In compliance with the
Canadian Privacy Legislation
some supporting forms
may have been removed from
this dissertation.

While these forms may be included
in the document page count,
their removal does not represent
any loss of content from the dissertation.

# ANALYSIS OF UNSTEADY FLOWS PAST OSCILLATING WINGS

**Chih-Wei Huang**

Department of Mechanical Engineering

McGill University

Montréal, Québec, Canada

August 2002

A thesis submitted to the Faculty of the Graduate Studies and Research in partial fulfillment of the requirements of the degree of Master of Engineering

*Your file Votre référence*
*ISBN: 0-612-88359-0*
*Our file Notre référence*
*ISBN: 0-612-88359-0*

# ABSTRACT

This thesis presents a more accurate and efficient method for the study of finite span wings in steady and unsteady supersonic flows with more computing efficiency.

For steady flows, the boundary conditions are expressed in terms of the source distributions over wing surfaces. Specific theoretical solutions are derived for the calculations of pressure coefficient distribution and the lift, pitching moment, and rolling moment coefficients. The present solutions have been validated for delta and trapezoidal wings by comparison with high order conical flow results based on the theory developed by Carafoli, Mateescu, and Nastase. An excellent agreement was found between these results.

For unsteady flows, the boundary conditions of finite span wings are modeled by using pulsating sources distributing over the wing surface. The present method leads to more accurate solutions for rigid wings executing harmonic oscillations in translation, pitching rotation, and rolling rotation of various oscillating frequencies. These solutions were found in very good agreement with the available high order conical flow solutions obtained by Carafoli, Mateescu, and Nastase.

Then the method has been used to obtain solutions for the flexible wings executing flexural oscillations, which are of interest for the aeroelastic studies in the aeronautical applications.

# RÉSUMÉ

Cette thèse présente une méthode pour l'étude des ailes d'envergure finie en écoulement supersonique stationnaires et non-stationnaires.

Pour les écoulements stationnaires, les conditions de frontière sont exprimés en termes de distributions de source sur la surface de l'aile. Des solutions théoriques spécifiques sont dérivés pour les coefficients aérodynamiques de pression, de portance et des moments de tangage et de roulis. Les solutions obtenus ont été validées pour les ailes delta et les ailes trapézoïdales par comparaison avec des résultats d'écoulement conique d'ordre supérieur basés sur la théorie développée par Carafoli, Mateescu, et Nastase. Un excellent accord a été trouvé entre ces résultats.

Pour les écoulements instationnaires, les conditions de frontière des ailes d'envergure finie sont modelés en employant des sources pulsatoires distribuées sur la surface de l'aile. La méthode présentée mène à des solutions plus précises pour les ailes rigides exécutant des oscillations harmoniques en translation, et rotation de tangage et de roulis à des diverses fréquences d'oscillation. Ces solutions ont été trouvées dans une bonne concordance avec les solutions disponibles basées sur les écoulements conique d'ordre supérieur, obtenues par Carafoli, Mateescu, et Nastase.

Après la validation, la méthode a été utilisée pour obtenir des solutions pour les ailes flexibles exécutant des oscillations en flexion, qui sont d'intérêt pour les études aéroélastiques dans les applications aéronautiques.

# AKOWLEDGEMENTS

This thesis required the support and assistance of a variety of individuals that, in combination, lead to the completion of this research. At the top of my list is my thesis supervisor, Professor Dan Mateescu, who patiently introduced me to the vast world of aerodynamics and guided my efforts to accomplish this work.

Also to be mentioned are my parents, my parents in law, and my extremely talented colleague, friend, and wife, Shirley, for their help, support, and encouragement, without which I wouldn't have been able to complete my research. I express my profound gratitude to them who make even the most frustrating times more pleasant.

Also to be mentioned are all the academic and technical staffs of the Department of Mechanical Engineering. I wish to express my grateful thanks to them for their help with administrative details throughout my study at McGill University.

Last, I would like to thank all my friends in Canada for their friendship, help, interest, and attention.

# CONTENTS

ABSTRACT ..... i

RÉSUMÉ ..... ii

ACKNOWLEDGEMENTS ..... iii

TABLE OF CONTENTS ..... iv

NOMENCLATURE ..... ix

LIST OF FIGURES ..... xii

LIST OF TABLES ..... xviii

**1. INTRODUCTION ..... 1**

1.1 Literature review ..... 1

1.2 Aims and scope of this thesis ..... 3

**2. PROBLEM FORMULATION ..... 5**

2.1 General geometrical configuration of polygonal wings and boundary condition ..... 5

2.2 The potential flow model with small disturbance approximation ..... 9

2.3 Low frequency harmonic motion of wing in supersonic flows ..... 12

2.4 Aerodynamic forces and moments coefficients on wings ..... 16

**3. PREVIOUS STUDIES – ANALYTICAL METHOD BASED ON THEORY OF CONICAL FLOWS AND SOLUTIONS TO STEADY AND UNSTEADY FLOWS PAST SUPERSONIC WINGS** ..... **18**

3.1 Compatibility relation of conical motions in supersonic flows ..... 18

3.2 Compatibility relation of high order conical motions in supersonic flows ..... 21

3.3 High order conical flow solutions of fixed wings placing in steady supersonic flows ..... 23

3.3.1 High order conical flow solutions to thin delta wing with supersonic leading edges and symmetry of incidence ..... 23

3.3.2 High order conical flow solutions to thin delta wing with supersonic leading edges and antisymmetry of incidence ..... 25

3.3.3 High order conical flow solutions to trapezoidal thin wing with supersonic leading edges ..... 26

3.4 High order conical flow solutions to wings executing unsteady motions in supersonic flows ..... 29

3.4.1 Calculation of the reduced pressure coefficient for thin delta wing ..... 30

3.4.2 Calculation of the reduced pressure coefficient for thin trapezoidal wing ..... 32

**4. ANALYSIS OF SUPERSONIC FLOW ON WING SURFACE BY METHOD OF SOURCE DISTRIBUTION** ..... **33**

4.1 Velocity potential of sources distributing over wing surface in steady supersonic flows ... 33

4.2 Velocity potential of pulsating sources distributing over wing surface in supersonic flows 40

**5. PRESENT STEADY FLOW SOLUTIONS FOR FIXED WINGS** ..... **44**

5.1 General steady flow solutions for thin wings ..... 44

5.2 Calculation of integral for thin delta wing in steady supersonic flows ..... 47

5.3 Calculation of integral for thin trapezoidal wing in steady supersonic flows ..... 53

**6. PRESENT UNSTEADY FLOW SOLUTIONS FOR OSCILLATING WINGS ..... 58**

6.1 General unsteady flow solutions for oscillating thin wings ..... 58

6.2 Calculation of integral for oscillating thin delta wing ..... 64

6.3 Calculation of integral for oscillating thin trapezoidal wing ..... 65

**7. RESULTS AND CONCLUSION ..... 66**

7.1 Steady flow results for delta wings ..... 66

7.2 Steady flow results for trapezoidal wings ..... 70

7.3 Unsteady flow results for oscillating rigid wings ..... 72

7.3.1 Case of wings executing oscillatory vertical translation ..... 72

7.3.1.1 Thin delta wing executing oscillatory vertical translation ..... 72

7.3.1.2 Thin trapezoidal wing executing oscillatory vertical translation ..... 80

7.3.2 Case of wings executing oscillatory pitching rotation ..... 84

7.3.2.1 Thin delta wing executing oscillatory pitching rotation ..... 84

7.3.2.2 Thin trapezoidal wing executing oscillatory pitching rotation ..... 92

7.3.3 Case of wings executing oscillatory rolling rotation ..... 96

7.3.3.1 Thin delta wing executing oscillatory rolling rotation ..... 96

7.3.3.2 Thin trapezoidal wing executing oscillatory rolling rotation ..... 104

7.4 Unsteady flow results for oscillating rigid wings ..... 108

7.4.1 Thin delta wing executing flexural harmonic oscillatory deformation ..... 109

7.4.2 Thin trapezoidal wing executing flexural harmonic oscillatory deformation ..... 111

**8. CONCLUSIONS ..... 113**

**APPENDIX A. Derivation of $\Phi_1'$ related to the calculation of the reduced pressure coefficient by theory of high-order conical flows** ..... **115**

A-1 Case of thin delta Wing ..... 115

A-2 Case of thin trapezoidal wing ..... 116

**APPENDIX B. Real part of specific inverse triangular functions** ..... **117**

**APPENDIX C. Integrals related to the calculation of $C_l$, $C_{m1}$, and $C_{m2}$ based on method of source distribution** ..... **118**

C-1 Case of thin delta wing in steady supersonic flows ..... 118

C-2: Case of thin trapezoidal wing in steady supersonic flows ..... 122

C-3: Case of oscillating delta wing in supersonic flows ..... 126

C-4: Case of oscillating trapezoidal wing in supersonic flows ..... 129

C-5 Recurrence formulae for the integral $I_a$ ..... 133

C-6 Recurrence formulae for the integral $I_b$ ..... 134

C-7 Recurrence formulae for integral $\int (l-y)^m I_g dy$ ..... 135

C-8 Recurrence formulae for integral $\int_{\frac{1}{B}}^{\frac{1}{B}} (l-y)^m dI_g$ ..... 136

C-9 Recurrence formulae for integral $\int (l+y)^n J_g dy$ ..... 137

C-10 Recurrence formulae for integral $\int_{\frac{1}{B}}^{\frac{1}{B}} (l+y)^n dJ_g$ ..... 139

C-11 Recurrence formulae for integral $\int y^n \tilde{J}_p dy$ ..... 140

C-12 Recurrence formulae for integral $\int_{\frac{1}{B}}^{B} y^n d\tilde{J}_p$ ..... 141

C-13 Integrals related to $I_g^*$ and $J_g^*$, for $g = 1$ ..... 142

**Appendix D: General integral and integration limits for calculation of aerodynamics coefficients for delta and trapezoidal wings ..... 144**

D-1: Case of thin delta wing ..... 144

D-2: Case of thin trapezoidal wing ..... 147

**BIBLIOGRAPHY ..... 150**

# NOMENCLATURE

| | |
|---|---|
| $a$ | speed of sound |
| $p$ | pressure |
| $\rho$ | density |
| $M$ | Mach number |
| $U_\infty$ | free stream velocity |
| $a_\infty$ | speed of sound in the free stream |
| $p_\infty$ | pressure in the undisturbed free stream |
| $\rho_\infty$ | density in the undisturbed free stream |
| $M_\infty$ | free stream Mach number ($M_\infty = U_\infty / a_\infty$) |
| $\gamma$ | ratio of specific heat coefficients at constant pressure and volume ($\gamma$=1.4 for air) |
| $\mu$ | Mach angle, $\mu = \sin^{-1}(1/M_\infty)$ |
| $\chi$ | wing sweep angle |
| $\tau$ | deflexion angle of the wing surface |
| $c_0$ | root chord |
| $b$ | span of trapezoidal wing |
| $l$ | span of delta wing; semi-span of trapezoidal wing |
| $V$ | flow velocity |
| $\lambda$ | reduced frequency |
| $\omega$ | angular frequency |
| $\Phi$ | velocity potential in steady flows; total reduced velocity potential in unsteady flows |
| $\varphi$ | perturbation velocity potential in steady flows; total velocity potential in unsteady flows |
| $\alpha$ | angle of attack |
| $\beta$ | rolling angle |
| $\Lambda$ | specific area containing series of infinitesimal sources |
| $\sigma$ | specific area covered by the forward Mach cone within $\Lambda$ |
| $S$ | total delta wing surface area; half of the total trapezoidal wing surface area; exponent used |
| $\mathbf{n}$ | normal unit vector to wing surface |

| | |
|---|---|
| $n_1, n_2, n_3$ | components of the normal unit vector to wing surfaces along axes $x_1$, $x_2$, and $x_3$ |
| $\xi_1, \xi_2$ | coordinates of sources distributing over the wing surfaces |
| $x_1, x_2, x_3$ | Cartesian coordinates |
| $y, z$ | non-dimensional conical coordinates ($y = x_2 / x_1$; $z = x_3 / x_1$) |
| $x, y, z$ | Busemann geometrical transformation coordinates |
| $X, Y$ | homogeneous coordinates |
| $X_1^*, X_2^*$ | auxiliary functions of the upper integral limits for two specific integration domains |
| $C_q^n$ | coefficients of binomial series |
| $h_0$ | amplitude of the vertical oscillatory translation |
| $\psi_h$ | phase angle of the vertical oscillatory translation |
| $\hat{h}$ | complex amplitude of the vertical oscillatory translation ($\hat{h} = h_0 e^{i\psi_h}$) |
| $\psi_0$ | amplitude of the rolling oscillatory rotation |
| $\psi_\psi$ | phase angle of the rolling oscillatory rotation |
| $\hat{\psi}$ | complex amplitude of the rolling oscillatory rotation ($\hat{\psi} = \psi_0 e^{i\psi_\psi}$) |
| $\theta_0$ | amplitude of the pitching oscillatory rotation |
| $\psi_\theta$ | phase angle of the pitching oscillatory rotation |
| $\hat{\theta}$ | complex amplitude of the pitching oscillatory rotation ($\hat{\theta} = \theta_0 e^{i\psi_\theta}$) |
| **i, j, k** | unit vectors along axes $x_1$, $x_2$, and $x_3$ |
| **q** | perturbation velocity (**q** = $u$**i** + $v$**j** + $w$**k**) |
| $u$ | perturbation velocity in the $x_1$ direction |
| $v$ | perturbation velocity in the $x_2$ direction |
| $w$ | perturbation velocity in the $x_3$ direction |
| $\hat{w}$ | reduced downwash ($\hat{w} = w/e^{i\omega t}$) |
| $\mathscr{U}$ | analytical complex function of perturbation velocity in the $x_1$ direction (Re[$\mathscr{U}$] = $u$) |
| $\mathscr{V}$ | analytical complex function of perturbation velocity in the $x_2$ direction (Re[$\mathscr{V}$] = $v$) |
| $\mathscr{W}$ | analytical complex function of perturbation velocity in the $x_3$ direction (Re[$\mathscr{W}$] = $w$) |
| $t$ | time |
| $\mathscr{F}_{n\text{-}q\text{-}r,\,q,r}$ | analytical function with respect to the complex variable x |
| $n$ | the degree of the homogeneous polynomial |
| $N$ | the highest degree of the homogeneous polynomial |

$c_{n-q,q}$ coefficients of the geometry of the thin wing surface equation expressed in homogeneous polynomial

$w_{n-q,q}$ coefficients of the downwash equation expressed in homogeneous polynomial

$Cp$ pressure coefficient

$\hat{C}p$ reduced pressure coefficient

$C_l$ lift coefficient

$\hat{C}_l$ reduced lift coefficient

$C_{m2}$ pitching moment coefficient

$\hat{C}_{m2}$ reduced pitching moment coefficient

$C_{m1}$ rolling moment coefficient

$\hat{C}_{m1}$ reduced rolling moment coefficient

**Exponents used:** $a, b, m, n, k, q, j, g, f, p, s, S, r, R, t, i_1, i_2$

# LIST OF FIGURES


2.1 Geometry of delta and trapezoidal wings at an incidence $\alpha$ in uniform free stream $U_\infty$ . . . 8

2.2 Geometry of thin wings of longitudinal cross-section at root chord at an incidence, $\alpha$, in uniform free stream $U_\infty$ . . . . . 8

3.1 Conformal transformation of wing geometry with supersonic edges . . . . . 20

3.2 The separation of half trapezoidal thin wing surface into $\widetilde{S}_0$, $S_0$, $S_i$, and $S_l$ . . . . . 27

4.1 A single source situated in uniform supersonic flow . . . . . 34

4.2 Distribution of series of infinitesimal sources in specific area $\Lambda$ . . . . . 35

4.3 Coordinates system and integral limits for the downwash calculation . . . . . 37

4.4 Calculation of the integral limit '$a_2$' . . . . . 38

5.1 Integral limits of the thin delta wing . . . . . 47

5.2 Integral limits of the thin trapezoidal wing . . . . . 53

7.1 The longitudinal and spanwise variation of the axial velocity for thin delta wing with supersonic leading edges and symmetry incidence $\alpha = -w_{10}x_1 / U_\infty$ . . . . . 68
(root chord, $c_0 = 1.0$; semi-span, $l = 0.75$; Mach number, $M_\infty = 2.0$)

7.2 The longitudinal and spanwise variation of the axial velocity for thin delta wing with supersonic leading edges and antisymmetry incidence $\alpha = -w_{01}x_2 / U_\infty$ . . . . . 69
(root chord, $c_0 = 1.0$; semi-span, $l = 0.75$; Mach number, $M_\infty = 2.0$)

7.3 The spanwise variation of the axial velocity for steady thin trapezoidal wing with supersonic leading edges and incidence $\alpha = -w_{10}x_1 / U_\infty$ ..... 71

(root chord, $c_0 = 1.0$; wing span, $b = 1.0$; wing semi-span, $l = 0.75$; Mach number, $M_\infty = 2.0$)

7.4 The real and imaginary parts of the reduced pressure coefficients for thin delta wing executing harmonic vertical translation oscillations ..... 75

(The reduced frequency of oscillations, $\lambda = 0.0147$; spanwise variation, $x_1 = 1.0$; root chord, $c_0 = 1.0$; wing span, $l = 0.75$; Mach number, $M_\infty = 2.0$)

7.5 The real and imaginary parts of the reduced pressure coefficients for thin delta wing executing harmonic vertical translation oscillations ..... 76

(The reduced frequency of oscillations, $\lambda = 0.0735$; spanwise variation, $x_1 = 1.0$; root chord, $c_0 = 1.0$; wing span, $l = 0.75$; Mach number, $M_\infty = 2.0$)

7.6 The real and imaginary parts of the reduced pressure coefficients for thin delta wing executing harmonic vertical translation oscillations ..... 77

(The reduced frequency of oscillations, $\lambda = 0.1470$; spanwise variation, $x_1 = 1.0$; root chord, $c_0 = 1.0$; wing span, $l = 0.75$; Mach number, $M_\infty = 2.0$)

7.7 The real and imaginary parts of the reduced pressure coefficients for thin delta wing executing harmonic vertical translation oscillations ..... 78

(The reduced frequency of oscillations, $\lambda = 0.735$; spanwise variation, $x_1 = 1.0$; root chord, $c_0 = 1.0$; wing span, $l = 0.75$; Mach number, $M_\infty = 2.0$)

7.8 The real and imaginary parts of the reduced pressure coefficients for thin delta wing executing harmonic vertical translation oscillations ..... 79

(The reduced frequency of oscillations, $\lambda = 1.0$; spanwise variation, $x_1 = 1.0$; root chord, $c_0 = 1.0$; wing span, $l = 0.75$; Mach number, $M_\infty = 2.0$)

7.9 The real and imaginary parts of the reduced pressure coefficients for thin trapezoidal wing executing harmonic vertical translation oscillations ..... 81
(The reduced frequency of oscillations, $\lambda = 0.0147$; spanwise variation, $x_1 = 1.0$; root chord, $c_0 = 1.0$; span, $b = 1.0$; wing span, $l = 0.75$; Mach number, $M_\infty = 2.0$)

7.10 The real and imaginary parts of the reduced pressure coefficients for thin trapezoidal wing executing harmonic vertical translation oscillations ..... 82
(The reduced frequency of oscillations, $\lambda = 0.0735$; spanwise variation, $x_1 = 1.0$; root chord, $c_0 = 1.0$; span, $b = 1.0$; wing span, $l = 0.75$; Mach number, $M_\infty = 2.0$)

7.11 The real and imaginary parts of the reduced pressure coefficients for thin trapezoidal wing executing harmonic vertical translation oscillations ..... 83
(The reduced frequency of oscillations, $\lambda = 0.1470$; spanwise variation, $x_1 = 1.0$; root chord, $c_0 = 1.0$; span, $b = 1.0$; wing span, $l = 0.75$; Mach number, $M_\infty = 2.0$)

7.12 The real and imaginary parts of the reduced pressure coefficients for thin delta wing executing harmonic pitching rotation oscillations ..... 87
(The reduced frequency of oscillations, $\lambda = 0.0147$; spanwise variation, $x_1 = 1.0$; root chord, $c_0 = 1.0$; wing span, $l = 0.75$; Mach number, $M_\infty = 2.0$)

7.13 The real and imaginary parts of the reduced pressure coefficients for thin delta wing executing harmonic pitching rotation oscillations ..... 88
(The reduced frequency of oscillations, $\lambda = 0.0735$; spanwise variation, $x_1 = 1.0$; root chord, $c_0 = 1.0$; wing span, $l = 0.75$; Mach number, $M_\infty = 2.0$)

7.14 The real and imaginary parts of the reduced pressure coefficients for thin delta wing executing harmonic pitching rotation oscillations ..... 89
(The reduced frequency of oscillations, $\lambda = 0.1470$; spanwise variation, $x_1 = 1.0$; root chord, $c_0 = 1.0$; wing span, $l = 0.75$; Mach number, $M_\infty = 2.0$)

7.15 The real and imaginary parts of the reduced pressure coefficients for thin delta wing executing harmonic pitching rotation oscillations ..... 90
(The reduced frequency of oscillations, $\lambda = 0.735$; spanwise variation, $x_1 = 1.0$; root chord, $c_0 = 1.0$; wing span, $l = 0.75$; Mach number, $M_\infty = 2.0$)

7.16 The real and imaginary parts of the reduced pressure coefficients for thin delta wing executing harmonic pitching rotation oscillations ..... 91
(The reduced frequency of oscillations, $\lambda = 1.0$; spanwise variation, $x_1 = 1.0$; root chord, $c_0 = 1.0$; wing span, $l = 0.75$; Mach number, $M_\infty = 2.0$)

7.17 The real and imaginary parts of the reduced pressure coefficients for thin trapezoidal wing executing harmonic pitching rotation oscillations ..... 93
(The reduced frequency of oscillations, $\lambda = 0.0147$; spanwise variation, $x_1 = 1.0$; root chord, $c_0 = 1.0$; span, $b = 1.0$; wing span, $l = 0.75$; Mach number, $M_\infty = 2.0$)

7.18 The real and imaginary parts of the reduced pressure coefficients for thin trapezoidal wing executing harmonic pitching rotation oscillations ..... 94
(The reduced frequency of oscillations, $\lambda = 0.0735$; spanwise variation, $x_1 = 1.0$; root chord, $c_0 = 1.0$; span, $b = 1.0$; wing span, $l = 0.75$; Mach number, $M_\infty = 2.0$)

7.19 The real and imaginary parts of the reduced pressure coefficients for thin trapezoidal wing executing harmonic pitching rotation oscillations ..... 95
(The reduced frequency of oscillations, $\lambda = 0.1470$; spanwise variation, $x_1 = 1.0$; root chord, $c_0 = 1.0$; span, $b = 1.0$; wing span, $l = 0.75$; Mach number, $M_\infty = 2.0$)

7.20 The real and imaginary parts of the reduced pressure coefficients for thin delta wing executing harmonic rolling rotation oscillations ..... 99
(The reduced frequency of oscillations, $\lambda = 0.0147$; spanwise variation, $x_1 = 1.0$; root chord, $c_0 = 1.0$; wing span, $l = 0.75$; Mach number, $M_\infty = 2.0$)

7.21 The real and imaginary parts of the reduced pressure coefficients for thin delta wing executing harmonic rolling rotation oscillations ..... 100
(The reduced frequency of oscillations, $\lambda = 0.0735$; spanwise variation, $x_1 = 1.0$; root chord, $c_0 = 1.0$; wing span, $l = 0.75$; Mach number, $M_\infty = 2.0$)

7.22 The real and imaginary parts of the reduced pressure coefficients for thin delta wing executing harmonic rolling rotation oscillations ..... 101
(The reduced frequency of oscillations, $\lambda = 0.1470$; spanwise variation, $x_1 = 1.0$; root chord, $c_0 = 1.0$; wing span, $l = 0.75$; Mach number, $M_\infty = 2.0$)

7.23 The real and imaginary parts of the reduced pressure coefficients for thin delta wing executing harmonic rolling rotation oscillations ..... 102
(The reduced frequency of oscillations, $\lambda = 0.735$; spanwise variation, $x_1 = 1.0$; root chord, $c_0 = 1.0$; wing span, $l = 0.75$; Mach number, $M_\infty = 2.0$)

7.24 The real and imaginary parts of the reduced pressure coefficients for thin delta wing executing harmonic rolling rotation oscillations ..... 103
(The reduced frequency of oscillations, $\lambda = 1.0$; spanwise variation, $x_1 = 1.0$; root chord, $c_0 = 1.0$; wing span, $l = 0.75$; Mach number, $M_\infty = 2.0$)

7.25 The real and imaginary parts of the reduced pressure coefficients for thin trapezoidal wing executing harmonic rolling rotation oscillations ..... 105
(The reduced frequency of oscillations, $\lambda = 0.0147$; spanwise variation, $x_1 = 1.0$; root chord, $c_0 = 1.0$; span, $b = 1.0$; wing span, $l = 0.75$; Mach number, $M_\infty = 2.0$)

7.26 The real and imaginary parts of the reduced pressure coefficients for thin trapezoidal wing executing harmonic rolling rotation oscillations ..... 106
(The reduced frequency of oscillations, $\lambda = 0.0735$; spanwise variation, $x_1 = 1.0$; root chord, $c_0 = 1.0$; span, $b = 1.0$; wing span, $l = 0.75$; Mach number, $M_\infty = 2.0$)

7.27 The real and imaginary parts of the reduced pressure coefficients for thin trapezoidal wing executing harmonic rolling rotation oscillations ..... 107

(The reduced frequency of oscillations, $\lambda = 0.1470$; spanwise variation, $x_1 = 1.0$; root chord, $c_0 = 1.0$; span, $b = 1.0$; wing span, $l = 0.75$; Mach number, $M_\infty = 2.0$)

7.28 The real and imaginary parts of the reduced pressure coefficients for delta thin wing executing flexural oscillations, $Z = g_1 x_1^2 e^{i\omega t}$ ..... 109

(The reduced frequency of oscillations, $\lambda = 0.0147$; spanwise variation at $x_1 = 1.0$; root chord, $c_0 = 1.0$; semi-span, $l = 0.75$; Mach number, $M_\infty = 2.0$)

7.29 The imaginary part of the reduced pressure coefficients for delta thin wing executing flexural oscillations, $Z = g_2 x_2^2 e^{i\omega t}$ ..... 110

(The reduced frequency of oscillations, $\lambda = 0.0147$; spanwise variation at $x_1 = 1.0$; root chord, $c_0 = 1.0$; semi-span, $l = 0.75$; Mach number, $M_\infty = 2.0$)

7.30 The real and imaginary parts of the reduced pressure coefficients for trapezoidal thin wing executing flexural oscillations, $Z = g_1 x_1^2 e^{i\omega t}$ ..... 111

(The reduced frequency of oscillations, $\lambda = 0.0147$; spanwise variation at $x_1 = 1.0$; root chord, $c_0 = 1.0$; span, $b = 1.0$; semi-span, $l = 0.75$; Mach number, $M_\infty = 2.0$)

7.31 The imaginary part of the reduced pressure coefficients for trapezoidal thin wing executing flexural oscillations, $Z = g_2 x_2^2 e^{i\omega t}$ ..... 112

(The reduced frequency of oscillations, $\lambda = 0.0147$; spanwise variation at $x_1 = 1.0$; root chord, $c_0 = 1.0$; semi-span, $l = 0.75$; Mach number, $M_\infty = 2.0$)

# LIST OF TABLES


7.1 $C_l$, $C_{m2}$, and $C_{m1}$ for steady thin delta wing with supersonic leading edges and symmetry incidence $\alpha = -w_{10}x_1 / U_\infty$ ..... 67

7.2 $C_l$, $C_{m2}$, and $C_{m1}$ for steady thin delta wing with supersonic leading edges and antisymmetry incidence $\alpha = -w_{01}x_2 / U_\infty$ ..... 67

7.3 $C_l$, $C_{m2}$, and $C_{m1}$ for steady thin trapezoidal wing with supersonic leading edges for $\alpha = -w_{10}x_1 / U_\infty$ ..... 70

7.4 $\hat{C}_l$ and $\hat{C}_{m2}$ for thin delta wing executing oscillatory vertical translation ($\lambda = 0.0147$) ... 73

7.5 $\hat{C}_l$ and $\hat{C}_{m2}$ for thin delta wing executing oscillatory vertical translation ($\lambda = 0.0735$) ... 74

7.6 $\hat{C}_l$ and $\hat{C}_{m2}$ for thin delta wing executing oscillatory vertical translation ($\lambda = 0.1470$) ... 74

7.7 $\hat{C}_l$ and $\hat{C}_{m2}$ for thin delta wing executing oscillatory vertical translation ($\lambda = 0.735$) ..... 74

7.8 $\hat{C}_l$ and $\hat{C}_{m2}$ for thin delta wing executing oscillatory vertical translation ($\lambda = 1.0$) ..... 74

7.9 $\hat{C}_l$ and $\hat{C}_{m2}$ for thin trapezoidal wing executing oscillatory vertical translation ($\lambda$ = 0.0147, 0.0735, and 0.1470) ..... 80

7.10 $\hat{C}_l$ and $\hat{C}_{m2}$ for thin delta wing executing oscillatory pitching rotation ($\lambda = 0.0147$) .... 85

7.11 $\hat{C}_l$ and $\hat{C}_{m2}$ for thin delta wing executing oscillatory pitching rotation ($\lambda = 0.0735$) .... 85

7.12 $\hat{C}_l$ and $\hat{C}_{m2}$ for thin delta wing executing oscillatory pitching rotation ($\lambda = 0.1470$) .... 85

7.13 $\hat{C}_l$ and $\hat{C}_{m2}$ for thin delta wing executing oscillatory pitching rotation ($\lambda = 0.735$) ..... 85

7.14 $\hat{C}_l$ and $\hat{C}_{m2}$ for thin delta wing executing oscillatory pitching rotation ($\lambda = 1.0$) ..... 86

7.15 $\hat{C}_l$ and $\hat{C}_{m2}$ for thin trapezoidal wing executing oscillatory pitching rotation ($\lambda$ = 0.0147, 0.0735, and 0.1470) ..... 92

7.16 $\hat{C}_{m1}$ for thin delta wing executing oscillatory rolling rotation ($\lambda = 0.0147$) ..... 97

7.17 $\hat{C}_{m1}$ for thin delta wing executing oscillatory rolling rotation ($\lambda = 0.0735$) ..... 97

7.18 $\hat{C}_{m1}$ for thin delta wing executing oscillatory rolling rotation ($\lambda = 0.1470$) ..... 98

7.19 $\hat{C}_{m1}$ for thin delta wing executing oscillatory rolling rotation ($\lambda = 0.735$) ..... 98

7.20 $\hat{C}_{m1}$ for thin delta wing executing oscillatory rolling rotation ($\lambda = 1.0$) ..... 98

7.21 $\hat{C}_{m1}$ for thin trapezoidal wing executing oscillatory rolling rotation ($\lambda$ = 0.0147, 0.0735, 0.1470) ..... 104

# CHAPTER 1

# INTRODUCTION

## 1.1 Literature review

In the past few decades, the steady and unsteady supersonic flows over wings have been investigated theoretically and experimentally, using various mathematical, numerical, and experimental approaches. The problem of predicting accurately the aerodynamic characteristics of wings of various plane forms is among the most important ones that have been studied in the development of the aeronautical sciences. The invention of the digital computer and its introduction into the world of science and technology has led to the development, and increased awareness, of the analytical and computational methods for achieving more accurate solutions to the complexity of the physical world. Following is a brief literature review on which the present work is based.

Theoretically, the behavior of supersonic flow can be described by fundamental equation systems, but one may think that the analytical results is often no practically possible to describe completely the evolution of the system in its full complexity. Therefore, approximate numerical solutions have been sought based on finite difference and finite volume approaches. MacCormack et al. [13], [14] & [28]-[32] developed an explicit technique for numerical solutions in the form of the finite difference expression of governing equation systems based on predictor-corrector method. Jameson et al. [13]-[20] highlight the considerable flexibility of the application to the explicit finite

volume method for the analysis of wings and aircraft configurations by introducing the artificial dissipation for flux term calculation. Mateescu et al. [45] compared their numerical results with those given by MacCormack et al. and Jameson et al.. Mateescu et al. developed the biased-flux method to approximate and evaluate directly the direction of perturbation propagation of different flux variables. He determined the optimum values for upwind and downwind bias factor by carrying out series of numerical experiments and resulted in more accurate solutions.

On the other hand, analytical solutions can be applied to advanced and conceptual designs embedded with reasonable linearized assumptions, which will reduce the complexity of the original basic equations and make them tractable within certain limits. For long time, scientists have been concentrated in the studies of triangular and polygonal wing plan forms in supersonic flows based on theory of conical flows and high order conical motions, established by Carafoli, Mateescu, and Nastase [2], Mateescu [36] & [38]-[41], Paul Germain [9]-[12], and Krasilsciova [24]-[26]. Carafoli et al. established a unified method on the basis of high order conical flows, delivering series of analytical solutions to all these problems and for the actual calculation for cases of isolated simple wings, cruciform wings, and wings with vertical plane tail, simple or cruciform wings fitted with a body, and so on, which could be applied to practical aeronautical applications.

The analytical approach of supersonic flows past oscillating wings carried out by Carafoli et al. was based on the frequency expansion method. This method determined the unsteady pressure coefficients and the unsteady lift, pitching moment, and rolling moment coefficients of polygonal wings with subsonic or supersonic leading edges executing harmonic oscillations in supersonic flows. However, the high order conical flow solutions provided zero real values of the reduced pressure coefficient and the reduce lift and moment coefficient in the cases of oscillatory translation and rolling oscillation.

Pines et al. [54] developed a numerical scheme based on the Mach Box method by frequency expansion technique to obtain generalized forces on an oscillating flexible and rigid wing in

supersonic flows with both subsonic and supersonic leading edges. Their procedure is limited to Mach number to 1.414 and higher. Zartanian and Zsu applied Bassel functions series representation of the integral to implement the Mach Box method and improved by Fenain M. and Guirand-Wallee D. [7] in 1967. Improving on the work done by Chipman [4] analytically refined the Mach Box method, greatly increasing the accuracy of the supersonic oscillatory pressure distribution. Although the improvement in the accuracy has been obtained, the grid refinement implies an important increase in the computational running time. Accordingly, Appa and Smith [49] introduced triangular elements representation and linear distribution of sources over wing surfaces. This produces more accurate geometric representation of the wing with fewer elements on the wing and the finite element grid does not change with the Mach number.

## 1.2 Aims and scope of this thesis

In the light of considerable researches done regarding the analysis of steady and unsteady supersonic flows, the difficulties of fitting rigorously the body geometry and the requirement of improving computing efficiency are inherent deficiency of some of the previous studies in terms of the accuracy of solutions and calculation complication. Rather, the main concern of this thesis is to find out an analytical method of approach with more accuracy and better computational efficiency in calculations of the aerodynamic forces and moments coefficients for general wing configuration not only for the steady flows, but also for the unsteady flows past wings executing higher oscillations frequency.

The present thesis consists in the presentation of the new analytical solutions for the study of the steady and unsteady flows past fixed and oscillating rigid wings and past flexible wings executing flexural oscillations. A summary of the content of the thesis is given in the following.

Chapter 2 is dedicated to the problem formation of the steady and unsteady supersonic flows past fixed and oscillating thin wing plan form. The wing geometry and boundary conditions, the governing potential equation, and equations of aerodynamic forces and moments coefficients are presented.

In Chapter 3, previous method and analytical solutions based on high order conical flows theory developed by Carafoli, Mateescu, and Nastase [2], [38]-[41], are presented.

Chapter 4 is devoted to the presentation of theory and fundamentals of source distribution on the wing in supersonic flows and the determination of the velocity potential equations of the distribution of sources in steady state and pulsating sources over wing surfaces executing unsteady motions.

In chapter 5, the analytical solutions for steady cases are presented for delta and trapezoidal wings in supersonic flows. The present solutions are validated by comparison with the previous results observed using the theory of high order conical flows.

In chapter 6, analytical unsteady solutions are presented for the rigid delta and trapezoidal wings executing harmonic oscillations in translation and pitching and rolling rotation. Then, the method has been used to study the flexible wings executing flexural oscillations, which are of interest for the aeroelastic studies in the aeronautical applications.

Chapter 7 presents a summary of results and discussion for various cases of steady and unsteady flows past rigid wings and flexible wings executing the flexural oscillations by the method presented in Chapter 4, 5 and 6. The solutions for the rigid wings have been validated by comparison with the previous results based on high order conical flows.

The last chapter is devoted to conclusions and suggestions for further research work.

# CHAPTER 2

# PROBLEM FORMULATION

## 2.1 General geometrical configuration of polygonal wings and boundary condition

In supersonic flows, the leading edges and the ridges play fundamental roles in unified theory of angular wings based on high order conical flows. First, let's consider an orthogonal system $OX_1X_2X_3$, with axis $OX_1$ parallel to the free stream velocity, $U_\infty$ (Fig. 2.1). The edges, such as $OA_1$ and $OA_2$ in delta wing, $O_1O_2, OA_1$ and $OA_2$ in trapezoidal wing, are called leading edges; while $A_1A_2$ are called tailing edges. The Mach cone is defined by the Mach angle, $\mu$, and the circle representing the intersection of this cone with physical plane normal to $OX_1$ at distance $x_1 = 1$ is called the Mach circle with radius equal to $\tan\mu = 1/B$, where $B = \sqrt{M_\infty^2 - 1}$. The position of leading edges can be defined by two angles, $\chi_1$ and $\chi_2$, and their traces in the physical plane at $x_1 = 1$ are $l_1 = \cot\chi_1$ and $l_2 = \cot\chi_2$. When the leading edges are situated outside the Mach cone, i.e., $l_1$ and $l_2$ are larger then the radius of Mach circle, $1/B$, they are denoted as supersonic leading edges.

The geometry of the thin wing surface is defined by the equation $x_3 = Z(x_1, x_2)$, where $Z(x_1, x_2)$ can be defined in the form as a superposition of homogeneous polynomials in $x_1$ and $x_2$.

$$Z = \sum_{n=1}^{N} \sum_{q=0}^{n} c_{n-q,q} x_1^{n-q} x_2^q , \tag{2.1.1}$$

where $N$ is the degree of the homogeneous polynomial of the highest order and the coefficients, $c_{n-q,q}$, are constants.

The deflexion angle, $\tau$, of wing surfaces with respect to the free stream direction can be expressed as

$$\tan\tau = \frac{\partial Z}{\partial x_1} = \sum_{n=1}^{N} \sum_{q=0}^{n-1} (n-q) c_{n-q,q} x_1^{n-q-1} x_2^q . \tag{2.1.2}$$

Generally, we denote $f$ as function of wing surface suitable for both fixed situation and general unsteady motion in uniform flows and can be written as $f(\mathbf{r}, t) = f(x_1, x_2, x_3, t) = 0$. And the normal unit vector to the wing surface can be defined by,

$$\mathbf{n} = \frac{\nabla f}{|\nabla f|} . \tag{2.1.3}$$

Let's denote the perturbation velocity on the wing surface by $\mathbf{q}_b$, with which is satisfied the continuous equation and we have

$$\frac{\partial f}{\partial t} + \mathbf{q}_b \cdot \nabla f = 0. \tag{2.1.4}$$

As well, the boundary condition on the wing can be defined as

$$\mathbf{q}_b \cdot \mathbf{n} = \mathbf{V} \cdot \mathbf{n} = (\mathbf{U}_\infty + \mathbf{q}) \cdot \mathbf{n} = 0, \tag{2.1.5}$$

or we can reorganize the boundary condition equation like

$$\mathbf{q} \cdot \mathbf{n} = -\mathbf{U}_\infty \cdot \mathbf{n} + \mathbf{q}_b \cdot \mathbf{n}, \tag{2.1.6}$$

where $\mathbf{V} = \mathbf{U}_\infty + \mathbf{q} = (U_\infty \cos\alpha + u)\mathbf{i} + v\mathbf{j} + (U_\infty \sin\alpha + w)\mathbf{k}$ is the fluid velocity on the wing surface; however, $\mathbf{q}$ is equal to zero for the undisturbed portion outside the Mach cone.

By substituting the definition of normal unit vector, the boundary condition can then be expressed in terms of $\nabla f$ and it shows

$$\mathbf{q} \cdot \nabla f = -\mathbf{U}_\infty \cdot \nabla f + \mathbf{q}_b \cdot \nabla f. \tag{2.1.7}$$

Let's take account of the material derivative of $f$ and we have

$$\frac{Df}{Dt} = \frac{\partial f}{\partial t} + \mathbf{V}\nabla f = \frac{\partial f}{\partial t} + (\mathbf{U}_\infty + \mathbf{q})\nabla f = \frac{\partial f}{\partial t} + (\mathbf{U}_\infty + \nabla\varphi)\nabla f = 0. \tag{2.1.8}$$

Accordingly, the boundary condition for wings executing unsteady motion can be rearranged as,

$$U_\infty \sin\alpha + w = (U_\infty \cos\alpha + u)\frac{\partial f}{\partial x_1} + v\frac{\partial f}{\partial x_2} + \frac{\partial f}{\partial t}. \tag{2.1.9}$$

For wings in steady state, we have,

$$U_\infty \sin\alpha + w = (U_\infty \cos\alpha + u)\frac{\partial f}{\partial x_1} + v\frac{\partial f}{\partial x_2}. \tag{2.1.10}$$

The perturbation velocity $u$ and $v$ are assumed small, and hence the boundary condition on the wings executing unsteady motions can then be recast in the form as

$$w = -U_\infty \sin\alpha + U_\infty \cos\alpha \frac{\partial f}{\partial x_1} + \frac{\partial f}{\partial t} = \sum_{n=1}^{N}\sum_{q=0}^{n-1} w_{n-q-1,q} x_1^{n-q-1} x_2^q + \frac{\partial f}{\partial t}. \tag{2.1.11}$$

And for wings in steady state, we have

$$w = -U_\infty \sin\alpha + U_\infty \cos\alpha \frac{\partial f}{\partial x_1} = \sum_{n=1}^{N}\sum_{q=0}^{n-1} w_{n-q-1,q} x_1^{n-q-1} x_2^q, \tag{2.1.12}$$

where $w_{n-q-1,q}$ are constants and $\sum_{n=1}^{N}\sum_{q=0}^{n-1} w_{n-q-1,q} x_1^{n-q-1} x_2^q$ is part of the downwash velocity expressed by the geometry of the thin wing surface. According to the linearized theory, each specific solution of a single polynomial of order ($n$-1) is sufficient for problems with more general geographical configurations. Hence, the part of the downwash velocity based on the geometry of the thin wing surface in ($n$-1) order can be replaced by $\sum_{q=0}^{n-1} w_{n-q-1,q} x_1^{n-q-1} x_2^q$.

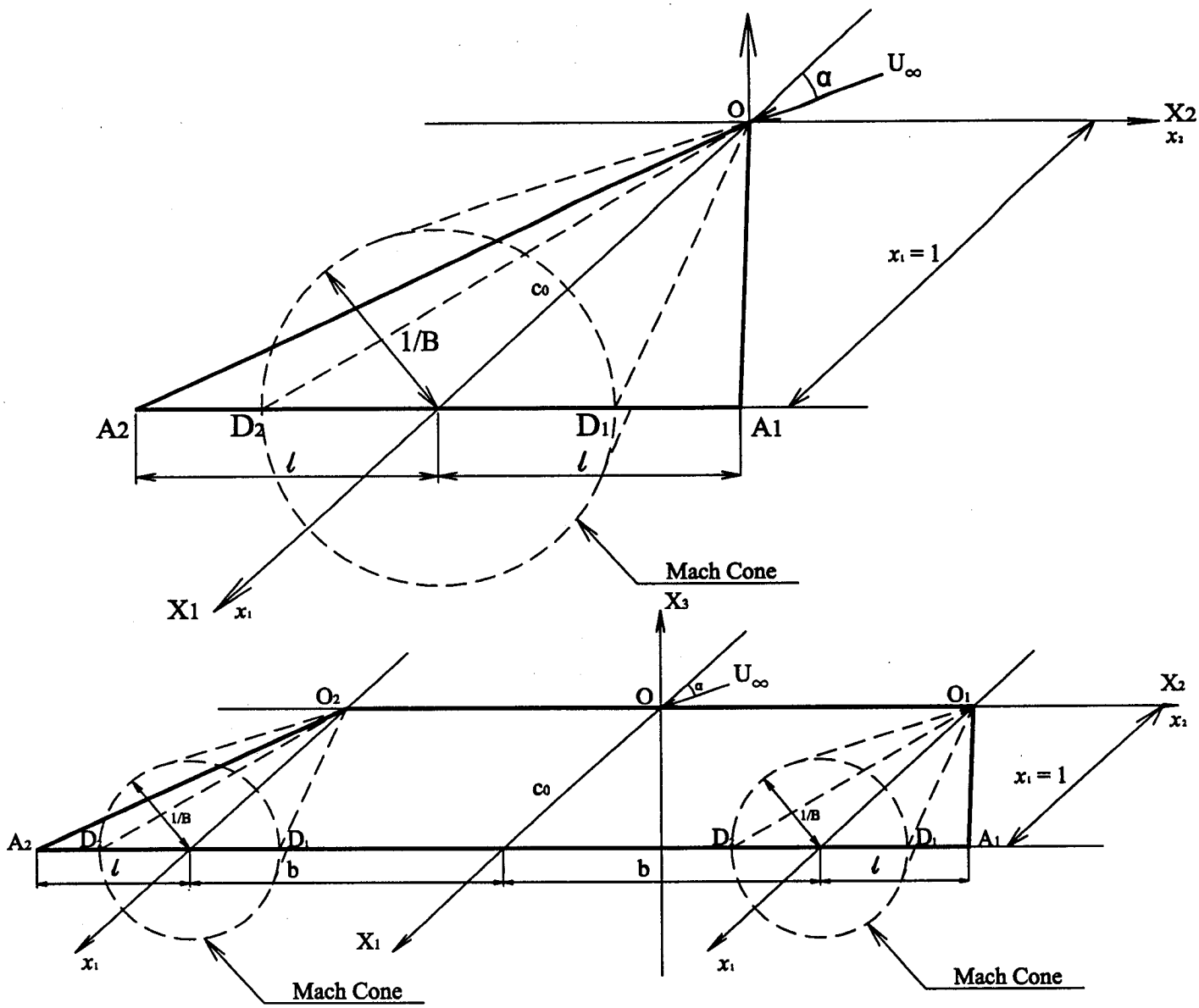


Figure 2.1 Geometry of delta and trapezoidal wings at an incidence α in uniform free stream $U_\infty$.

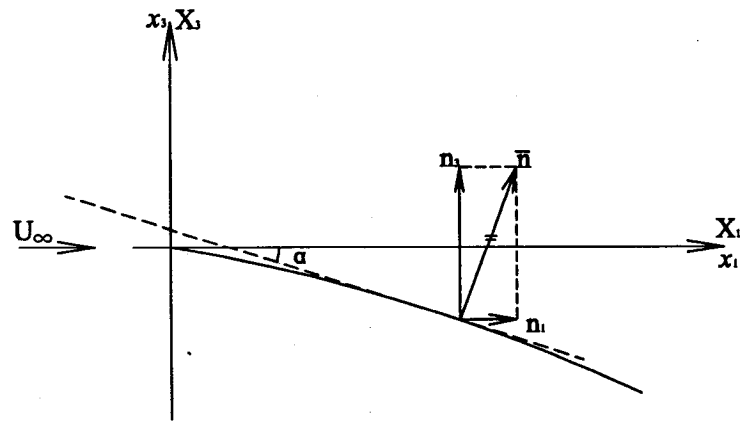


Figure 2.2 Geometry of thin wings of longitudinal cross-section at root chord at an incidence, α, in uniform free stream $U_\infty$.

## 2.2 The potential flow model with small disturbance approximation

Compared to the full system of Navier-Stokes equations, the potential flow model is the simplest mathematical description of inviscid and irrotational flows. As known from Prandtl's boundary layer analysis, this is a valid approximation for flows in high Reynolds numbers outside viscous regions developing in the vicinity of solid surface. Thus, the curl of the velocity is zero; i.e., $\nabla\times\vec{V}=0$, where $\vec{V}$ is the three-dimensional velocity field. Basically, the three-dimensional velocity field of the potential flows is the gradient of one specific scalar property, defined as the velocity potential functions, $\Phi$, and can be expressed by a single velocity potential function as $\vec{V}=\nabla\Phi$.

According to the non-viscous approximation, the entropy is constant along streamlines and the flow is isentropic throughout the whole flow field. Hence the equation of isentropic flow can be written as $\frac{p}{\rho^{\gamma}}=const.$, where $\gamma$ is the ratio of specific heat coefficients at constant pressure and constant volume ($\gamma$ = 1.4 for air). The speed of sound for isentropic assumption can be expressed as

$$a=\sqrt{\gamma\frac{p}{\rho}}=\sqrt{\gamma RT}\,. \tag{2.2.1}$$

And the continuity and momentum equations can be expressed as

$$\frac{\partial\rho}{\partial t}+\nabla\left(\rho\vec{V}\right)=0\,, \tag{2.2.2}$$

$$\frac{dV}{dt}=\frac{\partial\vec{V}}{\partial t}+\nabla\left(\frac{1}{2}V^{2}\right)+\left(\nabla\times\vec{V}\right)\times\vec{V}=\frac{\partial\vec{V}}{\partial t}+\nabla\left(\frac{1}{2}V^{2}\right)=-\frac{1}{\rho}\nabla p\,. \tag{2.2.3}$$

The rate of change of pressure with respect to density is an isentropic change and thus we have

$$\int\frac{dp}{\rho}=\frac{\gamma}{\gamma-1}\frac{p}{\rho}\rightarrow\frac{\nabla p}{\rho}=\nabla\left(\frac{\gamma}{\gamma-1}\frac{p}{\rho}\right). \tag{2.2.4}$$

By substituting Eq.(2.2.4) and $\vec{V}=\nabla\Phi$ into Eq.(2.2.3), the momentum equation can be recast by the following two forms as

$$\frac{\partial\vec{V}}{\partial t}+\nabla\left(\frac{1}{2}V^{2}\right)+\frac{1}{\rho}\nabla p=\nabla\left(\frac{\partial\varphi}{\partial t}+\frac{1}{2}V^{2}+\frac{\gamma}{\gamma-1}\frac{p}{\rho}\right)=0\,, \tag{2.2.5}$$

and

$$\nabla\left(\frac{\partial\varphi}{\partial t}+\frac{1}{2}V^2\right)=-\frac{1}{\rho}\nabla p=-a^2\frac{1}{\rho}\nabla\rho \rightarrow d\left(\frac{\partial\varphi}{\partial t}+\frac{1}{2}V^2\right)=-\frac{1}{\rho}dp=-a^2\frac{1}{\rho}d\rho. \qquad (2.2.6)$$

Substituting Eq.(2.2.6) into the continuity equation, Eq.(2.2.2), we have

$$\frac{1}{\rho}\frac{\partial\rho}{\partial t}+\vec{V}\frac{\nabla\rho}{\rho}+\nabla\vec{V}=0\rightarrow \nabla\vec{V}-\frac{1}{a^2}\left[\vec{V}\nabla\left(\frac{1}{2}V^2+\frac{\partial\varphi}{\partial t}\right)+\frac{\partial}{\partial t}\left(\frac{1}{2}V^2+\frac{\partial\varphi}{\partial t}\right)\right]=0. \qquad (2.2.7)$$

And from the Eq.(2.2.5), the pressure equation in differential form and finite form are presented, respectively.

$$d\left(\frac{\partial\Phi}{\partial t}\right)+\vec{V}d\vec{V}+\frac{dp}{\rho}=d\left(\frac{\partial\Phi}{\partial t}+\frac{1}{2}V^2+\frac{\gamma}{\gamma-1}\frac{p}{\rho}\right)=0. \qquad (2.2.8)$$

$$\frac{\partial\Phi}{\partial t}+\frac{1}{2}V^2+\frac{\gamma}{\gamma-1}\frac{p}{\rho}=const. \text{ (Bernoulli-Lagrange equation)} \qquad (2.2.9)$$

In turn, because of the complexity of the direct application to coordinate systems and in accordance with employing the small disturbances approximation, we assume that the free stream velocity $U_\infty$ is disturbed due to additional small velocity in the vicinity of the wing surface. The projection of small disturbing velocity on each orthogonal axis is $u$, $v$, $w$, respectively. Let's denote $\varphi(x,y,z,t)$ as the disturbance velocity potential and the total velocity components is written as

$$\vec{V}=\nabla\Phi=(U_\infty\cos\alpha+u)\mathbf{i}+v\mathbf{j}+(U_\infty\sin\alpha+w)\mathbf{k}, \qquad (2.2.10)$$

where $\mathbf{q}=u\mathbf{i}+v\mathbf{j}+w\mathbf{k}$, $u=\frac{\partial\varphi}{\partial x}$, $v=\frac{\partial\varphi}{\partial y}$, $w=\frac{\partial\varphi}{\partial z}$, and $\Phi=U_\infty(x\cos\alpha+z\sin\alpha)+\varphi$

As a result,

$$V^2=U^2+u^2+w^2=U_\infty^2+2U_\infty\frac{\partial\varphi}{\partial x}, \qquad (2.2.11)$$

$$\nabla\left(\frac{1}{2}V^2\right)\approx\nabla\left(U_\infty\frac{\partial\varphi}{\partial x}\right)=\nabla(U_\infty u), \qquad (2.2.12)$$

$$V\nabla\left(\frac{1}{2}V^2\right)\approx V\nabla\left(U_\infty\frac{\partial\varphi}{\partial x}\right)\approx U_\infty^2\frac{\partial u}{\partial x}=U_\infty^2\frac{\partial^2\varphi}{\partial x^2}, \qquad (2.2.13)$$

$$V\nabla\left(\frac{\partial\varphi}{\partial t}\right)\approx(U_\infty+u)\frac{\partial^2\varphi}{\partial t\partial x}+v\frac{\partial^2\varphi}{\partial t\partial y}+w\frac{\partial^2\varphi}{\partial t\partial z}\approx U_\infty\frac{\partial^2\varphi}{\partial t\partial x}, \tag{2.2.14}$$

$$\frac{\partial}{\partial t}\left(\frac{1}{2}V^2\right)\approx U_\infty\frac{\partial u}{\partial t}=U_\infty\frac{\partial^2\varphi}{\partial t\partial x}. \tag{2.2.15}$$

In addition, the Bernoulli-Lagrange equations, Eq.(2.2.9), can also be recast as

$$\frac{\partial\varphi}{\partial t}+\frac{1}{2}V^2+\frac{a^2}{\gamma-1}=\frac{1}{2}U_\infty^2+\frac{a_\infty^2}{\gamma-1}=\frac{a_0^2}{\gamma-1}=const, \tag{2.2.16}$$

where $a^2=a_\infty^2-\frac{\gamma-1}{2}\left(V^2-U^2+2\frac{\partial\varphi}{\partial t}\right)\approx a_\infty^2$.

Accordingly, by substituting Eq.(2.2.12) ~ (2.2.16) into Eq.(2.2.7), the differential velocity potential equation for unsteady potential flow is written as

$$-B^2\frac{\partial^2\varphi}{\partial x^2}+\frac{\partial^2\varphi}{\partial y^2}+\frac{\partial^2\varphi}{\partial z^2}=\frac{1}{a_\infty^2}\left(\frac{\partial^2\varphi}{\partial t^2}+2U_\infty\frac{\partial^2\varphi}{\partial x\partial t}\right), \tag{2.2.17}$$

where $M_\infty=\frac{U_\infty}{a_\infty}$, $B=\sqrt{M_\infty^2-1}$, $\mu=\tan^{-1}\frac{1}{B}$.

Also, for steady flows, the velocity potential equation is simplified as

$$-B^2\frac{\partial^2\varphi}{\partial x^2}+\frac{\partial^2\varphi}{\partial y^2}+\frac{\partial^2\varphi}{\partial z^2}=0 \tag{2.2.18}$$

## 2.3 Low frequency harmonic motion of wings in supersonic flows

According to the assumption of small disturbances, the low frequency harmonic motion of wings can be decomposed into three elementary parts: the vertical linear translation, h(t), the pitching rotation, θ(t), with respect to axis $OX_2$, and the rolling rotation, $\psi(t)$, with respect to $OX_1$. All three elementary parts are defined as follows.

$$h(t) = h_0 \cos(\omega t + \psi_h) = \mathrm{Re}\left[\hat{h} \cdot e^{i\omega t}\right] = \mathrm{Re}\left[h_0 \cdot e^{i(\omega t + \psi_h)}\right], \tag{2.3.1-a}$$

$$\theta(t) = \theta_0 \cos(\omega t + \psi_\theta) = \mathrm{Re}\left[\hat{\theta} \cdot e^{i\omega t}\right] = \mathrm{Re}\left[\theta_0 \cdot e^{i(\omega t + \psi_\theta)}\right], \tag{2.3.1-b}$$

$$\psi(t) = \psi_0 \cos(\omega t + \psi_\psi) = \mathrm{Re}\left[\hat{\psi} \cdot e^{i\omega t}\right] = \mathrm{Re}\left[\psi_0 \cdot e^{i(\omega t + \psi_\psi)}\right], \tag{2.3.1-c}$$

where $\omega$ and $t$ are the frequency of the oscillatory motions and the time, respectively. In linear vertical translation oscillations, $h_0$ and $\psi_h$ are the amplitude and the phase angle. Similarly, $\theta_0$ and $\psi_\theta$ are the amplitude and the phase angle of the pitching rotation oscillations, and $\psi_0$ and $\psi_\psi$ are the amplitude and the phase angle of the rolling rotation oscillations. If taken as complex forms, the complex amplitudes are defined as $\hat{h} = h_0 e^{i\psi_h}$, $\hat{\theta} = \theta_0 e^{i\psi_\theta}$, $\hat{\psi} = \psi_0 e^{i\psi_\psi}$.

In addition, the velocity potential for harmonic motion can be written as [52]

$$\varphi(x_1, x_2, x_3, t) = U_\infty e^{i(\omega t + kx_1)} \Phi(x_1, x_2, x_3), \tag{2.3.2}$$

where $\Phi(x_1, x_2, x_3)$ is independent of time and represents the total reduced velocity potential. Substitute Eq.(2.3.2) into Eq.(2.2.17) and the unsteady velocity potential equation can be recast as

$$-B^2 \frac{\partial^2 \Phi}{\partial x_1^{\,2}} + \frac{\partial^2 \Phi}{\partial x_2^{\,2}} + \frac{\partial^2 \Phi}{\partial x_3^{\,2}} = \lambda^2 \frac{1+B^2}{B^2} \Phi \approx 0, \tag{2.3.3}$$

where $\lambda = \dfrac{\omega}{U_\infty}$ and $k = -\lambda \dfrac{1+B^2}{B^2} = -\lambda \dfrac{M_\infty^2}{B^2}$.

For equation of a point on the general wing model surface, $P_n(x_1, x_2)$ represents a summation of the homogeneous polynomials, $P_n(x_1, x_2)$, of various orders with respect to $x_1$ and $x_2$.

$$P_n(x_1, x_2) = \sum_{n=0}^{N} P_n(x_1, x_2). \tag{2.3.4}$$

The equation of a point on the wing surface can also be expressed in terms of the variation in time in harmonic oscillatory motions and we have

$$Z = e^{i\omega t} P(x_1, x_2). \tag{2.3.5}$$

In turn, by considering the harmonic oscillatory motions with three elementary motions, Eq.(2.3.5) can then be expressed as

$$Z = h(t) - x_1 \tan(\theta(t)) + x_2 \sin(\psi(t)). \tag{2.3.6}$$

As well, based on the small disturbance assumption, $\tan(\theta) \approx \theta; \sin(\psi) \approx \psi$, Eq.(2.3.5) becomes

$$Z = h(t) - x_1\theta(t) + x_2\psi(t) = e^{i\omega t}\left(\hat{h} - x_1\hat{\theta} + x_2\hat{\psi}\right) = e^{i\omega t} P(x_1, x_2), \tag{2.3.7-a}$$

where

$$P(x_1, x_2) = \sum_{n=0}^{N} P_n(x_1, x_2) = \hat{h} - x_1\hat{\theta} + x_2\hat{\psi}. \tag{2.3.7-b}$$

Apply the equation of points on the surface of wings to the boundary condition equation in Eq.(2.3.6), the boundary condition of wings executing harmonic oscillatory motions with small angle of attack can then be recast as

$$w = \frac{\partial \varphi}{\partial x_3} \approx U_\infty \frac{\partial Z}{\partial x_1} + \frac{\partial Z}{\partial t} \tag{2.3.8-a}$$

$$= U_\infty e^{i\omega t}\left(\frac{\partial P(x_1, x_2)}{\partial x_1} + \frac{i\omega}{U_\infty} P(x_1, x_2)\right) \tag{2.3.8-b}$$

$$= U_\infty e^{i\omega t}\left(-\hat{\theta} + i\lambda\left(\hat{h} - x_1\hat{\theta} + x_2\hat{\psi}\right)\right). \tag{2.3.8-c}$$

The vertical downwash, $w$, can also be written directly from Eq.(2.3.2) as

$$w = \frac{\partial \varphi}{\partial x_3} = U_\infty e^{i(\omega t + kx_1)} \frac{\partial \Phi}{\partial x_3} = U_\infty e^{i(\omega t + kx_1)} \hat{w}, \tag{2.3.9-a}$$

where $\hat{w}$ is denoted as the reduced downwash and can then be expressed explicitly as follows.

$$\hat{w} = \frac{\partial \Phi}{\partial x_3} = -\frac{1}{U_\infty} e^{-i(\omega t + kx_1)} \frac{\partial \varphi}{\partial x_3}. \tag{2.3.9-b}$$

In turn, Eq.(2.3.9-b) can be written successively by taking $\frac{\partial \varphi}{\partial x_3}$ in Eq.(2.3.8-b).

$$\hat{w} = \frac{\partial \Phi}{\partial x_3} = -\frac{1}{U_\infty} e^{-i(\omega t + kx_1)} \frac{\partial \varphi}{\partial x_3} = e^{-ikx_1} \left( \frac{\partial P(x_1, x_2)}{\partial x_1} + \frac{i\omega}{U_\infty} P(x_1, x_2) \right) = e^{-ikx_1} \hat{W}(x_1, x_2). \tag{2.3.9-c}$$

Under the assumption of high order conical flows, $k$ is very small, and expand $e^{-ikx_1}$ by Taylor expansion neglecting terms in $k$ and higher.

$$e^{\pm ikx_1} = 1 \pm ikx_1 + O(k^2). \tag{2.3.10}$$

Substitute Eq.(2.3.10) into Eq.(2.3.9-c), and one has

$$\hat{w} = e^{-ikx_1} \left( \frac{\partial P(x_1, x_2)}{\partial x_1} + \frac{i\omega}{U_\infty} P(x_1, x_2) \right) = \frac{\partial P}{\partial x_1} - \lambda^2 x_1 \frac{1 + B^2}{B^2} P + i\lambda \left( P + x_1 \frac{1 + B^2}{B^2} \frac{\partial P}{\partial x_1} \right)$$

$$\approx \frac{\partial P}{\partial x_1} + i\lambda \left( P + x_1 \frac{1 + B^2}{B^2} \frac{\partial P}{\partial x_1} \right). \tag{2.3.11-a}$$

By taking account of $P(x_1, x_2)$ in Eq.(2.3.7-b), the reduce downwash becomes

$$\hat{w} = -\hat{\theta} + i\lambda \left( \hat{h} - x_1 \frac{2B^2 + 1}{B^2} \hat{\theta} + x_2 \hat{\psi} \right). \tag{2.3.11-b}$$

From Eq. (2.3.11-b), the total reduced velocity potential, $\Phi$, consist of real and imaginary parts.

$$\Phi = \Phi' + i\lambda \Phi'' = \sum_{n=1}^{N} \Phi'_n + i\lambda \sum_{n=0}^{N} \Phi''_{n+1}, \tag{2.3.12}$$

where $N$ is the highest order of the polynomial $P(x_1, x_2)$. Consequently, the total reduced velocity potential of the second order of the polynomial $P(x_1, x_2)$ ($N$ = 1) is $\Phi = \Phi'_1 + i\lambda(\Phi''_1 + \Phi''_2)$. And

reduced downwash can be expressed in complex form as

$$\hat{w} = -\hat{\theta} + i\lambda\left(\hat{h} - x_1\frac{2B^2+1}{B^2}\hat{\theta} + x_2\hat{\psi}\right) = \frac{\partial\Phi'}{\partial x_3} + i\lambda\frac{\partial\Phi''}{\partial x_3} = \frac{\partial\Phi_1'}{\partial x_3} + i\lambda\left(\frac{\partial\Phi_1''}{\partial x_3} + \frac{\partial\Phi_2''}{\partial x_3}\right), \tag{2.3.13}$$

where $\frac{\partial\Phi_1'}{\partial x_3} = -\hat{\theta}$, $\frac{\partial\Phi_1''}{\partial x_3} = \hat{h}$, and $\frac{\partial\Phi_2''}{\partial x_3} = -x_1\frac{2B^2+1}{B^2}\hat{\theta} + x_2\hat{\psi}$.

All those reduced downwash velocity coefficients for harmonic motions can then be determined as

$$w_{00}' = -\hat{\theta}. \tag{2.3.14}$$

$$w_{00}'' = \hat{h}. \tag{2.3.15}$$

$$w_{10}'' = -\frac{2B^2+1}{B^2}\hat{\theta}. \tag{2.3.16}$$

$$w_{00}' = \hat{\psi}. \tag{2.3.17}$$

## 2.4 Aerodynamic forces and moments coefficients of wings

The pressure coefficient equation in the first approximation, denoted by *Cp*, is defined as

$$Cp \equiv \frac{p - p_\infty}{\frac{1}{2}\rho_\infty U_\infty^2} = \frac{2}{\gamma M_\infty^2}\left(\frac{p}{p_\infty} - 1\right). \tag{2.4.1}$$

Based on Eq.(2.2.6), the pressure difference equation can be given as

$$\frac{p - p_\infty}{\rho_\infty} = -\delta\left(\frac{\partial \varphi}{\partial t} + \frac{1}{2}V^2\right) = \frac{1}{2}\left(V^2 - U_\infty^2\right) + \frac{\partial \varphi}{\partial t} \approx U_\infty u + \frac{\partial \varphi}{\partial t}. \tag{2.4.2}$$

As a result, the pressure coefficient equation for unsteady case becomes

$$Cp = -\frac{2}{U_\infty^2}\left(U_\infty \frac{\partial \varphi}{\partial x_1} + \frac{\partial \varphi}{\partial t}\right) = -2e^{i(\omega t + kx_1)}\left[\frac{\partial \Phi}{\partial x_1} + i(\lambda + k)\Phi\right] = -2e^{i(\omega t + kx_1)}\left[\frac{\partial \Phi}{\partial x_1} - \frac{i\lambda}{B^2}\Phi\right]. \tag{2.4.3}$$

Taking account of the total reduced velocity potential of the second order, $\Phi = \Phi_1' + i\lambda(\Phi_1'' + \Phi_2'')$,

$$Cp = -2e^{i\omega t}\left[\frac{\partial \Phi'}{\partial x_1} - \frac{i\lambda}{B^2}\left(\Phi' - B^2\frac{\partial \Phi''}{\partial x_1} + M_\infty^2 x_1 \frac{\partial \Phi'}{\partial x_1}\right)\right]$$

$$= -2e^{i\omega t}\left[\frac{\partial \Phi_1'}{\partial x_1} - \frac{i\lambda}{B^2}\left(\Phi_1' - B^2\frac{\partial(\Phi_1'' + \Phi_2'')}{\partial x_1} + M_\infty^2 x_1 \frac{\partial \Phi_1'}{\partial x_1}\right)\right]. \tag{2.4.4}$$

For steady flow, we have

$$Cp = -\frac{2}{U_\infty}\frac{\partial \varphi}{\partial x_1} = -2\frac{u}{U_\infty}. \tag{2.4.5}$$

The lift coefficient, pitching moment coefficient, and the rolling moment coefficient are calculated by integrating the pressure coefficient equation, Eq.(2.4.4) and (2.4.5), over the wing area. As far as the thin wing plan form is concerned, the pressure difference across the wing profile in dimensionless form as

$$\Delta Cp = Cp_l - Cp_u = -2Cp. \tag{2.4.6}$$

Thus, the dimensionless lift coefficient ($C_l$), pitching moment coefficient ($C_{m2}$), and rolling moment coefficient ($C_{m1}$) equations are defined as

$$C_l = \frac{-2}{S}\int_S CpdA = \frac{-2}{S}\int_S Cpx_1 dx_1 dy\,. \tag{2.4.7}$$

$$C_{m2} = \frac{-2}{Sc_0}\int_S x_1 CpdA = \frac{-2}{Sc_0}\int_S Cpx_1^2 dx_1 dy\,. \tag{2.4.8}$$

$$C_{m1} = \frac{-2}{S(2b)}\int_S x_2 CpdA = \frac{-2}{S(2b)}\int_S Cpx_1^2 y dx_1 dy\,. \tag{2.4.9}$$

We consider an element $dA$ of the wing on both surfaces as $dA = dx_1 dx_2 = x_1 dx_1 dy$ and generally denote by $S$ the total delta wing surface area or half of the total trapezoidal wing surface area, $c_0$ the root chord, and $2b$ the total wing span at $x_1 = 1.0$.

# CHAPTER 3

# PREVIOUS STUDIES – ANALYTICAL METHOD BASED ON THEORY OF CONICAL FLOWS AND SOLUTIONS TO STEADY AND UNSTEADY FLOWS PAST SUPERSONIC WINGS

## 3.1 Compatibility relation of conical motions in supersonic flows

The perturbation velocity, **q**, can be expressed as the gradient of the perturbation velocity potential $\varphi$.

$$\mathbf{q} = u\mathbf{i} + v\mathbf{j} + w\mathbf{k} = \nabla\varphi, \tag{3.1.1}$$

where $q_1 = \frac{\partial\varphi}{\partial x_1} = u$, $q_2 = \frac{\partial\varphi}{\partial x_2} = v$, and $q_3 = \frac{\partial\varphi}{\partial x_3} = w$.

Accordingly, the perturbation velocity potential in steady case can be recast as

$$-B^2\frac{\partial u}{\partial x_1} + \frac{\partial v}{\partial x_2} + \frac{\partial w}{\partial x_3} = 0. \tag{3.1.2}$$

Then, differentiating Eq.(3.1.2) above with respect to $x_1$, $x_2$, and $x_3$, one has

$$-B^2\frac{\partial q_k}{\partial x_1^2} + \frac{\partial q_k}{\partial x_2^2} + \frac{\partial q_k}{\partial x_3^2} = 0, \tag{3.1.3}$$

where $q_k = \frac{\partial\varphi}{\partial x_k}$, $k = 1, 2, 3$.

Based on the theory of conical motions and the assumption of small disturbances, developed by Busemann in 1935, the non-dimensional coordinates are given as $y=\frac{x_2}{x_1}$ and $z=\frac{x_3}{x_1}$. In general, we can denote $q_k$ as function of $y$ and $z$ and thus Eq.(3.1.3) can be recast by y and z.

$$\left(1-B^2y^2\right)\frac{\partial^2 q_k}{\partial y^2}+\left(1-B^2z^2\right)\frac{\partial^2 q_k}{\partial z^2}-2B^2yz\frac{\partial^2 q_k}{\partial y\partial z}-2B^2y\frac{\partial q_k}{\partial y}-2B^2z\frac{\partial q_k}{\partial z}=0. \qquad (3.1.4)$$

Let's consider the Busemann geometrical transformation as

$$\mathrm{y}^* = \mathcal{y}=\frac{y}{1-B^2z^2} \text{ and } z^* =\mathcal{z}=\frac{z}{1-B^2z^2}\sqrt{1-B^2\left(y^2+z^2\right)}, \qquad (3.1.5)$$

and thus Eq.(3.1.4) can be recast in the form of Laplace equation; i.e., $q_k$ becomes harmonic function in Busemann's auxiliary plane ($\mathcal{y}$, $\mathcal{z}$) (Fig. 3.1), and can be related to its corresponding harmonic functions, denoted as $q_k'$. As a result, and complex variable, $x$, in Busemann's auxiliary plan is defined as

$$x=\mathcal{y}+\mathrm{i}\mathcal{z}. \qquad (3.1.6)$$

And the harmonic functions in terms of the complex variable, $x$, can be expressed as

$$\frac{\partial^2 q_k}{\partial y^{*2}}+\frac{\partial^2 q_k}{\partial z^{*2}}=0, \qquad (3.1.7)$$

where $q_k=\frac{\partial\varphi}{\partial x_k}$, $k=1, 2, 3$.

The perturbation velocities can be expressed as the real part of the associated analytical complex functions and are shown as

$$\begin{aligned} &u(\mathcal{y},\ \mathcal{z}) = \mathrm{Re}[\mathcal{U}(x)],\ \mathcal{U}(x) = u(\mathcal{y},\ \mathcal{z}) + \mathrm{i}\, u'(\mathcal{y},\ \mathcal{z}),\\ &v(\mathcal{y},\ \mathcal{z}) = \mathrm{Re}[\mathcal{V}(x)],\ \mathcal{V}(x) = v(\mathcal{y},\ \mathcal{z}) + \mathrm{i}\, v'(\mathcal{y},\ \mathcal{z}), \qquad (3.1.8)\\ &w(\mathcal{y},\ \mathcal{z}) = \mathrm{Re}[\mathcal{W}(x)],\ \mathcal{W}(x) = w(\mathcal{y},\ \mathcal{z}) + \mathrm{i}\, w'(\mathcal{y},\ \mathcal{z}). \end{aligned}$$

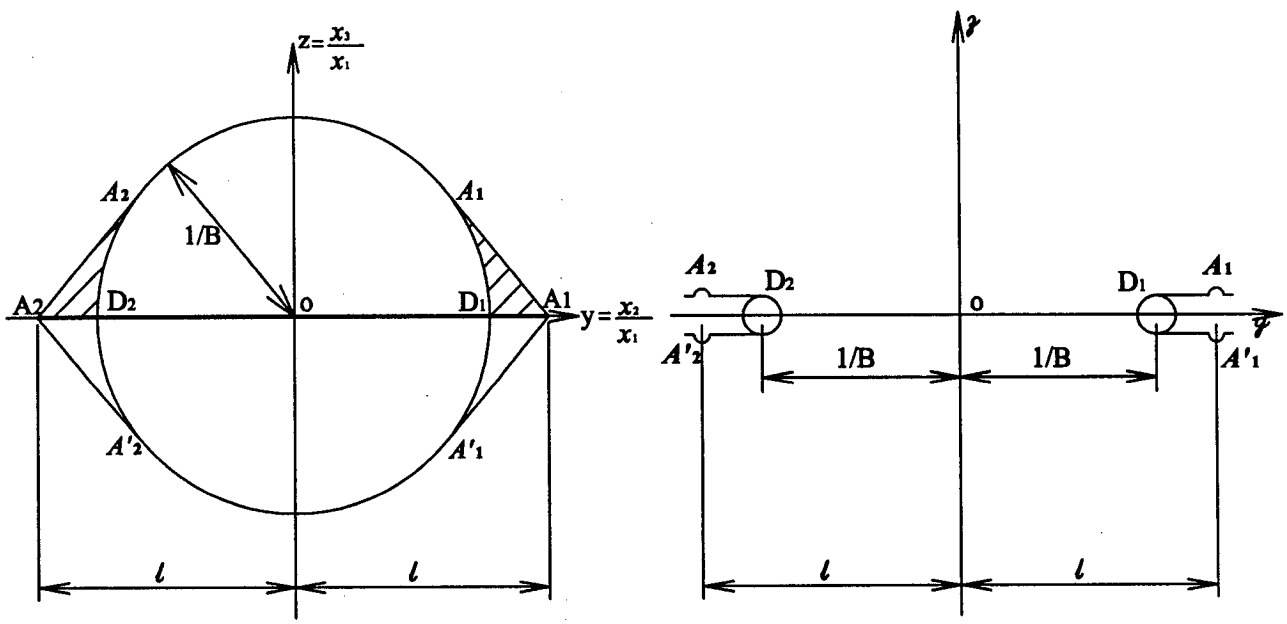


Figure 3.1 Conformal transformation of wing geometry with supersonic edges

Additionally, the curl of the velocity field is zero ($\nabla \times \mathbf{q} = 0$) and we have

$$\frac{\partial u}{\partial x_2} = \frac{\partial v}{\partial x_1}, \frac{\partial v}{\partial x_3} = \frac{\partial w}{\partial x_2}, \text{ and } \frac{\partial w}{\partial x_1} = \frac{\partial u}{\partial x_3}. \tag{3.1.9}$$

Similarly, by taking account of the Busemann geometrical transformation, the irrotationality conditions can be expressed in complex form as

$$\mathrm{d}\mathscr{U} = -x\,\mathrm{d}\mathscr{V} = \frac{ix}{\sqrt{1-B^2x^2}}\,\mathrm{d}\mathscr{W}. \tag{3.1.10}$$

This is the compatibility relation in the study of conical flow motions.

## 3.2 Compatibility relation of high order conical motions in supersonic flows

Conical flow motion of order $n$ with respect to the vertex O, is the flow for which the disturbance velocity potential $\varphi(x_1, x_2, x_3)$ is an $n$-th order homogeneous function with respect to $x_1$, $x_2$, and $x_3$. It follows that the $n$-th order derivatives of the velocity potential are constants on any radius vector issuing from vertex O, whence they are zero order homogeneous functions in this manner; e.g., the true conical flow is defined by $n = 1$. Accordingly, let's denote $\varphi_{p,q,r}$ by the derivative of the disturbance velocity potential of order $p$ with respect to $x_1$, or order $q$ with respect to $x_2$, and of order $r$ with respect to $x_3$. Explicitly, it is shown as

$$\varphi_{p,q,r} = \frac{\partial^{p+q+r}\varphi}{\partial x_1^p \partial x_2^q \partial x_3^r}. \tag{3.2.1}$$

If we consider $n$ is equal to $p + q + r$, $\varphi_{p,q,r} = \varphi_{n-q-r,q,r}$ is homogeneous function of zero order, which plays the same part as the perturbation velocity $u$, $v$, and $w$ in the true conical flow motion ($n = 1$), since the perturbation velocity $u$, $v$, and $w$ are also zero order homogeneous functions. In other word, $\varphi_{n-q-r,q,r}$ can be expressed as harmonic function in Busemann's auxiliary plane $(\psi,\zeta)$ and the corresponding conjugate harmonic function can be denote by $\varphi'_{n-q-r,q,r}$. Therefore, let's denote $\mathcal{F}_{n\text{-}q\text{-}r,q,r}$ as the analytical function in terms of the complex variable $x$ and we have

$$\mathcal{F}_{n\text{-}q\text{-}r,q,r} = \varphi_{n-q-r,q,r} + i\,\varphi'_{n-q-r,q,r}. \tag{3.2.2}$$

In turn, we consider ($n$-1) order derivatives of the function $\varphi$ with respect to $x_1$, $x_2$, and $x_3$, respectively. Here we choose $\varphi_{n-1,0,0}$ as example and its corresponding disturbance velocities are zero order homogeneous functions.

$$u_n = \frac{\partial \varphi_{n-1,0,0}}{\partial x_1} = \varphi_{n,0,0},\ v_n = \frac{\partial \varphi_{n-1,0,0}}{\partial x_2} = \varphi_{n-1,1,0},\ w_n = \frac{\partial \varphi_{n-1,0,0}}{\partial x_3} = \varphi_{n-1,0,1}. \tag{3.2.3}$$

These zero order homogeneous functions are the disturbance velocities $u$, $v$, $w$ of a true conical flow motions ($n = 1$), which represent the real part of the analytical functions $\mathcal{U},\mathcal{V},\mathcal{W}$. Namely, $u_n$, $v_n$, and $w_n$ represent the real parts of analytical functions $\mathcal{F}_{n,0,0}$, $\mathcal{F}_{n-1,1,0}$, and $\mathcal{F}_{n-1,0,1}$, replacing the analytical functions $\mathcal{U},\mathcal{V}$,and $\mathcal{W}$, respectively for unified mathematical expressions in the assumption of high order conical flows. The compatibility relation, Eq.(3.1.10), can also be recast in terms of analytical functions for cases in high order conical flow motions in the form as

$$d\mathcal{F}_{n,0,0} = -x\, d\mathcal{F}_{n-1,1,0} = \frac{ix}{\sqrt{1-B^2x^2}}\, d\mathcal{F}_{n-1,0,1}. \tag{3.2.4}$$

According to Eq.(3.2.4), we first consider the first two left hand side terms with successive sequential functions as

$$d\mathcal{F}_{n,0,0} = (-x)^q\, d\mathcal{F}_{n-q,q,0} = (-x)^{q-1}\, d\mathcal{F}_{n-q+1,q-1,0} = \cdots \tag{3.2.5}$$

Similarly, by considering the first and the third terms of Eq.(3.2.4), we obtain

$$d\mathcal{F}_{n,0,0} = \left(\frac{ix}{\sqrt{1-B^2x^2}}\right)^r d\,\mathcal{F}_{n-r,0,r} = \left(\frac{ix}{\sqrt{1-B^2x^2}}\right)^{r-1} d\mathcal{F}_{n-r+1,0,r-1} = \cdots \tag{3.2.6}$$

As well, relations between $\mathcal{F}_{n-q,q,0}$ in Eq.(3.2.6) and $\mathcal{F}_{n-r,0,r}$ in Eq.(3.2.5) can be obtained as

$$d\mathcal{F}_{n-q,q,0} = \left(\frac{ix}{\sqrt{1-B^2x^2}}\right)^r d\mathcal{F}_{n-q-r,q,r}, \tag{3.2.7}$$

$$d\mathcal{F}_{n-r,0,r} = (-x)^q\, d\mathcal{F}_{n-q-r,q,r}. \tag{3.2.8}$$

Substituting Eq.(3.2.7) into (3.2.5) and Eq.(3.2.8) into (3.2.6) leads to the general compatibility relation shown as

$$d\mathcal{F}_{n,0,0} = (-x)^q\left(\frac{ix}{\sqrt{1-B^2x^2}}\right)^r d\,\mathcal{F}_{n-q-r,q,r}, \tag{3.2.9}$$

which is valid if and only if $0 \le q+r \le n$.

## 3.3 High order conical flow solutions of fixed wings placing in steady supersonic flows

In the first place, a thin wing surface can generally be defined in the form as a superposition of homogeneous polynomials in $x_1$ and $x_2$, so as the perturbation downwash, $w$, expressed by the homogeneous polynomials of order ($n$-1).

$$w = \sum_{q=0}^{n-1} w_{n-q-1,q} x_1^{n-q-1} x_2^q = x_1^{n-1} \sum_{q=0}^{n-1} w_{n-q-1,q} y^q , \tag{3.3.1}$$

where $x = \mathcal{y} = y = \dfrac{x_2}{x_1}$, for $x_3$ is equal to zero.

On the other hand, the perturbation downwash, $w$, can be carried out by the compatibility relation known as Eq.(3.2.4) in terms of the real part of the analytical function $\mathscr{U}_{n-1}$.

$$u^{(n-1)} = x_1^{n-1} u_{n-1} = \mathrm{Re}[\, x_1^{n-1} \mathscr{U}_{n-1}]. \tag{3.3.2}$$

The analytical function of perturbation axial velocity, $\mathscr{U}$, is presented with respect to several wing models of interest in this study; e.g., steady thin delta wing with supersonic leading edges with (a) symmetry of incidence, $\alpha = -w_{10} x_1 / U_\infty$ , (b) antisymmetry of incidence, $\alpha = -w_{10} x_1 / U_\infty$, and the thin trapezoidal wing placing in incidence, $\alpha = -w_{10} x_1 / U_\infty$, with supersonic leading edges without the intersection of Mach lines from both sides.

### 3.3.1 High order conical flow solutions to thin delta wing with supersonic leading edges and symmetry of incidence

The analytical function corresponding to the disturbance axial velocity, $u$, can be expressed by theory of high order conical flows of order 1 and 2 and shown as

$$\mathscr{U}_{n-1} = \sum_{q=o}^{n-1} K_{n,q} x^q \left[ \cos^{-1} \sqrt{\frac{(1+Bl)(1-Bx)}{2B(l-x)}} + (-1)^q \cos^{-1} \sqrt{\frac{(1+Bl)(1+Bx)}{2B(l+x)}} \right] + \sum_{q=0}^{E\left(\frac{n-2}{2}\right)} D_{n,2q} x^{2q} \sqrt{\frac{1-B^2x^2}{B^2}}, \tag{3.3.3}$$

where $E(t)$ represents the greatest integer which does not exceed t. Following are the constants in the above equation, which are calculated in terms of the coefficients of the downwashes, Eq.(3.3.1).

$$K_{10} = -\frac{2w_{00}}{\pi B}\frac{Bl}{\sqrt{B^2l^2-1}}; \text{ for } n = 1. \tag{3.3.4}$$

And for $n = 2$, we have

$$K_{20} = -\frac{2}{\pi\left(B^2l^2-1\right)^{3/2}}\left[\left(B^2l^2-2\right)w_{10} - lw_{01}\right], \tag{3.3.5}$$

$$K_{21} = -\frac{2}{\pi\left(B^2l^2-1\right)^{3/2}}\left[w_{10} - B^2l^3w_{01}\right], \tag{3.3.6}$$

$$D_{20} = -\frac{2Bl}{\pi\left(B^2l^2-1\right)}\left[w_{10} + lw_{01}\right]. \tag{3.3.7}$$

By Eq.(2.4.5), the pressure coefficient of $n$-th order conical flows can be calculated by taking the real part of $\mathscr{U}_{n-1}$, which is equal to $u_{n-1}$.

$$Cp^{(n)} = -2\frac{u^{(n-1)}}{U_\infty} = -2x_1^{n-1}\frac{u_{n-1}}{U_\infty}. \tag{3.3.8}$$

Accordingly, the total pressure coefficient of the complex wing with multiple components can be expressed as

$$Cp = -2\frac{u}{U_\infty} = -2\sum_{n=1}^{N} x_1^{n-1}\frac{u_{n-1}}{U_\infty} = \sum_{n=1}^{N} Cp^{(n)} \tag{3.3.9}$$

As well, calculation of the lift coefficient and the pitching moment coefficient can be performed by integrating $Cp^{(n)}$ in Eq.(2.4.7) and (2.4.8), respectively.

$$C_l^{(n)} = \frac{-2}{S}\int_S Cp^{(n)}x_1\,dx_1\,dy = \frac{4}{(n+1)SU_\infty}\int_l u_{n-1}\,dy \tag{3.3.10}$$

$$C_{m2}^{(n)} = \frac{-2}{S}\int_S Cp^{(n)}x_1^2\,dx_1\,dy = \frac{4}{(n+2)SU_\infty}\int_l u_{n-1}\,dy = \frac{n+1}{n+2}C_l^{(n)} \tag{3.3.11}$$

Explicitly, for n = 1 and 2,

$$C_l^{(1)} = \frac{2\pi}{U_\infty}\frac{\sqrt{B^2l^2-1}}{Bl}K_{10} \tag{3.3.12}$$

$$C_l^{(2)} = \frac{4\pi}{3BlU_\infty}\left[\sqrt{B^2l^2-1}\left(K_{20}+\frac{l}{2}K_{21}\right)+\frac{1}{2B}D_{20}\right] \tag{3.3.13}$$

The pitching moment coefficients for n = 1 and 2 are

$$C_{m2}^{(1)} = \frac{2}{3}C_l^{(1)} \tag{3.3.14}$$

$$C_{m2}^{(2)} = \frac{3}{4}C_l^{(2)} \tag{3.3.15}$$

### 3.3.2 High order conical flow solutions to thin delta wing with supersonic leading edges and antisymmetry of incidence

The analytical function corresponding to the disturbance axial velocity, $u$, can be expressed by theory of high order conical flows of order 1 and 2 and shown as

$$\mathcal{U}_{n-1} = \sum_{q=o}^{n-1} K_{n,q}x^q\left[\cos^{-1}\sqrt{\frac{(1+Bl)(1-Bx)}{2B(l-x)}} - (-1)^q\cos^{-1}\sqrt{\frac{(1+Bl)(1+Bx)}{2B(l+x)}}\right] + \sum_{q=0}^{E\left(\frac{n-3}{2}\right)} D_{n,2q+1}x^{2q+1}\sqrt{\frac{1-B^2x^2}{B^2}}$$
$$+ \sum_{q=0}^{E\left(\frac{n-2}{2}\right)} Q_{n,2q+1}x^{2q+1}\cosh^{-1}\sqrt{\frac{1}{B^2x^2}}, \tag{3.3.16}$$

where $E(t)$ represents the greatest integer which does not exceed t. The constants, $K_{n,q}$ have the same values as indicated in Eq.(3.3.4) ~ (3.3.6), while the remaining for order $n = 2$ is

$$Q_{21} = -\frac{2w_{10}}{\pi}. \tag{3.3.17}$$

Accordingly, Eq.(3.3.8) can be applied for the calculation of $n$-th order pressure coefficient, $Cp^{(n)}$. The rolling moment coefficients, $C_{m1}^{(n)}$, can be expressed by integrating $Cp^{(n)}$ in Eq.(2.4.9) and we have

$$C_{m1}^{(n)} = \frac{-2}{S(2b)}\int_S Cp^{(n)}x_1^2\,ydx_1dy = \frac{4}{(n+2)SU_\infty(2b)}\int_l^t u_{n-1}ydy. \tag{3.3.18}$$

Explicitly, for n = 1 and 2, we have

$$C_{m1}^{(1)} = \frac{2\pi}{3BU_\infty}\sqrt{B^2l^2-1}K_{10}, \tag{3.3.19}$$

$$C_{m1}^{(1)} = \frac{\pi}{2BU_\infty}\left[\sqrt{B^2l^2-1}\left(K_{20}+\frac{2B^2l^2+1}{3B^2l^2}lK_{21}\right)+\frac{l}{3B^2l^2}Q_{21}\right]. \tag{3.3.20}$$

### 3.3.3 High order conical flow solutions to trapezoidal thin wing with supersonic leading edges

For thin trapezoidal wing with supersonic leading edges and symmetric in respect of axis $OX_1$, the general expression for the analytical function of disturbance axial velocity for order of 1 and 2 is

$$\mathscr{U}_{n-1} = \sum_{q=0}^{n-1}\left(K_{n,q}x^q\cos^{-1}\sqrt{\frac{(1+Bl)(1-Bx)}{2B(l-x)}}+H_{n,q}x^q\cos^{-1}\sqrt{\frac{1+Bx}{2}}\right)+\sum_{q=0}^{n-2}D_{n,q}x^q\sqrt{\frac{1-B^2x^2}{B^2}}. \tag{3.3.21}$$

Following are the constants in the above equation, which are calculated in terms of the coefficients of the downwashes, Eq.(3.3.1).

For n = 1,

$$K_{10} = -\frac{2w_{00}}{\pi B}\frac{Bl}{\sqrt{B^2l^2-1}},\quad H_{10} = -\frac{2w_{00}}{\pi B}. \tag{3.3.22}$$

For n = 2,

$$K_{20} = \frac{2l}{\pi\left(B^2l^2-1\right)^{3/2}}\left[\left(2-B^2l^2\right)w_{10}+lw_{01}\right], \tag{3.3.23}$$

$$K_{21} = -\frac{2}{\pi\left(B^2l^2-1\right)^{3/2}}\left[w_{10}+B^2l^3w_{01}\right], \tag{3.3.24}$$

$$H_{20} = -\frac{2w_{10}}{\pi B},\quad H_{21} = -\frac{2w_{01}}{\pi B}, \tag{3.3.25}$$

$$D_{20} = -\frac{w_{01}+Bl\cdot Bw_{10}}{\pi B\left(B^2l^2-1\right)}. \tag{3.3.26}$$

Applying formulae (3.3.21) and (3.3.8), the pressure coefficients of $n$-th order conical flow can be calculated. In turn, based on Eq.(2.4.7) ~ (2.4.9), calculations of the lift coefficient and the pitching moment coefficient need to be based on the calculation of the integration of the pressure coefficients over half of the symmetric trapezoidal wing, which can be divided into four portions: (a) $\widetilde{S}_0$ and $S_0$, the left hand side of surface, outside the Mach cone, (b) $S_i$, the wing surface covered by the Mach cone, and (c) $S_1$, the right hand side of surface, also outside the Mach cone (Fig. 3.2).

$$\int_S = \int_{\widetilde{S}_0} + \int_{S_0} + \int_{S_i} + \int_{S_1} \tag{3.3.27}$$

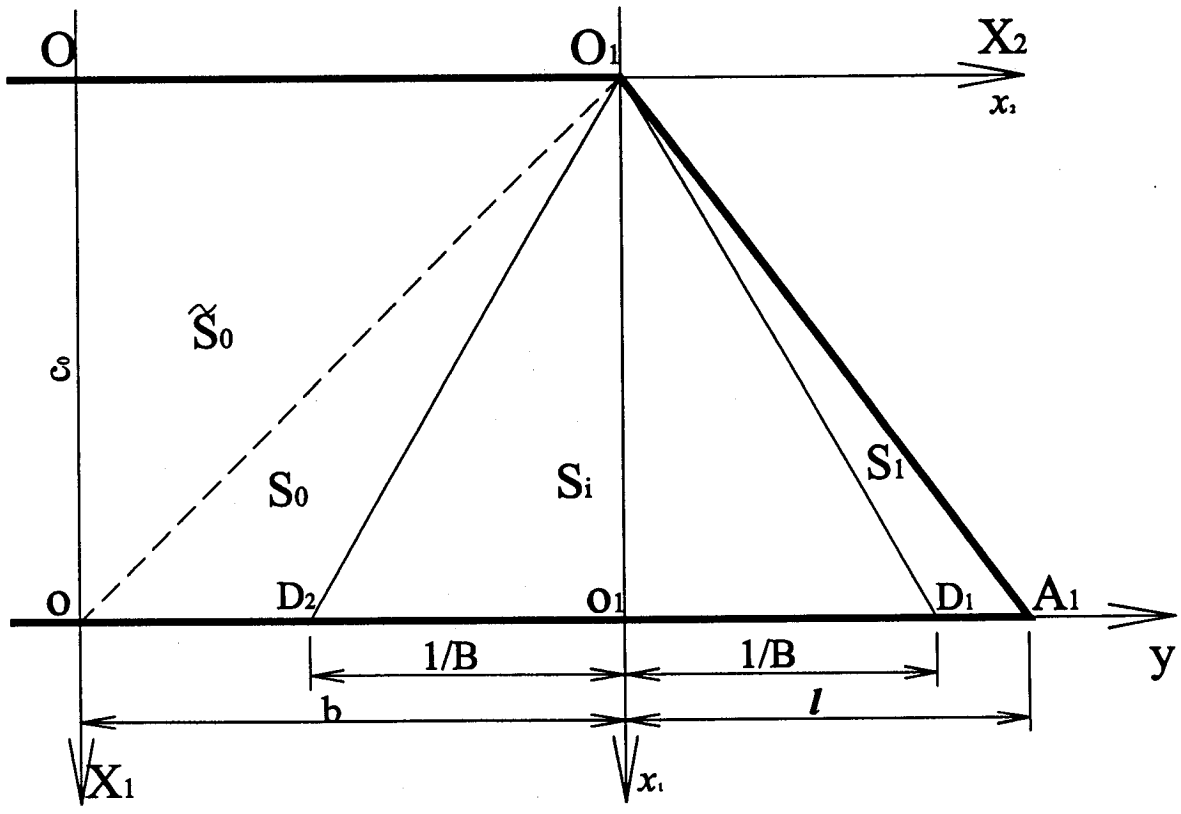


Figure 3.2 The separation of half trapezoidal thin wing surface into $\widetilde{S}_0$, $S_0$, $S_i$, and $S_1$.

On wing portions, $\widetilde{S}_0$, $S_0$, and $S_1$, the velocity $u$ and $w$ are expressed by homogeneous polynomials in terms of $x_1$ and $x_2$ and thus we have $E_{pr}x_1^{p-1}x_2^{r-1}$, where $E_{pr}$ is a constant. This term can be seen as the expression of the aerodynamic characteristics acting on any point on the elementary surface $dx_1dx_2 = x_1dx_1dy$. As a consequence, the integration over each portion of wing surface can be performed separately as follows.

(a) For integral domain, $\widetilde{S}_0$ and $S_0$,

$$\int_{\widetilde{S}_0} E_{pr}x_1^{p-1}x_2^{r-1}dx_1dx_1 + \int_{S_0} E_{pr}x_1^{p-1}x_2^{r-1}dx_1dx_1 = E_{pr}\left( \int_{\frac{b}{x_1}}^{b} x_1^{p+r-1}\int_0^1 ydx_1dy + \int_b^{\frac{1}{B}}\int_0^1 x_1^{p+r-1}y^{r-1}dx_1dy \right)$$

$$= -\frac{(-1)^r}{r}\left[\frac{b^r}{p} - \frac{1}{(p+r)B^r}\right]E_{pr}. \qquad (3.3.28)$$

(b) For integral domain, $S_1$,

$$\int_{S_1} E_{pr}x_1^{p-1}x_2^{r-1}dx_1dx_1 = E_{pr}\left( \int_{\frac{1}{B}}^{l}\int_0^1 x_1^{p+r-1}y^{r-1}dx_1dy \right) = \frac{1}{(p+r)r}\left[l^r - \left(\frac{1}{B}\right)^r\right]E_{pr}. \qquad (3.3.29)$$

(c) For integral domain, $S_i$, we apply Eq.(3.3.19) to the equations for calculation of those specific aerodynamic characteristics of which the integration limits are from $-\frac{1}{B}$ to $\frac{1}{B}$.

As a consequence, the lift coefficient and pitching moment coefficient of conical flows for order of 1 and 2 are presented as follows.

$$C_l^{(1)} = \frac{2\pi}{B(2b+l)U_\infty}\left(K_{10}\sqrt{B^2l^2-1} + 2BbH_{10}\right) \qquad (3.3.30)$$

$$C_l^{(2)} = \frac{\pi}{3B^2(2b+l)U_\infty}\left[2B\sqrt{B^2l^2-1}(2K_{20}+lK_{21}) + 4D_{20} + 6B^2bH_{20} + (1-6B^2b^2)H_{21}\right] \qquad (3.3.31)$$

$$C_{m2}^{(1)} = \frac{2\pi}{3B(2b+l)U_\infty}\left(2K_{10}\sqrt{B^2l^2-1} + 3BbH_{10}\right) \qquad (3.3.32)$$

$$C_{m2}^{(2)} = \frac{\pi}{12B^2(2b+l)U_\infty}\left[6B\sqrt{B^2l^2-1}(2K_{20}+lK_{21}) + 12D_{20} + 16B^2bH_{20} + 3(1-4B^2b^2)H_{21}\right] \qquad (3.3.33)$$

## 3.4 High order conical flow solutions to wings executing unsteady motions in supersonic flows

According to Eq.(2.4.4), the pressure coefficient of wings executing unsteady motions linearized by theory of high order conical flows is recalled as

$$Cp = -2e^{i\omega t}\left[\frac{\partial \Phi'}{\partial x_1} - \frac{i\lambda}{B^2}\left(\Phi' - B^2\frac{\partial \Phi''}{\partial x_1} + M_\infty^2 x_1 \frac{\partial \Phi'}{\partial x_1}\right)\right]$$

$$= -2e^{i\omega t}\left[\frac{\partial \Phi_1'}{\partial x_1} - \frac{i\lambda}{B^2}\left(\Phi_1' - B^2\frac{\partial(\Phi_1'' + \Phi_2'')}{\partial x_1} + M_\infty^2 x_1 \frac{\partial \Phi_1'}{\partial x_1}\right)\right], \tag{3.4.1}$$

where $\Phi = \Phi' + i\lambda\Phi'' = \Phi_1' + i\lambda(\Phi_1'' + \Phi_2'')$.

It follows that the calculation of the pressure coefficient in unsteady cases consists of calculations of the reduced velocity potential and the perturbation axial velocity.

$$u = \frac{\partial \Phi}{\partial x_1} = \frac{\partial \Phi'}{\partial x_1} + i\lambda\frac{\partial \Phi''}{\partial x_1} = \sum_{n=1}^{N}\frac{\partial \Phi_n'}{\partial x_1} + i\lambda\sum_{n=0}^{N}\frac{\partial \Phi_{n+1}''}{\partial x_1}, \tag{3.4.2}$$

$$\frac{\partial \Phi_n'}{\partial x_1} = x_1^{n-1}u_{n-1}' = x_1^{n-1}\mathrm{Re}[\mathscr{U}'_{n-1}], \tag{3.4.3}$$

$$\frac{\partial \Phi_{n+1}''}{\partial x_1} = x_1^n u_n'' = x_1^n \mathrm{Re}[\mathscr{U}''_n]. \tag{3.4.4}$$

Namely, for case when $n = 1$,

$$u = \frac{\partial \Phi_1'}{\partial x_1} + i\lambda\left(\frac{\partial \Phi_1''}{\partial x_1} + \frac{\partial \Phi_2''}{\partial x_1}\right), \tag{3.4.5}$$

$$\frac{\partial \Phi_1'}{\partial x_1} = u_0' = \mathrm{Re}[\mathscr{U}'_0], \tag{3.4.6}$$

$$\frac{\partial \Phi_1''}{\partial x_1} + \frac{\partial \Phi_2''}{\partial x_1} = u_0'' + x_1 u_1'' = \mathrm{Re}[\mathscr{U}''_0] + \mathrm{x_1Re}[\mathscr{U}''_1]. \tag{3.4.7}$$

Additionally, $\Phi_1'$ can be express as

$$\Phi_1' = x_1u_0' + x_2v_0' = x_1(u_0' + yv_0') = \mathrm{Re}[x_1 x\int \mathscr{U}'_0 d\left(\frac{1}{x}\right)]. \tag{3.4.8}$$

By substituting Eq.(3.4.6) ~ (3.6.8) into (3.4.1), the reduced pressure coefficient can be recast as

$$\hat{C}p = -2\left[u_0' - \frac{i\lambda}{B^2}\left(\Phi_1' - B^2\left(u_0'' + x_1 u_1''\right) + M_\infty^2 x_1 u_0'\right)\right]. \tag{3.4.9}$$

### 3.4.1 Calculation of the reduced pressure coefficient for thin delta wing

For thin delta wing with supersonic leading edges, $u_0'$, $u_0''$, and $u_1''$ are calculated by substituting $w_{00}'$ in Eq.(3.3.4), $w_{00}''$ in Eq.(3.3.4), and $w_{10}''$ and $w_{01}''$ in Eq.(3.3.5) ~ (3.3.7), where $w_{00}'$, $w_{00}''$, $w_{10}''$ and $w_{01}''$ have been delivered in Eq.(2.3.14) ~ (2.3.17), respectively.

$$\mathscr{U}'_0 = \frac{2}{\pi}\frac{\hat{\theta}l}{\sqrt{B^2l^2-1}}\left[\cos^{-1}\sqrt{\frac{(1+Bl)(1-Bx)}{2B(l-x)}} + \cos^{-1}\sqrt{\frac{(1+Bl)(1+Bx)}{2B(l+x)}}\right], \tag{3.4.10}$$

$$\mathscr{U}''_0 = -\frac{2}{\pi}\frac{\hat{h}l}{\sqrt{B^2l^2-1}}\left[\cos^{-1}\sqrt{\frac{(1+Bl)(1-Bx)}{2B(l-x)}} + \cos^{-1}\sqrt{\frac{(1+Bl)(1+Bx)}{2B(l+x)}}\right], \tag{3.4.11}$$

$$\begin{aligned}\mathscr{U}''_1 = {} & \frac{2}{\pi}\frac{1}{\left(B^2l^2-1\right)^{3/2}}\left[\hat{\theta}\frac{2B^2+1}{B^2}\left(l\left(B^2l^2-2\right)+x\right)+\hat{\psi}l^2\left(1-B^2lx\right)\right]\cos^{-1}\sqrt{\frac{(1+Bl)(1-Bx)}{2B(l-x)}} \\ & + \frac{2}{\pi}\frac{1}{\left(B^2l^2-1\right)^{3/2}}\left[\hat{\theta}\frac{2B^2+1}{B^2}\left(l\left(B^2l^2-2\right)-x\right)-\hat{\psi}l^2\left(1+B^2lx\right)\right]\cos^{-1}\sqrt{\frac{(1+Bl)(1+Bx)}{2B(l+x)}} \\ & + \frac{2}{\pi}\frac{Bl}{\left(B^2l^2-1\right)}\hat{\theta}\frac{2B^2+1}{B^2}\sqrt{\frac{1-B^2x^2}{B^2}},\end{aligned} \tag{3.4.12}$$

$$\Phi_1' = x_1\frac{2\hat{\theta}}{\pi\sqrt{B^2l^2-1}}\left[(l-x)\cos^{-1}\sqrt{\frac{(1+Bl)(1-Bx)}{2B(l-x)}} + (l+y)\cos^{-1}\sqrt{\frac{(1+Bl)(1+Bx)}{2B(l+x)}}\right]. \tag{3.4.13}$$

Accordingly, the general equation of $\hat{C}p$ can be calculated in terms of the real part of $\mathscr{U}'_0$, $\mathscr{U}''_0$, $\mathscr{U}''_1$, and $\Phi'_1$.

$$\hat{C}p = -\frac{4l}{\pi\sqrt{B^2l^2-1}}\left\{(\theta_0 - i\lambda h_0)\left[\cos^{-1}\sqrt{\frac{(1+Bl)(1-Bx)}{2B(l-x)}} + \cos^{-1}\sqrt{\frac{(1+Bl)(1+Bx)}{2B(l+x)}}\right]\right.$$

$$-i\lambda x_1\left[\left(\theta_0\frac{3+l^2-B^2l^2-(2+l^2)x/l}{B^2l^2-1} - \psi_0 l\frac{1-B^2lx}{B^2l^2-1}\right)\cos^{-1}\sqrt{\frac{(1+Bl)(1-Bx)}{2B(l-x)}}\right.$$

$$+\left(\theta_0\frac{3+l^2-B^2l^2+(2+l^2)x/l}{B^2l^2-1} + \psi_0 l\frac{1+B^2lx}{B^2l^2-1}\right)\cos^{-1}\sqrt{\frac{(1+Bl)(1+Bx)}{2B(l+x)}}$$

$$\left.\left.-\theta_0\frac{2B^2+1}{B^2}\frac{\sqrt{1-B^2x^2}}{\sqrt{B^2l^2-1}}\right]\right\}. \qquad (3.4.14)$$

For the reduced lift coefficient, we apply the similar formulae from the steady conical motions and obtain respectively.

$$\hat{C}_l = \frac{4}{B}\left[\theta_0 + i\lambda\left(\theta_0\frac{2B^2-1}{3B^2} - h_0\right)\right]. \qquad (3.4.15)$$

For the reduced pitching and rolling moment coefficients, we have

$$\hat{C}_{m2} = \frac{1}{B}\left[\frac{8}{3}\theta_0 + i\lambda\left(\theta_0\frac{2B^2-1}{B^2} - \frac{8}{3}h_0\right)\right], \qquad (3.4.16)$$

$$\hat{C}_{m1} = i\lambda\frac{2l^2}{3B}\psi_0. \qquad (3.4.17)$$

### 3.4.2 Calculation of the reduced pressure coefficient for thin trapezoidal wing

For case of thin trapezoidal wing with supersonic leading edges, $u'_0$, $u''_0$, and $u''_1$ are calculated by substituting $w'_{00}$ in Eq.(3.3.22), $w''_{00}$ in Eq.(3.3.22), and $w''_{10}$ and $w''_{01}$ in Eq.(3.3.23) ~ (3.3.26), where $w'_{00}$, $w''_{00}$, $w''_{10}$ and $w''_{01}$ have been carried out in Eq.(2.3.14) ~ (2.3.17), respectively. Explicitly, the real parts of $\mathscr{U}'_0$, $\mathscr{U}''_0$, $\mathscr{U}''_1$, and $\Phi'_1$ calculating as follows are devoted to calculating the reduce pressure coefficient for thin trapezoidal wing.

$$\mathscr{U}'_0 = \frac{2}{\pi}\frac{\hat{\theta}l}{\sqrt{B^2l^2-1}}\cos^{-1}\sqrt{\frac{(1+Bl)(1+Bx)}{2B(l+x)}} + \frac{2\hat{\theta}}{\pi B}\cos^{-1}\sqrt{\frac{1+Bx}{2}}, \tag{3.4.18}$$

$$\mathscr{U}''_0 = -\frac{2}{\pi}\frac{\hat{h}l}{\sqrt{B^2l^2-1}}\cos^{-1}\sqrt{\frac{(1+Bl)(1+Bx)}{2B(l+x)}} - \frac{2\hat{h}}{\pi B}\cos^{-1}\sqrt{\frac{1+Bx}{2}}, \tag{3.4.19}$$

$$\begin{aligned}\mathscr{U}''_1 = {} & \frac{2}{\pi}\frac{1}{\left(B^2l^2-1\right)^{3/2}}\left[\hat{\theta}\frac{2B^2+1}{B^2}\left(l\left(B^2l^2-2\right)+x\right)+\hat{\psi}l^2\left(1-B^2lx\right)\right]\cos^{-1}\sqrt{\frac{(1+Bl)(1-Bx)}{2B(l-x)}} \\ & + \frac{2}{\pi B}\left[\hat{\theta}\frac{2B^2+1}{B^2}-\hat{\psi}x\right]\cos^{-1}\sqrt{\frac{(1+Bx)}{2B}} + \frac{1}{\pi B\left(B^2l^2-1\right)}\left[l\hat{\theta}\left(2B^2+1\right)-\hat{\psi}\right]\sqrt{\frac{1-B^2x^2}{B^2}},\end{aligned} \tag{3.4.20}$$

$$\Phi'_1 = x_1\left[\frac{2\hat{\theta}(l-x)}{\pi\sqrt{B^2l^2-1}}\cos^{-1}\sqrt{\frac{(1+Bl)(1-Bx)}{2B(l-x)}} + \frac{2\hat{\theta}}{\pi B}\cos^{-1}\sqrt{\frac{(1+Bx)}{2}}\right], \tag{3.4.21}$$

Accordingly, substituting real parts of $\mathscr{U}'_0$, $\mathscr{U}''_0$, $\mathscr{U}''_1$, and $\Phi'_1$ into Eq.(3.4.9) follows the resultant form of the calculation of the reduced pressure coefficient.

# CHAPTER 4

# ANALYSIS OF SUPERSONIC FLOW ON WING SURFACE BY METHOD OF SOURCE DISTRIBUTION

## 4.1 Velocity potential of sources distributing over wing surface in steady supersonic flow

In the first place, a three dimensional source with intensity $q$ placed in a uniform supersonic flow characterized by $M_\infty = 2.0$ is described in Cartesian coordinate system with origin, O, and three axes, $Ox_1$, $Ox_2$, and $Ox_3$, where $Ox_1$ is parallel to the free stream velocity and the source is placed in plane $Ox_1x_2$ (Fig. 4.1); e.g., we may specify the location of the source on plane $Ox_1x_2$ at $x_1 = \xi_1$, $x_2 = \xi_2$, $x_3 = 0$. we denote as an arbitrary point and thus

As well, the velocity potential equation in respect to $P(x_1, x_2, x_3)$ within the velocity field in steady flow is recalled as

$$-B^2 \frac{\partial^2 \varphi}{\partial x_1^{\,2}} + \frac{\partial^2 \varphi}{\partial x_2^{\,2}} + \frac{\partial^2 \varphi}{\partial x_3^{\,2}} = 0, \qquad (4.1.1)$$

where $\varphi$ is denoted as the perturbation velocity potential with respect to point $P$ in space $(x_1, x_2, x_3)$.

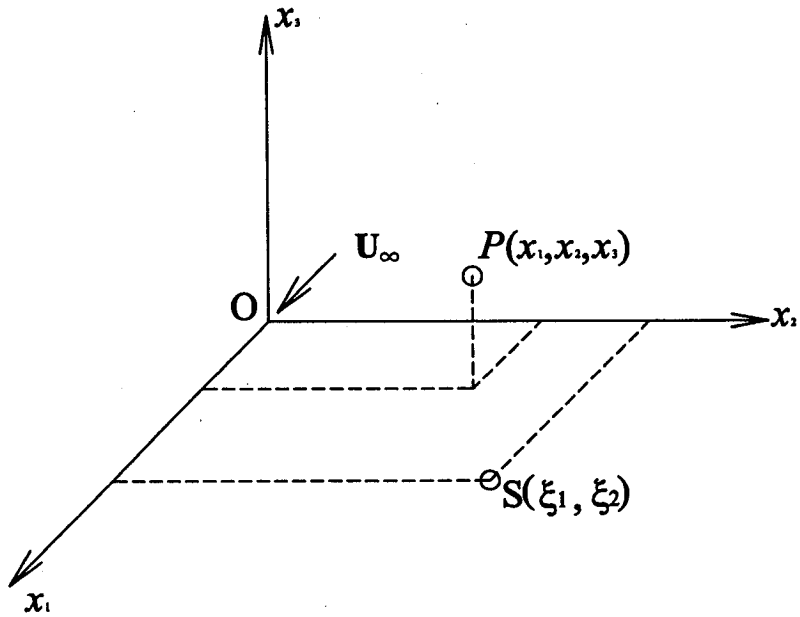


Figure 4.1 A single source situated in uniform supersonic flow

In turn, Eq.(4.1.1) can be recast in the form as the Laplace's equation by considering the coordinate transformation with the following three relations.

$$x_1 = iBX_1, x_2 = X_2,\ x_3 = X_3. \tag{4.1.2}$$

And the velocity potential equations becomes

$$\frac{\partial^2 \hat{\varphi}}{\partial X_1^{\,2}} + \frac{\partial^2 \hat{\varphi}}{\partial X_2^{\,2}} + \frac{\partial^2 \hat{\varphi}}{\partial X_3^{\,2}} = 0, \tag{4.1.3}$$

where $\hat{\varphi}$ is a harmonic function with respect to point $P$ in the transformed space ($X_1$, $X_2$, $X_3$) and represents the velocity potential of a fictitious incompressible flow around point $P$, situated in the new space. Therefore, this incompressible flow potential can be determined with the methods discussed for the wings in incompressible flow. Accordingly, the velocity potential, $\hat{\varphi}$, of this incompressible flow of point $P(X_1, X_2, X_3)$ related to the source with intensity $q$ can be determined as

$$\hat{\varphi} = \frac{1}{4\pi} \frac{q}{\sqrt{(X_1 - \xi_1')^2 + (X_2 - \xi_2')^2 + X_3^{\,2}}}. \tag{4.1.4}$$

As a result, the perturbation velocity potential of point $P$ related to a source with intensity $q$ in the original coordinate system $(x_1, x_2, x_3)$ is carried out and shown as follows.

$$\varphi = \frac{q}{\sqrt{(x_1 - \xi_1)^2 - B^2\left[(x_2 - \xi_2)^2 + x_3{}^2\right]}}. \tag{4.1.5}$$

Following is the determination of the velocity potential, $\varphi$, of point $P$ in space $(x_1, x_2, x_3)$ corresponding to sources distributing over a specific area, $\Lambda$, on plane $Ox_1x_2$ (Fig. 4.2). Firstly, the intensity of source related to the specific location $(\xi_1, \xi_2)$ is assumed uniform within the infinitesimal area $d\xi_1 d\xi_2$ and proportional to a given function $f(\xi_1, \xi_2)$. Explicitly, the intensity of source related to the specific location $(\xi_1, \xi_2)$ is denoted as $q_s$ and expressed as

$$q_s = f(\xi_1, \xi_2)\, d\xi_1 d\xi_2. \tag{4.1.6}$$

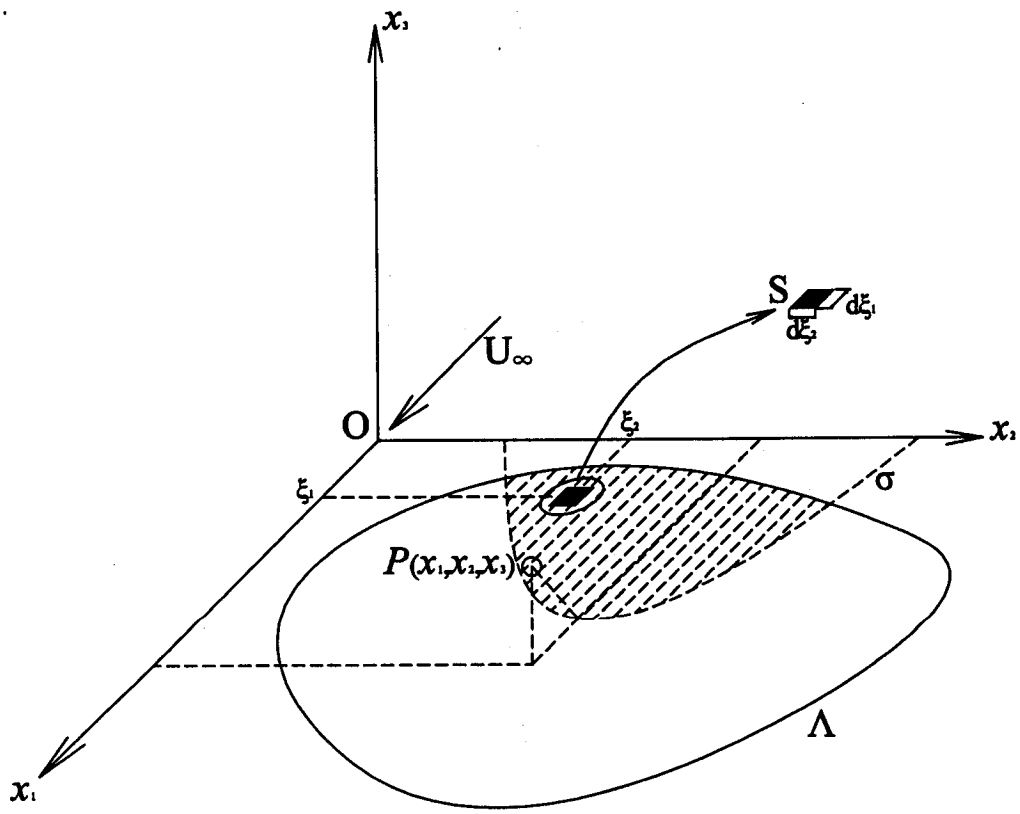


Figure 4.2 Distribution of series of sources in specific area $\Lambda$

Based on Eq.(4.1.5), the perturbation velocity potential of point $P$ related to a source placed in the specific location $(\xi_1, \xi_2)$ with intensity $q_s$ is expressed as

$$d\varphi = \frac{f(\xi_1, \xi_2) d\xi_1 d\xi_2}{\sqrt{(x_1 - \xi_1)^2 - B^2\left[(x_2 - \xi_2)^2 + x_3{}^2\right]}}, \tag{4.1.7}$$

where $d\varphi$ is a real value, and it follows that the denominator of Eq.(4.1.7) is supposed to be larger than zero.

$$(x_1 - \xi_1)^2 - B^2\left[(x_2 - \xi_2)^2 + x_3^2\right] \geq 0. \tag{4.1.8}$$

Mathematically, Eq.(4.1.8) represents the hyperbolic cones and the major axis is parallel to $Ox_1$ axis and the slope of asymptotes is $\frac{1}{B}$. In other words, such hyperbolic cone can be seen as the Mach cone specified by the Mach angle, $\mu = \tan^{-1}\frac{1}{B}$ in aerodynamic point of view. In this sense, only sources located inside the area, $\sigma$, covered by the forward Mach cone (Fig. 4.2) with the vertex, $P(x_1, x_2, x_3)$ and the specific area, $\Lambda$, count on the contribution to the calculation of the velocity potential of point $P$. Thus, the velocity potential, $\varphi$, related to sources distributing inside the area, $\sigma$, is expressed as

$$\varphi(x_1, x_2, x_3) = \iint_{\sigma} d\varphi \; d\xi_1 d\xi_2. \tag{4.1.9}$$

In turn, the perturbation downwash can be written as the derivative of $\varphi$ with respect to $x_3$ based on Eq.(4.1.9) due to the boundary condition as introduced in Eq.(2.1.10).

$$w = \frac{\partial \varphi}{\partial x_3} = \frac{\partial}{\partial x_3}\left(\iint_{\sigma} d\varphi d\xi_1 d\xi_2\right). \tag{4.1.10}$$

Denote the perturbation velocity potential of point $P$ related to sources distributing in the infinitesimal integration domain $\delta\xi_1\delta\xi_2$ by $\delta\varphi$. Then

$$\delta\varphi = f(\xi_1, \xi_2)\int_{a_1}^{a_2} d\xi_1 \int_{b_1}^{b_2} \frac{d\xi_2}{\sqrt{(x_1 - \xi_1)^2 - B^2\left[(x_2 - \xi_2)^2 + x_3^2\right]}}. \tag{4.1.11}$$

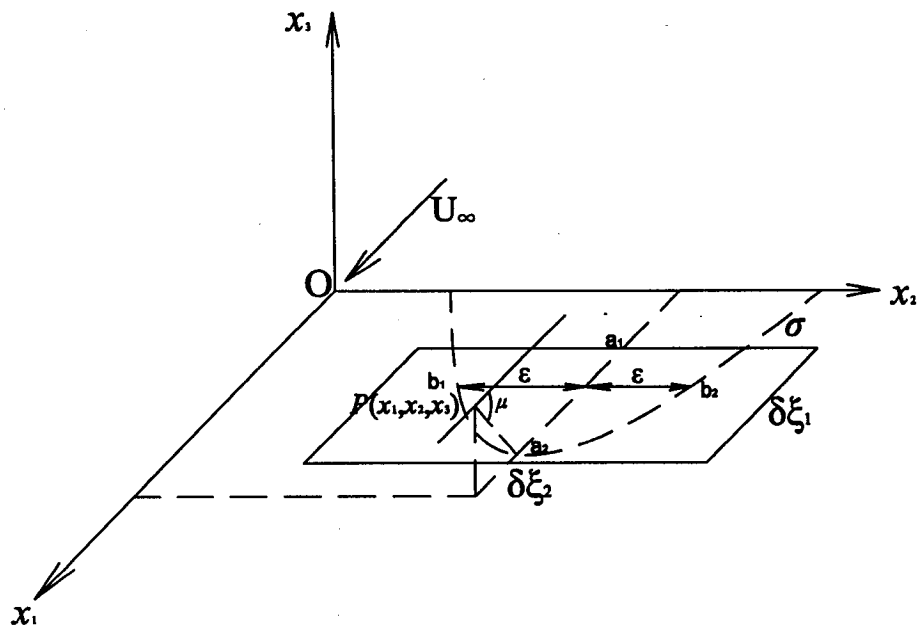


Figure 4.3 Coordinates system and integral limits for the downwash calculation

Firstly, we perform the integration with respect to variable $\xi_2$ in Eq.(4.1.11) and the upper and lower integration limits with respect to variable $\xi_2$ (Fig. 4.3) are expressed as $b_1 = x_2 - \varepsilon$ and $b_2 = x_2 + \varepsilon$.

$$\int_{b_1}^{b_2} \frac{d\xi_2}{\sqrt{(x_1-\xi_1)^2 - B^2\left[(x_2-\xi_2)^2 + x_3^2\right]}} = -\frac{1}{B}\sin^{-1}\frac{B(x_2-\xi_2)}{\sqrt{(x_1-\xi_1)^2 - B^2x_3^2}}\Bigg|_{b_1}^{b_2}$$

$$= \frac{2}{B}\sin^{-1}\frac{B\varepsilon}{\sqrt{(x_1-\xi_1)^2 - B^2x_3^2}}. \qquad (4.1.12)$$

As well, the integration limits, $b_1$ and $b_2$, are situated on the boundary of the hyperbola, and one obtains that

$$B\varepsilon = \sqrt{(x_1-\xi_1)^2 - B^2x_3^2}\,. \qquad (4.1.13)$$

Thus, Eq.(4.1.12) becomes

$$\int_{b_1}^{b_2} \frac{d\xi_2}{\sqrt{(x_1-\xi_1)^2 - B^2\left[(x_2-\xi_2)^2 + x_3^2\right]}} = \frac{\pi}{B}. \qquad (4.1.14)$$

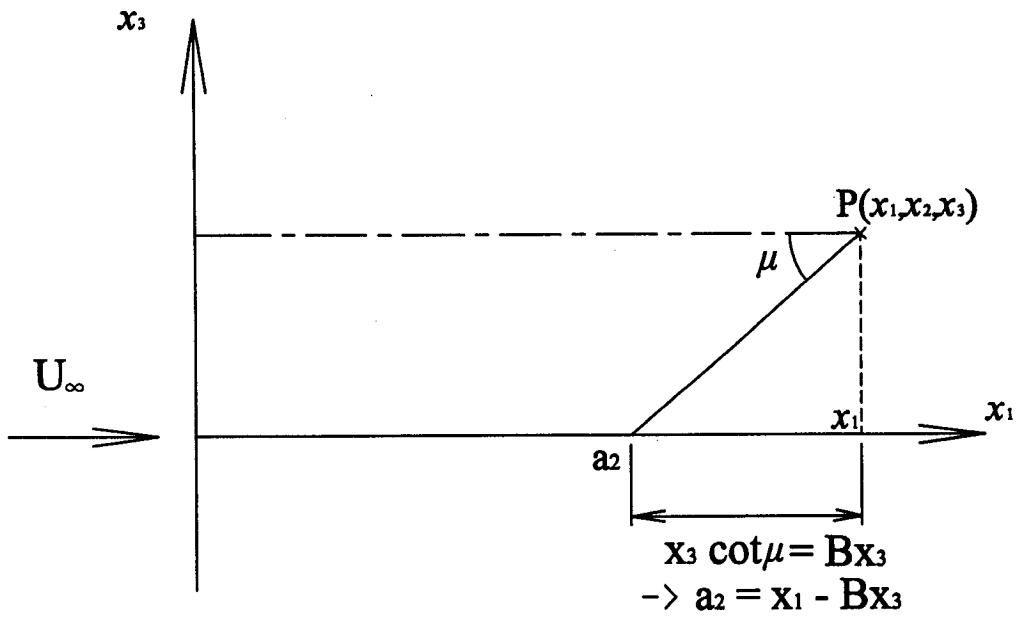


Figure 4.4 Calculation of the integral limit '$a_2$'

Secondly, we perform the integration with respect to variable $\xi_1$ with integration limits $a_1$ and $a_2$ in Eq.(4.1.11) and the perturbation velocity potential of point $P$ related to sources distributing in the infinitesimal integration domain $\delta\xi_1\delta\xi_2$ is carried out as

$$\delta\varphi = f(\xi_1,\xi_2)\frac{\pi}{B}\int_{a_1}^{a_2} d\xi_1 = f(\xi_1,\xi_2)\frac{\pi}{B}(a_2 - a_1) = f(\xi_1,\xi_2)\frac{\pi}{B}(x_1 - Bx_3 - a_1), \tag{4.1.15}$$

where $a_2$ is equal to $x_1 - Bx_3$ as shown in figure 4.4.

Accordingly, the perturbation downwash, $w$, is calculated as

$$w = \frac{\partial\varphi}{\partial x_3} = -\pi f(\xi_1,\xi_2). \tag{4.1.16}$$

And thus $f(\xi_1,\xi_2)$ can be expressed in terms of the function of downwash as

$$f(\xi_1,\xi_2) = -\frac{w}{\pi}. \tag{4.1.17}$$

As a consequence, the velocity potential of point $P$ related to sources distributing in the integration domain $\sigma$ with intensity proportional to the magnitude of $w(\xi_1,\xi_1)$ becomes

$$\varphi = -\frac{1}{\pi}\int_{a_1}^{a_2} d\xi_1 \int_{b_1}^{b_2} \frac{w(\xi_1,\xi_2)d\xi_2}{\sqrt{(x_1-\xi_1)^2 - B^2\left[(x_2-\xi_2)^2 + x_3^2\right]}}. \tag{4.1.18}$$

And for point $P$ located on plane $Ox_1x_2$, the velocity potential equation of point $P$ related to sources distributing in the integration domain $\sigma$ can be expressed as

$$\varphi(x_1,x_2) = -\frac{1}{\pi}\iint_{\sigma}\frac{w(\xi_1,\xi_2)}{R}d\xi_1 d\xi_2\,, \tag{4.1.19}$$

where $R = \sqrt{(x_1-\xi_1)^2 - B^2(x_2-\xi_2)^2}$ and $w(\xi_1,\xi_2)$ can be defined in the form as a superposition of homogeneous polynomial in $\xi_1$ and $\xi_2$ with respect to each location of a source in the integration domain $\sigma$.

## 4.2 Velocity potential of pulsating sources distributing over wing surface in supersonic flows

A three dimensional pulsating source with intensity $q$ in supersonic flow is of interest for analyzing wings executing unsteady motions. And as could be recalled, the velocity potential equation of point $P(x_1, x_2, x_3)$ in the unsteady supersonic flow is expressed as

$$-B^2\frac{\partial^2\varphi}{\partial x^2}+\frac{\partial^2\varphi}{\partial y^2}+\frac{\partial^2\varphi}{\partial z^2}=\frac{1}{a_\infty^2}\left(\frac{\partial^2\varphi}{\partial t^2}+2U_\infty\frac{\partial^2\varphi}{\partial x\partial t}\right). \tag{4.2.1}$$

By considering the velocity potential of point $P(x_1, x_2, x_3)$ for harmonic motion [52] shown as

$$\varphi(x_1, x_2, x_3, t)=U_\infty e^{i(\omega t+kx_1)}\Phi(x_1, x_2, x_3), \tag{4.2.2}$$

where $\Phi(x_1, x_2, x_3)$ is the reduced velocity potential of point $P(x_1, x_2, x_3)$,

Eq.(4.2.1) can be recast as

$$-B^2\frac{\partial^2\Phi}{\partial x_1^{\,2}}+\frac{\partial^2\Phi}{\partial x_2^{\,2}}+\frac{\partial^2\Phi}{\partial x_3^{\,2}}=\lambda^2\frac{1+B^2}{B^2}\Phi=\frac{\lambda^2M_\infty^2}{B^2}\Phi=K^2\Phi, \tag{4.2.3}$$

where we denote $\lambda=\dfrac{\omega}{U_\infty}$ by the reduced oscillating frequency, $K=\dfrac{\lambda M_\infty}{B}$, and $k=-K\dfrac{M_\infty}{B}$.

According to the boundary condition of the Mach cone, all the perturbation velocity, *u*, *v*, *w*, disappear outside of the Mach cone; i.e., the perturbation velocity potential, $\varphi$, is also zero.

$$\Phi=0, u=\frac{\partial\Phi}{\partial x_1}=0, v=\frac{\partial\Phi}{\partial x_2}=0, w=\frac{\partial\Phi}{\partial x_3}=0. \tag{4.2.4}$$

And similar to the steady supersonic flow, only sources distributing in area $\sigma$ covered by the forwarded Mach cone with the vertex point *P* and the specific area, Λ, contribute to the calculation of the velocity potential of point *P*. Explicitly, the boundary condition is recalled as

$$R=\sqrt{(x_1-\xi_1)^2-B^2\left[(x_2-\xi_2)^2+(x_3-\xi_3)^2\right]}\geq 0. \tag{4.2.5}$$

Let's consider Eq.(4.2.4) by the Lorenz transformation, including $\tau = t - K\frac{M_\infty}{B}x_1$, the reduced velocity potential of point $P$ can be expressed as

$$\Phi(x_1, x_2, x_3) = \Phi_1(R)\Phi_2(\psi)\Phi_3(\theta), \tag{4.2.6}$$

where $\psi = \frac{R}{x_1 - \xi_1}$ and $\theta = \tan^{-1}\frac{x_3 - \xi_3}{x_2 - \xi_2}$.

In this study, all wings are restricted to planar thin wing plan form (i.e., $x_3 = \xi_3 = 0$) and this condition leads to $\theta = 0$ and $\Phi_3(\theta) = 1$. As well, with the regard of non-singularity solution even when $x_1 = \xi_1$, taking $\Phi_2(\psi)$ as unit is a way for it. Accordingly, $\Phi(x_1, x_2, x_3)$ can be recast as

$$\Phi(x_1, x_2, x_3) = \Phi_1(R). \tag{4.2.7}$$

Thus, the derivative of $\Phi$ in respect to $x_1$ in first order is shown as

$$\frac{\partial\Phi}{\partial x_1} = \frac{\partial\Phi_1}{\partial R}\frac{\partial R}{\partial x_1}. \tag{4.2.8}$$

And then the derivative with respect to $x_1$ in second order is

$$\frac{\partial^2\Phi}{\partial x_1^{\,2}} = \frac{\partial^2\Phi_1}{\partial R^2}\left(\frac{\partial R}{\partial x_1}\right)^2 + \frac{\partial\Phi_1}{\partial R}\left(\frac{\partial^2 R}{\partial x_1^{\,2}}\right). \tag{4.2.9}$$

Similarly, the derivative of $\Phi$ in respect to $x_2$ and $x_3$ in second order are shown as

$$\frac{\partial^2\Phi}{\partial x_2^{\,2}} = \frac{\partial^2\Phi_1}{\partial R^2}\left(\frac{\partial R}{\partial x_2}\right)^2 + \frac{\partial\Phi_1}{\partial R}\left(\frac{\partial^2 R}{\partial x_2^{\,2}}\right). \tag{4.2.10}$$

$$\frac{\partial^2\Phi}{\partial x_3^{\,2}} = \frac{\partial^2\Phi_1}{\partial R^2}\left(\frac{\partial R}{\partial x_3}\right)^2 + \frac{\partial\Phi_1}{\partial R}\left(\frac{\partial^2 R}{\partial x_3^{\,2}}\right), \tag{4.2.11}$$

where

$$\frac{\partial R}{\partial x_1} = \frac{x_1 - \xi_1}{R},\ \frac{\partial^2 R}{\partial x_1^{\,2}} = \frac{-B^2\left[(x_2 - \xi_2)^2 - (x_3 - \xi_3)^2\right]}{R^3}, \tag{4.2.12}$$

$$\frac{\partial R}{\partial x_2} = \frac{-B^2(x_2 - \xi_2)}{R},\ \frac{\partial^2 R}{\partial x_2^{\,2}} = \frac{-B^2\left[(x_1 - \xi_1)^2 - B^2(x_3 - \xi_3)^2\right]}{R^3}, \tag{4.2.13}$$

$$\frac{\partial R}{\partial x_3}=\frac{-B(x_3-\xi_3)}{R},\ \text{and}\ \frac{\partial^2 R}{\partial x_3{}^2}=\frac{-B^2\left[(x_1-\xi_1)^2-B^2(x_2-\xi_2)^2\right]}{R^3}. \tag{4.2.14}$$

Substitute Eq.(4.2.9) ~ (4.2.14) into the velocity potential equation in terms of the reduced velocity potential as introduced in Eq.(4.2.3), and we have

$$\frac{\partial\Phi_1}{\partial R}\left\{-B^2\frac{-B^2\left[(x_2-\xi_2)^2+(x_3-\xi_3)^2\right]}{R^3}+\frac{-B^2\left[(x_1-\xi_1)^2-B^2(x_3-\xi_3)^2\right]-B^2\left[(x_1-\xi_1)^2+(x_2-\xi_2)^2\right]}{R^3}\right\}+$$

$$\frac{\partial^2\Phi_1}{\partial R^2}\left\{-B^2\frac{(x_1-\xi_1)^2}{R^2}+\frac{B^4\left[(x_2-\xi_2)^2+(x_3-\xi_3)^2\right]}{R^2}\right\}=K^2\Phi_1(R). \tag{4.2.15}$$

After simplifying the whole set of Eq.(4.2.15), the velocity potential equation in terms of the reduced velocity potential of point $P$ can be recast as

$$\frac{d^2\Phi_1}{dR^2}+\frac{2}{R}\frac{d\Phi_1}{dR}+\frac{K^2}{B^2}\Phi_1=0. \tag{4.2.16}$$

Mathematically, Eq.(4.2.16) is a homogeneous ordinary differential equation with respect to single variable, $R$, and one of the non-trivial general solutions of this O.D.E. can be written by

$$\Phi_1(R)=\frac{1}{R}\cos\left(\frac{K}{B}R\right). \tag{4.2.17}$$

Likewise, the velocity potential of point $P$ on wing surface in steady supersonic flow can then be applied to wings executing unsteady motions in terms of all time-independent variables and the non-trivial solution shown in Eq.(4.2.17).

$$\Phi(x_1,x_2)=-\frac{1}{\pi}\iint_\sigma\hat{w}(\xi_1,\xi_2)\frac{1}{R}\cos\left(\frac{KR}{B}\right)d\xi_1 d\xi_2\,, \tag{4.2.18}$$

where $\hat{w}=e^{-ik\xi_1}\hat{W}(\xi_1,\xi_2)$. According to the discussion of boundary condition in chapter 2.1, $\hat{W}$ is fully dependent on the geometry of the wing model surface. Replace $\hat{w}$ by $\hat{W}$ in Eq.(4.2.18) and put one $e^{ikx_1}$ inside the integral and set $e^{-ikx_1}$ outside the integral; that's it, Eq.(4.2.18) becomes

$$\Phi(x_1,x_2)=-\frac{1}{\pi}e^{-ikx_1}\iint_\sigma\frac{\hat{W}(\xi_1,\xi_2)}{R}e^{ik(x_1-\xi_1)}\cos\left(\frac{KR}{B}\right)d\xi_1 d\xi_2\,. \tag{4.2.19}$$

And $\hat{W}(\xi_1,\xi_2)$ can be defined as a superposition of homogeneous polynomial in $\xi_1$ and $\xi_2$ with respect to each location of a pulsating source in the integration domain $\sigma$. Explicitly, $w(\xi_1,\xi_2)$ in steady case and $\hat{W}(\xi_1,\xi_2)$ in unsteady case can then be unified in the form as

$$w_0(\xi_1,\xi_2)=\sum_{n=0}^{N}\sum_{j=0}^{n} w_{n-j,j}\xi_1^{n-j}\xi_2^{j}\,, \tag{4.2.20}$$

where $N$ and $w_{i,j}$; i = 0...$N$ and j = 0...$N$ are determined with the regard of physical conditions imposed on the wing model directly.

# CHAPTER 5

# PRESENT STEADY FLOW SOLUTIONS FOR FIXED WINGS

## 5.1 General steady flow solutions for thin wings

The velocity potential of point $P$ has been carried out by performing the integral of downwash in the integration domain $\sigma$ covered by the forward Mach cone and the fixed wing surface in supersonic flows. Accordingly, the axial disturbance velocity, $u$, can be written in the form as

$$u = \frac{\partial \varphi(x_1, x_2)}{\partial x_1} = -\frac{1}{\pi}\frac{\partial}{\partial x_1}\left( \iint_{\sigma} \frac{w(\xi_1, \xi_2)}{R} d\xi_1 d\xi_2 \right), \tag{5.1.1}$$

where $R = \sqrt{(x_1 - \xi_1)^2 - B^2(x_2 - \xi_2)^2}$ .

Let's consider the coordinate transformation with the following two relations.

$$X = x_1 - \xi_1 \text{ and } Y = \frac{x_2 - \xi_2}{x_1 - \xi_1}. \tag{5.1.2}$$

Thus, equations $w(\xi_1, \xi_2)$, $R$, and $d\xi_1 d\xi_2$ in Eq.(5.1.1) can then be recasted as functions of the transformed variables $X$ and $Y$.

$$w_0(\xi_1,\xi_2)=\sum_{n=0}^{N}\sum_{j=0}^{n}w_{n-j,j}\xi_1^{n-j}\xi_2^{j}=\sum_{n=0}^{N}\sum_{j=0}^{n}w_{n-j,j}(x_1-X)^{n-j}(x_2-XY)^{j}$$

$$=\sum_{n=0}^{N}\sum_{j=0}^{n}w_{n-j,j}\left(\sum_{k=0}^{n-j}\sum_{q=0}^{j}C_k^{n-j}C_q^{j}(-1)^{k+q}x_1^{\,n-j-k}x_2^{\,j-q}X^{k+q}Y^{q}\right), \tag{5.1.3}$$

where $C_k^{n-j}$ and $C_q^{j}$ are coefficients of Newton binomial formula.

$$R=X\sqrt{1-B^2Y^2}=X\Re\text{, where }\Re=\sqrt{1-B^2Y^2}\,. \tag{5.1.4}$$

The Jacobean of the coordinate transformation is calculated as

$$\begin{bmatrix}\dfrac{\partial\xi_1}{\partial X} & \dfrac{\partial\xi_1}{\partial Y}\\ \dfrac{\partial\xi_2}{\partial X} & \dfrac{\partial\xi_2}{\partial Y}\end{bmatrix}=X\,. \tag{5.1.5-a}$$

And thus

$$d\xi_1 d\xi_2 = XdXdY\,. \tag{5.1.5-b}$$

Substitute the Eq.(5.1.3), (5.1.4), and (5.1.5-b) into the perturbation velocity potential, $\varphi$, in terms of variables $X$ and $Y$ and one has

$$\varphi(X,Y)=-\frac{1}{\pi}\left\{\sum_{n=0}^{N}\sum_{j=0}^{n}w_{n-j,j}\bar{L}_0\left[\sum_{k=0}^{n-j}\sum_{q=0}^{j}x_1^{n-j-k}x_2^{j-q}I_0\right]\right\}, \tag{5.1.6}$$

where

$$I_0=\iint_{\sigma}\frac{X^{k+q}Y^{q}}{\Re}dXdY\,, \tag{5.1.7}$$

$$\bar{L}_0=C_k^{n-j}C_q^{j}(-1)^{k+q}. \tag{5.1.8}$$

The calculation of integral $I_0$ has to be performed based on the specific geometrical configuration of delta and trapezoidal wings separately. The following two sections are the detailed analytical solutions of the calculation of integral with which the both wing plan forms are concerned.

The axial perturbation velocity, $u$, is given by the following equation.

$$u = \frac{\partial \varphi}{\partial x_1} = -\frac{1}{\pi}\left\{\sum_{n=0}^{N}\sum_{j=0}^{n} w_{n-j,j}\bar{L}_0\left[\sum_{k=0}^{n-j}\sum_{q=0}^{j}(n-j-k)x_1^{n-j-k-1}x_2^{j-q}I_0 + x_1^{n-j-k}x_2^{j-q}\frac{\partial I_0}{\partial x_1}\right]\right\}. \quad (5.1.9)$$

Accordingly, the pressure coefficient, $Cp$, of wing in steady flow can be calculated as

$$Cp = -2\frac{u}{U_\infty} = \frac{2}{\pi U_\infty}\left\{\sum_{n=0}^{N}\sum_{j=0}^{n} w_{n-j,j}\bar{L}_0\left[\sum_{k=0}^{n-j}\sum_{q=0}^{j}(n-j-k)x_1^{n-j-k-1}x_2^{j-q}I_0 + x_1^{n-j-k}x_2^{j-q}\frac{\partial I_0}{\partial x_1}\right]\right\}. \quad (5.1.10)$$

As well, the lift coefficient, $C_l$, pitching moment coefficient, $C_{m2}$, and rolling moment coefficient, $C_{m1}$, can be calculated as follows.

For calculation of the lift coefficient,

$$C_l = \frac{-2}{S}\int_S Cpx_1 dx_1 dy$$

$$= \frac{-4}{S\pi}\left\{\sum_{n=0}^{N}\sum_{j=0}^{n} w_{n-j,j}\left[\sum_{k=0}^{n-j}\sum_{q=0}^{j}\bar{L}_0\left((n-k-q)\int_S (x_1^{n-k-q}y^{j-q})I_0 dx_1 dy + \int_S (x_1^{n-k-q+1}y^{j-q})\frac{\partial I_0}{\partial x_1}dx_1 dy\right)\right]\right\}. \quad (5.1.11)$$

For calculation of the pitching moment coefficient,

$$C_{m2} = \frac{-2}{Sc_0}\int_S Cpx_1^2 dx_1 dy$$

$$= \frac{-4}{c_0 S\pi}\left\{\sum_{n=0}^{N}\sum_{j=0}^{n} w_{n-j,j}\left[\sum_{k=0}^{n-j}\sum_{q=0}^{j}\bar{L}_0\left((n-k-q)\int_S (x_1^{n-k-q+1}y^{j-q})I_0 dx_1 dy + \int_S (x_1^{n-k-q+2}y^{j-q})\frac{\partial I_0}{\partial x_1}dx_1 dy\right)\right]\right\}. \quad (5.1.12)$$

For calculation of the rolling moment coefficient,

$$C_{m1} = \frac{-2}{S(2b)}\int_S Cpx_1^2 y dx_1 dy$$

$$= \frac{-4}{(2b)S\pi}\left\{\sum_{n=0}^{N}\sum_{j=0}^{n} w_{n-j,j}\left[\sum_{k=0}^{n-j}\sum_{q=0}^{j}\bar{L}_0\left((n-k-q)\int_S (x_1^{n-k-q+1}y^{j-q+1})I_0 dx_1 dy + \int_S (x_1^{n-k-q+2}y^{j-q+1})\frac{\partial I_0}{\partial x_1}dx_1 dy\right)\right]\right\}. \quad (5.1.13)$$

## 5.2 Calculation of integral for thin delta wing in steady supersonic flow

Let's consider figure 5.1 and the integration domain, $\sigma$, representing the specific area of wing surface covered by the forward Mach cone with the vertex at point $P$, can be split into two sections as $\Delta PA'_1O$ and $\Delta POA'_2$. It follows that the integral $I_0$ for thin delta wing can then be written related to domains $\Delta PA'_1O$ and $\Delta POA'_2$, respectively.

$$I_0 = \iint_{\sigma} \frac{X^{k+q}Y^q}{\Re} dXdY = \iint_{\Delta PA'_1O} \frac{X^{k+q}Y^q}{\Re} dXdY + \iint_{\Delta POA'_2} \frac{X^{k+q}Y^q}{\Re} dXdY . \qquad (5.2.1)$$

The integral limits in respect of both triangular domains are defined by the location of each point $P(x_1, x_2)$ on wing surface with variable, $y = x_2 / x_1$ and can be expressed in the form as function $f$(y).

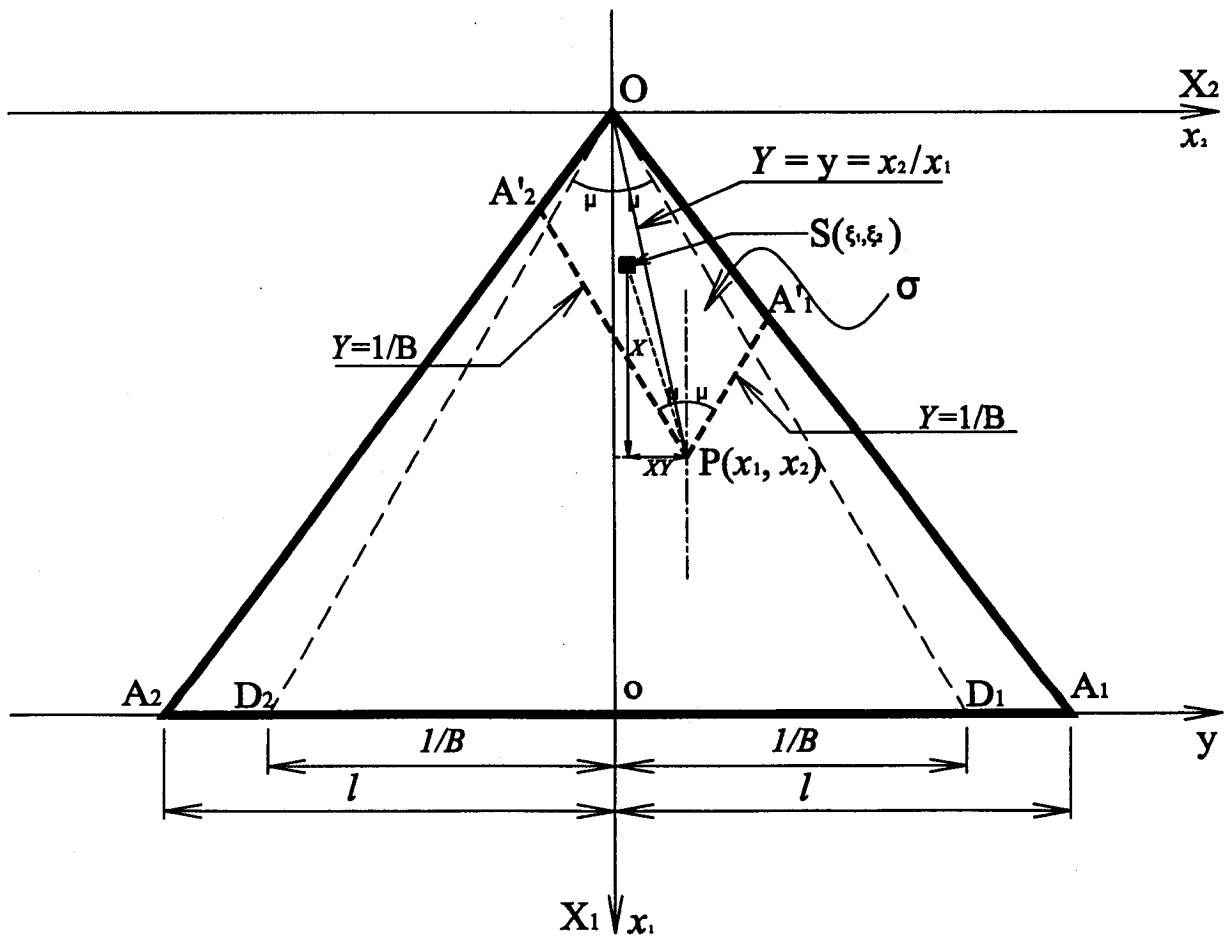


Figure 5.1 Integral limits of the thin delta wing

Explicitly, the integral limits, $f(y)$, with respect to $Y$ are expressed as

$$\text{For } \tan\mu = \frac{1}{B} \le y \le l,\ f(y) = \frac{1}{B}.$$

$$\text{For } -\frac{1}{B} \le y \le \frac{1}{B},\ f(y) = y. \tag{5.2.2}$$

$$\text{For } -l \le y \le -\frac{1}{B},\ f(y) = -\frac{1}{B}.$$

And for the integral limits with respect to $X$, we denote $X_1^*$ and $X_2^*$ by auxiliary functions representing the upper integral limits for integration domains $\Delta PA'_1O$ and $\Delta PA'_2O$, respectively.

For $\Delta PA'_1O$ domain, we have

$$X_{\Delta PA'_1O} = X_1^* = x_1 \frac{l-y}{l-Y}. \tag{5.2.3-a}$$

For $\Delta PA'_2O$ domain, we have

$$X_{\Delta PA'_2O} = X_2^* = x_1 \frac{l+y}{l+Y}. \tag{5.2.3-b}$$

Accordingly, $I_0$ can be recast as follows by considering all these integral limits in Eq.(5.2.1).

$$I_0 = \iint_{\sigma} \frac{X^{k+q}Y^q}{\Re} dXdY = \iint_{\Delta PA'_1O} \frac{X^{k+q}Y^q}{\Re} dXdY + \iint_{\Delta POA'_2} \frac{X^{k+q}Y^q}{\Re} dXdY$$

$$= \int_{\frac{1}{B}}^{f(y)} \frac{Y^q}{\Re} \left( \int_0^{X_1^*} X^{k+q} dX \right) dY + \int_{f(y)}^{\frac{1}{B}} \frac{Y^q}{\Re} \left( \int_0^{X_2^*} X^{k+q} dX \right) dY$$

$$= \int_{\frac{1}{B}}^{f(y)} \frac{X_1^{*k+q+1} Y^q}{(k+q+1)\Re} dY + \int_{f(y)}^{\frac{1}{B}} \frac{X_2^{*k+q+1} Y^q}{(k+q+1)\Re} dY$$

$$= \frac{[x_1(l-y)]^{k+q+1}}{k+q+1} \int_{\frac{1}{B}}^{f(y)} \frac{Y^q}{(l-Y)^{k+q+1}\Re} dY + \frac{[x_1(l+y)]^{k+q+1}}{k+q+1} \int_{f(y)}^{\frac{1}{B}} \frac{Y^q}{(l+Y)^{k+q+1}\Re} dY. \tag{5.2.4}$$

In turn, we consider $Y^q = [l-(l-Y)]^q$ in the first integral and $Y^q = [-l+(l+Y)]^q$ in the second integral shown in Eq.(5.2.4) and these two relations can be recast by the Newton binomial formula. It follows that the two integrals in Eq.(5.2.4) can be recast as

$$\int_{\frac{1}{B}}^{f(y)} \frac{Y^q}{(l-Y)^{k+q+1}\Re} dY = \sum_{f=0}^{q} (-1)^f C_f^q l^{q-f} \int_{\frac{1}{B}}^{f(y)} \frac{1}{(l-Y)^g \Re} dY, \tag{5.2.5-a}$$

$$\int_{f(y)}^{\frac{1}{B}} \frac{Y^q}{(l+Y)^{k+q+1}\Re} dY = \sum_{f=0}^{q} (-1)^{q-f} C_f^q l^{q-f} \int_{f(y)}^{\frac{1}{B}} \frac{1}{(l+Y)^g \Re} dY, \tag{5.2.5-b}$$

where $g = k+q-f+1$ and denote the integrals of two kinds above by $I_g$ and $J_g$, respectively.

$$I_g = \int_{\frac{1}{B}}^{f(y)} \frac{1}{(l-Y)^g \Re} dY, \tag{5.2.6-a}$$

$$J_g = \int_{f(y)}^{\frac{1}{B}} \frac{1}{(l+Y)^g \Re} dY. \tag{5.2.6-b}$$

Analytically, Integrals in Eq.(5.2.5-a) and (5.2.5-b) can be solved by using the recurrence formulae. Let's take Eq.(5.2.6-a) as an example. Firstly, denote the an auxiliary integral by $A_g$ and the following equation can be carried out straightforward as

$$A_g = \int_{\frac{1}{B}}^{f(y)} \frac{\Re}{(l-Y)^g} dY = \int_{\frac{1}{B}}^{f(y)} \frac{\Re^2}{(l-Y)^g \Re} dY = \int_{\frac{1}{B}}^{f(y)} \frac{1-B^2[l-(l-Y)]^2}{(l-Y)^g \Re} dY$$

$$= (1-B^2 l^2) \int_{\frac{1}{B}}^{f(y)} \frac{1}{(l-Y)^g \Re} dY + 2B^2 l \int_{\frac{1}{B}}^{f(y)} \frac{1}{(l-Y)^{g-1} \Re} dY - B^2 \int_{\frac{1}{B}}^{f(y)} \frac{1}{(l-Y)^{g-2} \Re} dY. \tag{5.2.7}$$

On the other hand, $A_g$ can also be integrated by part and we have,

$$A_g = \int_{\frac{1}{B}}^{f(y)} \frac{\Re}{(l-Y)^g} dY = \frac{\sqrt{1-B^2(f(y))^2}}{(g-1)(l-f(y))^{g-1}} - \frac{B^2}{(g-1)} \int_{\frac{1}{B}}^{f(y)} \frac{Y}{(l-Y)^{g-1}\sqrt{1-B^2Y^2}} dY \tag{5.2.8}$$

By arranging Eq.(5.2.7) and Eq.(5.2.8) together, the recurrence formulae for integral, $I_g$, are given as

$$I_g = \frac{1}{(1-B^2l^2)}\left[\frac{\sqrt{1-B^2[f(y)]^2}}{(g-1)[l-f(y)]^{g-1}} + B^2 l \frac{3-2g}{g-1} I_{g-1} + B^2 \frac{g-2}{g-1} I_{g-2}\right], \text{ for } g \geq 2. \quad (5.2.9\text{-a})$$

$$I_g = \frac{1}{B}\left[\sin^{-1}(Bf(y)) + \frac{\pi}{2}\right], \text{ for } g = 0. \quad (5.2.9\text{-b})$$

$$I_g = \frac{2}{\sqrt{B^2l^2-1}} \cos^{-1} \sqrt{\frac{(1-Bf(y))(1+Bl)}{2B(l-f(y))}}, \text{ for } g = 1, \quad (5.2.9\text{-c})$$

where $I_g = \int_{\frac{1}{B}}^{f(y)} \frac{1}{(l-Y)^g \Re} dY$, $I_{g-1} = \int_{\frac{1}{B}}^{f(y)} \frac{1}{(l-Y)^{g-1} \Re} dY$, $I_{g-2} = \int_{\frac{1}{B}}^{f(y)} \frac{1}{(l-Y)^{g-2} \Re} dY \ldots$

Similarly, the recurrence formulae for the integral, $J_g$, are given as

$$J_g = \frac{1}{(1-B^2l^2)}\left[\frac{\sqrt{1-B^2[f(y)]^2}}{(g-1)[l+f(y)]^{g-1}} + B^2 l \frac{3-2g}{g-1} I_{g-1} + B^2 \frac{g-2}{g-1} I_{g-2}\right], \text{ for } g \geq 2. \quad (5.2.10\text{-a})$$

$$J_g = \frac{1}{B}\left[\frac{\pi}{2} - \sin^{-1}(Bf(y))\right], \text{ for } g = 0. \quad (5.2.10\text{-b})$$

$$J_g = \frac{2}{\sqrt{B^2l^2-1}} \cos^{-1} \sqrt{\frac{(1+Bf(y))(1+Bl)}{2B(l+f(y))}}, \text{ for } g = 1, \quad (5.2.10\text{-c})$$

where $J_g = \int_{f(y)}^{\frac{1}{B}} \frac{1}{(l+Y)^g \Re} dY$, $J_{g+1} = \int_{f(y)}^{\frac{1}{B}} \frac{1}{(l+Y)^{g+1} \Re} dY$, $J_{g+2} = \int_{f(y)}^{\frac{1}{B}} \frac{1}{(l+Y)^{g+2} \Re} dY \ldots$

As a consequence, the integral, $I_0$, and its derivative with limits are given separately in terms of the position of point $P(x_1, x_2)$.

**For position outside the Mach cone to the right,** $\frac{1}{B} \le y \le l$ and $f(y) = \frac{1}{B}$.

$$I_0 = \frac{[x_1(l-y)]^{k+q+1}}{k+q+1} \int_{\frac{1}{B}}^{\frac{1}{B}} \frac{Y^q}{(l-Y)^{k+q+1}\Re} dY, \tag{5.2.11}$$

$$\frac{\partial}{\partial x_1} I_0 = l[x_1(l-y)]^{k+q} \int_{\frac{1}{B}}^{\frac{1}{B}} \frac{Y^q}{(l-Y)^{k+q+1}\Re} dY. \tag{5.2.12}$$

**For position inside the Mach cone,** $-\frac{1}{B} \le y \le \frac{1}{B}$ and $f(y) = y$.

$$I_0 = \frac{[x_1(l-y)]^{k+q+1}}{k+q+1} \int_{\frac{1}{B}}^{y} \frac{Y^q}{(l-Y)^{k+q+1}\Re} dY + \frac{[x_1(l+y)]^{k+q+1}}{k+q+1} \int_{y}^{\frac{1}{B}} \frac{Y^q}{(l+Y)^{k+q+1}\Re} dY. \tag{5.2.13}$$

$$\frac{\partial}{\partial x_1} I_0 = l[x_1(l-y)]^{k+q} \int_{\frac{1}{B}}^{y} \frac{Y^q}{(l-Y)^{k+q+1}\Re} dY + \frac{[x_1(l-y)]^{k+q+1}}{k+q+1} \frac{\partial}{\partial x_1} \left( \int_{\frac{1}{B}}^{y} \frac{Y^q}{(l-Y)^{k+q+1}\Re} dY \right) +$$

$$l[x_1(l+y)]^{k+q} \int_{y}^{\frac{1}{B}} \frac{Y^q}{(l+Y)^{k+q+1}\Re} dY + \frac{[x_1(l+y)]^{k+q+1}}{k+q+1} \frac{\partial}{\partial x_1} \left( \int_{y}^{\frac{1}{B}} \frac{Y^q}{(l+Y)^{k+q+1}\Re} dY \right), \tag{5.2.14}$$

where the derivative of integral $\int_{\frac{1}{B}}^{y} \frac{Y^q}{(l-Y)^{k+q+1}\Re} dY$ and $\int_{y}^{\frac{1}{B}} \frac{Y^q}{(l+Y)^{k+q+1}\Re} dY$ with respect to $x_1$ can be derived as

$$\frac{\partial}{\partial x_1} \left( \int_{\frac{1}{B}}^{y} \frac{Y^q}{(l-Y)^{k+q+1}\Re} dY \right) = \sum_{f=0}^{q} (-1)^f C_f^q l^{q-f} \frac{\partial I_g}{\partial x_1} = -\frac{x_2}{x_1^2} \sum_{f=0}^{q} (-1)^f C_f^q l^{q-f} \frac{\partial I_g}{\partial y}, \tag{5.2.15}$$

$$\frac{\partial}{\partial x_1} \left( \int_{y}^{\frac{1}{B}} \frac{Y^q}{(l+Y)^{k+q+1}\Re} dY \right) = \sum_{f=0}^{q} (-1)^{q-f} C_f^q l^{q-f} \frac{\partial J_g}{\partial x_1} = -\frac{x_2}{x_1^2} \sum_{f=0}^{q} (-1)^{q-f} C_f^q l^{q-f} \frac{\partial J_g}{\partial y}, \tag{5.2.16}$$

where the derivative of $I_g$ and $J_g$ with respect to y are then given by the recurrence formulae as follows.

For $g \geq 2$,

$$\frac{\partial I_g}{\partial y} = \frac{1}{1-B^2 l^2}\left[\frac{(g-1)\left|1-B^2y^2\right| - B^2 y(l-y)}{(g-1)(l-y)^g\sqrt{1-B^2y^2}} + B^2 l\frac{3-2g}{g-1}\frac{\partial I_{g-1}}{\partial y} + B^2\frac{g-2}{g-1}\frac{\partial I_{g-2}}{\partial y}\right]. \quad (5.2.17)$$

$$\frac{\partial J_g}{\partial y} = \frac{1}{1-B^2 l^2}\left[\frac{(g-1)\left|1-B^2y^2\right| - B^2 y(l+y)}{(g-1)(l+y)^g\sqrt{1-B^2y^2}} + B^2 l\frac{3-2g}{g-1}\frac{\partial J_{g-1}}{\partial y} + B^2\frac{g-2}{g-1}\frac{\partial J_{g-2}}{\partial y}\right]. \quad (5.2.18)$$

For $g = 1$,

$$\frac{\partial I_g}{\partial y} = \frac{1}{(l-y)\sqrt{1-B^2y^2}}. \quad (5.2.19)$$

$$\frac{\partial J_g}{\partial y} = \frac{-1}{(l+y)\sqrt{1-B^2y^2}}. \quad (5.2.20)$$

**For position outside the Mach cone to the left,** $-l \leq y \leq -\frac{1}{B}$ and $f(y) = -\frac{1}{B}$.

$$I_0 = \frac{[x_1(l+y)]^{k+q+1}}{k+q+1}\int_{\frac{1}{B}}^{\frac{1}{B}} \frac{Y^q}{(l+Y)^{k+q+1}\Re} dY \quad (5.2.21)$$

$$\frac{\partial}{\partial x_1} I_0 = l[x_1(l+y)]^{k+q}\int_{\frac{1}{B}}^{\frac{1}{B}} \frac{Y^q}{(l+Y)^{k+q+1}\Re} dY \quad (5.2.22)$$

In turn, considering the definition of the lift coefficient, pitching moment coefficient, and rolling moment coefficient in Eq.(5.1.11), (5.1.12), and (5.1.13), the integration of $I_0$ are essential at this stage. The detailed expressions for performing integrals in the calculation of the aerodynamic coefficients are given in Appendix C.

## 5.3 Calculation of integral for thin trapezoidal wing in steady supersonic flow

For analysis of thin trapezoidal wing situated in steady supersonic flow, let's consider figure 5.2 on which the calculation of integral is based. Because of the nature symmetry with respect to $OX_1$, the analysis of the aerodynamic characteristics can be performed in half of the wing. As well, we have two identical high-order conical motions at points $O_1$ and $O_2$, which are symmetric with respect to $OX_1$ axis but independent to each other; i.e., the interference of the two Mach cones is assumed small.

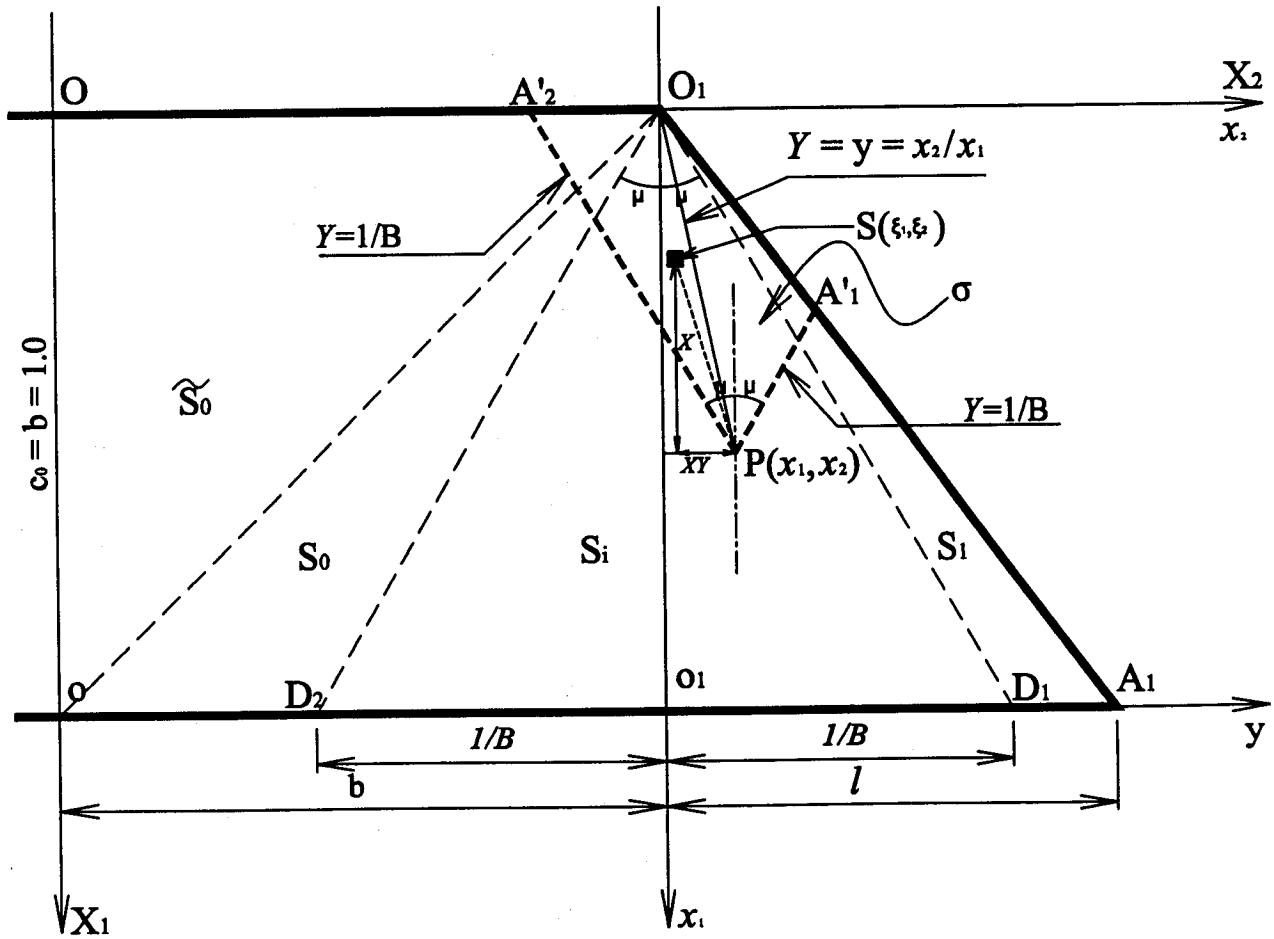


Figure 5.2 Integral limits of the thin trapezoidal wing

Likewise, the integration domain, $\sigma$, representing the specific area of wing surface covered by the forward Mach cone with the vertex at point $P$, can be split into two sections as $\Delta PA'_1O$ and $\Delta POA'_2$. The integral limit in respect of variable $X$ in domain $\Delta PA'_2O$ can be expressed as follows, while in domain $\Delta PA'_1O$, the integral limit in respect of variable $X$ is the same in Eq.(5.2.3-a).

$$X = X_2^* = x_1 . \tag{5.3.1}$$

Accordingly, the integral $I_0$ in respect of thin trapezoidal wing can be recast as

$$\begin{aligned} I_0 &= \iint \frac{X^{k+q}Y^q}{\Re} dXdY = \iint_{\Delta PA'_1O} \frac{X^{k+q}Y^q}{\Re} dXdY + \iint_{\Delta POA'_2} \frac{X^{k+q}Y^q}{\Re} dXdY \\ &= \int_{\frac{1}{B}}^{f(y)} \frac{Y^q}{\Re} \left( \int_0^{X_1^*} X^{k+q} dX \right) dY + \int_{f(y)}^{\frac{1}{B}} \frac{Y^q}{\Re} \left( \int_0^{X_2^*} X^{k+q} dX \right) dY \\ &= \int_{\frac{1}{B}}^{f(y)} \frac{X_1^{*k+q+1} Y^q}{(k+q+1)\Re} dY + \int_{f(y)}^{\frac{1}{B}} \frac{X_2^{*k+q+1} Y^q}{(k+q+1)\Re} dY \\ &= \frac{[x_1(l-y)]^{k+q+1}}{k+q+1} \int_{\frac{1}{B}}^{f(y)} \frac{Y^q}{(l-Y)^{k+q+1}\Re} dY + \frac{x_1^{k+q+1}}{k+q+1} \int_{f(y)}^{\frac{1}{B}} \frac{Y^q}{\Re} dY . \end{aligned} \tag{5.3.2}$$

The analytical solutions to the first integral in Eq.(5.3.2) have been carried out in Eq.(5.2.5-a), (5.2.6-a), and (5.2.9-a) ~ (5.2.9-c) by the recurrence formulae. Similarly, the second integral in Eq.(5.3.2) can also be calculated by the recurrence formulae.

Denote $\int_{f(y)}^{\frac{1}{B}} Y^p \Re dY$ by $\tilde{J}_p$, where $p$ is the power of $Y$ and equal to $q$.

$$\begin{aligned} \tilde{J}_p &= \int_{f(y)}^{\frac{1}{B}} Y^p \Re dY = \int_{f(y)}^{\frac{1}{B}} \frac{Y^p \Re^2}{\Re} dY = \int_{f(y)}^{\frac{1}{B}} \frac{Y^p \left(1 - B^2 Y^2\right)}{\Re} dY \\ &= \int_{f(y)}^{\frac{1}{B}} \frac{Y^p}{\Re} dY - B^2 \int_{f(y)}^{\frac{1}{B}} \frac{Y^{p+2}}{\Re} dY . \end{aligned} \tag{5.3.3}$$

On the other hand, by integrating by parts, integral $\tilde{J}_p$ is given by

$$\tilde{J}_p = \int_{f(y)}^{\frac{1}{B}} Y^p \Re dY = \frac{Y^{p+1}}{p+1}\Big|_{f(y)}^{\frac{1}{B}} + \int_{f(y)}^{\frac{1}{B}} \frac{Y^{p+1}}{p+1} \frac{B^2 Y}{\sqrt{1-B^2Y^2}} dY$$

$$= -\frac{\sqrt{1-B^2(f(y))^2}}{p+1}(f(y))^{p+1} + \frac{B^2}{p+1}\int_{f(y)}^{\frac{1}{B}} \frac{Y^{p+2}}{\Re} dY . \tag{5.3.4}$$

By rearranging Eq.(5.3.3) and Eq.(5.3.4), the recurrence formulae for integral $\tilde{J}_p$ are given by

$$\tilde{J}_p = \int_{f(y)}^{\frac{1}{B}} \frac{Y^p}{\Re} dY = \frac{p-1}{B^2 p}\left( \frac{\sqrt{1-B^2(f(y))^2}}{p-1}(f(y))^{p-1} + \tilde{J}_{p-2} \right), \text{ for } p \geq 2. \tag{5.3.5}$$

$$\tilde{J}_p = \int_{f(y)}^{\frac{1}{B}} \frac{1}{\Re} dY = \frac{1}{B}\left( \frac{\pi}{2} - \sin^{-1}(Bf(y)) \right), \text{ for } p = 0. \tag{5.3.6}$$

$$\tilde{J}_p = \int_{f(y)}^{\frac{1}{B}} \frac{\overline{Y}}{\underline{R}} d\overline{Y} = \frac{1}{B^2}\sqrt{1-B^2(f(y))^2}, \text{ for } p = 1, \tag{5.3.7}$$

where $\tilde{J}_p = \int_{f(y)}^{\frac{1}{B}} \frac{Y^p}{\Re} dY$ and $\tilde{J}_{p-2} = \int_{f(y)}^{\frac{1}{B}} \frac{Y^{p-2}}{\Re} dY$.

As a result, the analytical solutions to integral, $I_0$, and its derivative in respect to $x_1$ with limits for thin trapezoidal wing are given separately based on the location of point $P(x_1, x_2)$.

**For position in area** $S_1$, $\frac{1}{B} \leq y \leq l_1$ and $f(y) = \frac{1}{B}$.

$$I_0 = \frac{[x_1(l-y)]^{k+q+1}}{k+q+1} \int_{\frac{1}{B}}^{\frac{1}{B}} \frac{Y^q}{(l-Y)^{k+q+1}\Re} dY . \tag{5.3.8}$$

$$\frac{\partial}{\partial x_1} I_0 = l[x_1(l-y)]^{k+q} \int_{\frac{1}{B}}^{\frac{1}{B}} \frac{Y^q}{(l-Y)^{k+q+1}\Re} dY . \tag{5.3.9}$$

**For position in area $S_i$,** $-\frac{1}{B} \le y \le \frac{1}{B}$ and $f(y) = y$.

$$I_0 = \frac{[x_1(l-y)]^{k+q+1}}{k+q+1} \int_{\frac{1}{B}}^{f(y)} \frac{Y^q}{(l-Y)^{k+q+1}\Re} dY + \frac{x_1^{k+q+1}}{k+q+1} \int_{f(y)}^{\frac{1}{B}} \frac{Y^q}{\Re} dY. \tag{5.3.10}$$

$$\frac{\partial}{\partial x_1} I_0 = l[x_1(l-y)]^{k+q} \int_{\frac{1}{B}}^{y} \frac{Y^q}{(l-Y)^{k+q+1}\Re} dY + \frac{[x_1(l-y)]^{k+q+1}}{k+q+1} \frac{\partial}{\partial x_1} \left( \int_{\frac{1}{B}}^{y} \frac{Y^q}{(l-Y)^{k+q+1}\Re} dY \right) +$$

$$x_1^{k+q} \int_{y}^{\frac{1}{B}} \frac{Y^q}{\Re} dY + \frac{x_1^{k+q+1}}{k+q+1} \frac{\partial}{\partial x_1} \left( \int_{y}^{\frac{1}{B}} \frac{Y^q}{\Re} dY \right), \tag{5.3.11}$$

where the derivative of integral $\int_{\frac{1}{B}}^{y} \frac{Y^q}{(l-Y)^{k+q+1}\Re} dY$ and $\int_{y}^{\frac{1}{B}} \frac{Y^q}{\Re} dY$ with respect to $x_1$ can be derived as

$$\frac{\partial}{\partial x_1} \left( \int_{\frac{1}{B}}^{y} \frac{Y^q}{(l-Y)^{k+q+1}\Re} dY \right) = \sum_{f=0}^{q} (-1)^f C_f^q l^{q-f} \frac{\partial I_g}{\partial x_1} = -\frac{x_2}{x_1^2} \sum_{f=0}^{q} (-1)^f C_f^q l^{q-f} \frac{\partial I_g}{\partial y}, \tag{5.3.12}$$

$$\frac{\partial}{\partial x_1} \left( \int_{y}^{\frac{1}{B}} \frac{Y^q}{\Re} dY \right) = \frac{\partial \tilde{J}_p}{\partial x_1} = -\frac{y}{x_1} \frac{p-1}{B^2 p} \frac{\partial}{\partial y} \left( \frac{\sqrt{1-B^2y^2}}{p-1} y^{p-1} + \tilde{J}_{p-2} \right)$$

$$= -\frac{y}{x_1} \frac{p-1}{B^2 p} \left( \frac{-B^2}{p-1} \frac{y^p}{\sqrt{1-B^2y^2}} + \sqrt{1-B^2y^2} \times y^{p-2} + \frac{\partial \tilde{J}_{p-2}}{\partial y} \right), \text{ for } p \ge 2. \tag{5.3.13}$$

The derivatives of $I_g$ and $\tilde{J}_g$ with respect to y are derived based on the recurrence formulae.

For $g \ge 2$,

$$\frac{\partial I_g}{\partial y} = \frac{1}{1-B^2l^2} \left[ \frac{(g-1)|1-B^2y^2| - B^2y(l-y)}{(g-1)(l-y)^g \sqrt{1-B^2y^2}} + B^2 l \frac{3-2g}{g-1} \frac{\partial I_{g-1}}{\partial y} + B^2 \frac{g-2}{g-1} \frac{\partial I_{g-2}}{\partial y} \right]. \tag{5.3.14}$$

For $g = 1$,

$$\frac{\partial I_g}{\partial y} = \frac{1}{(l-y)\sqrt{1-B^2y^2}} \tag{5.3.15}$$

For $p = 0$,

$$\frac{\partial \tilde{J}_p}{\partial x_1} = \frac{\partial}{\partial x_1}\left( \int_y^{\frac{1}{B}} \frac{1}{\Re} dY \right) = \frac{y}{x_1\sqrt{1-B^2y^2}} \tag{5.3.16}$$

For $p = 1$,

$$\frac{\partial \tilde{J}_p}{\partial x_1} = \frac{\partial}{\partial x_1}\left( \int_y^{\frac{1}{B}} \frac{Y}{\Re} dY \right) = \frac{y^2}{x_1\sqrt{1-B^2y^2}} \tag{5.3.17}$$

**For position in area** $\tilde{S}_0$ **and** $S_0$, $-l_2 \le y \le -\frac{1}{B}$ and $f(y) = -\frac{1}{B}$.

$$I_0 = \frac{x_1^{\,k+q+1}}{k+q+1} \int_{-\frac{1}{B}}^{\frac{1}{B}} \frac{Y^q}{\Re} dY . \tag{5.3.18}$$

$$\frac{\partial}{\partial x_1} I_0 = x_1^{\,k+q} \int_{-\frac{1}{B}}^{\frac{1}{B}} \frac{Y^q}{\Re} dY \tag{5.3.19}$$

In turn, calculations of the lift coefficient and the pitching moment coefficient for trapezoidal wing models in steady supersonic flow are performed by integrating the integral $I_0$ for half of the wing plane form. As can be seen in figure 5.2, the half wing plane form is divided into four integral domains: $\tilde{S}_0$ and $S_0$, the first and second parts of the left hand surface outside the Mach cone, $S_i$, the surface inside the Mach cone, and $S_1$, the right hand surface outside the Mach cone. Within these specific integration domains, $I_g$ is zero and $\tilde{J}_g$ is constant for integration domains in $\tilde{S}_0$ and $S_0$, and for integration domain within $S_i$, $\tilde{J}_g$ is zero, and $I_g$ is constant. For integration domain inside the Mach cone, both $\tilde{J}_g$ and $I_g$ are function of y and thus, detailed expression used in the calculation of the aerodynamic coefficients are given in Appendix C.

# CHAPTER 6

# PRESENT UNSTEADY FLOW SOLUTIONS FOR OSCILLATING WINGS

## 6.1 General unsteady flow solutions for oscillating thin wings

Firstly, the reduced pressure coefficient of oscillating thin wings derived by Eq.(2.4.3) is recalled as

$$\hat{C}p = -2e^{ikx_1}\left[\frac{\partial\Phi}{\partial x_1} - \frac{i\lambda}{B^2}\Phi\right] = -2e^{ikx_1}\left[\frac{\partial\Phi}{\partial x_1} - \frac{ik}{M_\infty^2}\Phi\right], \tag{6.1.1}$$

where the analytical solutions to $\frac{\partial\Phi}{\partial x_1}$ and $\Phi$ are essential at this stage. According to Eq.(4.2.19), $\Phi$ has been carried out explicitly and recalled as

$$\Phi(x_1,x_2) = -\frac{1}{\pi}e^{-ikx_1}\iint_S \frac{\hat{W}(\xi_1,\xi_2)}{R}e^{ik(x_1-\xi_1)}\cos\left(\frac{KR}{B}\right)d\xi_1 d\xi_2 \,. \tag{6.1.2}$$

Let's also consider the coordinate transformation with the relations as shown in Eq.(5.1.2) and $\hat{W}(\xi_1,\xi_2)$, $R$, $d\xi_1 d\xi_2$, $e^{ik(x_1-\xi_1)}$, and $\cos\left(\frac{KR}{B}\right)$ in Eq.(6.1.2) can be recast as functions of the transformed variables $X$ and $Y$. Firstly, $e^{ik(x_1-\xi_1)}$ and $\cos\left(\frac{KR}{B}\right)$ can be expressed analytically by Taylor expansion series as

$$e^{ik(x_1-\xi_1)} = e^{ikX} = 1 + ikX + \frac{1}{2!}(ikX)^2 + \frac{1}{3!}(ikX)^3 + \ldots = 1 + \sum_{j_1}^{J_1} \frac{1}{j_1!}(ikX)^{j_1} = 1 + S_1, \tag{6.1.3}$$

where $S_1 = \sum_{j_1}^{J_1} \frac{1}{j_1!}(ikX)^{j_1}$.

$$\cos\left(\frac{KR}{B}\right) = \cos\left(\frac{kX}{M_\infty}\Re\right) = 1 - \frac{1}{2!}\left(\frac{kX}{M_\infty}\Re\right)^2 + \frac{1}{4!}\left(\frac{kX}{M_\infty}\Re\right)^4 - \frac{1}{6!}\left(\frac{kX}{M_\infty}\Re\right)^6 + \ldots$$

$$= 1 + \sum_{j_2=1}^{J_2} \frac{1}{(2j_2)!}(-1)^{j_2}\left(\frac{kX}{M_\infty}\Re\right)^{2j_2} = 1 + S_2, \tag{6.1.4}$$

where $S_2 = \sum_{j_2=1}^{J_2} \frac{1}{(2j_2)!}(-1)^{j_2}\left(\frac{kX}{M_\infty}\Re\right)^{2j_2}$.

Thus the product of $e^{ik(x_1-\xi_1)}$ and $\cos\left(\frac{KR}{B}\right)$ by Taylor expansion series is expressed as

$$e^{ikX}\cos\left(\frac{kX}{M_\infty}\Re\right) = 1 + S_1 + S_2 + S_1S_2. \tag{6.1.5}$$

According, by substituting Eq. (5.1.3) ~ (5.1.5), and (6.1.5) into Eq.(6.1.2), the reduced velocity potential, $\Phi$, can be recast as

$$\Phi(X,Y) = -\frac{1}{\pi}e^{-ikx_1}\iint_\sigma w_0(X,Y)\frac{1}{R}(1 + S_1 + S_2 + S_1S_2)dXdY$$

$$= \Phi_0 + \Phi_1 + \Phi_2 + \Phi_{12}, \tag{6.1.6}$$

where

$$\Phi_0 = -\frac{1}{\pi}e^{-ikx_1}\iint_\sigma w_0(X,Y)\frac{1}{\Re}dXdY, \tag{6.1.7}$$

$$\Phi_1 = -\frac{1}{\pi}e^{-ikx_1}\iint_\sigma w_0(X,Y)\frac{1}{\Re}S_1dXdY, \tag{6.1.8}$$

$$\Phi_2 = -\frac{1}{\pi}e^{-ikx_1}\iint_\sigma w_0(X,Y)\frac{1}{\Re}S_2dXdY, \tag{6.1.9}$$

$$\Phi_{12} = -\frac{1}{\pi}e^{-ikx_1}\iint_\sigma w_0(X,Y)\frac{1}{\Re}S_1S_2dXdY. \tag{6.1.10}$$

By substituting the unified expression of $w_0(X,Y)$ with homogeneous polynomial series in $X$ and $Y$, all above equations from (6.1.7) ~ (6.1.10) can then be recast as

$$\Phi_0 = -\frac{1}{\pi} e^{-ikx_1} \left\{ \sum_{n=0}^{N} \sum_{j=0}^{n} w_{n-j,j} \overline{L}_0 \left[ \sum_{k=0}^{n-j} \sum_{q=0}^{j} x_1^{n-j-k} x_2^{j-q} I_0 \right] \right\}, \tag{6.1.11}$$

where $I_0 = \iint_{\Re} \frac{X^{k+q} Y^q}{\Re} dXdY$ and $\overline{L}_0 = C_k^{n-j} C_q^j (-1)^{k+q}$.

$$\Phi_1 = -\frac{1}{\pi} e^{-ikx_1} \left\{ \sum_{n=0}^{N} \sum_{j=0}^{n} w_{n-j,j} \overline{L}_0 \left[ \sum_{k=0}^{n-j} \sum_{q=0}^{j} \sum_{s=1}^{S} \overline{L}_1 x_1^{n-j-k} x_2^{j-q} I_1 \right] \right\}, \tag{6.1.12}$$

where $I_1 = \iint_{\Re} \frac{X^{k+q+s} Y^q}{\Re} dXdY$ and $\overline{L}_1 = \frac{1}{s!}(ik)^s$.

$$\Phi_2 = -\frac{1}{\pi} e^{-ikx_1} \left\{ \sum_{n=0}^{N} \sum_{j=0}^{n} w_{n-j,j} \overline{L}_0 \left[ \sum_{k=0}^{n-j} \sum_{q=0}^{j} \sum_{r=1}^{R} \sum_{t=0}^{r} \overline{L}_2 x_1^{n-j-k} x_2^{j-q} I_2 \right] \right\}, \tag{6.1.13}$$

where $I_2 = \iint_{\Re} \frac{X^{k+q+2r} Y^{q-2t+2r}}{\Re} dXdY$ and $\overline{L}_2 = \frac{(-1)^r}{(2r)!} \left( \frac{k}{M_\infty} \right)^{2r} C_t^r \left( -B^2 \right)^{r-t}$.

$$\Phi_{12} = -\frac{1}{\pi} e^{-ikx_1} \left\{ \sum_{n=0}^{N} \sum_{j=0}^{n} w_{n-j,j} \overline{L}_0 \left[ \sum_{k=0}^{n-j} \sum_{q=0}^{j} \sum_{s=1}^{S} \sum_{r=1}^{R} \sum_{t=0}^{r} \overline{L}_{12} x_1^{n-j-k} x_2^{j-q} I_{12} \right] \right\}, \tag{6.1.14}$$

where $I_{12} = \iint_{\Re} \frac{X^{k+q+s+2r} Y^{q-2t+2r}}{\Re} dXdY$ and $\overline{L}_{12} = \overline{L}_1 \overline{L}_2$.

And the derivative of $\Phi$ with respect to $x_1$ is calculated as

$$\frac{\partial \Phi}{\partial x_1} = \frac{\partial \Phi_0}{\partial x_1} + \frac{\partial \Phi_1}{\partial x_1} + \frac{\partial \Phi_2}{\partial x_1} + \frac{\partial \Phi_{12}}{\partial x_1}. \tag{6.1.15}$$

Likely, each term of Eq.(6.1.15) can be derived separately as

$$\frac{\partial \Phi_0}{\partial x_1} = (-ik)\Phi_0 - \frac{1}{\pi} e^{-ikx_1} \left\{ \sum_{n=0}^{N} \sum_{j=0}^{n} w_{n-j,j} \bar{L}_0 \left[ \sum_{k=0}^{n-j} \sum_{q=0}^{j} (n-j-k) x_1^{n-j-k-1} x_2^{j-q} I_0 + x_1^{n-j-k} x_2^{j-q} \frac{\partial I_0}{\partial x_1} \right] \right\}. \quad (6.1.16)$$

$$\frac{\partial \Phi_1}{\partial x_1} = (-ik)\Phi_1 - \frac{1}{\pi} e^{-ikx_1} \left\{ \sum_{n=0}^{N} \sum_{j=0}^{n} w_{n-j,j} \bar{L}_0 \left[ \sum_{k=0}^{n-j} \sum_{q=0}^{j} \sum_{s=1}^{S} \bar{L}_1 \left( (n-j-k) x_1^{n-j-k-1} x_2^{j-q} I_1 + x_1^{n-j-k} x_2^{j-q} \frac{\partial I_1}{\partial x_1} \right) \right] \right\}. \quad (6.1.17)$$

$$\frac{\partial \Phi_2}{\partial x_1} = (-ik)\Phi_2 - \frac{1}{\pi} e^{-ikx_1} \left\{ \sum_{n=0}^{N} \sum_{j=0}^{n} w_{n-j,j} \bar{L}_0 \left[ \sum_{k=0}^{n-j} \sum_{q=0}^{j} \sum_{r=1}^{R} \sum_{t=0}^{r} \bar{L}_2 \left( (n-j-k) x_1^{n-j-k-1} x_2^{j-q} I_2 + x_1^{n-j-k} x_2^{j-q} \frac{\partial I_2}{\partial x_1} \right) \right] \right\}. \quad (6.1.18)$$

$$\frac{\partial \Phi_{12}}{\partial x_1} = (-ik)\Phi_{12} - \frac{1}{\pi} e^{-ikx_1} \left\{ \sum_{n=0}^{N} \sum_{j=0}^{n} w_{n-j,j} \bar{L}_0 \left[ \sum_{k=0}^{n-j} \sum_{q=0}^{j} \sum_{s=1}^{S} \sum_{r=1}^{R} \sum_{t=0}^{r} \bar{L}_{12} \left( (n-j-k) x_1^{n-j-k-1} x_2^{j-q} I_{12} + x_1^{n-j-k} x_2^{j-q} \frac{\partial I_{12}}{\partial x_1} \right) \right] \right\}. \quad (6.1.19)$$

Accordingly, the reduced pressure coefficient can then be expressed by method of pulsating sources distribution over wing surfaces by substituting Eq.(6.1.11) ~ (6.1.14) and Eq.(6.1.16) ~ (6.1.19) into Eq.(6.1.1).

$$\hat{C}p = \frac{2}{\pi} \sum_{n=0}^{N} \sum_{j=0}^{n} w_{n-j,j} \left\{ \sum_{k=0}^{n-j} \sum_{q=0}^{j} \bar{L}_0 \left[ \left( (n-k-q) x_1^{n-k-q-1} y^{j-q} + i\lambda x_1^{n-k-q} y^{j-q} \right) \left( I_0 + \sum_{s=1}^{S} \bar{L}_1 I_1 + \sum_{r=1}^{R} \sum_{t=0}^{r} \bar{L}_2 I_2 + \sum_{s=1}^{S} \sum_{r=1}^{R} \sum_{t=0}^{r} \bar{L}_{12} I_{12} \right) \right.$$

$$\left. + x_1^{n-k-q} y^{j-q} \left( \frac{\partial I_0}{\partial x_1} + \sum_{s=1}^{S} \bar{L}_1 \frac{\partial I_1}{\partial x_1} + \sum_{r=1}^{R} \sum_{t=0}^{r} \bar{L}_2 \frac{\partial I_2}{\partial x_1} + \sum_{s=1}^{S} \sum_{r=1}^{R} \sum_{t=0}^{r} \bar{L}_{12} \frac{\partial I_{12}}{\partial x_1} \right) \right] \right\}, \quad (6.1.20)$$

where $\lambda = \frac{\omega}{U_\infty}$ by taking the root chord $c_0 = 1.0$.

The present solutions to the calculation of the reduced lift coefficient, the pitching moment coefficient, and the rolling moment coefficient can be carried out by performing the integration of Eq.(6.1.20) through the whole wing area denoted by $S$ directly.

$$\hat{C}_l = \frac{-4}{S\pi}\sum_{n=0}^{N}\sum_{j=0}^{n} w_{n-j,j}\left\{\sum_{k=0}^{n-j}\sum_{q=0}^{j}\overline{L}_0\left[(n-k-q)\left(\int_S x_1^{n-j-k}y^{j-q}I_0dx_1dy + \sum_{s=1}^{S}\overline{L}_1\int_S x_1^{n-j-k}y^{j-q}I_1dx_1dy + \right.\right.\right.$$

$$\left.\sum_{r=1}^{R}\sum_{t=0}^{r}\overline{L}_2\int_S x_1^{n-j-k}y^{j-q}I_2dx_1dy + \sum_{s=1}^{S}\sum_{r=1}^{R}\sum_{t=0}^{r}\overline{L}_{12}\int_S x_1^{n-j-k}y^{j-q}I_{12}dx_1dy\right)$$

$$+i\lambda\left(\int_S x_1^{n-j-k+1}y^{j-q}I_0dx_1dy + \sum_{s=1}^{S}\overline{L}_1\int_S x_1^{n-j-k+1}y^{j-q}I_1dx_1dy + \right.$$

$$\left.\sum_{r=1}^{R}\sum_{t=0}^{r}\overline{L}_2\int_S x_1^{n-j-k+1}y^{j-q}I_2dx_1dy + \sum_{s=1}^{S}\sum_{r=1}^{R}\sum_{t=0}^{r}\overline{L}_{12}\int_S x_1^{n-j-k+1}y^{j-q}I_{12}dx_1dy\right)$$

$$+\left(\int_S\left(x_1^{n-k-q+1}y^{j-q}\right)\frac{\partial I_0}{\partial x_1}dx_1dy + \sum_{s=1}^{S}\overline{L}_1\int_S\left(x_1^{n-k-q+1}y^{j-q}\right)\frac{\partial I_1}{\partial x_1}dx_1dy + \right.$$

$$\left.\left.\left.\sum_{r=1}^{R}\sum_{t=0}^{r}\overline{L}_2\int_S\left(x_1^{n-k-q+1}y^{j-q}\right)\frac{\partial I_2}{\partial x_1}dx_1dy + \sum_{s=1}^{S}\sum_{r=1}^{R}\sum_{t=0}^{r}\overline{L}_{12}\int_S\left(x_1^{n-k-q+1}y^{j-q}\right)\frac{\partial I_{12}}{\partial x_1}dx_1dy\right)\right]\right\}. \quad (6.1.21)$$

$$\hat{C}_{m2} = \frac{-4}{c_0S\pi}\sum_{n=0}^{N}\sum_{j=0}^{n} w_{n-j,j}\left\{\sum_{k=0}^{n-j}\sum_{q=0}^{j}\overline{L}_0\left[(n-k-q)\left(\int_S x_1^{n-j-k+1}y^{j-q}I_0dx_1dy + \sum_{s=1}^{S}\overline{L}_1\int_S x_1^{n-j-k+1}y^{j-q}I_1dx_1dy + \right.\right.\right.$$

$$\left.\sum_{r=1}^{R}\sum_{t=0}^{r}\overline{L}_2\int_S x_1^{n-j-k+1}y^{j-q}I_2dx_1dy + \sum_{s=1}^{S}\sum_{r=1}^{R}\sum_{t=0}^{r}\overline{L}_{12}\int_S x_1^{n-j-k+1}y^{j-q}I_{12}dx_1dy\right)$$

$$+i\lambda\left(\int_S x_1^{n-j-k+2}y^{j-q}I_0dx_1dy + \sum_{s=1}^{S}\overline{L}_1\int_S x_1^{n-j-k+2}y^{j-q}I_1dx_1dy + \right.$$

$$\left.\sum_{r=1}^{R}\sum_{t=0}^{r}\overline{L}_2\int_S x_1^{n-j-k+2}y^{j-q}I_2dx_1dy + \sum_{s=1}^{S}\sum_{r=1}^{R}\sum_{t=0}^{r}\overline{L}_{12}\int_S x_1^{n-j-k+2}y^{j-q}I_{12}dx_1dy\right)$$

$$+\left(\int_S\left(x_1^{n-k-q+2}y^{j-q}\right)\frac{\partial I_0}{\partial x_1}dx_1dy + \sum_{s=1}^{S}\overline{L}_1\int_S\left(x_1^{n-k-q+2}y^{j-q}\right)\frac{\partial I_1}{\partial x_1}dx_1dy + \right.$$

$$\left.\left.\left.\sum_{r=1}^{R}\sum_{t=0}^{r}\overline{L}_2\int_S\left(x_1^{n-k-q+2}y^{j-q}\right)\frac{\partial I_2}{\partial x_1}dx_1dy + \sum_{s=1}^{S}\sum_{r=1}^{R}\sum_{t=0}^{r}\overline{L}_{12}\int_S\left(x_1^{n-k-q+2}y^{j-q}\right)\frac{\partial I_{12}}{\partial x_1}dx_1dy\right)\right]\right\}. \quad (6.1.22)$$

$$\hat{C}_{m1}=\frac{-4}{(2b)S\pi}\sum_{n=0}^{N}\sum_{j=0}^{n}w_{n-j,j}\left\{\sum_{k=0}^{n-j}\sum_{q=0}^{j}\overline{L}_0\left[(n-k-q)\left(\int_S x_1^{n-j-k+1}y^{j-q+1}I_0dx_1dy+\sum_{s=1}^{S}\overline{L}_1\int_S x_1^{n-j-k+1}y^{j-q+1}I_1dx_1dy+\right.\right.\right.$$

$$\sum_{r=1}^{R}\sum_{t=0}^{r}\overline{L}_2\int_S x_1^{n-j-k+1}y^{j-q+1}I_2dx_1dy+\sum_{s=1}^{S}\sum_{r=1}^{R}\sum_{t=0}^{r}\overline{L}_{12}\int_S x_1^{n-j-k+1}y^{j-q+1}I_{12}dx_1dy$$

$$+i\lambda\left(\int_S x_1^{n-j-k+2}y^{j-q+1}I_0dx_1dy+\sum_{s=1}^{S}\overline{L}_1\int_S x_1^{n-j-k+2}y^{j-q+1}I_1dx_1dy+\right.$$

$$\sum_{r=1}^{R}\sum_{t=0}^{r}\overline{L}_2\int_S x_1^{n-j-k+2}y^{j-q+1}I_2dx_1dy+\sum_{s=1}^{S}\sum_{r=1}^{R}\sum_{t=0}^{r}\overline{L}_{12}\int_S x_1^{n-j-k+2}y^{j-q+1}I_{12}dx_1dy$$

$$+\left(\int_S\left(x_1^{n-k-q+2}y^{j-q+1}\right)\frac{\partial I_0}{\partial x_1}dx_1dy+\sum_{s=1}^{S}\overline{L}_1\int_S\left(x_1^{n-k-q+2}y^{j-q+1}\right)\frac{\partial I_1}{\partial x_1}dx_1dy+\right.$$

$$\left.\left.\left.\sum_{r=1}^{R}\sum_{t=0}^{r}\overline{L}_2\int_S\left(x_1^{n-k-q+2}y^{j-q+1}\right)\frac{\partial I_2}{\partial x_1}dx_1dy+\sum_{s=1}^{S}\sum_{r=1}^{R}\sum_{t=0}^{r}\overline{L}_{12}\int_S\left(x_1^{n-k-q+2}y^{j-q+1}\right)\frac{\partial I_{12}}{\partial x_1}dx_1dy\right)\right]\right\}. \quad (6.1.23)$$

## 6.2 Calculation of integral for oscillating thin delta wing

In order to accomplish the calculations of those aerodynamic coefficients for thin delta wing executing harmonic oscillations in supersonic flows, the integrals, $I_0$, $I_1$, $I_2$, and $I_{12}$, and their derivatives in respect to $x_1$ would need to be performed exclusively on the basis of the geometrical configuration. For convenience, we arrange the calculation of integral systematically and denote the general integral by $I_{i_1,i_2}$ defined as

$$I_{i_1,i_2} = \iint_{\mathcal{S}} \frac{X^{i_1} Y^{i_2}}{\Re} dXdY = \frac{[x_1(l-y)]^{i_1+1}}{i_1+1} \int_{\frac{1}{B}}^{f(y)} \frac{Y^{i_2}}{(l-Y)^{i_1+1}\Re} dY + \frac{[x_1(l+y)]^{i_1+1}}{i_1+1} \int_{f(y)}^{\frac{1}{B}} \frac{Y^{i_2}}{(l+Y)^{i_1+1}\Re} dY, \quad (6.2.1)$$

where $i_1$ and $i_2$ are powers of variables $X$ and $Y$, respectively and $\Re = \sqrt{1-B^2Y^2}$.

Thus, the integrals, $I_0$, $I_1$, $I_2$, and $I_{12}$, can be defined in terms of $i_1$ and $i_2$ as

- For integral $I_0$, $i_1 = k+q$ and $i_2 = q$.
- For integral $I_1$, $i_1 = k+q+s$ and $i_2 = q$.
- For integral $I_2$, $i_1 = k+q+2r$ and $i_2 = q-2t+2r$.
- For integral $I_{12}$, $i_1 = k+q+s+2r$ and $i_2 = q-2t+2r$.

The expressions for these integrals perform in this case are given in Appendix D.

In turn, calculations of the lift coefficient, pitching moment coefficient, and the rolling moment coefficient can then be performed by integrating $I_{i_1,i_2}$ over the delta wing surface denoted as $S$. The detailed expressions for performing the integral for $I_{i_1,i_2}$ used in the calculation of the aerodynamic coefficients are given in Appendix C.

## 6.3 Calculation of integral for oscillating thin trapezoidal wing

For trapezoidal wings executing unsteady motions in supersonic flows, the calculations of those aerodynamic coefficients can be carried out by performing the calculation of integrals, $I_0$, $I_1$, $I_2$, $I_{12}$, and their derivatives with respect to $x_1$. Similarly, we denote the general integral by $I_{i_1,i_2}$ and we have

$$I_{i_1,i_2} = \iint_{\mathfrak{D}} \frac{X^{i_1} Y^{i_2}}{\mathfrak{R}} dXdY = \frac{[x_1(l-y)]^{i_1+1}}{i_1+1} \int_{\frac{1}{B}}^{f(y)} \frac{Y^{i_2}}{(l-Y)^{i_1+1}\mathfrak{R}} dY + \frac{x_1^{i_1+1}}{i_1+1} \int_{f(y)}^{\frac{1}{B}} \frac{Y^{i_2}}{\mathfrak{R}} dY, \tag{6.3.1}$$

where $i_1$ and $i_2$ are powers of variables $X$ and $Y$, respectively.

Accordingly, the integrals, $I_0$, $I_1$, $I_2$, $I_{12}$, respectively can be expressed in terms of $i_1$ and $i_2$ as

- For integral $I_0$, $i_1 = k+q$ and $i_2 = q$
- For integral $I_1$, $i_1 = k+q+s$ and $i_2 = q$
- For integral $I_2$, $i_1 = k+q+2r$ and $i_2 = q-2t+2r$
- For integral $I_{12}$, $i_1 = k+q+s+2r$ and $i_2 = q-2t+2r$

The expressions for these integrals perform in this case are given in Appendix D.

In turn, the calculations of the lift coefficient, pitching moment coefficient, and rolling moment coefficient for trapezoidal wing executing unsteady motions are performed by integrating the general integral $I_{i_1,i_2}$ for half of the trapezoidal wing. As one may recall by considering Figure 5.2 again, we notice that for integration domain within $\widetilde{S}_0$ and $S_0$, $I_g$ is zero, and $\widetilde{J}_g$ is constant, while within the integration domain, $S_1$, $\widetilde{J}_g$ is zero, and $I_g$ is constant, instead. And for integration domain inside the Mach cone, both $\widetilde{J}_g$ and $I_g$ are function of $y$. Accordingly, the detailed expressions used in the calculation of the aerodynamic coefficient are given in Appendix C.

# CHAPTER 7

# RESULTS AND DISCUSSION

## 7.1 Steady flow results for delta wings

The validation of the present method will first be devoted to the cases of thin delta wing in a uniform supersonic flow characterized by $M_\infty = 2.0$ with: (a) symmetry of incidence, $\alpha = -w_{10}x_1 / U_\infty$, and (b) antisymmetry of incidence, $\alpha = -w_{01}x_2 / U_\infty$. The semi-span, $l$, at $x_1 = 1.0$ is equal to 0.75 and for this geometrical configuration, both leading edges are outside the Mach cone with the vertex located at the wing apex and can be considered as supersonic leading edges. As can be seen in both figures 7.1 and 7.2, the variations of $u^{(1)} / w_{10}$ and $u^{(1)} / w_{01}$, which are proportional to the pressure coefficient, are plotted in the spanwise cross-section at $x_1 = 1.0$ and in the longitudinal section at $x_2 = 0.2$, respectively. The present solutions are compared in the same figures with the results obtained by the theory of high order conical flows (Carafoli, Mateescu, Nastase, [2]). An excellent agreement was found between these results.

As well, the lift coefficient, the pitching moment coefficient, and the rolling moment coefficient are also calculated and presented in the following tables 7.1 and 7.2.

| | $C_l$ | $C_{m2}$ | $C_{m1}$ |
|---|---|---|---|
| Present solutions | -0.00226 | -0.00170 | 0 |
| High order conical flow solutions | -0.00226 | -0.00170 | 0 |

Table 7.1 $C_l$, $C_{m2}$, and $C_{m1}$ for steady thin delta wing with supersonic leading edges and symmetry incidence $\alpha = -w_{10}x_1 / U_\infty$.

| | $C_l$ | $C_{m2}$ | $C_{m1}$ |
|---|---|---|---|
| Present solutions | 0 | 0 | 0.00031 |
| High order conical flow solutions | 0 | 0 | 0.00032 |

Table 7.2 $C_l$, $C_{m2}$, and $C_{m1}$ for steady thin delta wing with supersonic leading edges and antisymmetry incidence $\alpha = -w_{01}x_2 / U_\infty$.

Albeit results obtained in steady thin delta wing by both methods are in very good agreement, the present method developed in this thesis permits an enhanced flexibility to cope with cases in higher order approximations without deteriorating the calculation efficiency. Also, with the comparison to the previous method, the present method can easily be applied to unsteady cases from steady solutions directly without further magnificent modification throughout the whole equation system.

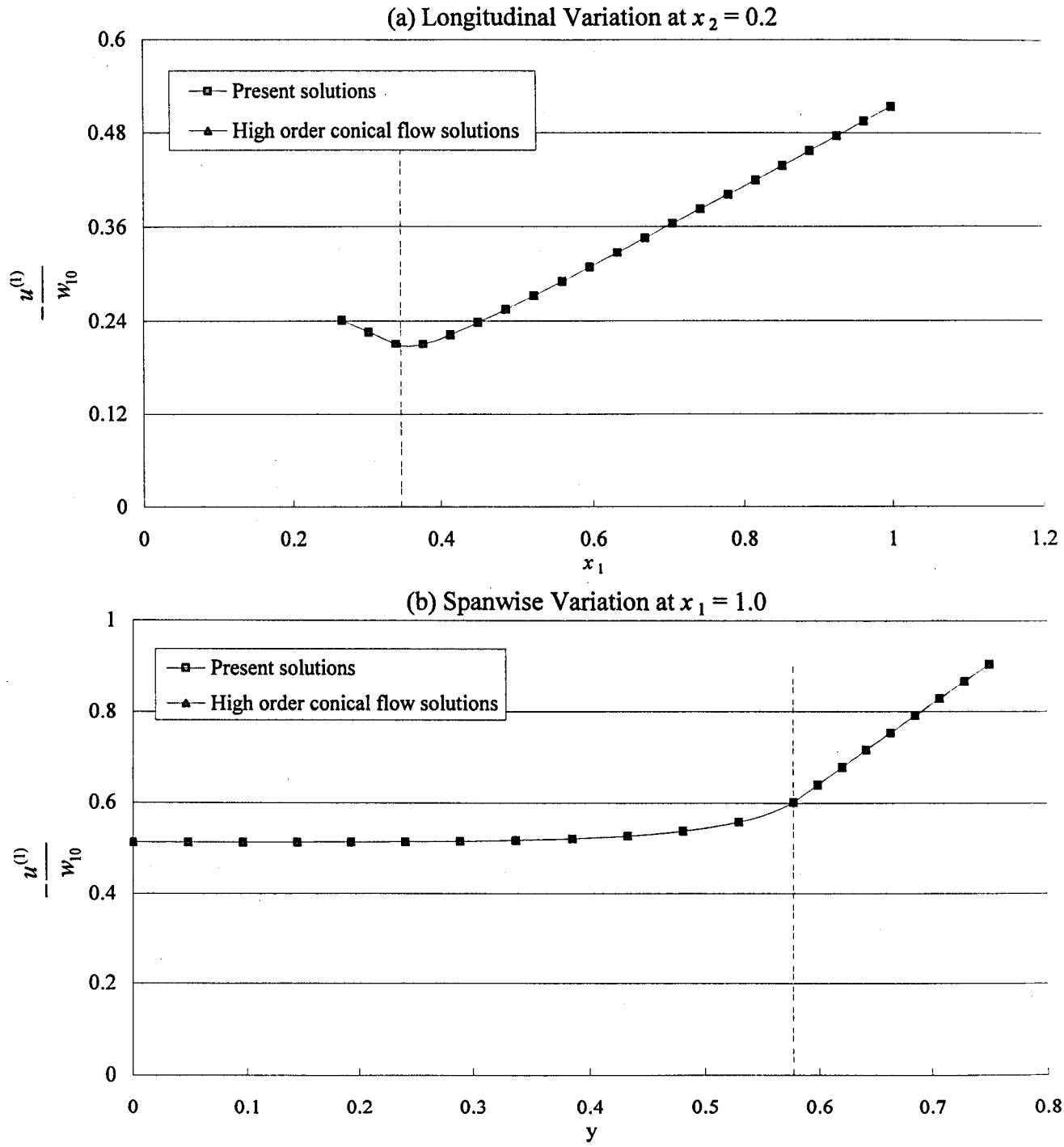


Figure 7.1 The longitudinal and spanwise variation of the axial velocity for steady thin delta wing with supersonic leading edges and symmetry of incidence $\alpha = -w_{10}x_1 / U_\infty$. (root chord, $c_0 = 1.0$; semi-span, $l = 0.75$; Mach number, $M_\infty = 2.0$)

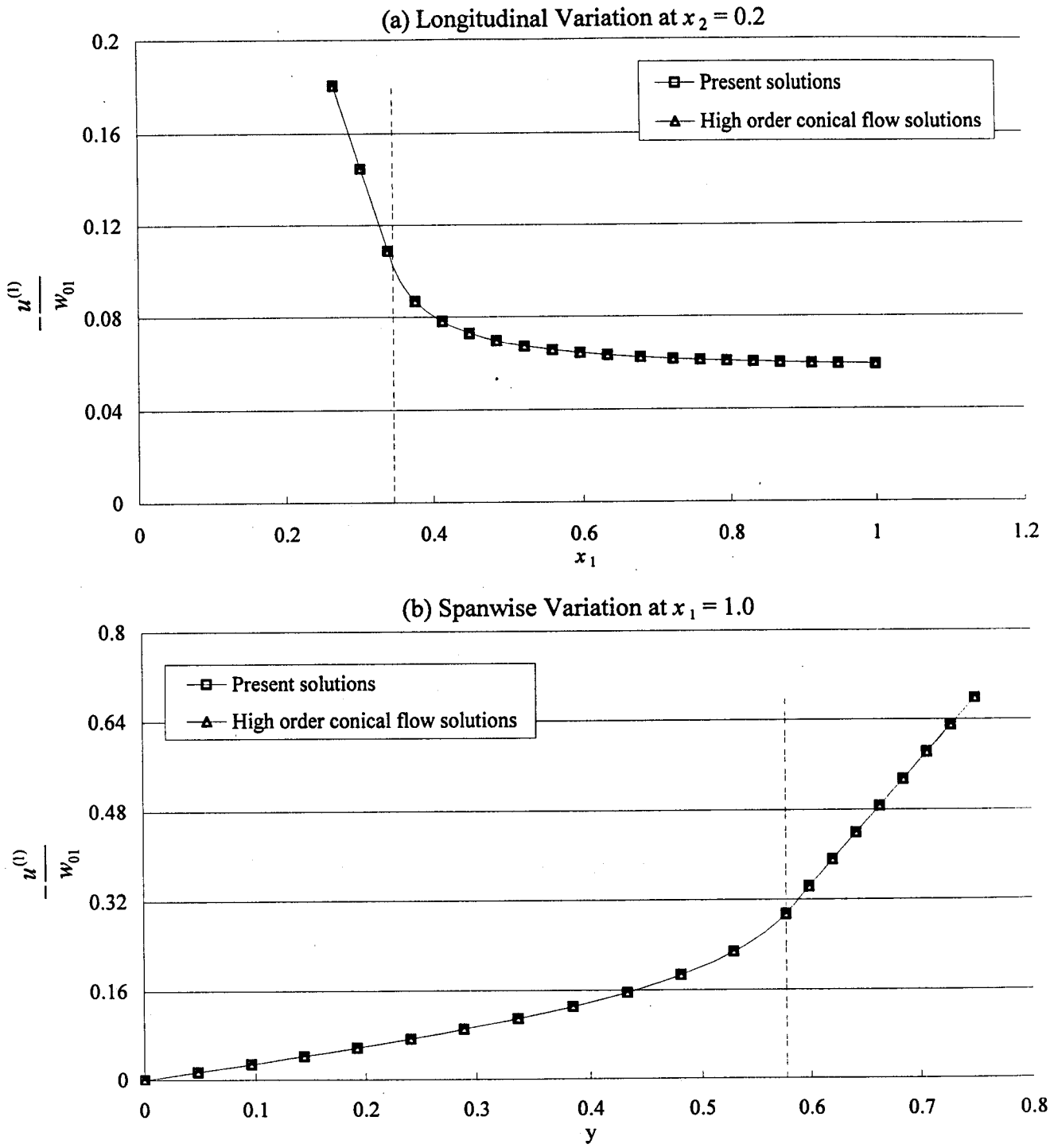


Figure 7.2 The longitudinal and spanwise variation of the axial velocity for steady thin delta wing with supersonic leading edges and antisymmetry of incidence $\alpha = -w_{01}x_2 / U_\infty$. (root chord, $c_0$ = 1.0; semi-span, $l$ = 0.75; Mach number, $M_\infty$ = 2.0)

## 7.2 Steady flow results for trapezoidal wings

Similarly, we consider the thin trapezoidal wing with wing span, $b$, is equal to 1.0 and the wing semi-span, $l$, is 0.75, placing in a uniform supersonic flow, characterized by $M_\infty = 2.0$ with incidence $\alpha = -w_{10}x_1 / U_\infty$. The spanwise variation of the perturbation axial velocity in the cross-section of trapezoidal wing plan form is plotted in figure 7.3. The present solutions are compared in the same figures with the results obtained by the theory of high order conical flows (Carafoli, Mateescu, Nastase, [2]). These results are in excellent agreement.

In addition, the corresponding aerodynamic characteristics coefficients are calculated and presented in table 7.3.

| | $C_l$ | $C_{m2}$ | $C_{m1}$ |
|---|---|---|---|
| Present solutions | -0.00185 | -0.00129 | 0 |
| High order conical flow solutions | -0.00185 | -0.00129 | 0 |

Table 7.3 $C_l$, $C_{m2}$, and $C_{m1}$ for steady thin trapezoidal wing with supersonic leading edges for $\alpha = -w_{10}x_1 / U_\infty$.

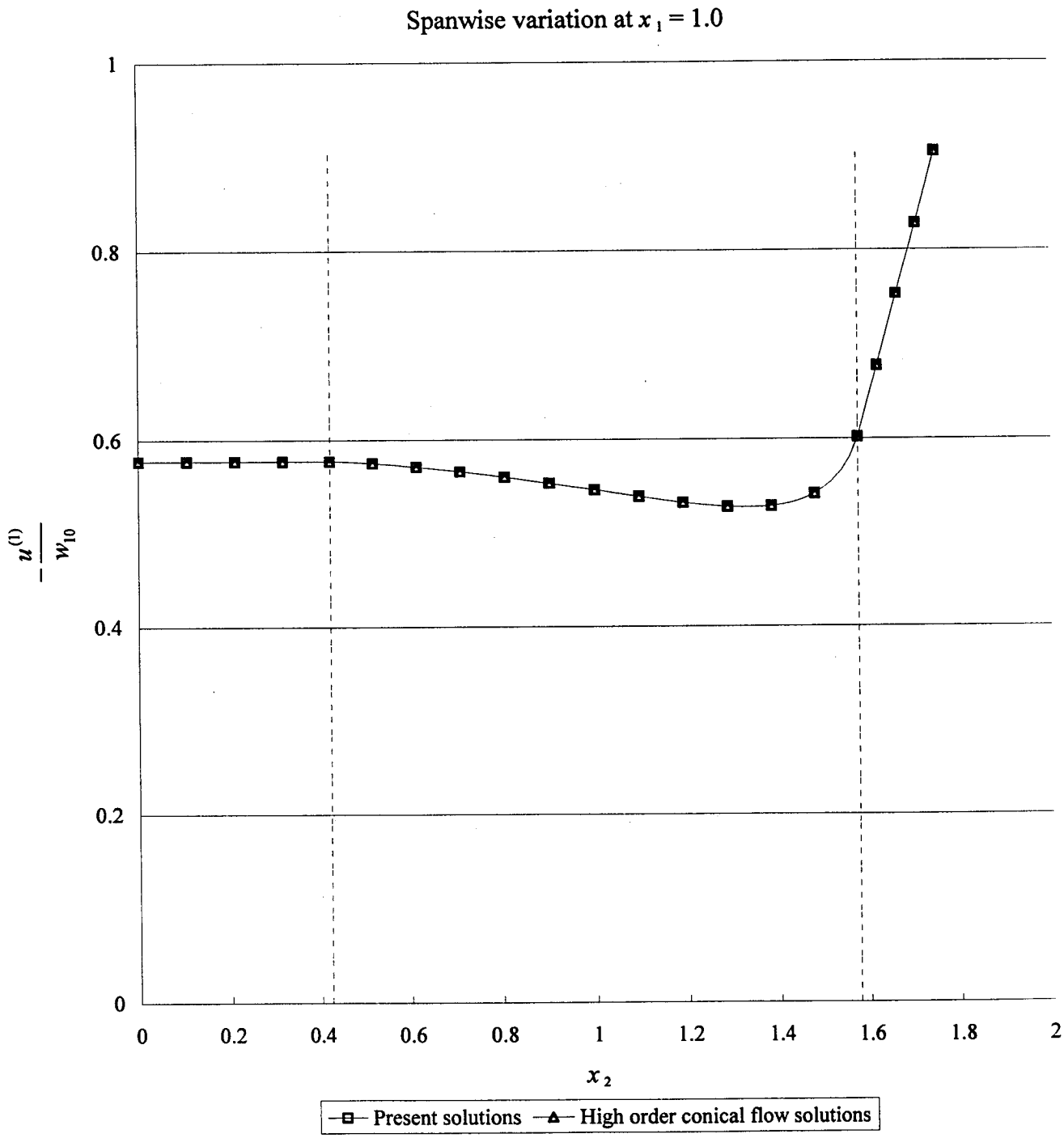


Figure 7.3 The spanwise variation of the axial velocity for steady thin trapezoidal wing with supersonic leading edges and incidence $\alpha = -w_{10}x_1 / U_\infty$. (root chord, $c_0 = 1.0$; span, $b = 1.0$; semi-span, $l = 0.75$; Mach number, $M_\infty = 2.0$)

## 7.3 Unsteady flow results for oscillating rigid wings

### 7.3.1 Case of wings executing oscillatory vertical translation

We first consider that each point over wing surface executes oscillatory movement of small amplitude, which can be defined by,

$$Z = h(t) = e^{i\omega t} h_0 \,;\; P = h_0 \tag{7.3.1}$$

In this case, the boundary condition can be expressed by

$$\hat{w} = i\lambda h_0 = w_{00},\; \lambda = \omega / U_\infty \tag{7.3.2}$$

The numerical results were obtained for various reduced frequency λ as 0.0147, 0.0735, 0.147, 0.735, and 1.0, where $h_0 = 0.02$.

#### 7.3.1.1 Thin delta wing executing oscillatory vertical translation

In this case, results of the spanwise variation of the real and imaginary parts of the reduced pressure coefficient over right hand side of wing surface along the wing trace at $x_1 = 1.0$ are plotted in figures 7.4, 7.5, 7.6, 7.7 and 7.8. The imaginary part of the present solutions is plotted in the same figure with the results obtained by the theory of high order conical flows (Carafoli, Mateescu, Nastase, [2]). A very good agreement was found for small oscillating frequency. For oscillations at higher frequency, the agreement, however, starts to deteriorate for wing surface near and outside the Mach cone due to the approximation introduced in high order conical flow solutions. The real part of the reduced pressure coefficient is assumed zero in the high order conical flow solutions due to the approximation made in the frequency expansion method related to the unsteady formulation using high order conical flows. The present solutions, however, are more accurate and provide non-zero solutions to the calculation of the reduced pressure coefficients even though it is comparatively small corresponding to the imaginary part for small oscillating frequency. For higher oscillating frequency, the real part of

the present solutions is no longer negligible compared to the related imaginary part, i.e., the present method proves to be more accurate especially for oscillations in higher frequency. This is due to the consideration of the complete governing equation for unsteady flows related to the unsteady formulation by using pulsating sources distribution over thin wing surface.

The results of the reduced lift coefficient and pitching moment coefficient are presented in tables 7.4, 7.5, 7.6, 7.7 and 7.8. An excellent agreement was found in imaginary part of specific aerodynamic characteristics calculated by both methods for small oscillating frequency. The agreement, however, becomes worse for higher oscillating frequency. Also, the present method is more accurate because the real part of the reduced lift and pitching moment coefficients can be calculated not only for small but also for higher oscillating frequency. For the high order conical flow solutions, the real part of the reduced lift coefficient and the reduced pitching moment coefficient are assumed zero due to the approximation related to the unsteady formulation using high order conical flows.

| | $\hat{C}_l$ | | $\hat{C}_{m2}$ | |
|---|---|---|---|---|
| | **REAL** | **IMAG** | **REAL** | **IMAG** |
| Present solutions | -0.00006 | -0.03396 | -0.00004 | -0.02264 |
| High order conical flow solutions | 0 | -0.03396 | 0 | -0.02264 |

Table 7.4 $\hat{C}_l$ and $\hat{C}_{m2}$ for thin delta wing executing oscillatory vertical translation ($\lambda = 0.0147$)

| | $\hat{C}_l$ | | $\hat{C}_{m2}$ | |
|---|---|---|---|---|
| | **REAL** | **IMAG** | **REAL** | **IMAG** |
| Present solutions | -0.00139 | -0.16977 | -0.00104 | -0.11318 |
| High order conical flow solutions | 0 | -0.16981 | 0 | -0.11321 |

Table 7.5 $\hat{C}_l$ and $\hat{C}_{m2}$ for thin delta wing executing oscillatory vertical translation ($\lambda = 0.0735$)

| | $\hat{C}_l$ | | $\hat{C}_{m2}$ | |
|---|---|---|---|---|
| | **REAL** | **IMAG** | **REAL** | **IMAG** |
| Present solutions | -0.00554 | -0.33934 | -0.00415 | -0.22619 |
| High order conical flow solutions | 0 | -0.33962 | 0 | -0.22641 |

Table 7.6 $\hat{C}_l$ and $\hat{C}_{m2}$ for thin delta wing executing oscillatory vertical translation ($\lambda = 0.1470$)

| | $\hat{C}_l$ | | $\hat{C}_{m2}$ | |
|---|---|---|---|---|
| | **REAL** | **IMAG** | **REAL** | **IMAG** |
| Present solutions | -0.13268 | -1.66087 | -0.09903 | -1.10211 |
| High order conical flow solutions | 0 | -1.69809 | 0 | -1.13206 |

Table 7.7 $\hat{C}_l$ and $\hat{C}_{m2}$ for thin delta wing executing oscillatory vertical translation ($\lambda = 0.7350$)

| | $\hat{C}_l$ | | $\hat{C}_{m2}$ | |
|---|---|---|---|---|
| | **REAL** | **IMAG** | **REAL** | **IMAG** |
| Present solutions | -0.23783 | -2.20994 | -0.17696 | -1.45908 |
| High order conical flow solutions | 0 | -2.31033 | 0 | -1.54022 |

Table 7.8 $\hat{C}_l$ and $\hat{C}_{m2}$ for thin delta wing executing oscillatory vertical translation ($\lambda = 1.0$)

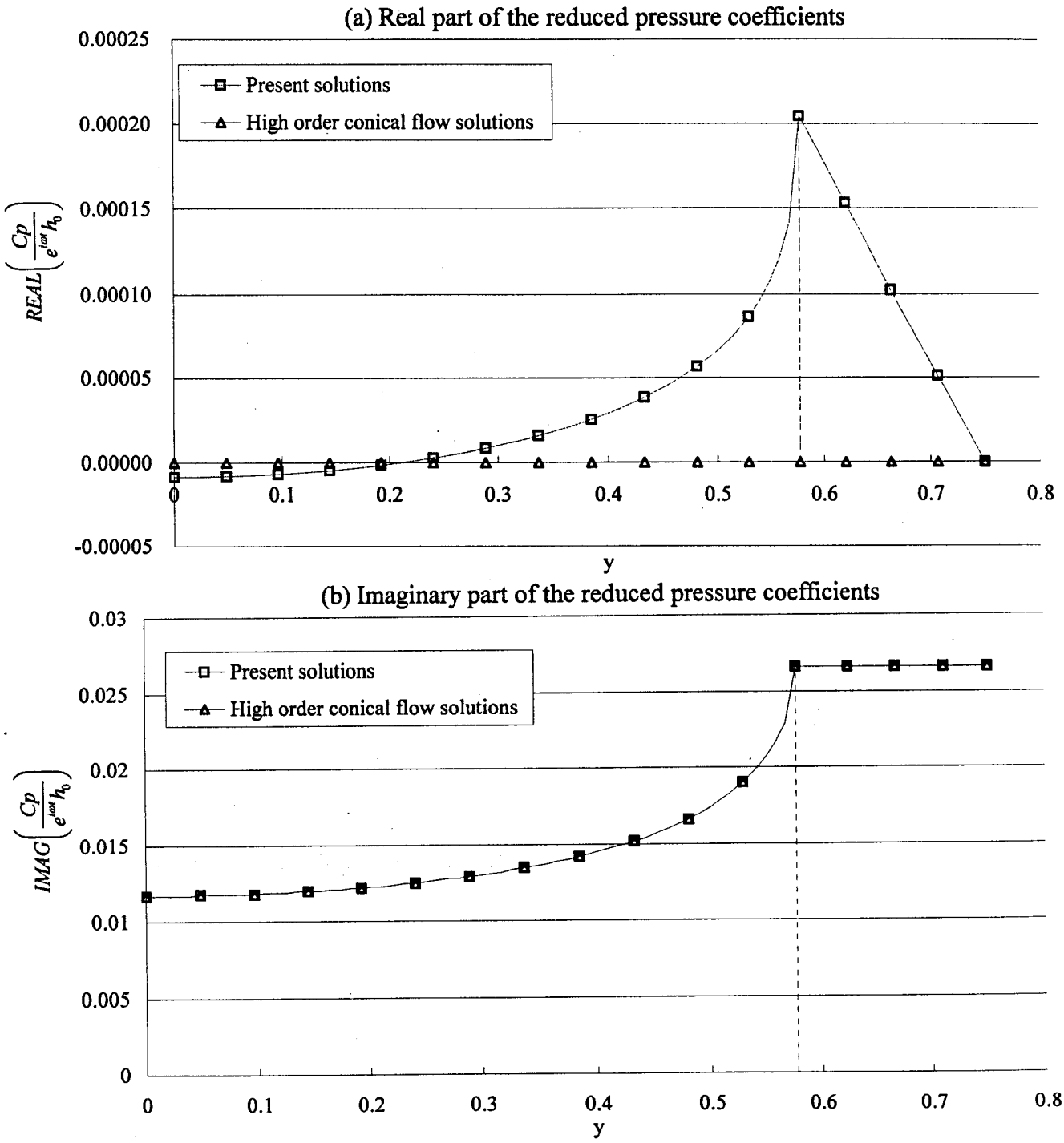


Figure 7.4 The real and imaginary parts of the reduced pressure coefficients for thin delta wing executing harmonic vertical translation oscillations.
(The reduced frequency of oscillations, $\lambda = 0.0147$; spanwise variation at $x_1 = 1.0$; root chord, $c_0 = 1.0$; semi-span, $l = 0.75$; Mach number, $M_\infty = 2.0$)

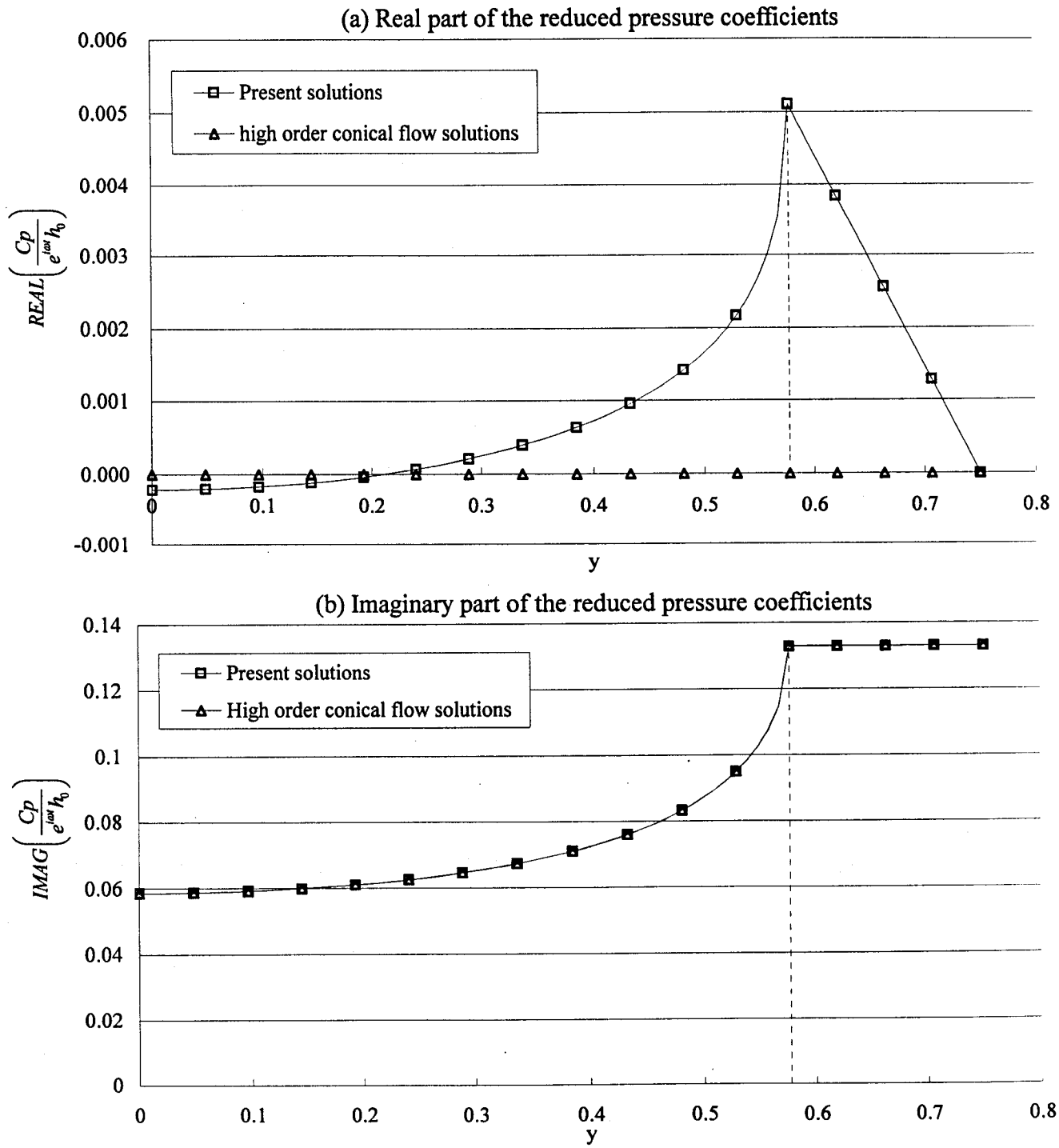


Figure 7.5 The real and imaginary parts of the reduced pressure coefficients for thin delta wing executing harmonic vertical translation oscillations.

(The reduced frequency of oscillations, $\lambda = 0.0735$; spanwise variation at $x_1 = 1.0$; root chord, $c_0 = 1.0$; semi-span, $l = 0.75$; Mach number, $M_\infty = 2.0$)

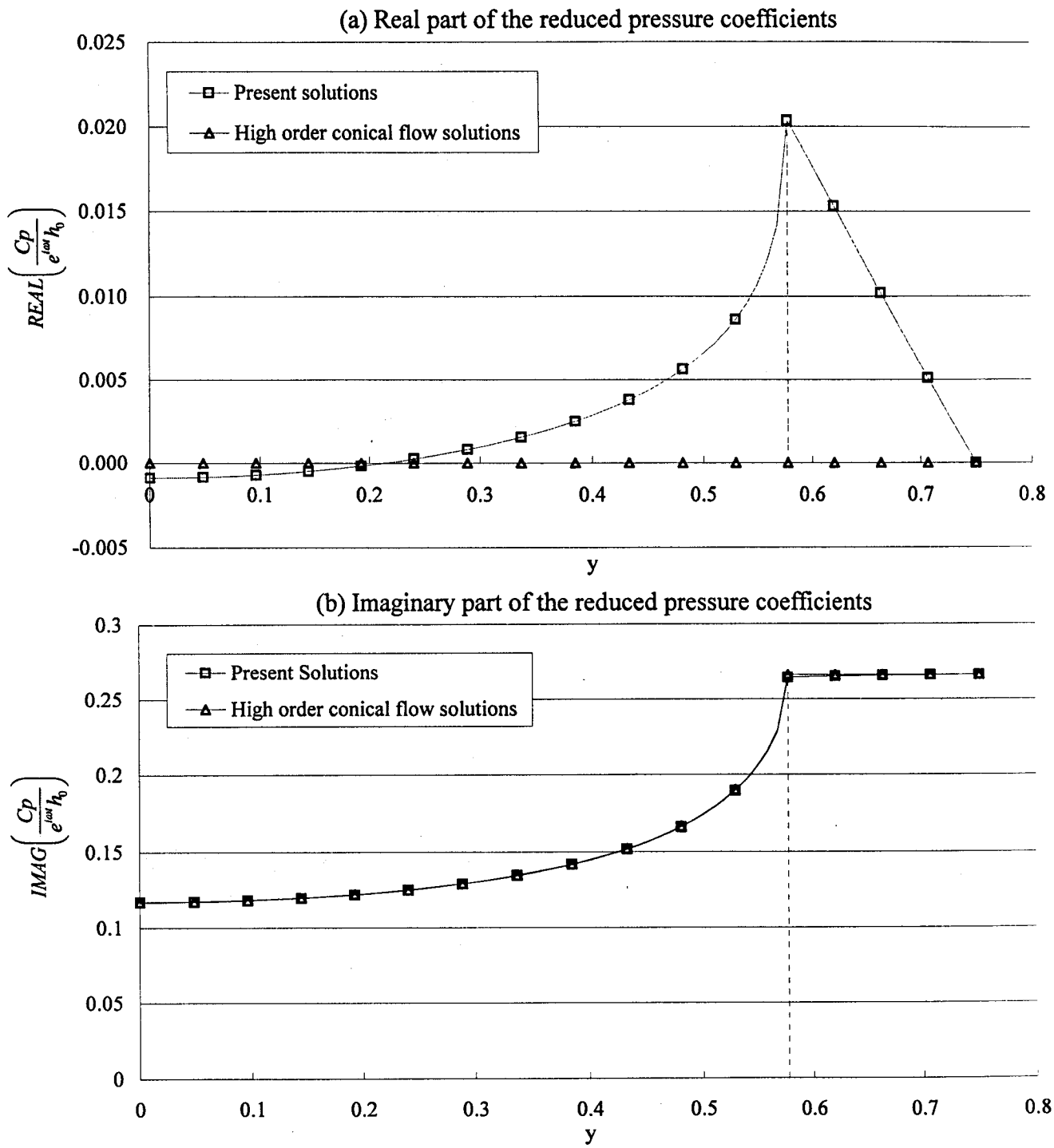


Figure 7.6 The real and imaginary parts of the reduced pressure coefficients for thin delta wing executing harmonic vertical translation oscillations.
(The reduced frequency of oscillations, $\lambda = 0.1470$; spanwise variation at $x_1 = 1.0$; root chord, $c_0 = 1.0$; semi-span, $l = 0.75$; Mach number, $M_\infty = 2.0$)

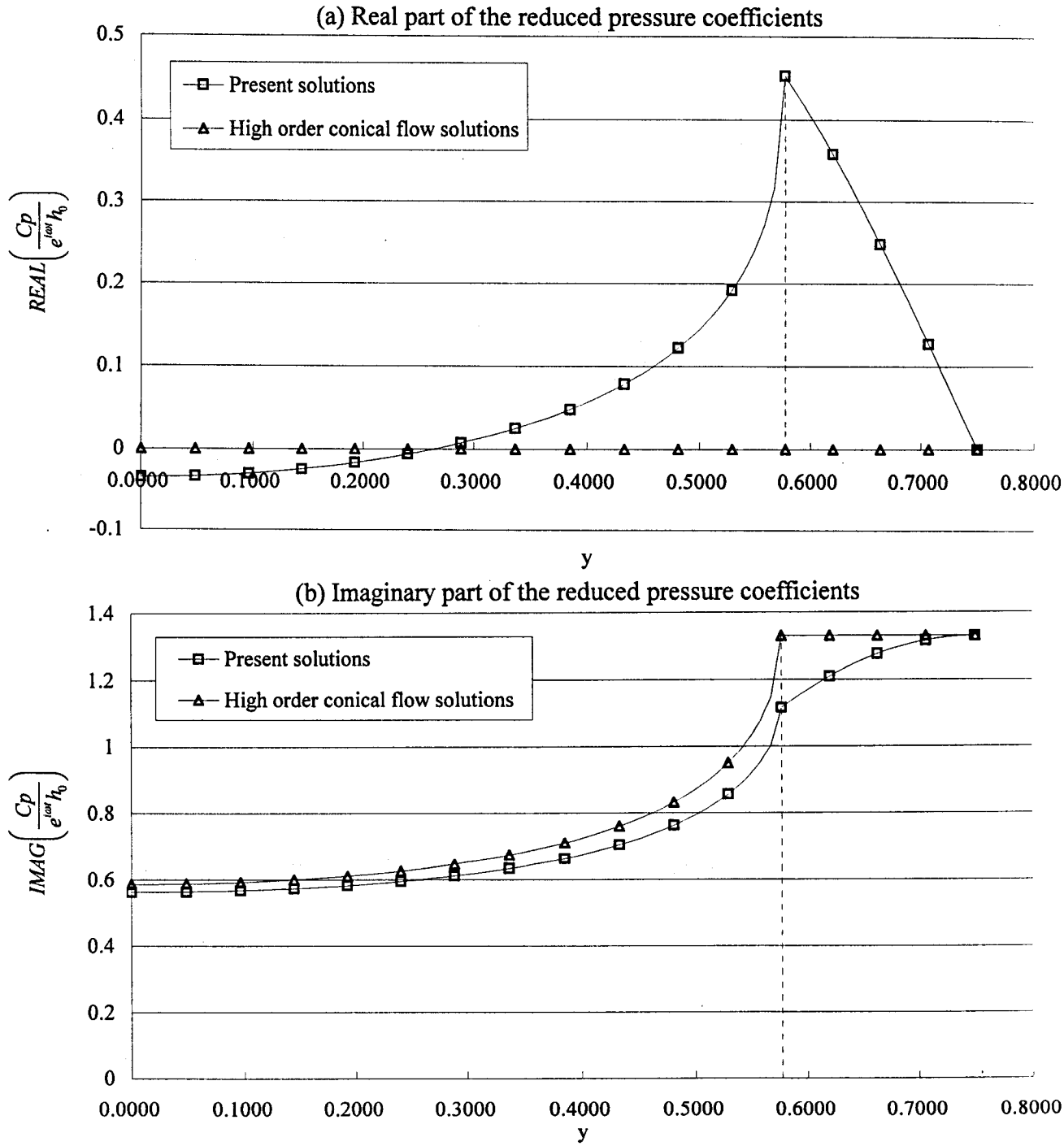


Figure 7.7 The real and imaginary parts of the reduced pressure coefficients for thin delta wing executing harmonic vertical translation oscillations.

(The reduced frequency of oscillations, $\lambda = 0.7350$; spanwise variation at $x_1 = 1.0$; root chord, $c_0 = 1.0$; semi-span, $l = 0.75$; Mach number, $M_\infty = 2.0$)

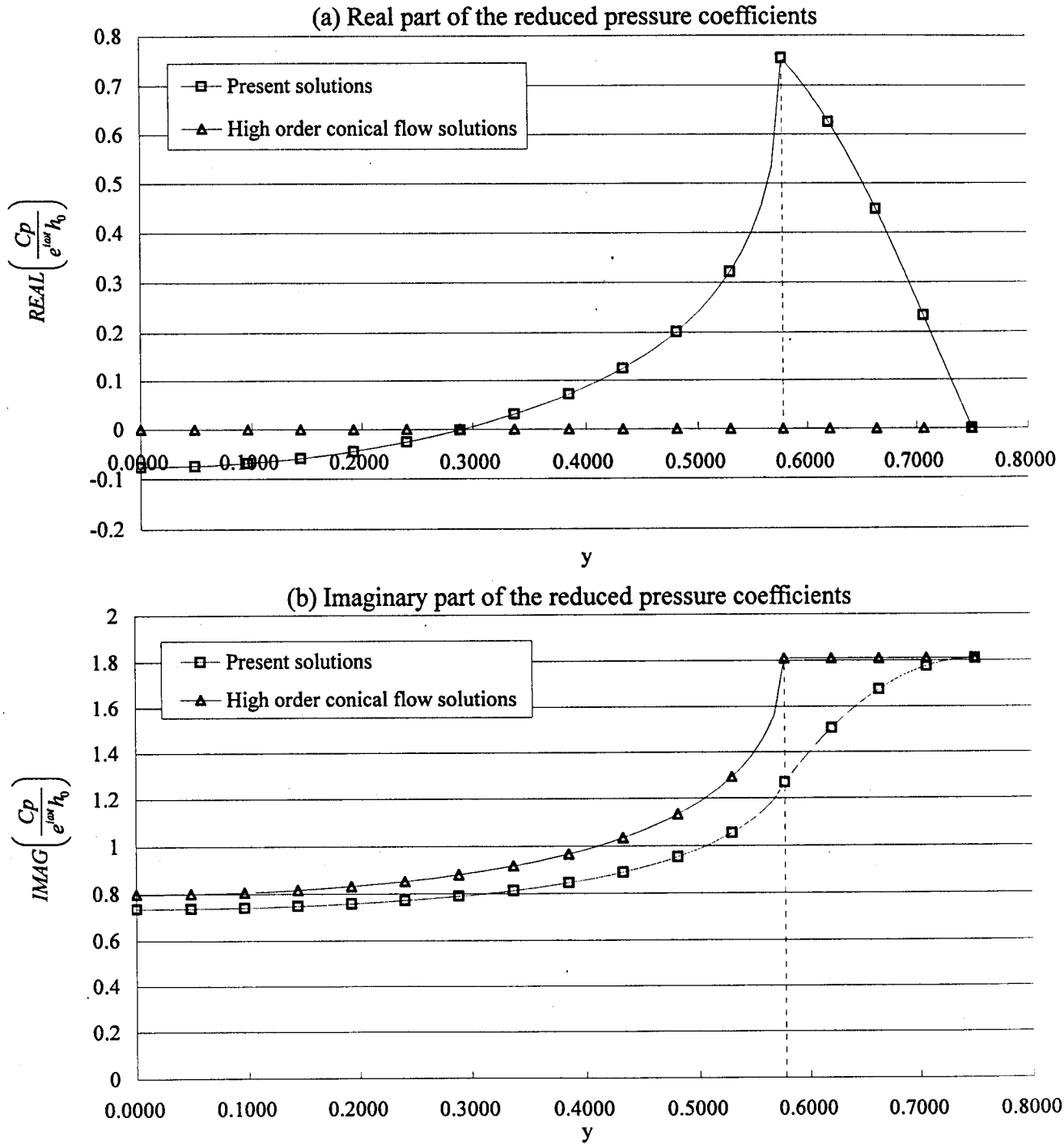


Figure 7.8 The real and imaginary parts of the reduced pressure coefficients for thin delta wing executing harmonic vertical translation oscillations.

(The reduced frequency of oscillations, $\lambda = 1.0$; spanwise variation at $x_1 = 1.0$; root chord, $c_0 = 1.0$; semi-span, $l = 0.75$; Mach number, $M_\infty = 2.0$)

### 7.3.1.2 Thin trapezoidal wing executing oscillatory vertical translation

Present solutions of the spanwise variation of the real and imaginary parts of the reduced pressure coefficient of trapezoidal wing are plotted in figures 7.9, 7.10, and 7.11. The imaginary part of the present solutions is compared in the same figures with the results obtained by the theory of high order conical flows (Carafoli, Mateescu, Nastase, [2]). An excellent agreement was found in these results. The present solutions are more accurate and provided non-zero solutions to the real part of the reduced pressure coefficient, while the high order conical flow solutions are assumed zero due to the approximation made in the frequency expansion method using high order conical flows.

The reduced lift coefficient and pitching moment coefficient are calculated by present method and are presented in table 7.9. However, high order conical flow solutions are not available in this case.

| Present solutions | $\hat{C}_l$ | | $\hat{C}_{m2}$ | |
|---|---|---|---|---|
| | **REAL** | **IMAG** | **REAL** | **IMAG** |
| $\lambda = 0.0147$ | -0.00008 | -0.03396 | -0.00006 | -0.01852 |
| $\lambda = 0.0735$ | -0.00189 | -0.16974 | -0.00159 | -0.09257 |
| $\lambda = 0.1470$ | -0.00754 | -0.33913 | -0.00636 | -0.18483 |

Table 7.9 $\hat{C}_l$ and $\hat{C}_{m2}$ for thin trapezoidal wing executing oscillatory vertical translation.

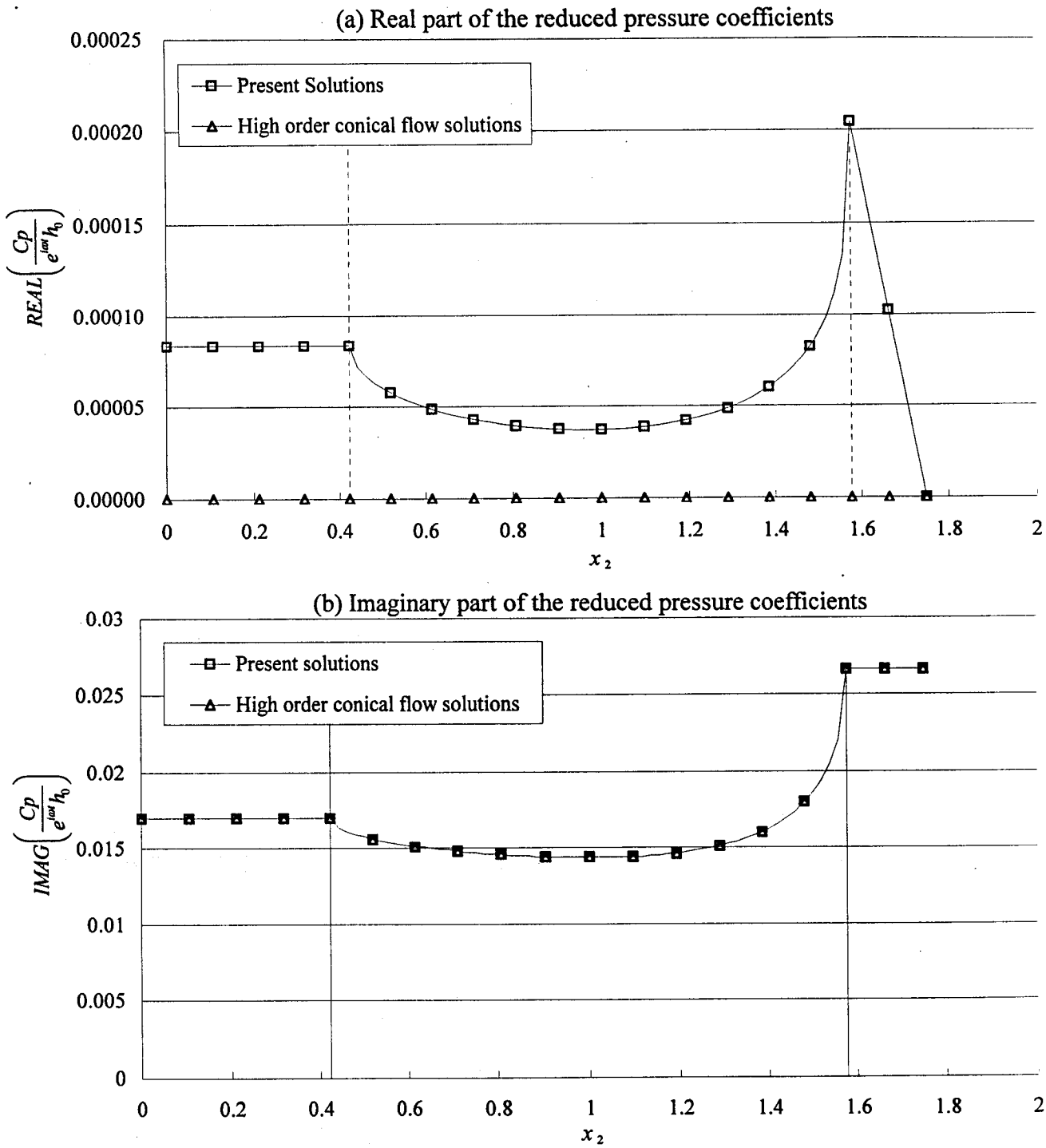


Figure 7.9 The real and imaginary parts of the reduced pressure coefficients for thin trapezoidal wing executing harmonic vertical translation oscillations.

(The reduced frequency of oscillations, $\lambda = 0.0147$; spanwise variation at $x_1 = 1.0$; root chord, $c_0 = 1.0$; span, $b = 1.0$; semi-span, $l = 0.75$; Mach number, $M_\infty = 2.0$)

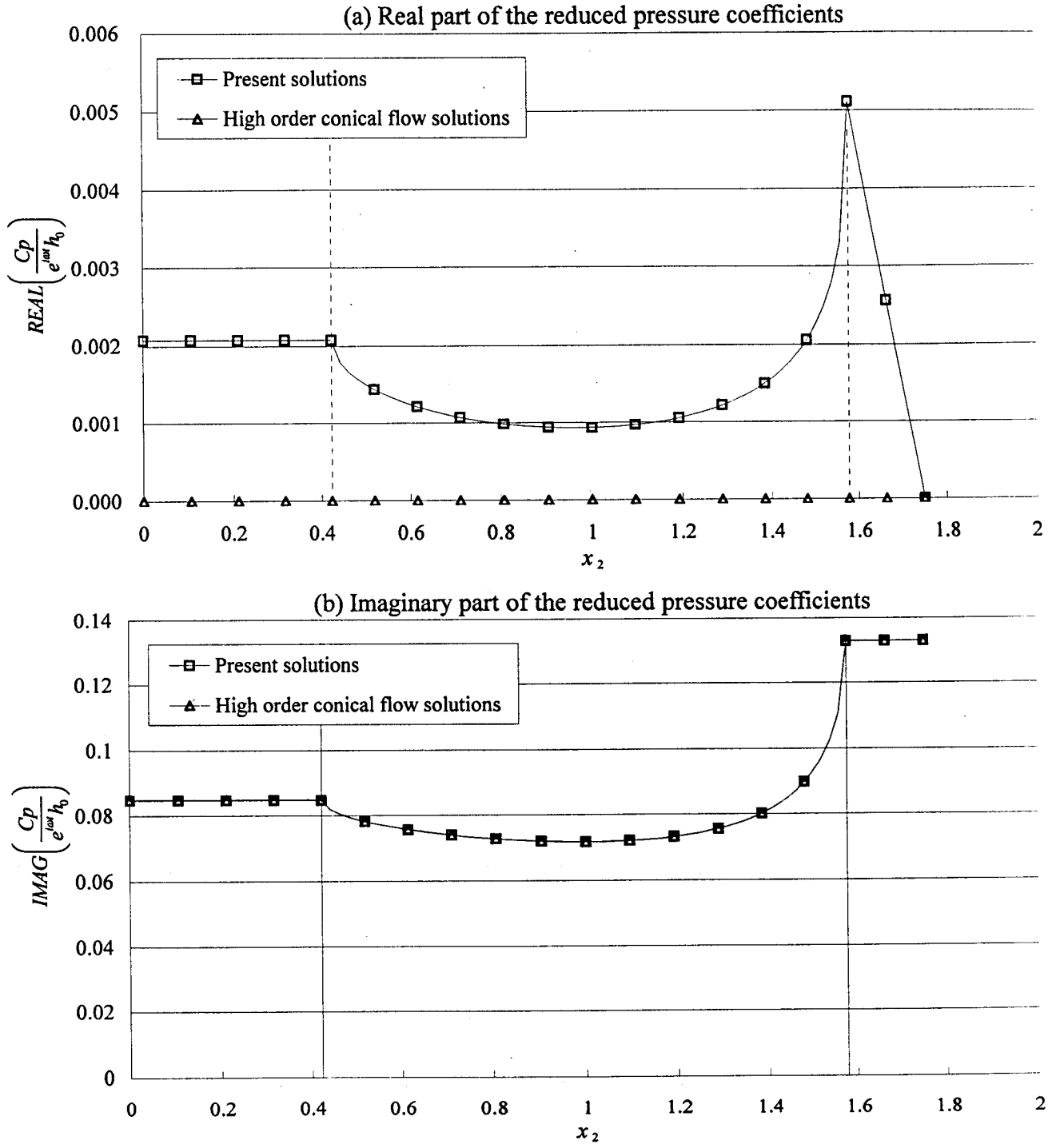


Figure 7.10 The real and imaginary parts of the reduced pressure coefficients for thin trapezoidal wing executing harmonic vertical translation oscillations.
(The reduced frequency of oscillations, $\lambda = 0.0735$; spanwise variation at $x_1 = 1.0$; root chord, $c_0 = 1.0$; span, $b = 1.0$; semi-span, $l = 0.75$; Mach number, $M_\infty = 2.0$)

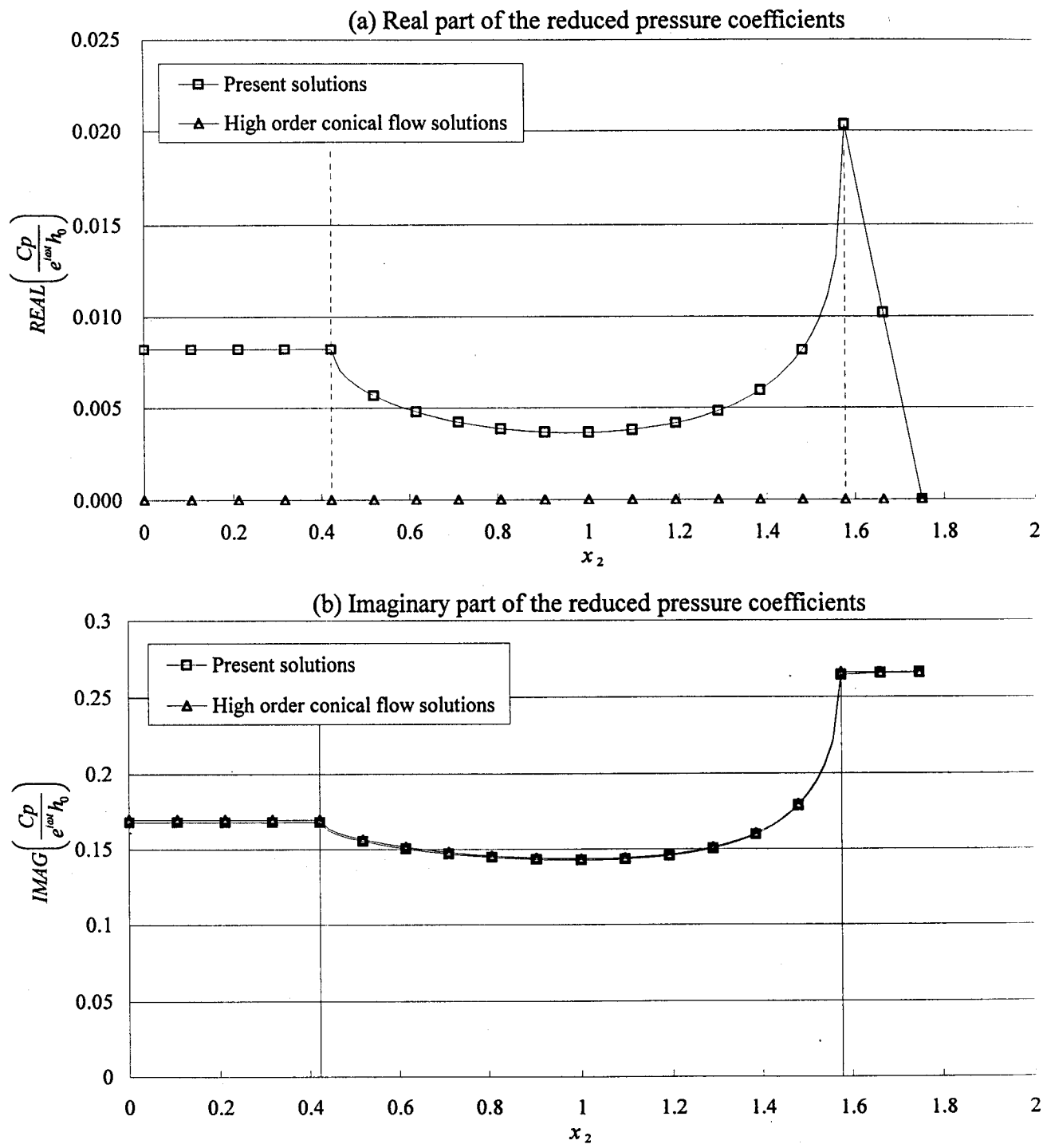


Figure 7.11 The real and imaginary parts of the reduced pressure coefficients for thin trapezoidal wing executing harmonic vertical translation oscillations.
(The reduced frequency of oscillations, $\lambda = 0.1470$; spanwise variation at $x_1 = 1.0$; root chord, $c_0 = 1.0$; span, $b = 1.0$; semi-span, $l = 0.75$; Mach number, $M_\infty = 2.0$)

### 7.3.2 Case of wings executing oscillatory pitching rotation

For case of wings executing oscillatory pitching rotation, we first consider that each point over wing surface executes oscillatory movement of small amplitude, which can be defined by,

$$Z = -x_1\theta(t) = -x_1\hat{\theta}e^{i\omega t} = e^{i\omega t}\left(-x_1\theta_0\right);\ P = -x_1\theta_0 . \tag{7.3.3}$$

The boundary condition can be expressed by,

$$\hat{w} = -\theta_0 - i\lambda\theta_0 x_1 = w_{00} + w_{10}x_1;\ \lambda = \omega/U_\infty . \tag{7.3.4}$$

The numerical results were calculated for various reduced frequency λ as 0.0147, 0.0735, 0.147, 0.735, and 1.0, where $\theta_0 = 0.02$.

#### 7.3.2.1 Thin delta wing executing oscillatory pitching rotation

For delta wing, results of the spanwise variation of the real and imaginary parts of the reduced pressure coefficient over the right hand side of wing surface along the wing trace at $x_1 = 1.0$ are plotted in figures 7.12, 7.13, 7.14, 7.15, and 7.16. The real and imaginary parts of the present solutions are compared in the same figures with the results obtained by the theory of high order conical flow (Carafoli, Mateescu, Nastase, [2]). An excellent agreement in real and imaginary parts was found for small oscillating frequency. For higher oscillating frequency the agreement, however, starts to deteriorate, especially in real part solutions for wing surface near and beyond the Mach cone. This is mainly due to the approximation related to the unsteady formulation using theory of high order conical flows.

The results of the reduced lift coefficient and the reduced pitching moment coefficient are presented in tables 7.10, 7.11, 7.12, 7.13, and 7.14. An excellent agreement was found in real and imaginary parts based on results for small oscillating frequency. The agreement starts to deteriorate for delta wing executing in high oscillating frequency.

| | $\hat{C}_l$ | | $\hat{C}_{m2}$ | |
|---|---|---|---|---|
| | **REAL** | **IMAG** | **REAL** | **IMAG** |
| Present solutions | 2.309 | 0.019 | 1.540 | 0.014 |
| High order conical flow solutions | 2.309 | 0.019 | 1.540 | 0.014 |

Table 7.10 $\hat{C}_l$ and $\hat{C}_{m2}$ for thin delta wing executing oscillatory pitching rotation ($\lambda = 0.0147$)

| | $\hat{C}_l$ | | $\hat{C}_{m2}$ | |
|---|---|---|---|---|
| | **REAL** | **IMAG** | **REAL** | **IMAG** |
| Present solutions | 2.310 | 0.094 | 1.540 | 0.071 |
| High order conical flow solutions | 2.309 | 0.094 | 1.540 | 0.071 |

Table 7.11 $\hat{C}_l$ and $\hat{C}_{m2}$ for thin delta wing executing oscillatory pitching rotation ($\lambda = 0.0735$)

| | $\hat{C}_l$ | | $\hat{C}_{m2}$ | |
|---|---|---|---|---|
| | **REAL** | **IMAG** | **REAL** | **IMAG** |
| Present solutions | 2.310 | 0.189 | 1.540 | 0.141 |
| High order conical flow solutions | 2.309 | 0.189 | 1.540 | 0.142 |

Table 7.12 $\hat{C}_l$ and $\hat{C}_{m2}$ for thin delta wing executing oscillatory pitching rotation ($\lambda = 0.1470$)

| | $\hat{C}_l$ | | $\hat{C}_{m2}$ | |
|---|---|---|---|---|
| | **REAL** | **IMAG** | **REAL** | **IMAG** |
| Present solutions | 2.326 | 0.937 | 1.553 | 0.702 |
| High order conical flow solutions | 2.309 | 0.943 | 1.540 | 0.708 |

Table 7.13 $\hat{C}_l$ and $\hat{C}_{m2}$ for thin delta wing executing oscillatory pitching rotation ($\lambda = 0.735$)

| | $\hat{C}_l$ | | $\hat{C}_{m2}$ | |
|---|---|---|---|---|
| | **REAL** | **IMAG** | **REAL** | **IMAG** |
| Present solutions | 2.331 | 1.264 | 1.556 | 0.946 |
| High order conical flow solutions | 2.309 | 1.284 | 1.540 | 0.963 |

Table 7.14 $\hat{C}_l$ and $\hat{C}_{m2}$ for thin delta wing executing oscillatory pitching rotation ($\lambda = 1.0$)

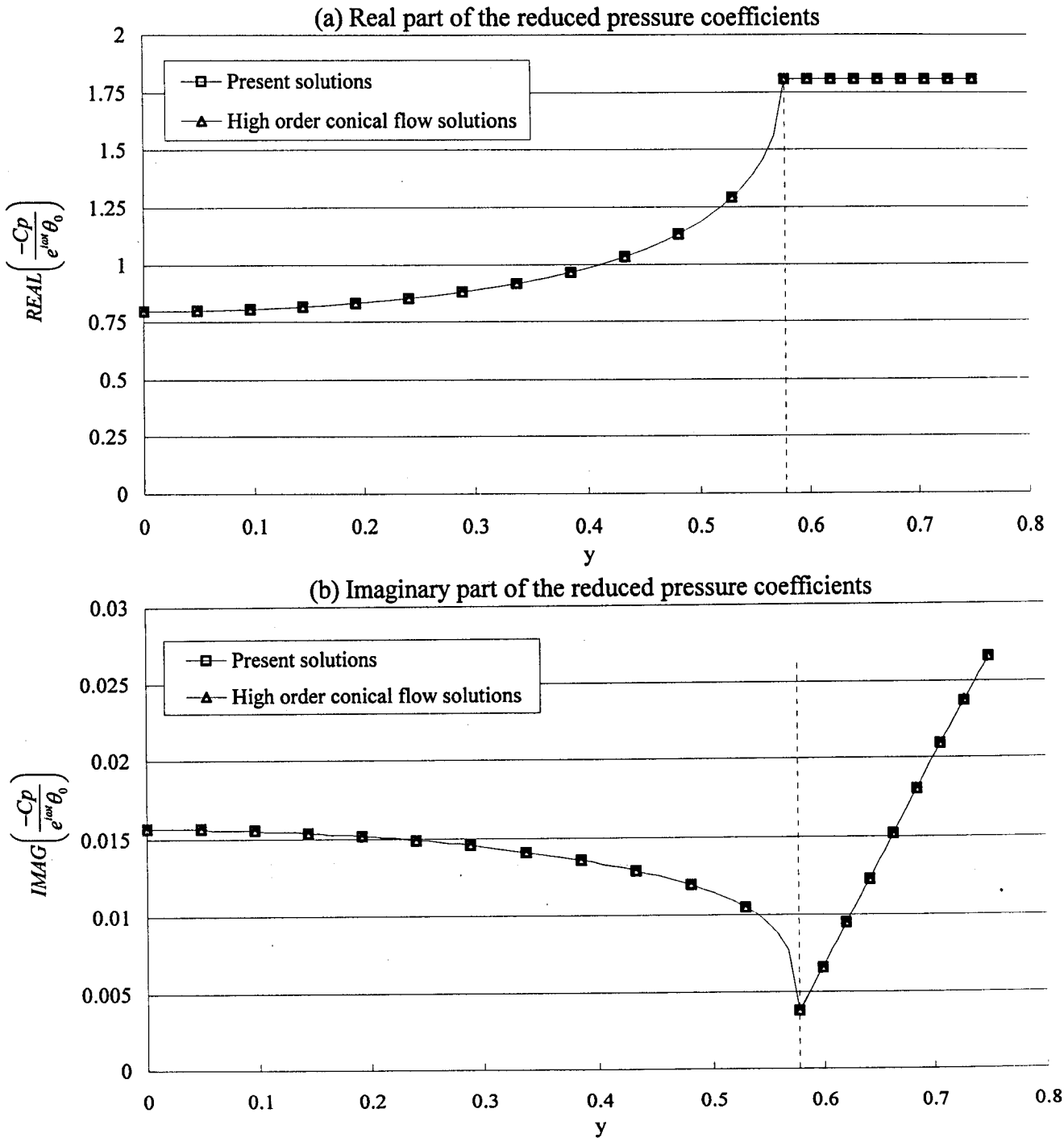


Figure 7.12 The real and imaginary parts of the reduced pressure coefficients for thin delta wing executing harmonic pitching rotation oscillations.
(The reduced frequency of oscillations, $\lambda = 0.0147$; spanwise variation at $x_1 = 1.0$; root chord, $c_0 = 1.0$; semi-span, $l = 0.75$; Mach number, $M_\infty = 2.0$)

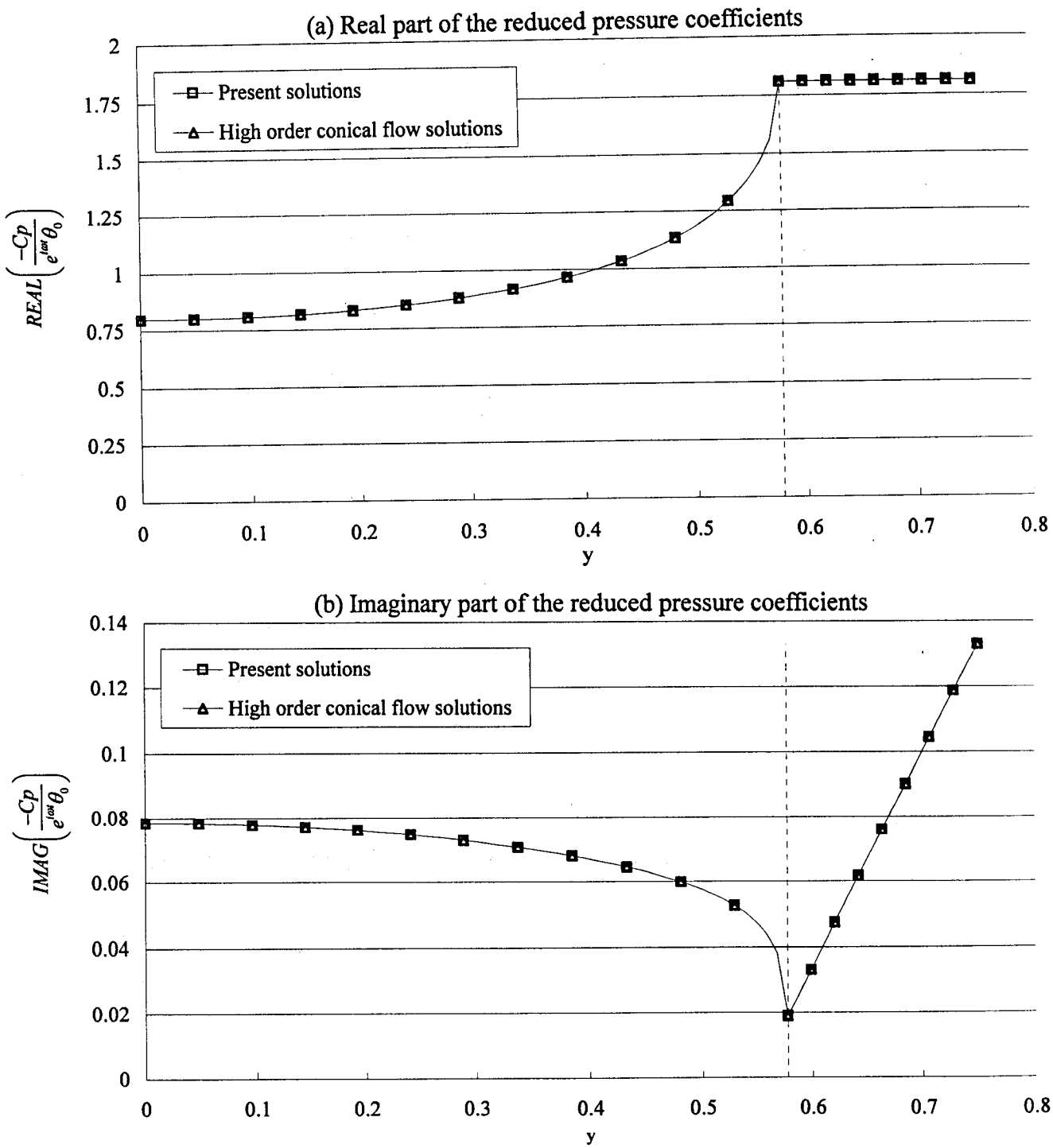


Figure 7.13 The real and imaginary parts of the reduced pressure coefficients for thin delta wing executing harmonic pitching rotation oscillations.
(The reduced frequency of oscillations, $\lambda = 0.0735$; spanwise variation at $x_1 = 1.0$; root chord, $c_0 = 1.0$; semi-span, $l = 0.75$; Mach number, $M_\infty = 2.0$)

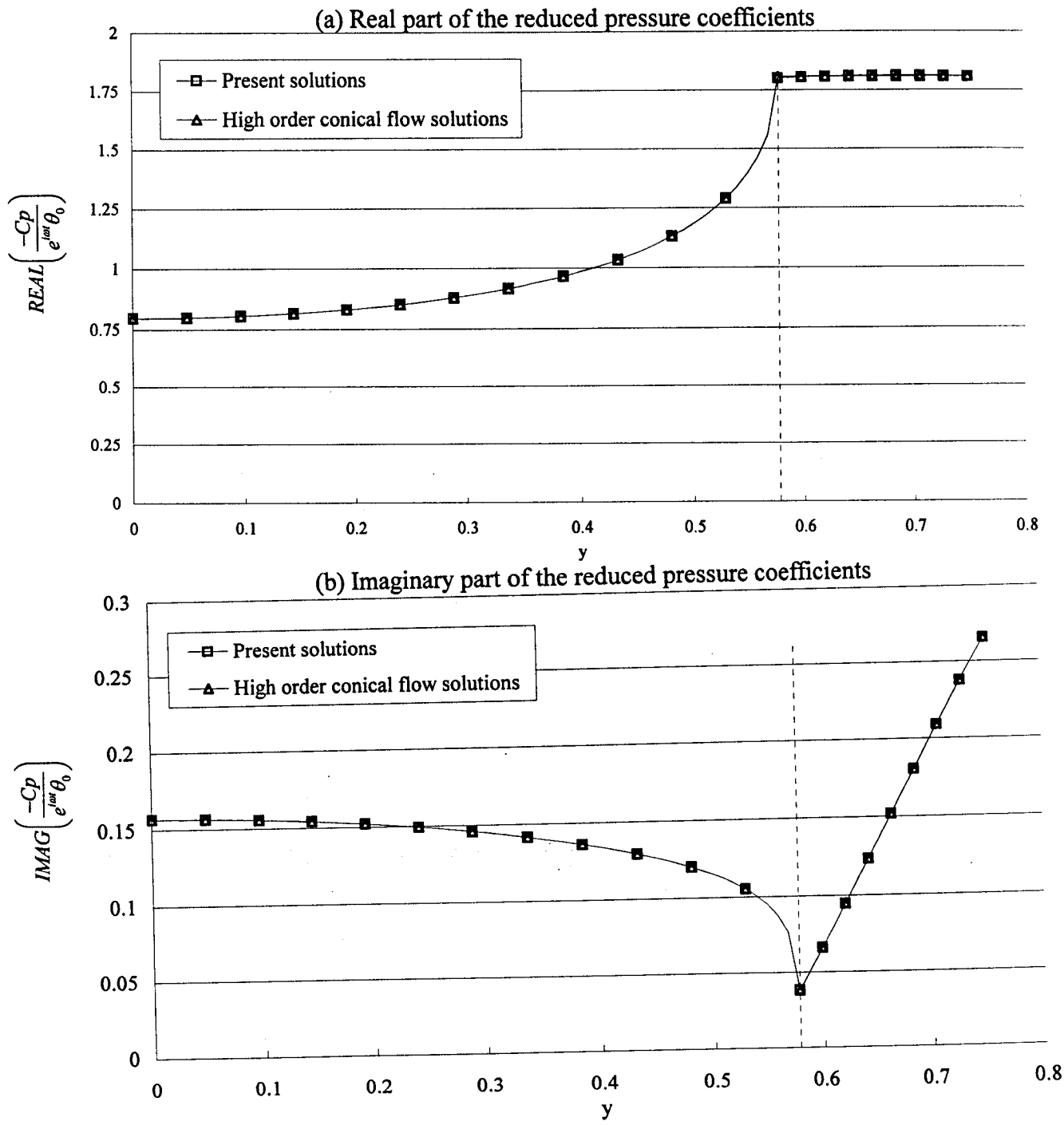


Figure 7.14 The real and imaginary parts of the reduced pressure coefficients for thin delta wing executing harmonic pitching rotation oscillations.
(The reduced frequency of oscillations, $\lambda = 0.1470$; spanwise variation at $x_1 = 1.0$; root chord, $c_0 = 1.0$; semi-span, $l = 0.75$; Mach number, $M_\infty = 2.0$)

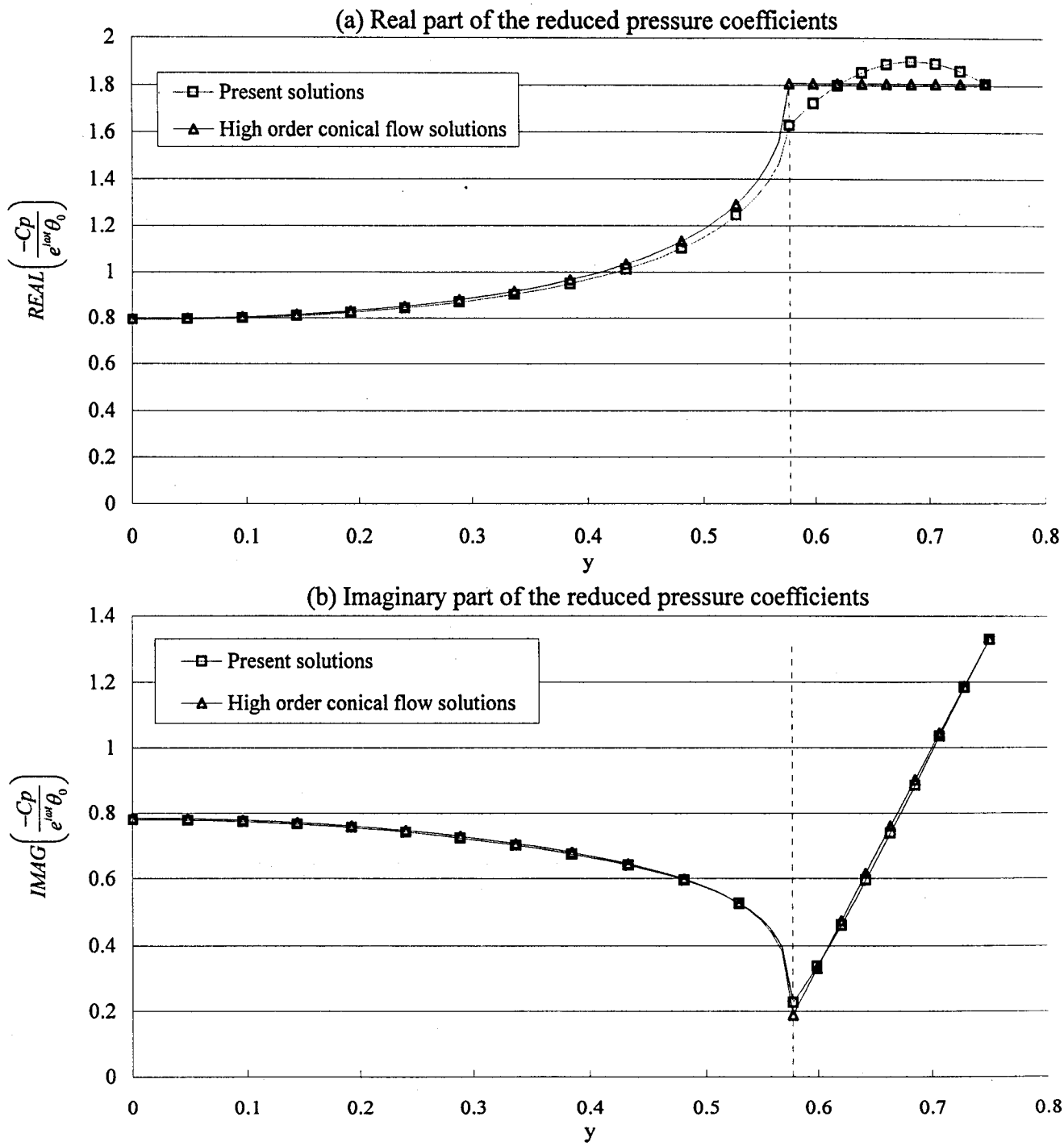


Figure 7.15 The real and imaginary parts of the reduced pressure coefficients for thin delta wing executing harmonic pitching rotation oscillations.
(The reduced frequency of oscillations, $\lambda = 0.735$; spanwise variation at $x_1 = 1.0$; root chord, $c_0 = 1.0$; semi-span, $l = 0.75$; Mach number, $M_\infty = 2.0$)

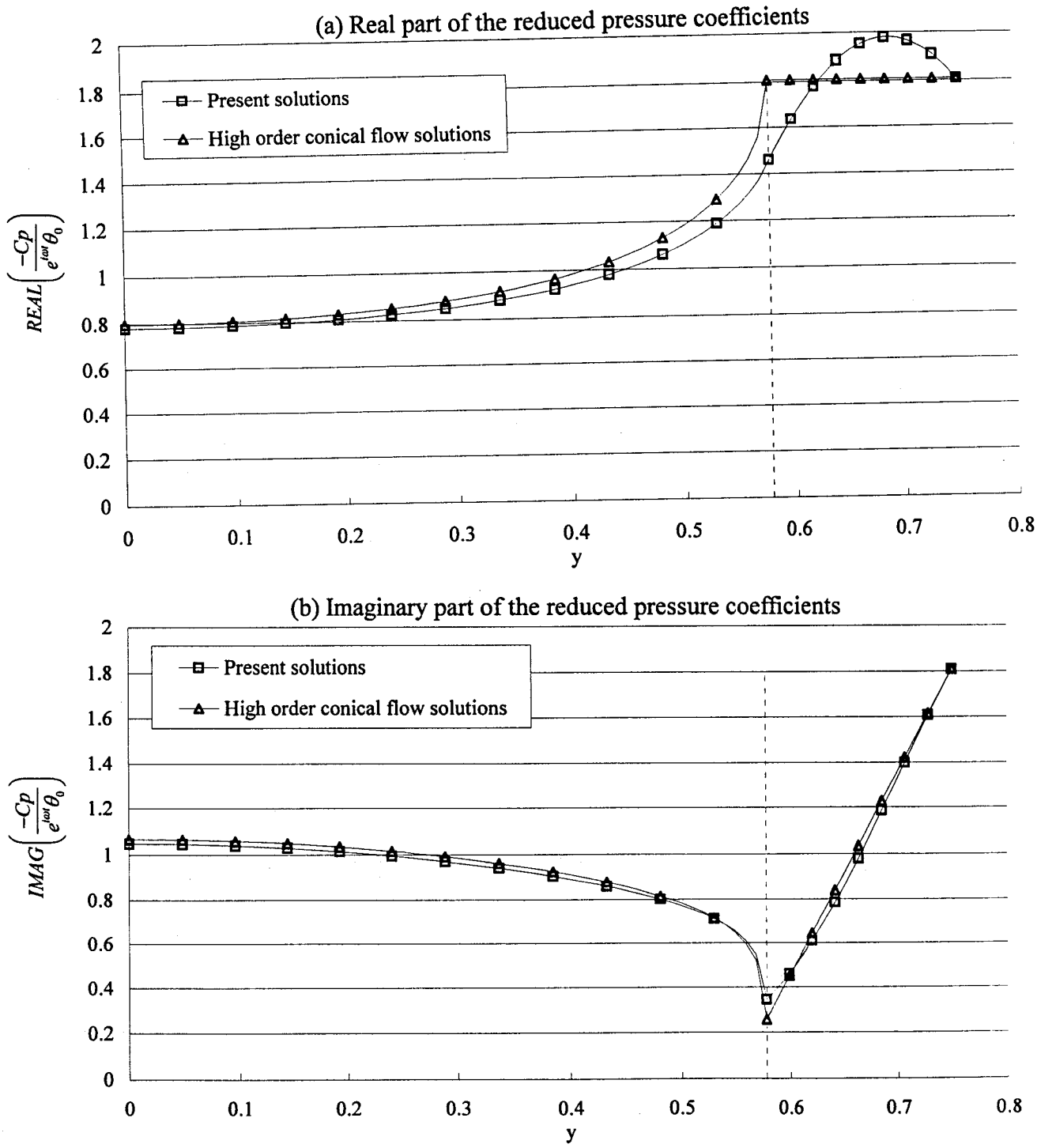


Figure 7.16 The real and imaginary parts of the reduced pressure coefficients for thin delta wing executing harmonic pitching rotation oscillations.
(The reduced frequency of oscillations, $\lambda = 1.0$; spanwise variation at $x_1 = 1.0$; root chord, $c_0 = 1.0$; semi-span, $l = 0.75$; Mach number, $M_\infty = 2.0$)

### 7.3.2.2 Thin trapezoidal wing executing oscillatory pitching rotation

Present solutions of the spanwise variation of the real and imaginary parts of the reduced pressure coefficient of trapezoidal wing are plotted in figures 7.17, 7.18, and 7.19. The results of the real and imaginary parts of the reduced pressure coefficients are in very good agreement and presented in the same figures in comparison with those obtained by the theory of high order conical flows (Carafoli, Mateescu, Nastase, [2]) in lower reduced frequency. However, for oscillations in higher reduced frequency, differences between two solutions are observed in light of the fact that the right hand side of the potential equation is neglected in the method by theory of high order conical flows.

The reduced lift coefficient and the reduced pitching moment coefficient are calculated by the present method and multiplied by 1000 for clear presentation in table 7.15.

| Present solutions | $1000\hat{C}_l$ | | $1000\hat{C}_{m2}$ | |
|---|---|---|---|---|
| | **REAL** | **IMAG** | **REAL** | **IMAG** |
| $\lambda = 0.0147$ | 2309.325 | 13.37868 | 1259.645 | 8.524725 |
| $\lambda = 0.0735$ | 2309.223 | 66.89601 | 1259.574 | 42.62622 |
| $\lambda = 0.1470$ | 2308.886 | 133.8084 | 1259.227 | 85.26791 |

Table 7.15 $\hat{C}_l$ and $\hat{C}_{m2}$ for thin trapezoidal wing executing oscillatory pitching rotation ($\lambda = 0.0147$, 0.0735, and 0.1470)

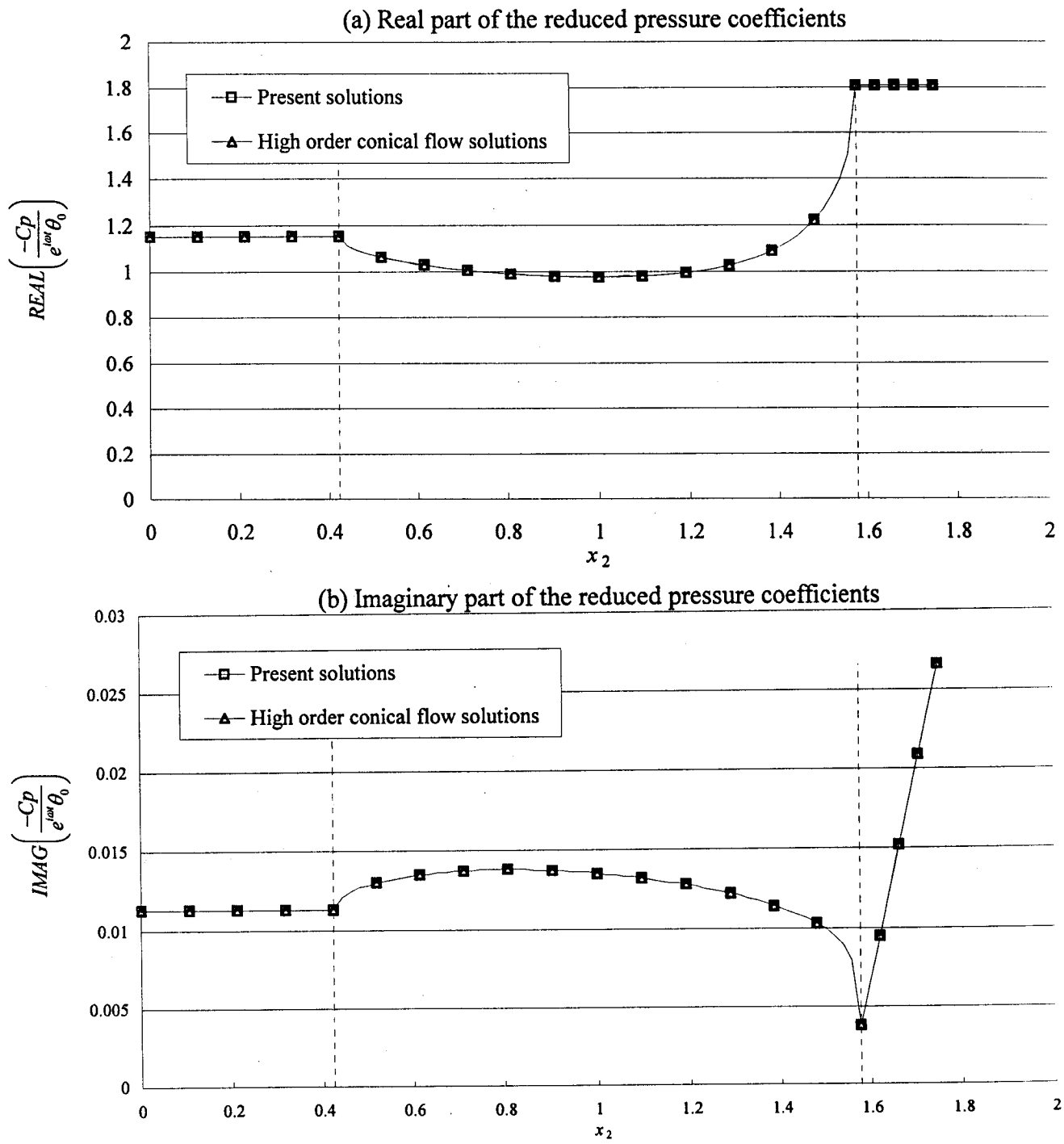


Figure 7.17 The real and imaginary parts of the reduced pressure coefficients for thin trapezoidal wing executing harmonic pitching rotation oscillations.

(The reduced frequency of oscillations, $\lambda = 0.0147$; spanwise variation at $x_1 = 1.0$; root chord, $c_0 = 1.0$; span, $b = 1.0$; semi-span, $l = 0.75$; Mach number, $M_\infty = 2.0$)

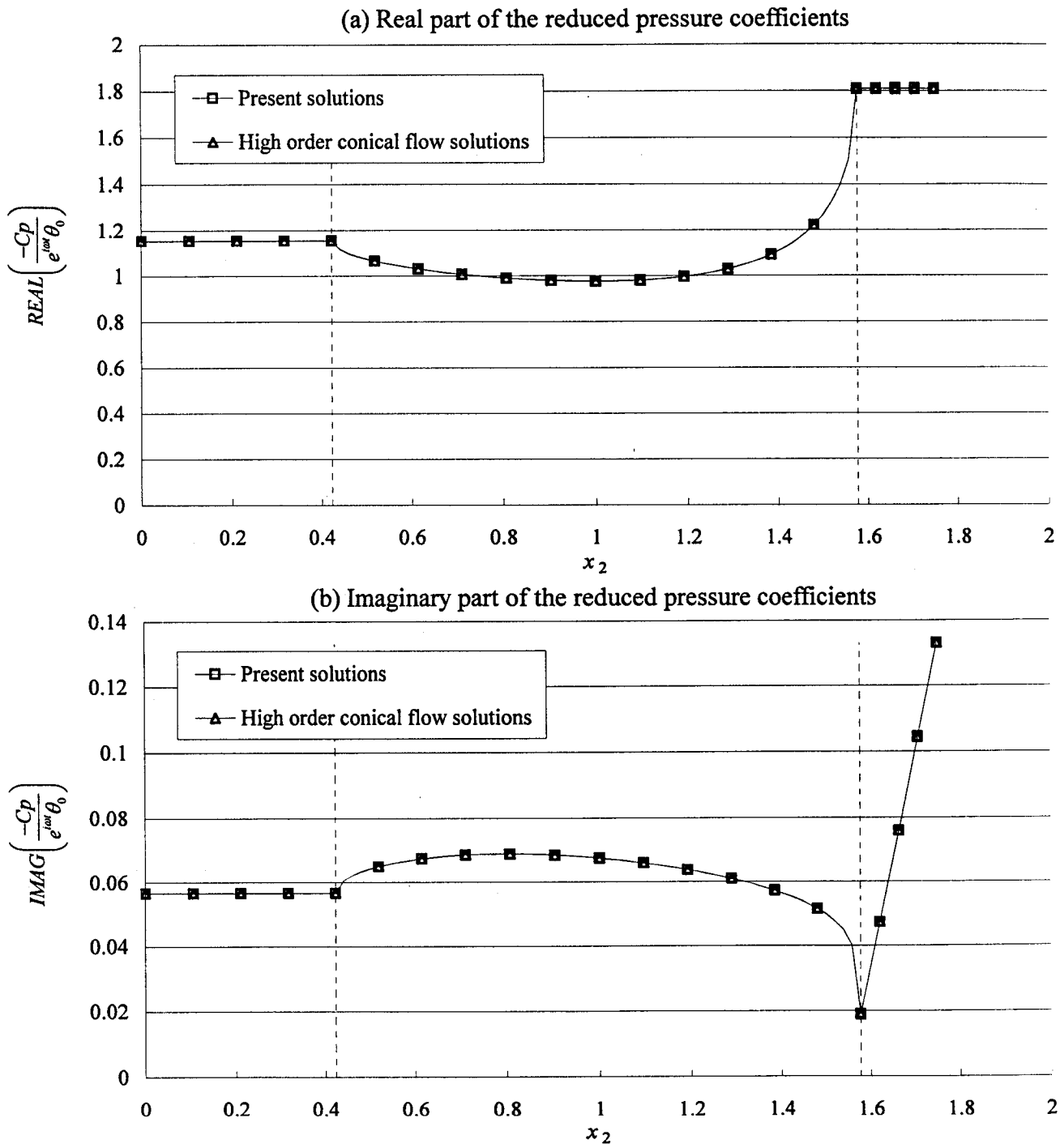


Figure 7.18 The real and imaginary parts of the reduced pressure coefficients for thin trapezoidal wing executing harmonic pitching rotation oscillations.

(The reduced frequency of oscillations, $\lambda = 0.0735$; spanwise variation at $x_1 = 1.0$; root chord, $c_0 = 1.0$; span, $b = 1.0$; semi-span, $l = 0.75$; Mach number, $M_\infty = 2.0$)

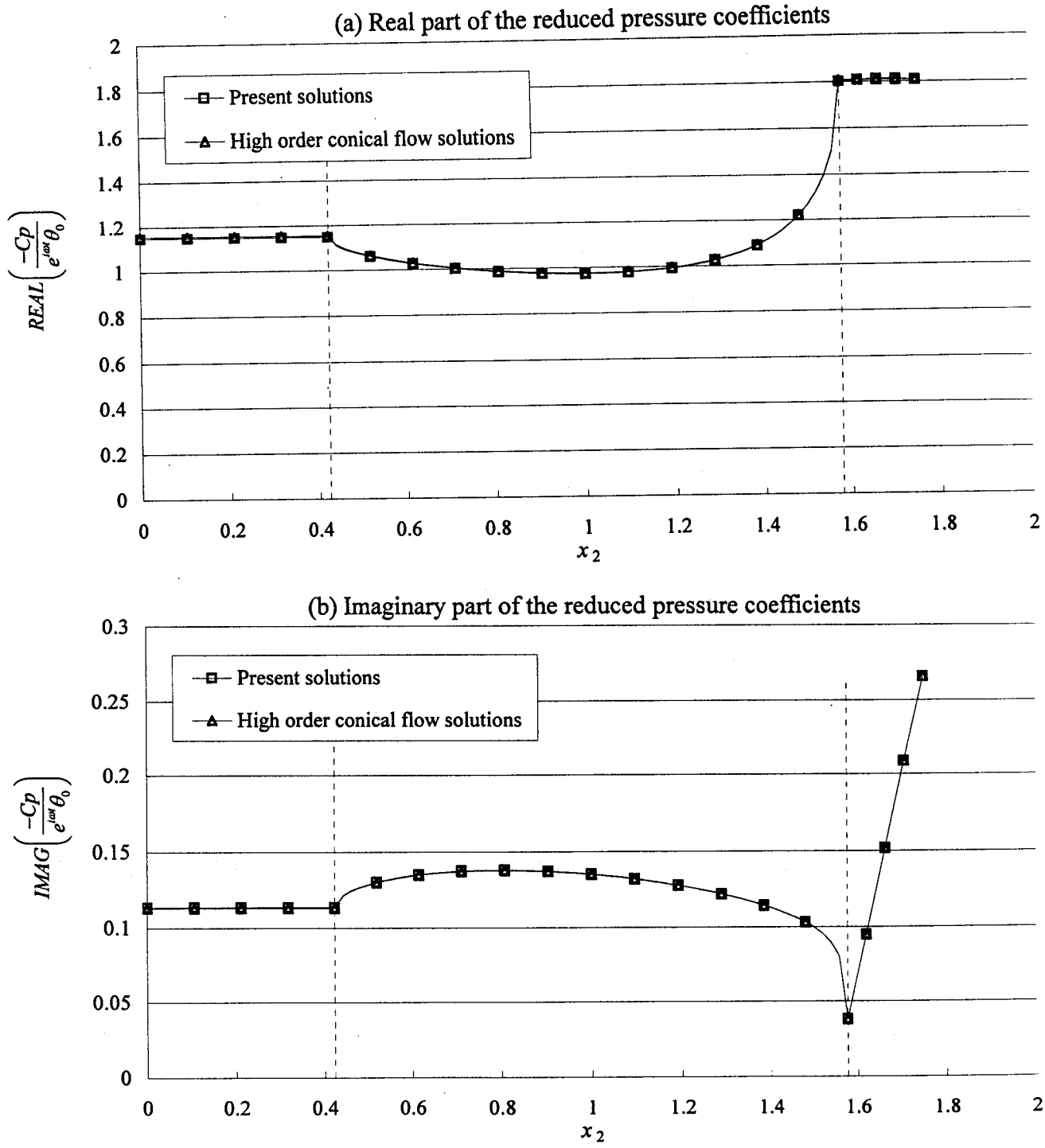


Figure 7.19 The real and imaginary parts of the reduced pressure coefficients for thin trapezoidal wing executing harmonic pitching rotation oscillations.

(The reduced frequency of oscillations, $\lambda = 0.1470$; spanwise variation at $x_1 = 1.0$; root chord, $c_0 = 1.0$; span, $b = 1.0$; semi-span, $l = 0.75$; Mach number, $M_\infty = 2.0$)

### 7.3.3 Case of wings executing oscillatory rolling rotation

We consider that each point over wing surface executes oscillatory rolling rotation of small amplitude, which can be defined by,

$$Z = x_2\psi(t) = x_2\hat{\psi}e^{i\omega t} = e^{i\omega t}(x_2\psi_0);\ P = x_2\psi_0 . \tag{7.3.5}$$

In turn, the boundary condition can be expressed by

$$\hat{w} = i\lambda x_2\psi_0 = w_{01}x_2 . \tag{7.3.6}$$

The numerical results were calculated for various reduced frequency $\lambda$ as 0.0147, 0.0735, 0.1470, 0.735, and 1.0, where $\psi_0 = 0.02$.

#### 7.3.3.1 Thin delta wing executing oscillatory rolling rotation

Present solutions to the spanwise variation of the real and imaginary parts of the reduced pressure coefficient over the right hand side of thin delta wing surface along the wing trace at $x_1$ = 1.0 are plotted in figures 7.20, 7.21, 7.22, 7.23, and 7.24. The imaginary part of the present solutions is compared in the same figures with the results obtained by the high order conical flow solutions. An excellent agreement was found for small oscillating frequency. However, the agreement starts to deteriorate for wing surface near and outside the Mach cone for high oscillating frequency. The present solutions are more accurate and provided non-zero solutions for the real part of the reduced pressure coefficients even it is small compared to the imaginary part of the solutions for small oscillating frequency. For high oscillating frequency, the weight of the real part of the present solutions is increasing and cannot be neglected with comparison of the imaginary counterpart so that the present method proves to be more accurate in this respect. Nevertheless, the high order conical flow solutions provided zero real values due to the approximation made in the frequency expansion method related to the unsteady formulation using high order conical flows.

The results of the reduced rolling moment coefficient are presented in tables 7.16, 7.17, 7.18, 7.19, and 7.20. Obviously, all results are in a very good agreement in imaginary part by the present solutions and high order conical flow solutions for oscillations at small frequency. However, for high oscillating frequency, the agreement becomes worse and the difference of the results from both methods goes up to around 28%. However, due to the approximation made in the frequency expansion method using the high order conical flows, the high order conical flow solutions provided zero values of the reduced lift coefficient and the reduced pitching moment coefficient, while the present solutions are more accurate and provide non-zero solutions in the calculation of the aerodynamic coefficients accordingly.

| | $\hat{C}_{m1}$ | |
|---|---|---|
| | **REAL** | **IMAG** |
| Present solutions | 0.00003 | 0.00314 |
| High order conical flow solutions | 0 | 0.00318 |

Table 7.16 $\hat{C}_{m1}$ for thin delta wing executing oscillatory rolling rotation ($\lambda = 0.0147$)

| | $\hat{C}_{m1}$ | |
|---|---|---|
| | **REAL** | **IMAG** |
| Present solutions | 0.00077 | 0.01570 |
| High order conical flow solutions | 0 | 0.01592 |

Table 7.17 $\hat{C}_{m1}$ for thin delta wing executing oscillatory rolling rotation ($\lambda = 0.0735$)

| | $\hat{C}_{m1}$ | |
|---|---|---|
| | **REAL** | **IMAG** |
| Present solutions | 0.00308 | 0.03127 |
| High order conical flow solutions | 0 | 0.03184 |

Table 7.18 $\hat{C}_{m1}$ for thin delta wing executing oscillatory rolling rotation ($\lambda = 0.1470$)

| | $\hat{C}_{m1}$ | |
|---|---|---|
| | **REAL** | **IMAG** |
| Present solutions | 0.0723 | 0.1343 |
| High order conical flow solutions | 0 | 0.1592 |

Table 7.19 $\hat{C}_{m1}$ for thin delta wing executing oscillatory rolling rotation ($\lambda = 0.735$)

| | $\hat{C}_{m1}$ | |
|---|---|---|
| | **REAL** | **IMAG** |
| Present solutions | 0.1268 | 0.2166 |
| High order conical flow solutions | 0 | 0.1557 |

Table 7.20 $\hat{C}_{m1}$ for thin delta wing executing oscillatory rolling rotation ($\lambda = 1.0$)

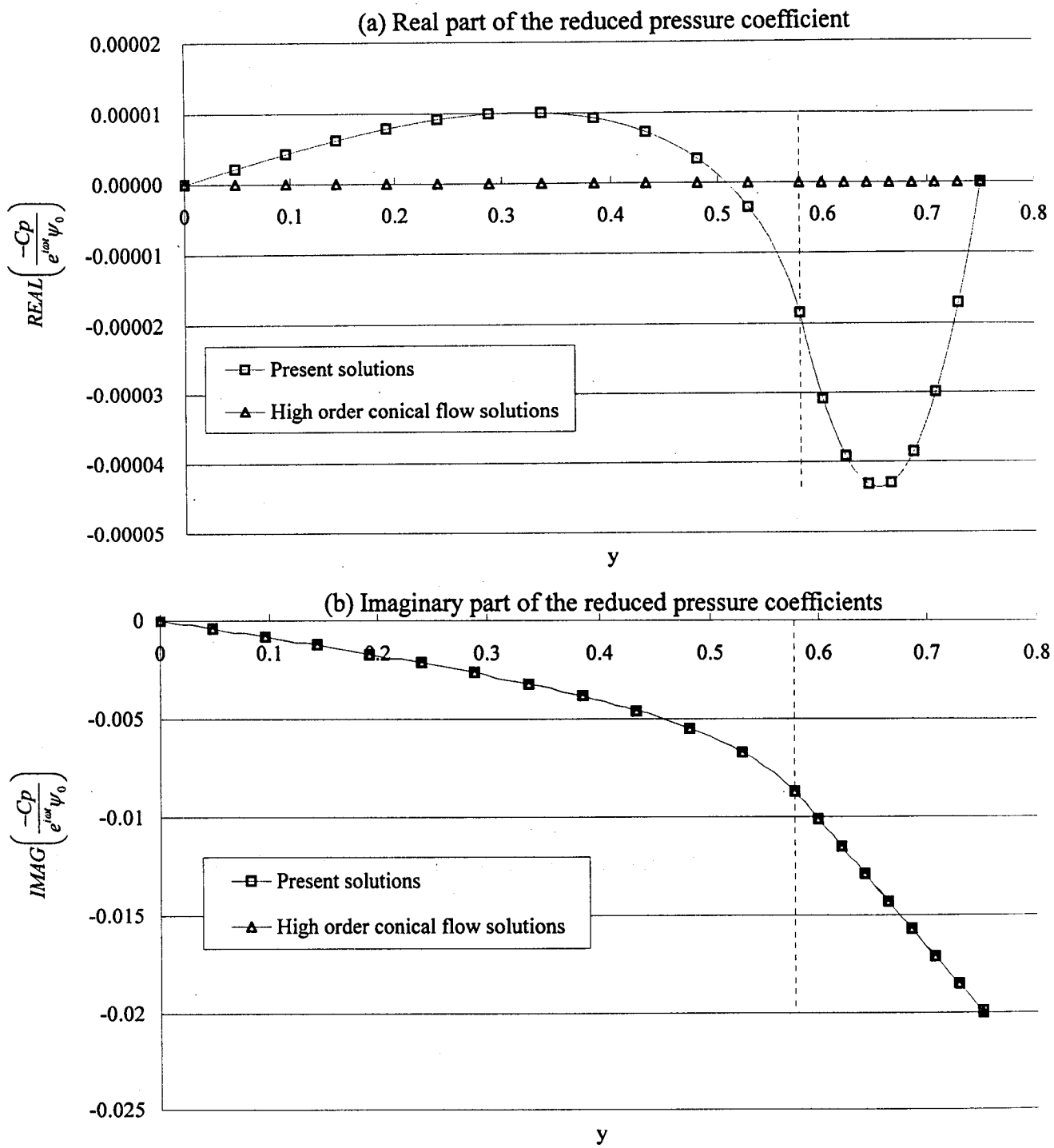


Figure 7.20 The real and imaginary parts of the reduced pressure coefficients for thin delta wing executing harmonic rolling rotation oscillations.
(The reduced frequency of oscillations, $\lambda = 0.0147$; spanwise variation at $x_1 = 1.0$; root chord, $c_0 = 1.0$; semi-span, $l = 0.75$; Mach number, $M_\infty = 2.0$)

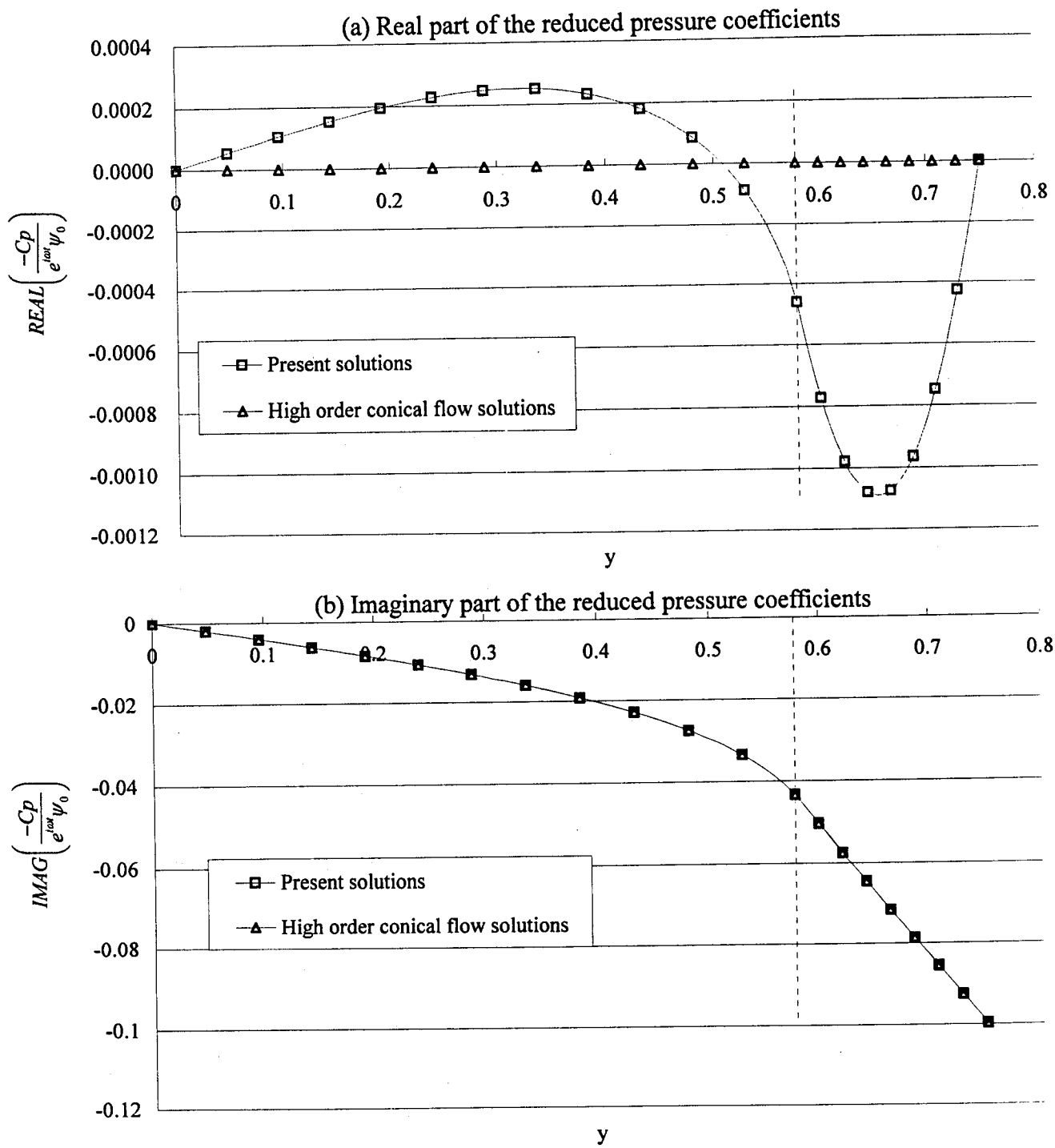


Figure 7.21 The real and imaginary parts of the reduced pressure coefficients for thin delta wing executing harmonic rolling rotation oscillations.
(The reduced frequency of oscillations, $\lambda = 0.0735$; spanwise variation at $x_1 = 1.0$; root chord, $c_0 = 1.0$; semi-span, $l = 0.75$; Mach number, $M_\infty = 2.0$)

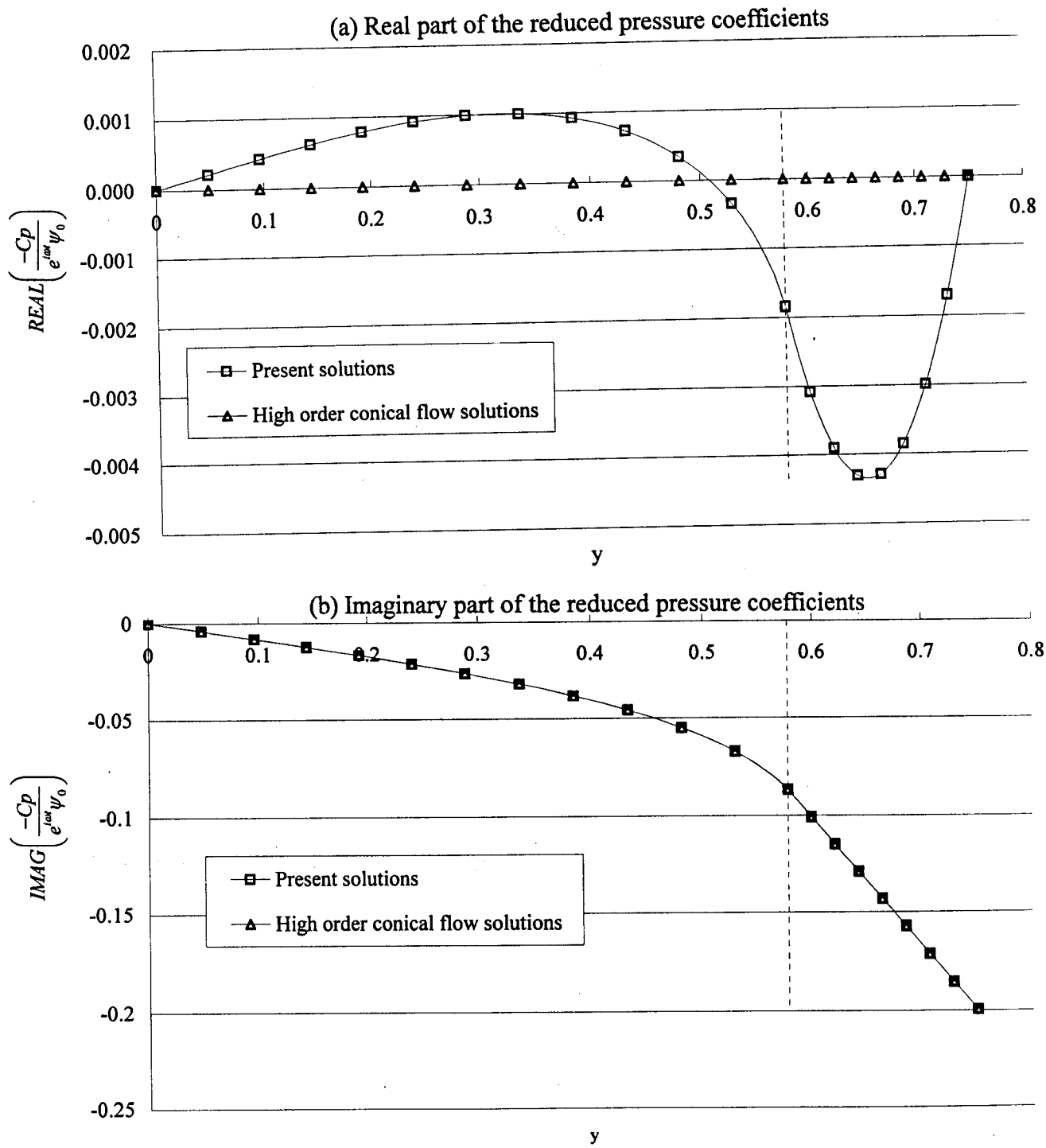


Figure 7.22 The real and imaginary parts of the reduced pressure coefficients for thin delta wing executing harmonic rolling rotation oscillations.
(The reduced frequency of oscillations, $\lambda = 0.1470$; spanwise variation at $x_1 = 1.0$; root chord, $c_0 = 1.0$; semi-span, $l = 0.75$; Mach number, $M_\infty = 2.0$)

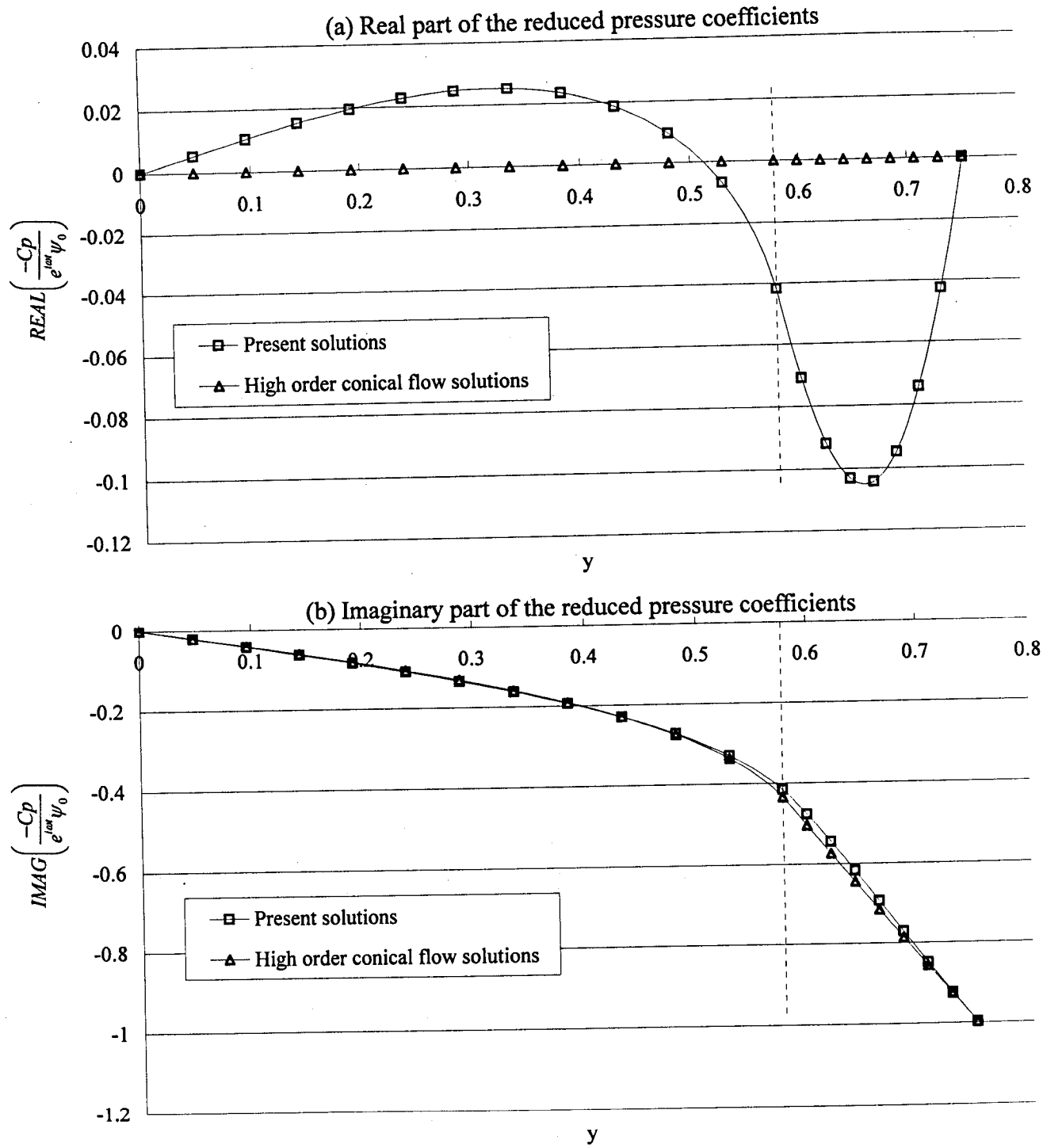


Figure 7.23 The real and imaginary parts of the reduced pressure coefficients for thin delta wing executing harmonic rolling rotation oscillations.
(The reduced frequency of oscillations, $\lambda = 0.735$; spanwise variation at $x_1 = 1.0$; root chord, $c_0 = 1.0$; semi-span, $l = 0.75$; Mach number, $M_\infty = 2.0$)

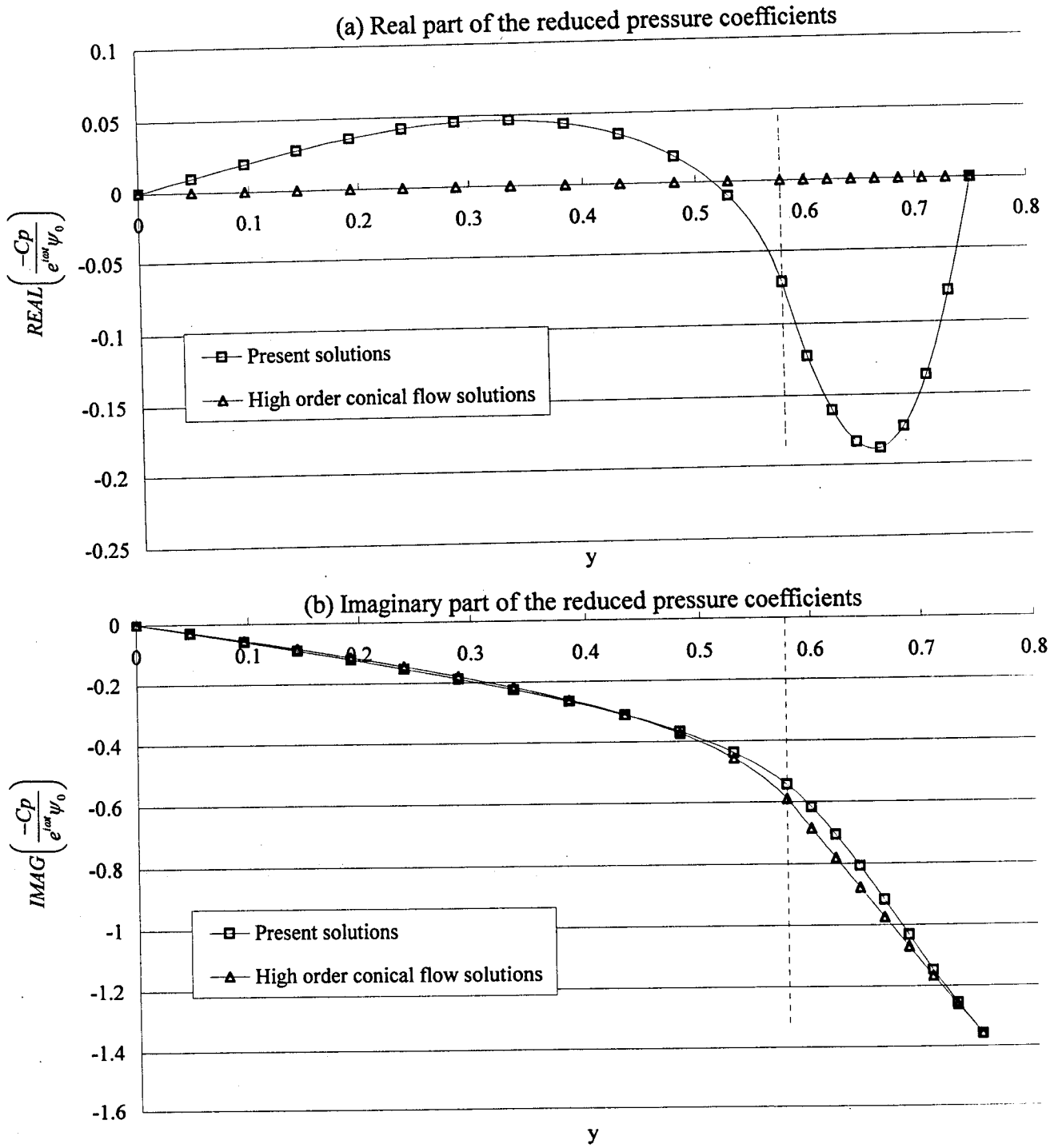


Figure 7.24 The real and imaginary parts of the reduced pressure coefficients for thin delta wing executing harmonic rolling rotation oscillations.
(The reduced frequency of oscillations, $\lambda = 1.0$; spanwise variation at $x_1 = 1.0$; root chord, $c_0 = 1.0$; semi-span, $l = 0.75$; Mach number, $M_\infty = 2.0$)

### 7.3.3.2 Thin trapezoidal wing executing oscillatory rolling rotation

Present solutions of the spanwise variations at $x_1 = 1.0$ of the real and imaginary parts of the reduced pressure coefficient of the thin trapezoidal wing are plotted in figures 7.25, 7.26, and 7.27. The imaginary part of the present solutions is plotted in the same figures in comparison to the high order conical flow solutions (Carafoli, Mateescu, Nastase, [2]). An excellent agreement was found among them. The real part of the reduced pressure coefficients is calculated by the present method and non-zero solutions are presented. However, the high order conical flow solutions provided zero real values, on which an approximation made in the frequency expansion method related to the unsteady formulation is based.

The reduced rolling moment coefficients are calculated by the present method and presented in table 7.21, while the previous results by the theory of high order conical flows are not available in this case.

| Present solutions | $\hat{C}_{m1}$ | |
|---|---|---|
| | **REAL** | **IMAG** |
| $\lambda = 0.0147$ | 0.000004 | 0.00037 |
| $\lambda = 0.0735$ | 0.00009 | 0.00184 |
| $\lambda = 0.1470$ | 0.00036 | 0.00366 |

Table 7.21 $\hat{C}_{m1}$ for thin trapezoidal wing executing oscillatory rolling rotation ($\lambda$ = 0.0147, 0.0735, and 0.1470)

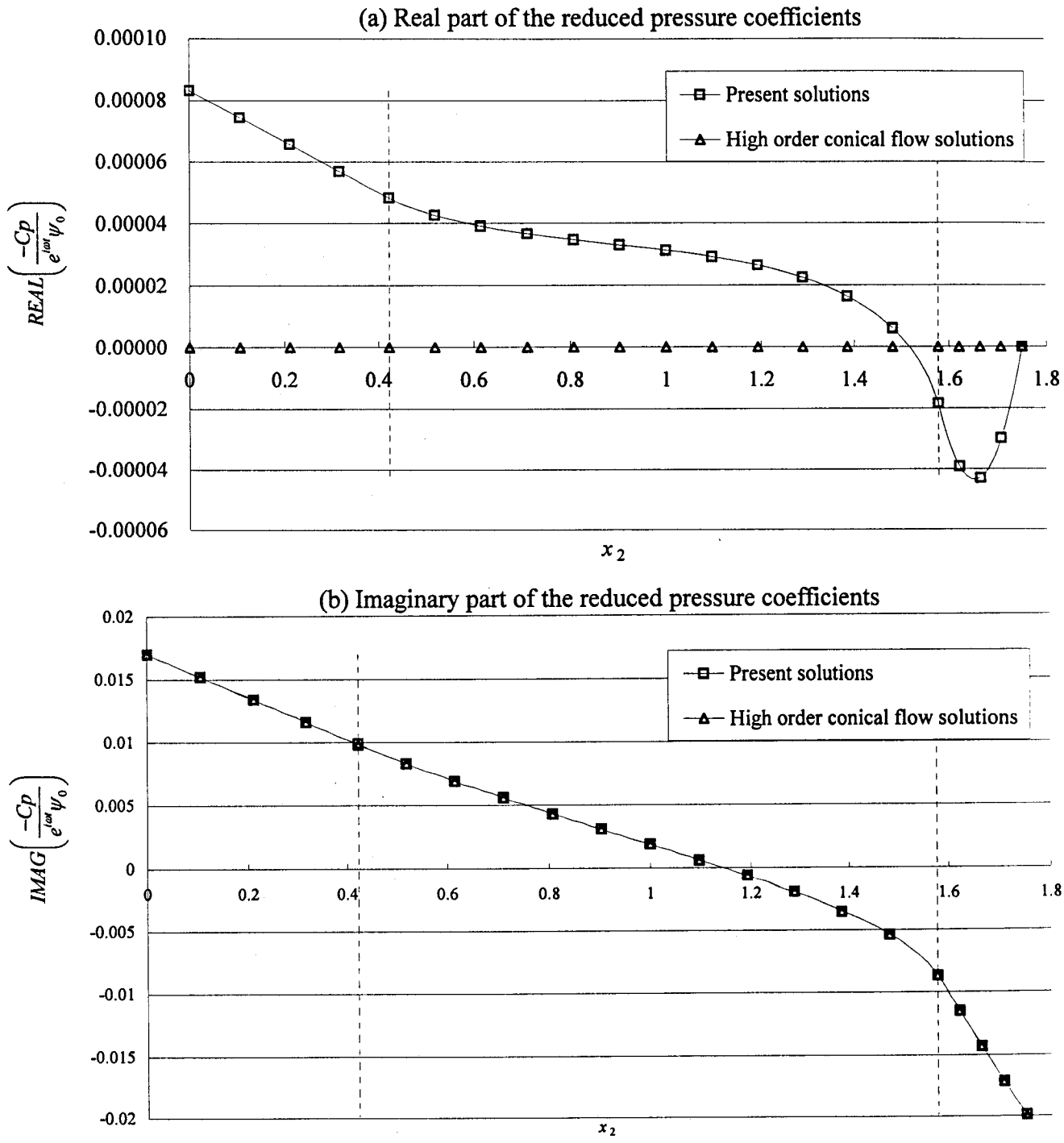


Figure 7.25 The real and imaginary parts of the reduced pressure coefficients for thin trapezoidal wing executing harmonic rolling rotation oscillations.
(The reduced frequency of oscillations, $\lambda = 0.0147$; spanwise variation at $x_1 = 1.0$; root chord, $c_0 = 1.0$; span, $b = 1.0$; semi-span, $l = 0.75$; Mach number, $M_\infty = 2.0$)

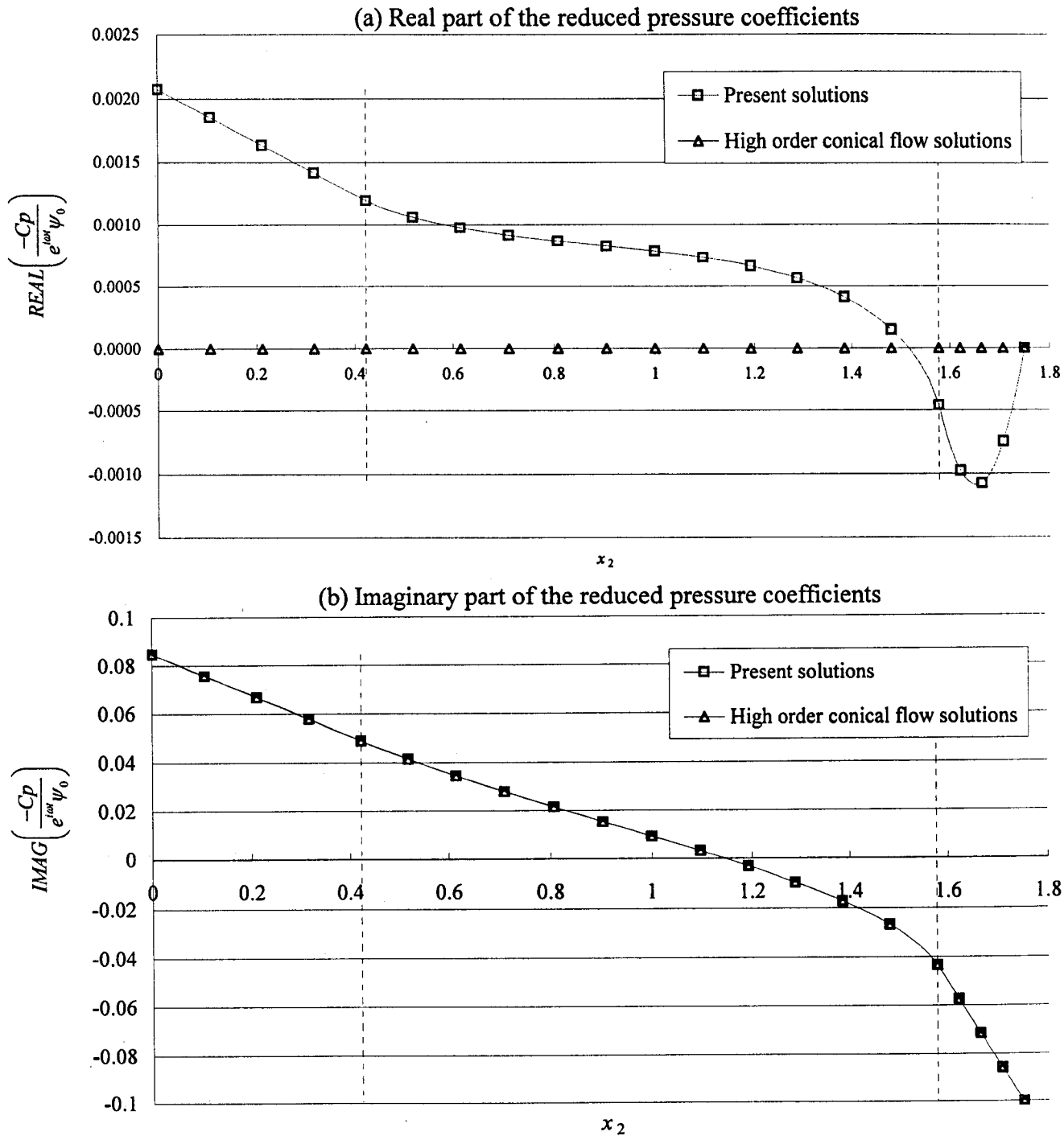


Figure 7.26 The real and imaginary parts of the reduced pressure coefficients for thin trapezoidal wing executing harmonic rolling rotation oscillations.
(The reduced frequency of oscillations, $\lambda = 0.0735$; spanwise variation at $x_1 = 1.0$; root chord, $c_0 = 1.0$; span, $b = 1.0$; semi-span, $l = 0.75$; Mach number, $M_\infty = 2.0$)

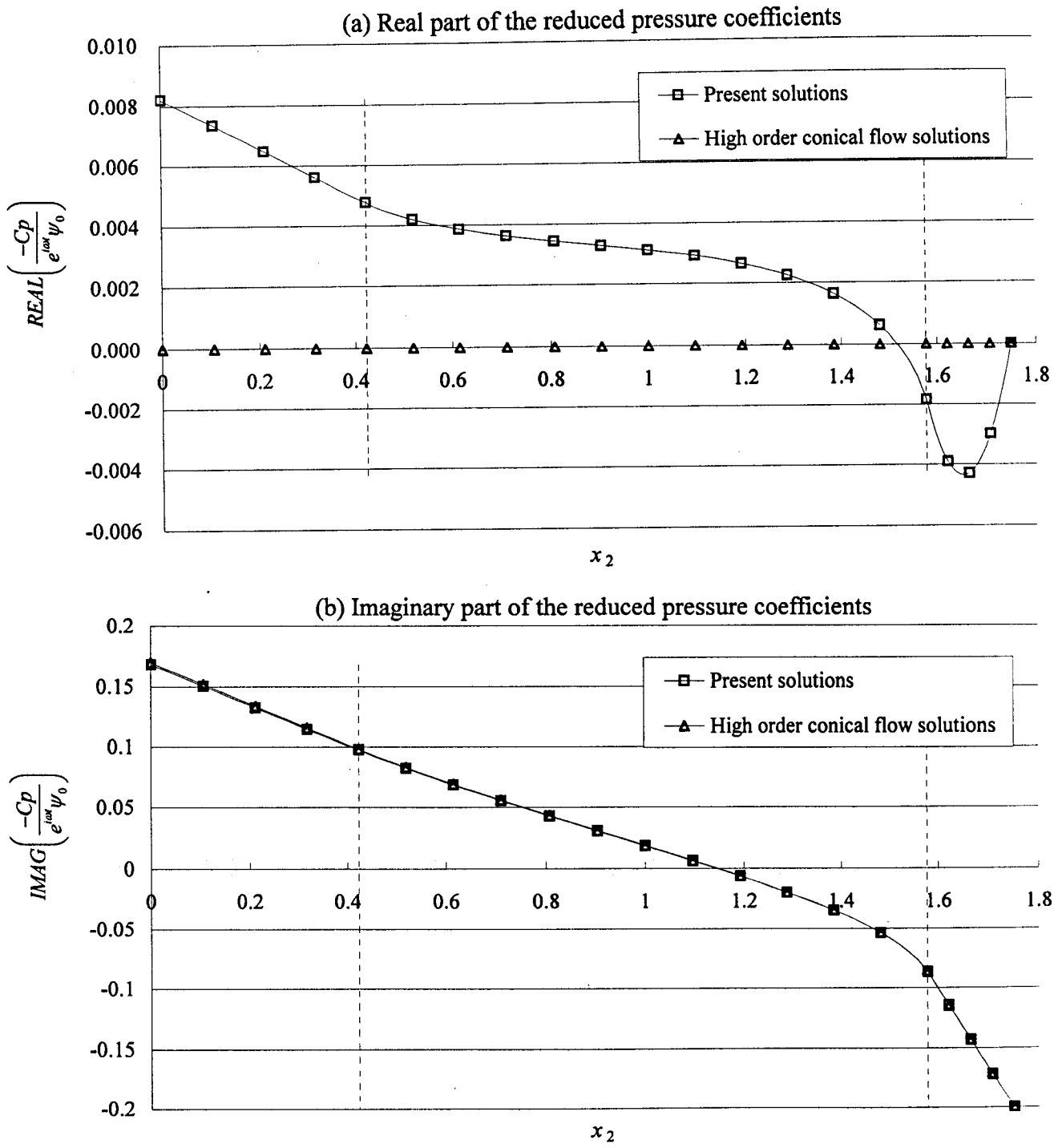


Figure 7.27 The real and imaginary parts of the reduced pressure coefficients for thin trapezoidal wing executing harmonic rolling rotation oscillations.

(The reduced frequency of oscillations, $\lambda = 0.1470$; spanwise variation at $x_1 = 1.0$; root chord, $c_0 = 1.0$; span, $b = 1.0$; semi-span, $l = 0.75$; Mach number, $M_\infty = 2.0$)

## 7.4 Unsteady flow results for flexible wings executing flexural oscillations

In this section, the flexural harmonic oscillating deformation of wings in supersonic flows are analyzed by method of distribution of pulsating sources. Likely, equations of any point over wing surface executing flexural harmonic oscillations in two directions, which are along $Ox_1$ and $Ox_2$ axes, respectively, can be described by two homogeneous polynomials.

$$Z_1 = e^{i\omega t} P_1(x_1, x_2) = g_1 x_1^2 e^{i\omega t}. \tag{7.4.1}$$

$$Z_2 = e^{i\omega t} P_2(x_1, x_2) = g_2 x_2^2 e^{i\omega t}. \tag{7.4.2}$$

Constants, $g_1$ and $g_2$, are coefficients of homogeneous polynomials, and the boundary conditions are given as

$$\hat{w}_1 = \left( \frac{\partial P_1}{\partial x_1} + i\lambda P_1 \right) = 2g_1 x_1 + i\lambda g_1 x_1^2, \tag{7.4.3}$$

$$\hat{w}_2 = \left( \frac{\partial P_2}{\partial x_1} + i\lambda P_2 \right) = i\lambda g_2 x_2^2. \tag{7.4.4}$$

The numerical results are obtained for the reduced frequency $\lambda$ as 0.0147, where $g_1$ and $g_2$ are equal to 0.02.

The spanwise variations of the reduced pressure coefficients at $x_1 = 1.0$ are plotted in figures 7.28 and 7.29 for thin delta wing and figures 7.30 and 7.31 for thin trapezoidal wing.

### 7.4.1 Thin delta wing executing flexural harmonic oscillatory deformation

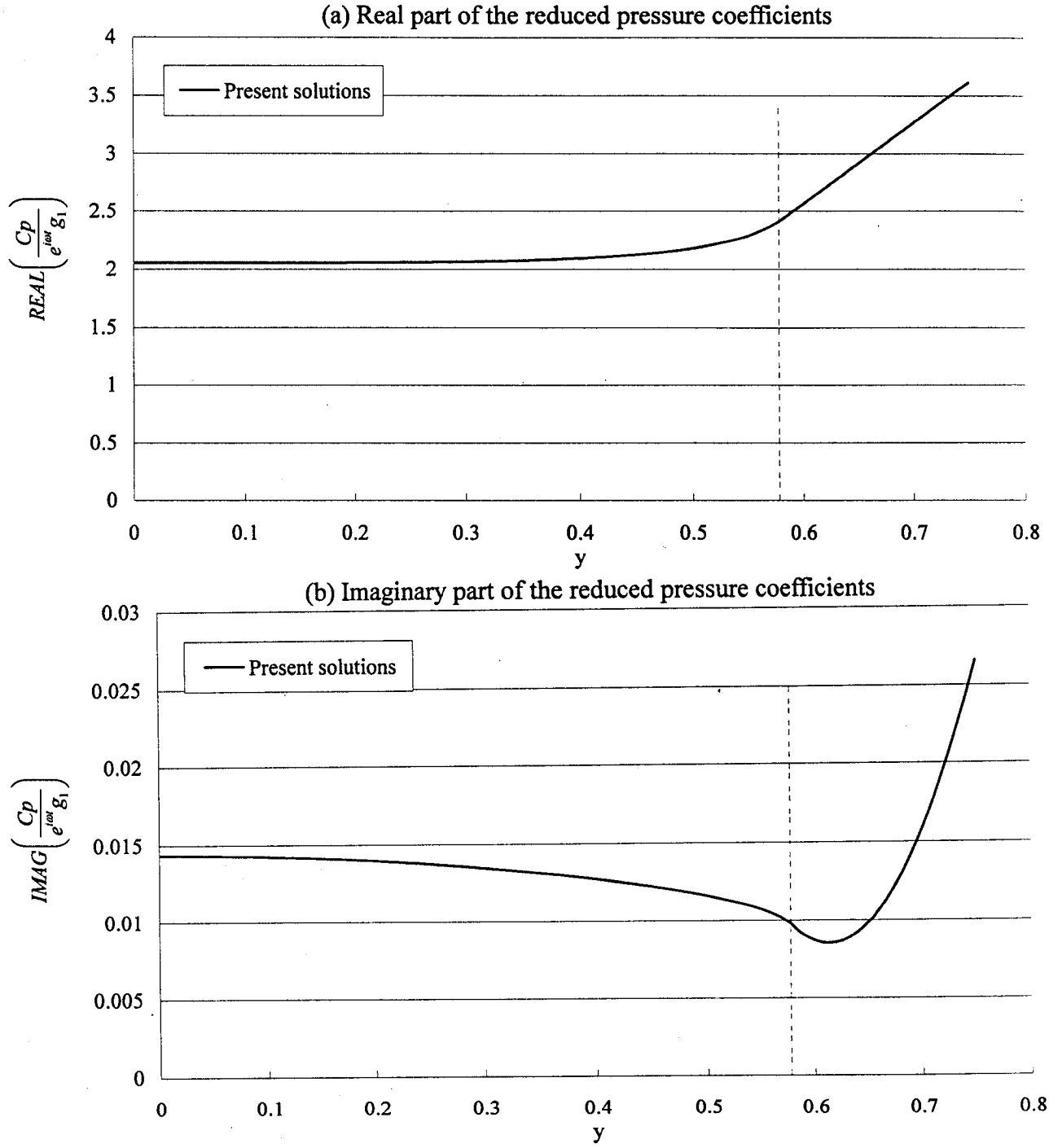


Figure 7.28 The real and imaginary parts of the reduced pressure coefficients for thin delta wing executing flexural oscillations, $Z = g_1 x_1^2 e^{i\omega t}$.
(The reduced frequency of oscillations, $\lambda = 0.0147$; spanwise variation at $x_1 = 1.0$; root chord, $c_0 = 1.0$; semi-span, $l = 0.75$; Mach number, $M_\infty = 2.0$)

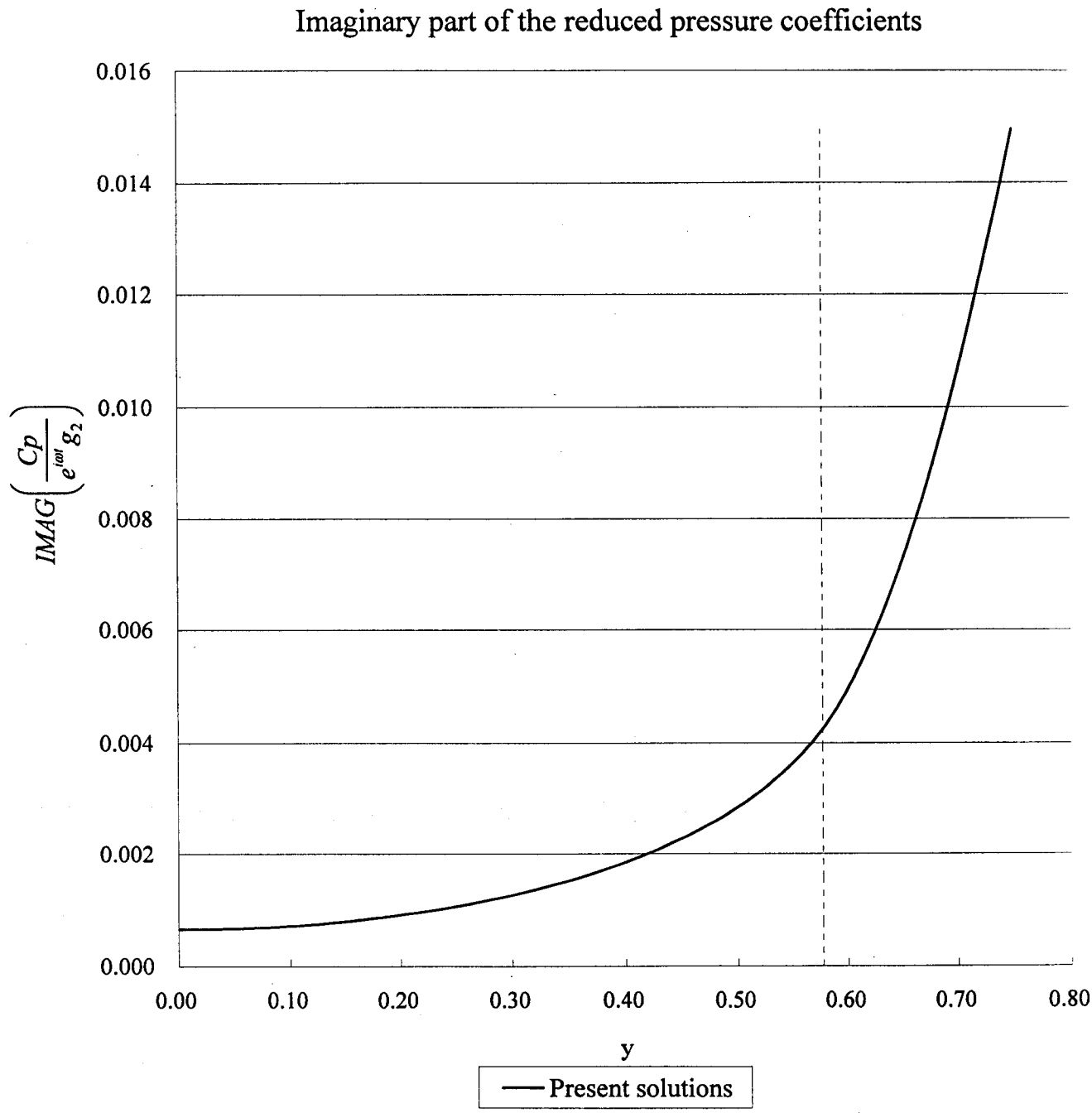


Figure 7.29 The imaginary part of the reduced pressure coefficients for thin delta wing executing flexural oscillations, $Z = g_2 x_2^2 e^{i\omega t}$.

(The reduced frequency of oscillations, $\lambda = 0.0147$; spanwise variation at $x_1 = 1.0$; root chord, $c_0 = 1.0$; semi-span, $l = 0.75$; Mach number, $M_\infty = 2.0$)

### 7.4.2 Thin trapezoidal wing executing flexural harmonic oscillatory deformation

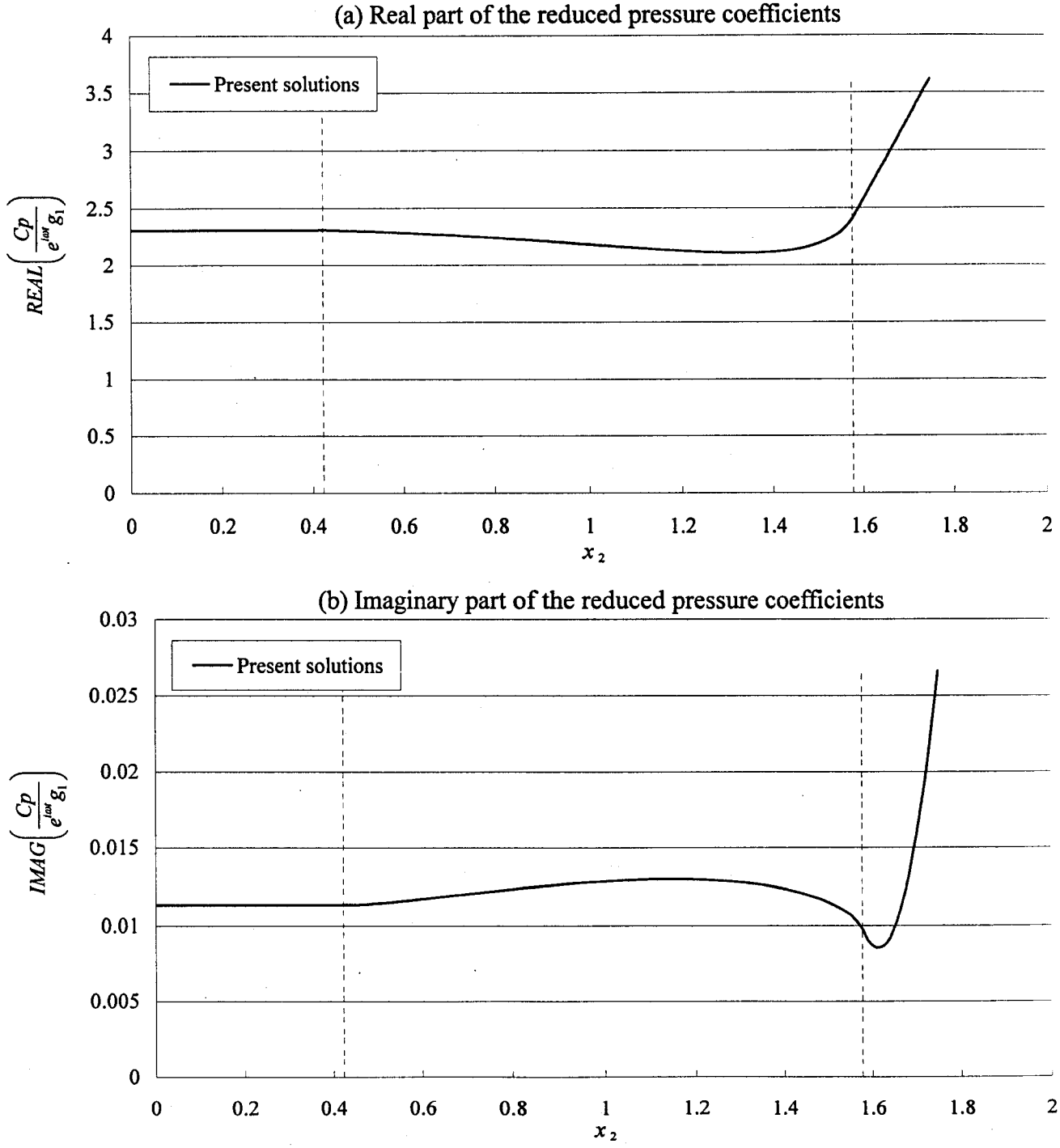


Figure 7.30 The real and imaginary parts of the reduced pressure coefficients for thin trapezoidal wing executing flexural oscillations, $Z = g_1 x_1^2 e^{i\omega t}$.
(The reduced frequency of oscillations, $\lambda = 0.0147$; spanwise variation at $x_1 = 1.0$; root chord, $c_0 = 1.0$; span, $b = 1.0$; semi-span, $l = 0.75$; Mach number, $M_\infty = 2.0$)

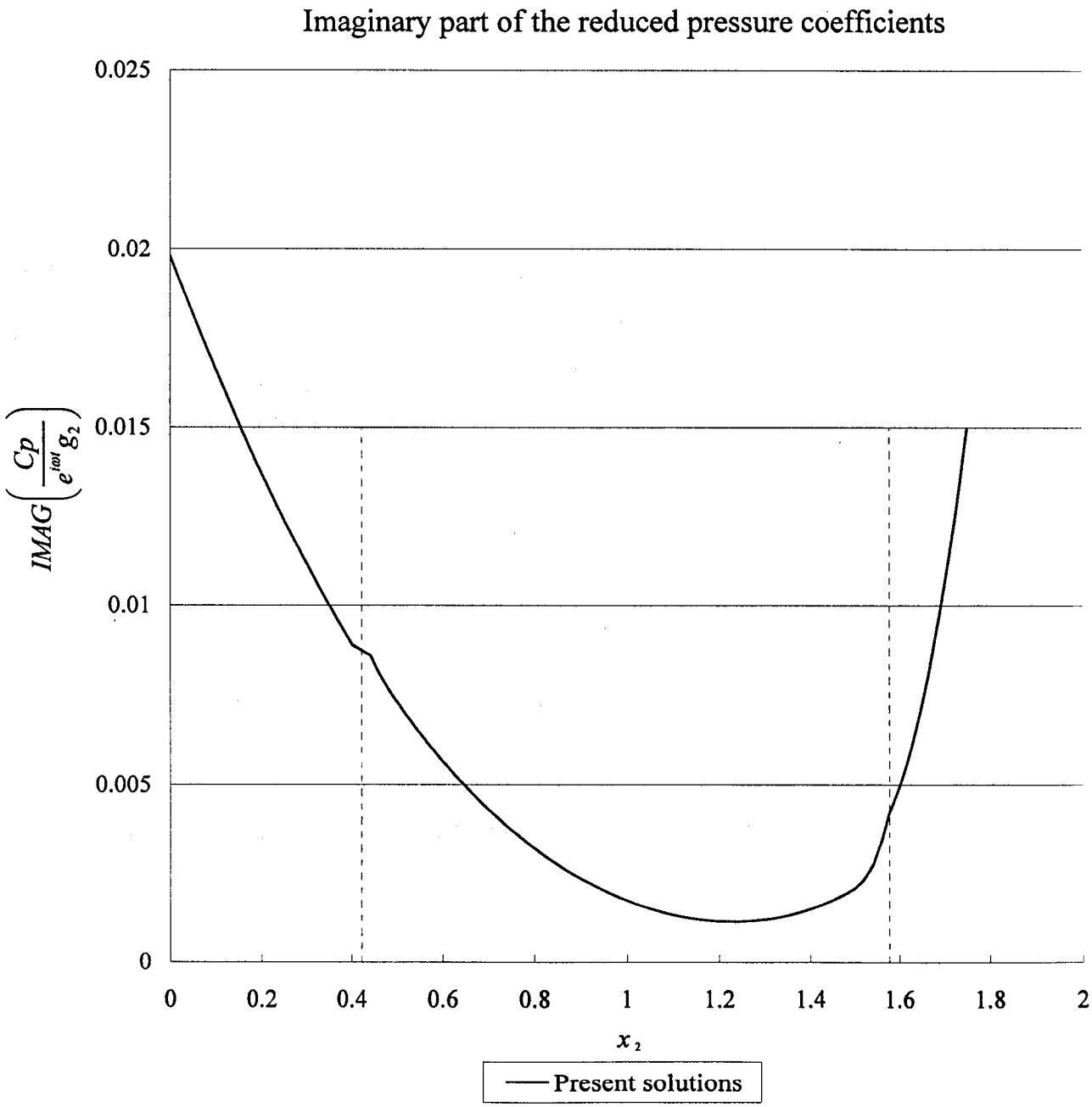


Figure 7.31 The imaginary part of the reduced pressure coefficients for thin trapezoidal wing executing flexural oscillations, $Z = g_2 x_2^2 e^{i\omega t}$.
(The reduced frequency of oscillations, $\lambda = 0.0147$; spanwise variation at $x_1 = 1.0$; root chord, $c_0 = 1.0$; span, $b = 1.0$; semi-span, $l = 0.75$; Mach number, $M_\infty = 2.0$)

# CHAPTER 8

# CONCLUSION

This thesis presents a method for the study of finite span wings in steady and unsteady supersonic flows.

For steady flows, the method uses a distribution of sources, which are integrated over the surface of the wing. Specific theoretical solutions have been derived for the pressure coefficient and the lift, pitching moment, and rolling moment coefficients. The present solutions have been validated for delta and trapezoidal wings by comparison with the results obtained by Carafoli, Mateescu, and Nastase [2], [38]-[41], using the high order conical flows method. An excellent agreement was found between these results.

The method of solutions for unsteady flows uses pulsating sources distributing on the wing surface, which are integrated over the surface of the oscillating wings. Specific theoretical solutions have been derived for the unsteady pressure coefficient and the unsteady lift, pitching moment, and rolling moment coefficients.

The present unsteady solutions have been validated for delta and trapezoidal wings executing harmonic oscillations in translation, pitching rotation and rolling rotation of various frequencies by compassion with the results obtained by Carafoli, Mateescu, and Nastase [2], [38]-[41], using the high order conical flows method. The present solutions were found in very good agreement with the

previous results available for small oscillating frequency. This agreement between the two methods starts to deteriorate for high oscillating frequency due to the approximation introduced in high order conical flow solutions. Moreover, the present solutions is proved to be more accurate and provided non-zero solutions for the real part of the reduced pressure coefficient, and the reduced lift and moment coefficients in the case of oscillatory translation and rolling oscillation. In these cases, the high order conical flow solutions only provided zero real values due to the approximations made in the frequency expansion method. Nevertheless, the actual real values obtained in the present unsteady solutions are small in the case of low frequencies but they are increasing for higher oscillating frequencies.

The method has then been applied for the analysis of wings with flexural oscillations, which are of interest for the aeroelastic studies in the aeronautical applications.

**Recommendation for future study:** The present method can be extended in the future for the trapezoidal and rectangular wings with subsonic leading edges. Also worthy of future research are the exponentially decaying amplitude in harmonic motions and wing surface deformation. This could be a very interesting problem as often being cases in practice.

# Appendix A: Derivation of $\Phi_1'$ related to the calculation of the reduced pressure coefficient by theory of high order conical flows

## A-1: Case of thin delta wing

$$\Phi_1' = \mathrm{Re}\left[x_1 x \int U_0' d\left(\frac{1}{x}\right)\right] = \mathrm{Re}\left[x_1 x \int \frac{2l\hat{\theta}}{\pi\sqrt{B^2l^2-1}}\left(\cos^{-1}\sqrt{\frac{(1+Bl)(1-Bx)}{2B(l-x)}} + \cos^{-1}\sqrt{\frac{(1+Bl)(1+Bx)}{2B(l+x)}}\right) d\left(\frac{1}{x}\right)\right]$$

$$= \mathrm{Re}\left[x_1 \frac{2\hat{\theta}}{\pi\sqrt{B^2l^2-1}} lx \int\left(\cos^{-1}\sqrt{\frac{(1+Bl)(1-Bx)}{2B(l-x)}} + \cos^{-1}\sqrt{\frac{(1+Bl)(1+Bx)}{2B(l+x)}}\right) d\left(\frac{1}{x}\right)\right]. \quad \text{(A-1)}$$

For the 1st integral, by method of integration by parts, we first set *u* and *dv* and then *du* and *v* are calculated straightforward as

$$u = \cos^{-1}\sqrt{\frac{(1+Bl)(1-Bx)}{2B(l-x)}},\ du = \frac{\sqrt{B^2l^2-1}}{2(l-x)\sqrt{1-B^2x^2}}dx. \quad \text{(A-2)}$$

$$dv = d\left(\frac{1}{x}\right),\ v = \frac{1}{x}. \quad \text{(A-3)}$$

Then,

$$\int\cos^{-1}\sqrt{\frac{(1+Bl)(1-Bx)}{2B(l-x)}} d\left(\frac{1}{x}\right) = \frac{1}{x}\cos^{-1}\sqrt{\frac{(1+Bl)(1-Bx)}{2B(l-x)}} - \int\frac{1}{x(l-x)}\frac{\sqrt{B^2l^2-1}}{2\sqrt{1-B^2x^2}}dx$$

$$= \frac{1}{x}\cos^{-1}\sqrt{\frac{(1+Bl)(1-Bx)}{2B(l-x)}} - \int\left[\frac{1}{l}\left(\frac{1}{x}+\frac{1}{l-x}\right)\right]\frac{\sqrt{B^2l^2-1}}{2\sqrt{1-B^2x^2}}dx$$

$$= \frac{1}{x}\cos^{-1}\sqrt{\frac{(1+Bl)(1-Bx)}{2B(l-x)}} - \frac{1}{l}\int\frac{\sqrt{B^2l^2-1}}{2(l-x)\sqrt{1-B^2x^2}}dx - \frac{1}{l}\int\frac{\sqrt{B^2l^2-1}}{2x\sqrt{1-B^2x^2}}dx$$

$$= \frac{1}{x}\cos^{-1}\sqrt{\frac{(1+Bl)(1-Bx)}{2B(l-x)}} - \frac{1}{l}\cos^{-1}\sqrt{\frac{(1+Bl)(1-Bx)}{2B(l-x)}} - \frac{\sqrt{B^2l^2-1}}{2l}\int\frac{1}{x\sqrt{1-B^2x^2}}dx. \quad \text{(A-4)}$$

The 2nd integral can be calculated in the same manner as

$$\int\cos^{-1}\sqrt{\frac{(1+Bl)(1+Bx)}{2B(l+x)}}d\left(\frac{1}{x}\right)=\frac{1}{x}\cos^{-1}\sqrt{\frac{(1+Bl)(1+Bx)}{2B(l+x)}}-\int\frac{1}{x(l+x)}\frac{-\sqrt{B^2l^2-1}}{2\sqrt{1-B^2x^2}}dx$$

$$=\frac{1}{x}\cos^{-1}\sqrt{\frac{(1+Bl)(1+Bx)}{2B(l+x)}}+\int\left[\frac{1}{l}\left(\frac{1}{x}-\frac{1}{l+x}\right)\right]\frac{\sqrt{B^2l^2-1}}{2\sqrt{1-B^2x^2}}dx$$

$$=\frac{1}{x}\cos^{-1}\sqrt{\frac{(1+Bl)(1+Bx)}{2B(l+x)}}+\frac{1}{l}\int\frac{-\sqrt{B^2l^2-1}}{2(l+x)\sqrt{1-B^2x^2}}dx+\frac{\sqrt{B^2l^2-1}}{2l}\int\frac{1}{x\sqrt{1-B^2x^2}}dx$$

$$=\frac{1}{x}\cos^{-1}\sqrt{\frac{(1+Bl)(1+Bx)}{2B(l+x)}}+\frac{1}{l}\cos^{-1}\sqrt{\frac{(1+Bl)(1+Bx)}{2B(l+x)}}+\frac{\sqrt{B^2l^2-1}}{2l}\int\frac{1}{x\sqrt{1-B^2x^2}}dx. \quad \text{(A-5)}$$

Accordingly, $\Phi_1'$ for thin delta wing is calculated as

$$\Phi_1'=\frac{2\hat{\theta}x_1}{\pi\sqrt{B^2l^2-1}}\left[(l-x)\cos^{-1}\sqrt{\frac{(1+Bl)(1-Bx)}{2B(l-x)}}+(l+x)\cos^{-1}\sqrt{\frac{(1+Bl)(1+Bx)}{2B(l+x)}}\right]. \quad \text{(A-6)}$$

## A-2: Case of thin trapezoidal wing

$$\Phi_1'=\mathrm{Re}\left[x_1x\int U_0'd\left(\frac{1}{x}\right)\right]=\mathrm{Re}\left[x_1x\int\left(\frac{2l\hat{\theta}}{\pi\sqrt{B^2l^2-1}}\cos^{-1}\sqrt{\frac{(1+Bl)(1-Bx)}{2B(l-x)}}+\frac{2\hat{\theta}}{\pi B}\cos^{-1}\sqrt{\frac{(1+Bx)}{2}}\right)d\left(\frac{1}{x}\right)\right]$$

$$=x_1\times\mathrm{Re}\left[\frac{2\hat{\theta}}{\pi\sqrt{B^2l^2-1}}lx\int\cos^{-1}\sqrt{\frac{(1+Bl)(1-Bx)}{2B(l-x)}}d\left(\frac{1}{x}\right)+\frac{2\hat{\theta}}{\pi B}x\int\cos^{-1}\sqrt{\frac{(1+Bx)}{2}}d\left(\frac{1}{x}\right)\right]. \quad \text{(A-7)}$$

The first integral is obtained already for case of thin delta wing. The second integral is calculated by parts and we set *u* and *dv* and then *du* and *v* are calculated straightforward as

$$u=\cos^{-1}\sqrt{\frac{1+Bx}{2}},\ du=\frac{-B}{2\sqrt{1-B^2x^2}}dx. \quad \text{(A-8)}$$

$$dv=d\left(\frac{1}{x}\right),\ v=\frac{1}{x}. \quad \text{(A-9)}$$

$$\int\cos^{-1}\sqrt{\frac{1+Bx}{2}}d\left(\frac{1}{x}\right)=\frac{1}{x}\cos^{-1}\sqrt{\frac{1+Bx}{2}}+\frac{B}{2}\int\frac{1}{x}\frac{1}{\sqrt{1-B^2x^2}}dx. \quad \text{(A-10)}$$

Accordingly, $\Phi_1'$ for thin trapezoidal wing is calculated as

$$\Phi_1' = x_1 \times \mathrm{Re}\left[\frac{2\hat{\theta}}{\pi\sqrt{B^2l^2-1}}(l-x)\cos^{-1}\sqrt{\frac{(1+Bl)(1-Bx)}{2B(l-x)}} - \frac{\hat{\theta}}{\pi}\int\frac{1}{x\sqrt{B^2l^2-1}}dx + \frac{2\hat{\theta}}{\pi B}\cos^{-1}\sqrt{\frac{1+Bx}{2}} + \frac{\hat{\theta}}{\pi}\int\frac{1}{x\sqrt{B^2l^2-1}}dx\right]$$

$$= x_1 \times \mathrm{Re}\left[\frac{2\hat{\theta}}{\pi\sqrt{B^2l^2-1}}(l-x)\cos^{-1}\sqrt{\frac{(1+Bl)(1-Bx)}{2B(l-x)}} + \frac{2\hat{\theta}}{\pi B}\cos^{-1}\sqrt{\frac{1+Bx}{2}}\right]. \qquad \text{(A-11)}$$

# Appendix B: REAL PART OF SPECIFIC INVERSE TRIANGULAR FUNCTIONS

In this part, the limits of the following triangular functions are presented as references for several calculations in this study.

$$\mathrm{Re}\left[\cos^{-1}\sqrt{\frac{(1+Bl_1)(1-Bx)}{2B(l_1-x)}}\right]_{\substack{x=y\\z=0}} = \begin{cases} \dfrac{\pi}{2} & y\in\left(\dfrac{1}{B},l_1\right) \\ \cos^{-1}\sqrt{\dfrac{(1+Bl_1)(1-Bx)}{2B(l_1-x)}}; & y\in\left(-l_2,\dfrac{1}{B}\right) \\ 0 & y\in(-\infty,-l_2)\cup(l_1,\infty) \end{cases}$$

$$\mathrm{Re}\left[\cos^{-1}\sqrt{\frac{(1+Bl_2)(1+Bx)}{2B(l_2+x)}}\right]_{\substack{x=y\\z=0}} = \begin{cases} \dfrac{\pi}{2} & y\in\left(-l_2,-\dfrac{1}{B}\right) \\ \cos^{-1}\sqrt{\dfrac{(1+Bl_2)(1+Bx)}{2B(l_2+x)}}; & y\in\left(-\dfrac{1}{B},l_1\right) \\ 0 & y\in(-\infty,-l_2)\cup(l_1,\infty) \end{cases}$$

# Appendix C: Integrals related to the calculation of $C_l$, $C_{m1}$, and $C_{m2}$ based on method of source distribution

## C-1: Case of thin delta wing in steady supersonic flows

**For calculation of the lift coefficient, $C_l$:**

$$(n-k-q)\int_l^1\int_0^1\left(x_1^{n-k-q-1}y^{j-q}\right)I_0 x_1 dx_1 dy$$

$$=\frac{n-k-q}{(k+q+1)(n+2)}\left[\sum_{f=0}^{q}(-1)^f C_f^q l^{q-f}\left(\sum_{t_1=0}^{j-q}(-1)^{t_1}C_{t_1}^{j-q}l^{j-q-t_1}\int_l^1(l-y)^{k+q+t_1+1}I_g dy\right)\right.$$

$$\left.+\sum_{f=0}^{i_2}(-1)^{i_2-f}C_f^{i_2}l^{i_2-f}\left(\sum_{t_2=0}^{j-q}(-1)^{j-q-t_2}C_{t_2}^{j-q}l^{j-q-t_2}\int_l^1(l+y)^{i_1+t_2+1}J_g dy\right)\right]. \qquad \text{(C-1)}$$

$$\int_l^1\int_0^1\left(x_1^{n-k-q}y^{j-q}\right)I_0 x_1 dx_1 dy$$

$$=\frac{1}{(k+q+1)(n+3)}\left[\sum_{f=0}^{q}(-1)^f C_f^q l^{q-f}\left(\sum_{t_1=0}^{j-q}(-1)^{t_1}C_{t_1}^{j-q}l^{j-q-t_1}\int_l^1(l-y)^{k+q+t_1+1}I_g dy\right)\right.$$

$$\left.+\sum_{f=0}^{q}(-1)^{q-f}C_f^q l^{q-f}\left(\sum_{t_2=0}^{j-q}(-1)^{j-q-t_2}C_{t_2}^{j-q}l^{j-q-t_2}\int_l^1(l+y)^{k+q+t_2+1}J_g dy\right)\right]. \qquad \text{(C-2)}$$

$$\int_l^1\int_0^1\left(x_1^{n-k-q}y^{j-q}\right)\frac{\partial I_0}{\partial x_1}x_1 dx_1 dy$$

$$=\frac{1}{n+2}\left[\sum_{f=0}^{q}(-1)^f C_f^q l^{q-f+1}\left(\sum_{t_3=0}^{j-q}(-1)^{t_3}C_{t_3}^{j-q}l^{j-q-t_3}\int_l^1(l-y)^{k+q+t_3}I_g dy\right)\right.$$

$$\left.+\sum_{f=0}^{q}(-1)^{q-f}C_f^q l^{q-f+1}\left(\sum_{t_4=0}^{j-q}(-1)^{j-q-t_4}C_{t_4}^{j-q}l^{j-q-t_4}\int_l^1(l+y)^{k+q+t_4}J_g dy\right)\right]$$

$$-\frac{1}{(n+2)(k+q+1)}\left\{\sum_{f=0}^{q}(-1)^f C_f^q l^{q-f}\left[\sum_{t_5=0}^{j-q+1}(-1)^{t_5} C_{t_5}^{j-q+1} l^{j-q+1-t_5}\left(\int_l (l-y)^{k+q+1+t_5}\, dI_g\right)\right]\right.$$

$$\left.+\sum_{f=0}^{q}(-1)^{q-f} C_f^q l^{q-f}\left[\sum_{t_6=0}^{j-q+1}(-1)^{j-q+1-t_6} C_{t_6}^{j-q+1} l^{j-q+1-t_6}\left(\int_l (l+y)^{k+q+1+t_6}\, dJ_g\right)\right]\right\}. \qquad \text{(C-3)}$$

**For calculation of the pitching moment coefficient, $C_{m2}$:**

$$(n-k-q)\int_{-l}^{l}\int_{0}^{1}\left(x_1^{n-k-q-1} y^{j-q}\right) I_0 x_1^2\, dx_1 dy$$

$$=\frac{n-k-q}{(k+q+1)(n+3)}\left[\sum_{f=0}^{q}(-1)^f C_f^q l^{q-f}\left(\sum_{t_1=0}^{j-q}(-1)^{t_1} C_{t_1}^{j-q} l^{j-q-t_1}\int_l (l-y)^{k+q+t_1+1} I_g dy\right)\right.$$

$$\left.+\sum_{f=0}^{q}(-1)^{q-f} C_f^q l^{q-f}\left(\sum_{t_2=0}^{j-q}(-1)^{j-q-t_2} C_{t_2}^{j-q} l^{j-q-t_2}\int_l (l+y)^{k+q+t_2+1} J_g dy\right)\right]. \qquad \text{(C-4)}$$

$$\int_{-l}^{l}\int_{0}^{1}\left(x_1^{n-k-q} y^{j-q}\right) I_0 x_1^2\, dx_1 dy$$

$$=\frac{1}{(k+q+1)(n+4)}\left[\sum_{f=0}^{q}(-1)^f C_f^q l^{q-f}\left(\sum_{t_1=0}^{j-q}(-1)^{t_1} C_{t_1}^{j-q} l^{j-q-t_1}\int_l (l-y)^{k+q+t_1+1} I_g dy\right)\right.$$

$$\left.+\sum_{f=0}^{q}(-1)^{q-f} C_f^q l^{q-f}\left(\sum_{t_2=0}^{j-q}(-1)^{j-q-t_2} C_{t_2}^{j-q} l^{j-q-t_2}\int_l (l+y)^{k+q+t_2+1} J_g dy\right)\right]. \qquad \text{(C-5)}$$

$$\int_{-l}^{l}\int_{0}^{1}\left(x_1^{n-k-q} y^{j-q}\right)\frac{\partial I_0}{\partial x_1} x_1^2\, dx_1 dy$$

$$=\frac{1}{n+2}\left[\sum_{f=0}^{q}(-1)^f C_f^q l^{q-f+1}\left(\sum_{t_3=0}^{j-q}(-1)^{t_3} C_{t_3}^{j-q} l^{j-q-t_3}\int_l (l-y)^{k+q+t_3} I_g dy\right)\right.$$

$$\left.+\sum_{f=0}^{q}(-1)^{q-f} C_f^q l^{q-f+1}\left(\sum_{t_4=0}^{j-q}(-1)^{j-q-t_4} C_{t_4}^{j-q} l^{j-q-t_4}\int_l (l+y)^{k+q+t_4} J_g dy\right)\right]$$

$$-\frac{1}{(n+2)(k+q+1)}\left\{\sum_{f=0}^{q}(-1)^f C_f^q l^{q-f}\left[\sum_{t_5=0}^{j-q+1}(-1)^{t_5} C_{t_5}^{j-q+1} l^{j-q+1-t_5}\left(\int_l (l-y)^{k+q+1+t_5} dI_g\right)\right]\right.$$

$$\left.+\sum_{f=0}^{q}(-1)^{q-f} C_f^q l^{q-f}\left[\sum_{t_6=0}^{j-q+1}(-1)^{j-q+1-t_6} C_{t_6}^{j-q+1} l^{j-q+1-t_6}\left(\int_l (l+y)^{k+q+1+t_6} dJ_g\right)\right]\right\}. \quad \text{(C-6)}$$

**For calculation of the rolling moment coefficient, $C_{m1}$:**

$$(n-k-q)\int_{-l}^{l}\int_{0}^{l}\left(x_1^{n-k-q-1} y^{j-q}\right) I_0 x_1^2 y dx_1 dy$$

$$=\frac{n-k-q}{(k+q+1)(n+3)}\left[\sum_{f=0}^{q}(-1)^f C_f^q l^{q-f}\left(\sum_{t_5=0}^{j-q+1}(-1)^{t_5} C_{t_5}^{j-q+1} l^{j-q+1-t_5}\int_l (l-y)^{k+q+t_5+1} I_g dy\right)\right.$$

$$\left.+\sum_{f=0}^{q}(-1)^{q-f} C_f^q l^{q-f}\left(\sum_{t_6=0}^{j-q+1}(-1)^{j-q+1-t_6} C_{t_6}^{j-q+1} l^{j-q+1-t_6}\int_l (l+y)^{k+q+t_6+1} J_g dy\right)\right]. \quad \text{(C-7)}$$

$$\int_{-l}^{l}\int_{0}^{l}\left(x_1^{n-k-q} y^{j-q}\right) I_0 x_1^2 y dx_1 dy$$

$$=\frac{1}{(k+q+1)(n+4)}\left[\sum_{f=0}^{q}(-1)^f C_f^q l^{q-f}\left(\sum_{t_5=0}^{j-q+1}(-1)^{t_5} C_{t_5}^{j-q+1} l^{j-q+1-t_5}\int_l (l-y)^{k+q+t_5+1} I_g dy\right)\right.$$

$$\left.+\sum_{f=0}^{q}(-1)^{q-f} C_f^q l^{q-f}\left(\sum_{t_6=0}^{j-q+1}(-1)^{j-q+1-t_6} C_{t_6}^{j-q+1} l^{j-q+1-t_6}\int_l (l+y)^{k+q+t_6+1} J_g dy\right)\right]. \quad \text{(C-8)}$$

$$\int_{-l}^{l}\int_{0}^{l}\left(x_1^{n-k-q} y^{j-q}\right)\frac{\partial I_0}{\partial x_1} x_1^2 y dx_1 dy$$

$$=\frac{1}{n+3}\left[\sum_{f=0}^{q}(-1)^f C_f^q l^{q-f+1}\left(\sum_{t_7=0}^{j-q+1}(-1)^{t_7} C_{t_7}^{j-q+1} l^{j-q+1-t_7}\int_l (l-y)^{k+q+t_7} I_g dy\right)\right.$$

$$\left.+\sum_{f=0}^{q}(-1)^{q-f} C_f^q l^{q-f+1}\left(\sum_{t_8=0}^{j-q+1}(-1)^{j-q+1-t_8} C_{t_8}^{j-q+1} l^{j-q+1-t_8}\int_l (l+y)^{k+q+t_8} J_g dy\right)\right]$$

$$-\frac{1}{(n+3)(k+q+1)}\left\{\sum_{f=0}^{q}(-1)^{f}C_{f}^{q}l^{q-f}\left[\sum_{t_9=0}^{j-q+2}(-1)^{t_9}C_{t_9}^{j-q+2}l^{j-q+2-t_9}\left(\int_{l}^{\frac{1}{B}}(l-y)^{k+q+1+t_9}dI_g\right)\right]\right.$$

$$\left.+\sum_{f=0}^{q}(-1)^{q-f}C_{f}^{q}l^{q-f}\left[\sum_{t_{10}=0}^{j-q+2}(-1)^{j-q+2-t_{10}}C_{t_{10}}^{j-q+2}l^{j-q+2-t_{10}}\left(\int_{l}^{\frac{1}{B}}(l+y)^{k+q+1+t_{10}}dJ_g\right)\right]\right\}. \qquad \text{(C-9)}$$

From Eq.(C-1) ~ (C-9), let's consider the following four general integrals with limits for case of thin delta wing. For integration limit of $y$ between $-l$ and $-\frac{1}{B}$, $I_g$ is zero, and $J_g$ is constant, and for integration limit of $y$ between $\frac{1}{B}$ and $l$, $J_g$ is zero, and $I_g$ is constant. Thus, one concludes that

$$\int_{l}^{\frac{1}{B}}(l-y)^{m}I_g dy = \int_{l}^{\frac{1}{B}}(l-y)^{m}I_g dy + \int_{\frac{1}{B}}^{\frac{1}{B}}(l-y)^{m}I_g dy + \int_{\frac{1}{B}}^{\frac{1}{B}}(l-y)^{m}I_g dy. \qquad \text{(C-10)}$$

$$\int_{l}^{\frac{1}{B}}(l-y)^{m}dI_g = \int_{l}^{\frac{1}{B}}(l-y)^{m}dI_g + \int_{\frac{1}{B}}^{\frac{1}{B}}(l-y)^{m}dI_g + \int_{\frac{1}{B}}^{\frac{1}{B}}(l-y)^{m}dI_g. \qquad \text{(C-11)}$$

$$\int_{l}^{\frac{1}{B}}(l+y)^{n}J_g dy = \int_{l}^{\frac{1}{B}}(l+y)^{n}J_g dy + \int_{\frac{1}{B}}^{\frac{1}{B}}(l+y)^{n}J_g dy + \int_{\frac{1}{B}}^{\frac{1}{B}}(l+y)^{n}J_g dy. \qquad \text{(C-12)}$$

$$\int_{l}^{\frac{1}{B}}(l+y)^{n}dJ_g = \int_{l}^{\frac{1}{B}}(l+y)^{n}dJ_g + \int_{\frac{1}{B}}^{\frac{1}{B}}(l+y)^{n}dJ_g + \int_{\frac{1}{B}}^{\frac{1}{B}}(l+y)^{n}dJ_g. \qquad \text{(C-13)}$$

Derivations for integrals in Eq.(C-10) ~ (C-13) are also solved by applying the recurrence formulae and presented in the following section.

# C-2: Case of thin trapezoidal wing in steady supersonic flows

**For calculation of the lift coefficient, $C_l$:**

$$\begin{aligned}(n-k-q)\iint_S\left(x_1^{n-k-q-1}y^{j-q}\right)I_0x_1dx_1dy&=(n-k-q)\iint_{\tilde{S}_0}\left(x_1^{n-k-q-1}y^{j-q}\right)I_0x_1dx_1dy+(n-k-q)\iint_{S_0+S_i+S_1}\left(x_1^{n-k-q-1}y^{j-q}\right)I_0x_1dx_1dy\\&=(n-k-q)\int_0^1\int_{\frac{b}{x_1}}^{b}\left(x_1^{n-k-q-1}y^{j-q}\right)I_0x_1dx_1dy+(n-k-q)\int_{LB}^{UB}\int_0^1\left(x_1^{n-k-q-1}y^{j-q}\right)I_0x_1dx_1dy\\&=\frac{-(n-k-q)(-b)^{j-q+1}}{(k+q+1)(n+2)[(n+q)-(j-1)]}\tilde{J}_p\left(-\frac{1}{B}\right)+\frac{n-k-q}{(k+q+1)(n+2)}\left\{\sum_{f=0}^{q}(-1)^fC_f^ql^{q-f}\left[\sum_{t_1=0}^{j-q}(-1)^{t_1}C_{t_1}^{j-q}l^{j-q-t_1}\right.\right.\\&\left.\left.\times\left(\int_{\frac{1}{B}}^{1}(l-y)^{k+q+t_1+1}I_gdy+\int_{\frac{1}{B}}^{1}(l-y)^{k+q+t_1+1}I_gdy\right)\right]+\left(\int_b^{\frac{1}{B}}y^{j-q}\tilde{J}_pdy+\int_{\frac{1}{B}}^{1}y^{j-q}\tilde{J}_pdy\right)\right\}.\end{aligned}\tag{C-14}$$

$$\begin{aligned}\iint_S\left(x_1^{n-k-q}y^{j-q}\right)I_0x_1dx_1dy&=\iint_{\tilde{S}_0}\left(x_1^{n-k-q}y^{j-q}\right)I_0x_1dx_1dy+\iint_{S_0+S_i+S_1}\left(x_1^{n-k-q}y^{j-q}\right)I_0x_1dx_1dy\\&=\int_0^1\int_{\frac{b}{x_1}}^{b}\left(x_1^{n-k-q}y^{j-q}\right)I_0x_1dx_1dy+\int_{LB}^{UB}\int_0^1\left(x_1^{n-k-q}y^{j-q}\right)I_0x_1dx_1dy\\&=\frac{-(-b)^{j-q+1}}{(k+q+1)(n+3)[(n+q)-(j-2)]}\tilde{J}_p\left(-\frac{1}{B}\right)+\frac{1}{(k+q+1)(n+3)}\left\{\sum_{f=0}^{q}(-1)^fC_f^ql^{q-f}\left[\sum_{t_1=0}^{j-q}(-1)^{t_1}C_{t_1}^{j-q}l^{j-q-t_1}\right.\right.\\&\left.\left.\times\left(\int_{\frac{1}{B}}^{1}(l-y)^{k+q+t_1+1}I_gdy+\int_{\frac{1}{B}}^{1}(l-y)^{k+q+t_1+1}I_gdy\right)\right]+\left(\int_b^{\frac{1}{B}}y^{j-q}\tilde{J}_pdy+\int_{\frac{1}{B}}^{1}y^{j-q}\tilde{J}_pdy\right)\right\}.\end{aligned}\tag{C-15}$$

$$\begin{aligned}\iint_S\left(x_1^{n-k-q}y^{j-q}\right)\frac{\partial I_0}{\partial x_1}x_1dx_1dy&=\iint_{\tilde{S}_0}\left(x_1^{n-k-q}y^{j-q}\right)\frac{\partial I_0}{\partial x_1}x_1dx_1dy+\iint_{S_0+S_i+S_1}\left(x_1^{n-k-q}y^{j-q}\right)\frac{\partial I_0}{\partial x_1}x_1dx_1dy\\&=\int_0^1\int_{\frac{b}{x_1}}^{b}\left(x_1^{n-k-q}y^{j-q}\right)\frac{\partial I_0}{\partial x_1}x_1dx_1dy+\int_{LB}^{UB}\int_0^1\left(x_1^{n-k-q}y^{j-q}\right)\frac{\partial I_0}{\partial x_1}x_1dx_1dy\\&=\frac{-(-b)^{j-q+1}}{(n+2)[(n+q)-(j-1)]}\tilde{J}_p\left(-\frac{1}{B}\right)+\frac{1}{n+2}\left\{\sum_{f=0}^{q}(-1)^fC_f^ql^{q-f+1}\left[\sum_{t_3=0}^{j-q}(-1)^{t_3}C_{t_3}^{j-q}l^{j-q-t_3}\right.\right.\end{aligned}$$

$$\times\left(\int_{\frac{1}{B}}^{\frac{1}{B}}(l-y)^{k+q+t_3}I_g dy+\int_{\frac{1}{B}}^{1}(l-y)^{k+q+t_3}I_g dy\right)\Bigg]+\left(\int_b^{\frac{1}{B}}y^{j-q}\tilde{J}_p dy+\int_{\frac{1}{B}}^{\frac{1}{B}}y^{j-q}\tilde{J}_p dy\right)\Bigg\}$$

$$-\frac{1}{(n+2)(k+q+1)}\left\{\sum_{f=0}^{q}(-1)^f C_f^q l^{q-f}\left[\sum_{t_5=0}^{j-q+1}(-1)^{t_5}C_{t_5}^{j-q+1}l^{j-q+1-t_5}\left(\int_{\frac{1}{B}}^{\frac{1}{B}}(l-y)^{k+q+1+t_5}dI_g\right)\right]+\left(\int_{\frac{1}{B}}^{\frac{1}{B}}y^{j-q+1}d\tilde{J}_p\right)\right\}. \tag{C-16}$$

**For calculation of the pitching moment coefficient, $C_{m2}$:**

$$(n-k-q)\int_S\left(x_1^{n-k-q-1}y^{j-q}\right)I_0x_1^2dx_1dy=(n-k-q)\int_{\tilde{S}_0}\left(x_1^{n-k-q-1}y^{j-q}\right)I_0x_1^2dx_1dy+(n-k-q)\int_{S_0+S_i+S_1}\left(x_1^{n-k-q-1}y^{j-q}\right)I_0x_1^2dx_1dy$$

$$=(n-k-q)\int_0^1\int_{\frac{b}{x_1}}^{b}\left(x_1^{n-k-q-1}y^{j-q}\right)I_0x_1^2dx_1dy+(n-k-q)\int_{LB}^{UB}\int_0^1\left(x_1^{n-k-q-1}y^{j-q}\right)I_0x_1^2dx_1dy$$

$$=\frac{-(n-k-q)(-b)^{j-q+1}}{(k+q+1)(n+3)[(n+q)-(j-2)]}\tilde{J}_p\left(-\frac{1}{B}\right)+\frac{n-k-q}{(k+q+1)(n+3)}\left\{\sum_{f=0}^{q}(-1)^f C_f^q l^{q-f}\left[\sum_{t_1=0}^{j-q}(-1)^{t_1}C_{t_1}^{j-q}l^{j-q-t_1}\right.\right.$$

$$\left.\left.\times\left(\int_{\frac{1}{B}}^{\frac{1}{B}}(l-y)^{k+q+t_1+1}I_g dy+\int_{\frac{1}{B}}^{1}(l-y)^{k+q+t_1+1}I_g dy\right)\right]+\left(\int_b^{\frac{1}{B}}y^{j-q}\tilde{J}_p dy+\int_{\frac{1}{B}}^{\frac{1}{B}}y^{j-q}\tilde{J}_p dy\right)\right\}. \tag{C-17}$$

$$\int_S\left(x_1^{n-k-q}y^{j-q}\right)I_0x_1^2dx_1dy=\int_{\tilde{S}_0}\left(x_1^{n-k-q}y^{j-q}\right)I_0x_1^2dx_1dy+\int_{S_0+S_i+S_1}\left(x_1^{n-k-q}y^{j-q}\right)I_0x_1^2dx_1dy$$

$$=\int_0^1\int_{\frac{b}{x_1}}^{b}\left(x_1^{n-k-q}y^{j-q}\right)I_0x_1^2dx_1dy+\int_{LB}^{UB}\int_0^1\left(x_1^{n-k-q}y^{j-q}\right)I_0x_1^2dx_1dy$$

$$=\frac{-(-b)^{j-q+1}}{(k+q+1)(n+4)[(n+q)-(j-5)]}\tilde{J}_p\left(-\frac{1}{B}\right)+\frac{1}{(k+q+1)(n+4)}\left\{\sum_{f=0}^{q}(-1)^f C_f^q l^{q-f}\left[\sum_{t_1=0}^{j-q}(-1)^{t_1}C_{t_1}^{j-q}l^{j-q-t_1}\right.\right.$$

$$\left.\left.\times\left(\int_{\frac{1}{B}}^{\frac{1}{B}}(l-y)^{k+q+t_1+1}I_g dy+\int_{\frac{1}{B}}^{1}(l-y)^{k+q+t_1+1}I_g dy\right)\right]+\left(\int_b^{\frac{1}{B}}y^{j-q}\tilde{J}_p dy+\int_{\frac{1}{B}}^{\frac{1}{B}}y^{j-q}\tilde{J}_p dy\right)\right\}. \tag{C-18}$$

$$\int_S \left(x_1^{n-k-q} y^{j-q}\right)\frac{\partial I_0}{\partial x_1} x_1^2 dx_1 dy = \int_{\tilde{S}_0} \left(x_1^{n-k-q} y^{j-q}\right)\frac{\partial I_0}{\partial x_1} x_1^2 dx_1 dy + \int_{S_0+S_i+S_1} \left(x_1^{n-k-q} y^{j-q}\right)\frac{\partial I_0}{\partial x_1} x_1^2 dx_1 dy$$

$$= \int_0^1 \int_{\frac{b}{x_1}}^{b} \left(x_1^{n-k-q} y^{j-q}\right)\frac{\partial I_0}{\partial x_1} x_1^2 dx_1 dy + \int_{LB}^{UB} \int_0^1 \left(x_1^{n-k-q} y^{j-q}\right)\frac{\partial I_0}{\partial x_1} x_1^2 dx_1 dy$$

$$= \frac{-(-b)^{j-q+1}}{(n+3)\left[(n+q)-(j-2)\right]}\tilde{J}_p\left(-\frac{1}{B}\right) + \frac{1}{n+3}\left\{\sum_{f=0}^{q}(-1)^f C_f^q l^{q-f+1}\left[\sum_{t_3=0}^{j-q}(-1)^{t_3} C_{t_3}^{j-q} l^{j-q-t_3}\right]\right.$$

$$\left.\times\left(\int_{\frac{1}{B}}^{\frac{1}{B}} (l-y)^{k+q+t_3} I_g dy + \int_{\frac{1}{B}}^{1} (l-y)^{k+q+t_3} I_g dy\right)\right] + \left(\int_b^{\frac{1}{B}} y^{j-q}\tilde{J}_p dy + \int_{\frac{1}{B}}^{\frac{1}{B}} y^{j-q}\tilde{J}_p dy\right)\right\}$$

$$-\frac{1}{(n+3)(k+q+1)}\left\{\sum_{f=0}^{q}(-1)^f C_f^q l^{q-f}\left[\sum_{t_5=0}^{j-q+1}(-1)^{t_5} C_{t_5}^{j-q+1} l^{j-q+1-t_5}\left(\int_{\frac{1}{B}}^{\frac{1}{B}} (l-y)^{k+q+1+t_5} dI_g\right)\right] + \left(\int_{\frac{1}{B}}^{\frac{1}{B}} y^{j-q+1} d\tilde{J}_p\right)\right\}. \quad \text{(C-19)}$$

**For calculation of the rolling moment coefficient, $C_{ml}$:**

$$(n-k-q)\int_S \left(x_1^{n-k-q-1} y^{j-q}\right) I_0 x_1^2 y dx_1 dy = (n-k-q)\int_{\tilde{S}_0} \left(x_1^{n-k-q-1} y^{j-q}\right) I_0 x_1^2 y dx_1 dy + (n-k-q)\int_{S_0+S_i+S_1} \left(x_1^{n-k-q-1} y^{j-q}\right) I_0 x_1^2 y dx_1 dy$$

$$= (n-k-q)\int_0^1 \int_{\frac{b}{x_1}}^{b} \left(x_1^{n-k-q-1} y^{j-q}\right) I_0 x_1^2 y dx_1 dy + (n-k-q)\int_{LB}^{UB} \int_0^1 \left(x_1^{n-k-q-1} y^{j-q}\right) I_0 x_1^2 y dx_1 dy$$

$$= \frac{-(n-k-q)(-b)^{j-q+2}}{(k+q+1)(n+3)\left[(n+q)-(j-1)\right]}\tilde{J}_p\left(-\frac{1}{B}\right) + \frac{n-k-q}{(k+q+1)(n+3)}\left\{\sum_{f=0}^{q}(-1)^f C_f^q l^{q-f}\left[\sum_{t_5=0}^{j-q+1}(-1)^{t_5} C_{t_5}^{j-q+1} l^{j-q+1-t_5}\right.\right.$$

$$\left.\left.\times\left(\int_{\frac{1}{B}}^{\frac{1}{B}} (l-y)^{k+q+t_5+1} I_g dy + \int_{\frac{1}{B}}^{1} (l-y)^{k+q+t_5+1} I_g dy\right)\right] + \left(\int_b^{\frac{1}{B}} y^{j-q+1}\tilde{J}_p dy + \int_{\frac{1}{B}}^{\frac{1}{B}} y^{j-q+1}\tilde{J}_p dy\right)\right\}. \quad \text{(C-20)}$$

$$\int_S \left(x_1^{n-k-q} y^{j-q}\right) I_0 x_1^2 y dx_1 dy = \int_{\tilde{S}_0} \left(x_1^{n-k-q} y^{j-q}\right) I_0 x_1^2 y dx_1 dy + \int_{S_0+S_i+S_1} \left(x_1^{n-k-q} y^{j-q}\right) I_0 x_1^2 y dx_1 dy$$

$$= \int_0^1 \int_{\frac{b}{x_1}}^b \left(x_1^{n-k-q} y^{j-q}\right) I_0 x_1^2 y dx_1 dy + \int_{LB}^{UB} \int_0^1 \left(x_1^{n-k-q} y^{j-q}\right) I_0 x_1^2 y dx_1 dy$$

$$= \frac{-(-b)^{j-q+2}}{(k+q+1)(n+4)[(n+q)-(j-2)]} \tilde{J}_p\left(-\frac{1}{B}\right) + \frac{1}{(k+q+1)(n+4)} \left\{ \sum_{f=0}^{q} (-1)^f C_f^q l^{q-f} \left[ \sum_{t_5=0}^{j-q+1} (-1)^{t_5} C_{t_5}^{j-q+1} l^{j-q+1-t_5} \right.\right.$$

$$\left.\left. \times \left( \int_{\frac{1}{B}}^{\frac{1}{B}} (l-y)^{k+q+t_5+1} I_g dy + \int_{\frac{1}{B}}^{l} (l-y)^{k+q+t_5+1} I_g dy \right) \right] + \left( \int_b^{\frac{1}{B}} y^{j-q+1} \tilde{J}_p dy + \int_{\frac{1}{B}}^{\frac{1}{B}} y^{j-q+1} \tilde{J}_p dy \right) \right\}. \quad \text{(C-21)}$$

$$\int_S \left(x_1^{n-k-q} y^{j-q}\right) \frac{\partial I_0}{\partial x_1} x_1^2 y dx_1 dy = \int_{\tilde{S}_0} \left(x_1^{n-k-q} y^{j-q}\right) \frac{\partial I_0}{\partial x_1} x_1^2 y dx_1 dy + \int_{S_0+S_i+S_1} \left(x_1^{n-k-q} y^{j-q}\right) \frac{\partial I_0}{\partial x_1} x_1^2 y dx_1 dy$$

$$= \int_0^1 \int_{\frac{b}{x_1}}^b \left(x_1^{n-k-q} y^{j-q}\right) \frac{\partial I_0}{\partial x_1} x_1^2 y dx_1 dy + \int_{LB}^{UB} \int_0^1 \left(x_1^{n-k-q} y^{j-q}\right) \frac{\partial I_0}{\partial x_1} x_1^2 y dx_1 dy$$

$$= \frac{-(-b)^{j-q+2}}{(n+3)[(n+q)-(j-1)]} \tilde{J}_p\left(-\frac{1}{B}\right) + \frac{1}{n+3} \left\{ \sum_{f=0}^{q} (-1)^f C_f^q l^{q-f+1} \left[ \sum_{t_7=0}^{j-q+1} (-1)^{t_7} C_{t_7}^{j-q+1} l^{j-q+1-t_7} \right] \right.$$

$$\left. \times \left( \int_{\frac{1}{B}}^{\frac{1}{B}} (l-y)^{k+q+t_7} I_g dy + \int_{\frac{1}{B}}^{l} (l-y)^{k+q+t_7} I_g dy \right) \right] + \left( \int_b^{\frac{1}{B}} y^{j-q+1} \tilde{J}_p dy + \int_{\frac{1}{B}}^{\frac{1}{B}} y^{j-q+1} \tilde{J}_p dy \right) \right\}$$

$$- \frac{1}{(n+3)(k+q+1)} \left\{ \sum_{f=0}^{q} (-1)^f C_f^q l^{q-f} \left[ \sum_{t_9=0}^{j-q+2} (-1)^{t_9} C_{t_9}^{j-q+2} l^{j-q+2-t_9} \left( \int_{\frac{1}{B}}^{\frac{1}{B}} (l-y)^{k+q+1+t_9} dI_g \right) \right] + \left( \int_{\frac{1}{B}}^{\frac{1}{B}} y^{j-q+2} d\tilde{J}_p \right) \right\}.$$

(C-22)

Similarly, detailed solutions for integrals in Eq.(C-14) ~ (C-22) with limits are solved by the recurrence formulae and one may refer to the following sections.

## C-3: Case of oscillating delta wing in supersonic flows

**For calculation of the lift coefficient, $C_l$:**

$$(n-k-q)\int_l^l\int_0^l\left(x_1^{n-k-q-1}y^{j-q}\right)I_{i_1,i_2}x_1dx_1dy$$

$$=\frac{n-k-q}{(i_1+1)(n-k-q+i_1+2)}\left[\sum_{f=0}^{i_2}(-1)^f C_f^{i_2}l^{i_2-f}\left(\sum_{t_1=0}^{j-q}(-1)^{t_1}C_{t_1}^{j-q}l^{j-q-t_1}\int_l^l(l-y)^{i_1+t_1+1}I_g dy\right)\right.$$

$$\left.+\sum_{f=0}^{i_2}(-1)^{i_2-f}C_f^{i_2}l^{i_2-f}\left(\sum_{t_2=0}^{j-q}(-1)^{j-q-t_2}C_{t_2}^{j-q}l^{j-q-t_2}\int_l^l(l+y)^{i_1+t_2+1}J_g dy\right)\right]. \quad \text{(C-23)}$$

$$\int_l^l\int_0^l\left(x_1^{n-k-q}y^{j-q}\right)I_{i_1,i_2}x_1dx_1dy$$

$$=\frac{1}{(i_1+1)(n-k-q+i_1+3)}\left[\sum_{f=0}^{i_2}(-1)^f C_f^{i_2}l^{i_2-f}\left(\sum_{t_1=0}^{j-q}(-1)^{t_1}C_{t_1}^{j-q}l^{j-q-t_1}\int_l^l(l-y)^{i_1+t_1+1}I_g dy\right)\right.$$

$$\left.+\sum_{f=0}^{i_2}(-1)^{i_2-f}C_f^{i_2}l^{i_2-f}\left(\sum_{t_2=0}^{j-q}(-1)^{j-q-t_2}C_{t_2}^{j-q}l^{j-q-t_2}\int_l^l(l+y)^{i_1+t_2+1}J_g dy\right)\right]. \quad \text{(C-24)}$$

$$\int_l^l\int_0^l\left(x_1^{n-k-q}y^{j-q}\right)\frac{\partial I_{i_1,i_2}}{\partial x_1}x_1dx_1dy$$

$$=\frac{1}{n-k-q+i_1+2}\left[\sum_{f=0}^{i_2}(-1)^f C_f^{i_2}l^{i_2-f+1}\left(\sum_{t_3=0}^{j-q}(-1)^{t_3}C_{t_3}^{j-q}l^{j-q-t_3}\int_l^l(l-y)^{i_1+t_3}I_g dy\right)\right.$$

$$\left.+\sum_{f=0}^{i_2}(-1)^{i_2-f}C_f^{i_2}l^{i_2-f+1}\left(\sum_{t_4=0}^{j-q}(-1)^{j-q-t_4}C_{t_4}^{j-q}l^{j-q-t_4}\int_l^l(l+y)^{i_1+t_4}J_g dy\right)\right]$$

$$-\frac{1}{(n-k-q+i_1+2)(i_1+1)}\left\{\sum_{f=0}^{i_2}(-1)^f C_f^{i_2}l^{i_2-f}\left[\sum_{t_5=0}^{j-q+1}(-1)^{t_5}C_{t_5}^{j-q+1}l^{j-q+1-t_5}\left(\int_l^l(l-y)^{i_1+1+t_5}dI_g\right)\right]\right.$$

$$\left.+\sum_{f=0}^{i_2}(-1)^{i_2-f}C_f^{i_2}l^{i_2-f}\left[\sum_{t_6=0}^{j-q+1}(-1)^{j-q+1-t_6}C_{t_6}^{j-q+1}l^{j-q+1-t_6}\left(\int_l^l(l+y)^{i_1+1+t_6}dJ_g\right)\right]\right\}. \quad \text{(C-25)}$$

**For calculation of the pitching moment coefficient, $C_{m2}$:**

$$(n-k-q)\int_{-l}^{l}\int_{0}^{1}\left(x_1^{n-k-q-1}y^{j-q}\right)I_{i_1,i_2}x_1^2\,dx_1dy$$

$$=\frac{n-k-q}{(i_1+1)(n-k-q+i_1+3)}\left[\sum_{f=0}^{i_2}(-1)^f C_f^{i_2}l^{i_2-f}\left(\sum_{t_1=0}^{j-q}(-1)^{t_1}C_{t_1}^{j-q}l^{j-q-t_1}\int_{-l}^{l}(l-y)^{i_1+t_1+1}I_g\,dy\right)\right.$$

$$\left.+\sum_{f=0}^{i_2}(-1)^{i_2-f}C_f^{i_2}l^{i_2-f}\left(\sum_{t_2=0}^{j-q}(-1)^{j-q-t_2}C_{t_2}^{j-q}l^{j-q-t_2}\int_{-l}^{l}(l+y)^{i_1+t_2+1}J_g\,dy\right)\right]. \qquad \text{(C-26)}$$

$$\int_{-l}^{l}\int_{0}^{1}\left(x_1^{n-k-q}y^{j-q}\right)I_{i_1,i_2}x_1^2\,dx_1dy$$

$$=\frac{1}{(i_1+1)(n-k-q+i_1+4)}\left[\sum_{f=0}^{i_2}(-1)^f C_f^{i_2}l^{i_2-f}\left(\sum_{t_1=0}^{j-q}(-1)^{t_1}C_{t_1}^{j-q}l^{j-q-t_1}\int_{-l}^{l}(l-y)^{i_1+t_1+1}I_g\,dy\right)\right.$$

$$\left.+\sum_{f=0}^{i_2}(-1)^{i_2-f}C_f^{i_2}l^{i_2-f}\left(\sum_{t_2=0}^{j-q}(-1)^{j-q-t_2}C_{t_2}^{j-q}l^{j-q-t_2}\int_{-l}^{l}(l+y)^{i_1+t_2+1}J_g\,dy\right)\right]. \qquad \text{(C-27)}$$

$$\int_{-l}^{l}\int_{0}^{1}\left(x_1^{n-k-q}y^{j-q}\right)\frac{\partial I_{i_1,i_2}}{\partial x_1}x_1^2\,dx_1dy$$

$$=\frac{1}{n-k-q+i_1+2}\left[\sum_{f=0}^{i_2}(-1)^f C_f^{i_2}l^{i_2-f+1}\left(\sum_{t_3=0}^{j-q}(-1)^{t_3}C_{t_3}^{j-q}l^{j-q-t_3}\int_{-l}^{l}(l-y)^{i_1+t_3}I_g\,dy\right)\right.$$

$$\left.+\sum_{f=0}^{i_2}(-1)^{i_2-f}C_f^{i_2}l^{i_2-f+1}\left(\sum_{t_4=0}^{j-q}(-1)^{j-q-t_4}C_{t_4}^{j-q}l^{j-q-t_4}\int_{-l}^{l}(l+y)^{i_1+t_4}J_g\,dy\right)\right]$$

$$-\frac{1}{(n-k-q+i_1+2)(i_1+1)}\left\{\sum_{f=0}^{i_2}(-1)^f C_f^{i_2}l^{i_2-f}\left[\sum_{t_5=0}^{j-q+1}(-1)^{t_5}C_{t_5}^{j-q+1}l^{j-q+1-t_5}\left(\int_{-l}^{l}(l-y)^{i_1+1+t_5}dI_g\right)\right]\right.$$

$$\left.+\sum_{f=0}^{i_2}(-1)^{i_2-f}C_f^{i_2}l^{i_2-f}\left[\sum_{t_6=0}^{j-q+1}(-1)^{j-q+1-t_6}C_{t_6}^{j-q+1}l^{j-q+1-t_6}\left(\int_{-l}^{l}(l+y)^{i_1+1+t_6}dJ_g\right)\right]\right\}. \qquad \text{(C-28)}$$

**For calculation of the rolling moment coefficient, $C_{ml}$:**

$$(n-k-q)\int_l^t\int_0^t\left(x_1^{n-k-q-1}y^{j-q}\right)I_{i_1,i_2}x_1^2\,y\,dx_1dy$$

$$=\frac{n-k-q}{(i_1+1)(n-k-q+i_1+3)}\left[\sum_{f=0}^{i_2}(-1)^f C_f^{i_2}l^{i_2-f}\left(\sum_{t_5=0}^{j-q+1}(-1)^{t_5}C_{t_5}^{j-q+1}l^{j-q+1-t_5}\int_l^t(l-y)^{i_1+t_5+1}I_g\,dy\right)\right.$$

$$\left.+\sum_{f=0}^{i_2}(-1)^{i_2-f}C_f^{i_2}l^{i_2-f}\left(\sum_{t_6=0}^{j-q+1}(-1)^{j-q+1-t_6}C_{t_6}^{j-q+1}l^{j-q+1-t_6}\int_l^t(l+y)^{i_1+t_6+1}J_g\,dy\right)\right]. \quad \text{(C-29)}$$

$$\int_l^t\int_0^t\left(x_1^{n-k-q}y^{j-q}\right)I_{i_1,i_2}x_1^2\,y\,dx_1dy$$

$$=\frac{1}{(i_1+1)(n-k-q+i_1+4)}\left[\sum_{f=0}^{i_2}(-1)^f C_f^{i_2}l^{i_2-f}\left(\sum_{t_5=0}^{j-q+1}(-1)^{t_5}C_{t_5}^{j-q+1}l^{j-q+1-t_5}\int_l^t(l-y)^{i_1+t_5+1}I_g\,dy\right)\right.$$

$$\left.+\sum_{f=0}^{i_2}(-1)^{i_2-f}C_f^{i_2}l^{i_2-f}\left(\sum_{t_6=0}^{j-q+1}(-1)^{j-q+1-t_6}C_{t_6}^{j-q+1}l^{j-q+1-t_6}\int_l^t(l+y)^{i_1+t_6+1}J_g\,dy\right)\right]. \quad \text{(C-30)}$$

$$\int_l^t\int_0^t\left(x_1^{n-k-q}y^{j-q}\right)\frac{\partial I_{i_1,i_2}}{\partial x_1}x_1^2\,y\,dx_1dy$$

$$=\frac{1}{n-k-q+i_1+3}\left[\sum_{f=0}^{i_2}(-1)^f C_f^{i_2}l^{i_2-f+1}\left(\sum_{t_7=0}^{j-q+1}(-1)^{t_7}C_{t_7}^{j-q+1}l^{j-q+1-t_7}\int_l^t(l-y)^{i_1+t_7}I_g\,dy\right)\right.$$

$$\left.+\sum_{f=0}^{i_2}(-1)^{i_2-f}C_f^{i_2}l^{i_2-f+1}\left(\sum_{t_8=0}^{j-q+1}(-1)^{j-q+1-t_8}C_{t_8}^{j-q+1}l^{j-q+1-t_8}\int_l^t(l+y)^{i_1+t_8}J_g\,dy\right)\right]$$

$$-\frac{1}{(n-k-q+i_1+3)(i_1+1)}\left\{\sum_{f=0}^{i_2}(-1)^f C_f^{i_2}l^{i_2-f}\left[\sum_{t_9=0}^{j-q+2}(-1)^{t_9}C_{t_9}^{j-q+2}l^{j-q+2-t_9}\left(\int_l^t(l-y)^{i_1+1+t_9}dI_g\right)\right]\right.$$

$$\left.+\sum_{f=0}^{i_2}(-1)^{i_2-f}C_f^{i_2}l^{i_2-f}\left[\sum_{t_{10}=0}^{j-q+2}(-1)^{j-q+2-t_{10}}C_{t_{10}}^{j-q+2}l^{j-q+2-t_{10}}\left(\int_l^t(l+y)^{i_1+1+t_{10}}dJ_g\right)\right]\right\}. \quad \text{(C-31)}$$

For the calculation of finite integrals of $I_g$, $J_g$ , $dI_g$, and $dJ_g$ with integral limits for case of delta wing, one may refer to the following section for detailed discussion.

# C-4: Case of oscillating trapezoidal wing in supersonic flows

**For calculation of the lift coefficient, $C_l$:**

$$\begin{aligned}(n-k-q)\iint_S\left(x_1^{n-k-q-1}y^{j-q}\right)I_{i_1,i_2}x_1dx_1dy&=(n-k-q)\iint_{\tilde{S}_0}\left(x_1^{n-k-q-1}y^{j-q}\right)I_{i_1,i_2}x_1dx_1dy+(n-k-q)\iint_{S_0+S_i+S_1}\left(x_1^{n-k-q-1}y^{j-q}\right)I_{i_1,i_2}x_1dx_1dy\\&=(n-k-q)\int_0^1\int_{\frac{b}{x_1}}^b\left(x_1^{n-k-q-1}y^{j-q}\right)I_{i_1,i_2}x_1dx_1dy+(n-k-q)\int_{LB}^{UB}\int_0^1\left(x_1^{n-k-q-1}y^{j-q}\right)I_{i_1,i_2}x_1dx_1dy\\&=\frac{-(n-k-q)(-b)^{j-q+1}}{(i_1+1)[(n-k+i_1)-(q-2)][(n-k+i_1)-(j-1)]}\tilde{J}_p\left(-\frac{1}{B}\right)\\&\quad+\frac{n-k-q}{(i_1+1)(n-k-q+i_1+2)}\left\{\sum_{f=0}^{i_2}(-1)^f C_f^{i_2}l^{i_2-f}\left[\sum_{t_1=0}^{j-q}(-1)^{t_1}C_{t_1}^{j-q}l^{j-q-t_1}\right.\right.\\&\quad\left.\left.\times\left(\int_{\frac{1}{B}}^{\frac{1}{B}}(l-y)^{i_1+t_1+1}I_g\,dy+\int_{\frac{1}{B}}^{1}(l-y)^{i_1+t_1+1}I_g\,dy\right)\right]+\left(\int_b^{\frac{1}{B}}y^{j-q}\tilde{J}_p\,dy+\int_{\frac{1}{B}}^{\frac{1}{B}}y^{j-q}\tilde{J}_p\,dy\right)\right\}.\end{aligned}\tag{C-32}$$

$$\begin{aligned}\iint_S\left(x_1^{n-k-q}y^{j-q}\right)I_{i_1,i_2}x_1dx_1dy&=\iint_{\tilde{S}_0}\left(x_1^{n-k-q}y^{j-q}\right)I_{i_1,i_2}x_1dx_1dy+\iint_{S_0+S_i+S_1}\left(x_1^{n-k-q}y^{j-q}\right)I_{i_1,i_2}x_1dx_1dy\\&=\int_0^1\int_{\frac{b}{x_1}}^b\left(x_1^{n-k-q}y^{j-q}\right)I_{i_1,i_2}x_1dx_1dy+\int_{LB}^{UB}\int_0^1\left(x_1^{n-k-q}y^{j-q}\right)I_{i_1,i_2}x_1dx_1dy\\&=\frac{-(-b)^{j-q+1}}{(i_1+1)[(n-k+i_1)-(q-3)][(n-k+i_1)-(j-2)]}\tilde{J}_p\left(-\frac{1}{B}\right)+\frac{1}{(i_1+1)(n-k-q+i_1+3)}\left\{\sum_{f=0}^{i_2}(-1)^f C_f^{i_2}l^{i_2-f}\right.\\&\quad\left.\times\left[\sum_{t_1=0}^{j-q}(-1)^{t_1}C_{t_1}^{j-q}l^{j-q-t_1}\left(\int_{\frac{1}{B}}^{\frac{1}{B}}(l-y)^{i_1+t_1+1}I_g\,dy+\int_{\frac{1}{B}}^{1}(l-y)^{i_1+t_1+1}I_g\,dy\right)\right]+\left(\int_b^{\frac{1}{B}}y^{j-q}\tilde{J}_p\,dy+\int_{\frac{1}{B}}^{\frac{1}{B}}y^{j-q}\tilde{J}_p\,dy\right)\right\}\end{aligned}\tag{C-33}$$

$$\int_S \left(x_1^{n-k-q} y^{j-q}\right)\frac{\partial I_{i_1,i_2}}{\partial x_1} x_1 dx_1 dy = \int_{\tilde{S}_0}\left(x_1^{n-k-q} y^{j-q}\right)\frac{\partial I_{i_1,i_2}}{\partial x_1} x_1 dx_1 dy + \int_{S_0+S_i+S_1}\left(x_1^{n-k-q} y^{j-q}\right)\frac{\partial I_{i_1,i_2}}{\partial x_1} x_1 dx_1 dy$$

$$= \int_0^1 \int_{\frac{b}{x_1}}^{b}\left(x_1^{n-k-q} y^{j-q}\right)\frac{\partial I_{i_1,i_2}}{\partial x_1} x_1 dx_1 dy + \int_{LB}^{UB}\int_0^1 \left(x_1^{n-k-q} y^{j-q}\right)\frac{\partial I_{i_1,i_2}}{\partial x_1} x_1 dx_1 dy$$

$$= \frac{-(-b)^{j-q+1}}{\left[(n-k+i_1)-(q-2)\right]\left[(n-k+i_1)-(j-1)\right]}\tilde{J}_p\left(-\frac{1}{B}\right) + \frac{1}{n-k-q+i_1+2}\left\{\sum_{f=0}^{i_2}(-1)^f C_f^{i_2} l^{i_2-f+1}\right.$$

$$\left.\times\left[\sum_{t_3=0}^{j-q}(-1)^{t_3} C_{t_3}^{j-q} l^{j-q-t_3}\left(\int_{\frac{1}{B}}^{\frac{1}{B}}(l-y)^{i_1+t_3} I_g dy + \int_{\frac{1}{B}}^{1}(l-y)^{i_1+t_3} I_g dy\right)\right] + \left(\int_b^{\frac{1}{B}} y^{j-q}\tilde{J}_p dy + \int_{\frac{1}{B}}^{\frac{1}{B}} y^{j-q}\tilde{J}_p dy\right)\right\}$$

$$-\frac{1}{(n-k-q+i_1+2)(i_1+1)}\left\{\sum_{f=0}^{i_2}(-1)^f C_f^{i_2} l^{i_2-f}\left[\sum_{t_5=0}^{j-q+1}(-1)^{t_5} C_{t_5}^{j-q+1} l^{j-q+1-t_5}\left(\int_{\frac{1}{B}}^{\frac{1}{B}}(l-y)^{i_1+1+t_5} dI_g\right)\right] + \left(\int_{\frac{1}{B}}^{\frac{1}{B}} y^{j-q+1} d\tilde{J}_p\right)\right\}.$$

(C-34)

**For calculation of the pitching moment coefficient, $C_{m2}$:**

$$(n-k-q)\int_S \left(x_1^{n-k-q-1} y^{j-q}\right) I_{i_1,i_2} x_1^2 dx_1 dy = (n-k-q)\int_{\tilde{S}_0}\left(x_1^{n-k-q-1} y^{j-q}\right) I_{i_1,i_2} x_1^2 dx_1 dy + (n-k-q)\int_{S_0+S_i+S_1}\left(x_1^{n-k-q-1} y^{j-q}\right) I_{i_1,i_2} x_1^2 dx_1 dy$$

$$= (n-k-q)\int_0^1 \int_{\frac{b}{x_1}}^{b}\left(x_1^{n-k-q-1} y^{j-q}\right) I_{i_1,i_2} x_1^2 dx_1 dy + (n-k-q)\int_{LB}^{UB}\int_0^1 \left(x_1^{n-k-q-1} y^{j-q}\right) I_{i_1,i_2} x_1^2 dx_1 dy$$

$$= \frac{-(n-k-q)(-b)^{j-q+1}}{(i_1+1)\left[(n-k+i_1)-(q-3)\right]\left[(n-k+i_1)-(j-2)\right]}\tilde{J}_p\left(-\frac{1}{B}\right) + \frac{n-k-q}{(i_1+1)(n-k-q+i_1+3)}\left\{\sum_{f=0}^{i_2}(-1)^f C_f^{i_2} l^{i_2-f}\right.$$

$$\left.\times\left[\sum_{t_1=0}^{j-q}(-1)^{t_1} C_{t_1}^{j-q} l^{j-q-t_1}\left(\int_{\frac{1}{B}}^{\frac{1}{B}}(l-y)^{i_1+t_1+1} I_g dy + \int_{\frac{1}{B}}^{1}(l-y)^{i_1+t_1+1} I_g dy\right)\right] + \left(\int_b^{\frac{1}{B}} y^{j-q}\tilde{J}_p dy + \int_{\frac{1}{B}}^{\frac{1}{B}} y^{j-q}\tilde{J}_p dy\right)\right\}$$

(C-35)

$$\int_S \left(x_1^{n-k-q} y^{j-q}\right) I_{i_1,i_2} x_1^2 dx_1 dy = \int_{\tilde{S}_0} \left(x_1^{n-k-q} y^{j-q}\right) I_{i_1,i_2} x_1^2 dx_1 dy + \int_{S_0+S_i+S_1} \left(x_1^{n-k-q} y^{j-q}\right) I_{i_1,i_2} x_1^2 dx_1 dy$$

$$= \int_0^1 \int_{\frac{b}{x_1}}^b \left(x_1^{n-k-q} y^{j-q}\right) I_{i_1,i_2} x_1^2 dx_1 dy + \int_{LB}^{UB} \int_0^1 \left(x_1^{n-k-q} y^{j-q}\right) I_{i_1,i_2} x_1^2 dx_1 dy$$

$$= \frac{-(-b)^{j-q+1}}{(i_1+1)[(n-k+i_1)-(q-4)][(n-k+i_1)-(j-5)]} \tilde{J}_p\left(-\frac{1}{B}\right) + \frac{1}{(i_1+1)(n-k-q+i_1+4)} \left\{ \sum_{f=0}^{i_2} (-1)^f C_f^{i_2} l^{i_2-f} \right.$$

$$\left. \times \left[ \sum_{t_1=0}^{j-q} (-1)^{t_1} C_{t_1}^{j-q} l^{j-q-t_1} \left( \int_{\frac{1}{B}}^{\frac{1}{B}} (l-y)^{i_1+t_1+1} I_g dy + \int_{\frac{1}{B}}^{1} (l-y)^{i_1+t_1+1} I_g dy \right) \right] + \left( \int_b^{\frac{1}{B}} y^{j-q} \tilde{J}_p dy + \int_{\frac{1}{B}}^{\frac{1}{B}} y^{j-q} \tilde{J}_p dy \right) \right\}$$

(C-36)

$$\int_S \left(x_1^{n-k-q} y^{j-q}\right) \frac{\partial I_{i_1,i_2}}{\partial x_1} x_1^2 dx_1 dy = \int_{\tilde{S}_0} \left(x_1^{n-k-q} y^{j-q}\right) \frac{\partial I_{i_1,i_2}}{\partial x_1} x_1^2 dx_1 dy + \int_{S_0+S_i+S_1} \left(x_1^{n-k-q} y^{j-q}\right) \frac{\partial I_{i_1,i_2}}{\partial x_1} x_1^2 dx_1 dy$$

$$= \int_0^1 \int_{\frac{b}{x_1}}^b \left(x_1^{n-k-q} y^{j-q}\right) \frac{\partial I_{i_1,i_2}}{\partial x_1} x_1^2 dx_1 dy + \int_{LB}^{UB} \int_0^1 \left(x_1^{n-k-q} y^{j-q}\right) \frac{\partial I_{i_1,i_2}}{\partial x_1} x_1^2 dx_1 dy$$

$$= \frac{-(-b)^{j-q+1}}{[(n-k+i_1)-(q-3)][(n-k+i_1)-(j-2)]} \tilde{J}_p\left(-\frac{1}{B}\right) + \frac{1}{n-k-q+i_1+3} \left\{ \sum_{f=0}^{i_2} (-1)^f C_f^{i_2} l^{i_2-f+1} \right.$$

$$\left. \times \left[ \sum_{t_3=0}^{j-q} (-1)^{t_3} C_{t_3}^{j-q} l^{j-q-t_3} \left( \int_{\frac{1}{B}}^{\frac{1}{B}} (l-y)^{i_1+t_3} I_g dy + \int_{\frac{1}{B}}^{1} (l-y)^{i_1+t_3} I_g dy \right) \right] + \left( \int_b^{\frac{1}{B}} y^{j-q} \tilde{J}_p dy + \int_{\frac{1}{B}}^{\frac{1}{B}} y^{j-q} \tilde{J}_p dy \right) \right\}$$

$$- \frac{1}{(n-k-q+i_1+3)(i_1+1)} \left\{ \sum_{f=0}^{i_2} (-1)^f C_f^{i_2} l^{i_2-f} \left[ \sum_{t_5=0}^{j-q+1} (-1)^{t_5} C_{t_5}^{j-q+1} l^{j-q+1-t_5} \left( \int_{\frac{1}{B}}^{\frac{1}{B}} (l-y)^{i_1+1+t_5} dI_g \right) \right] + \left( \int_{\frac{1}{B}}^{\frac{1}{B}} y^{j-q+1} d\tilde{J}_p \right) \right\}.$$

(C-37)

**For calculation of the rolling moment coefficient, $C_{ml}$ :**

$$(n-k-q)\iint_S \left(x_1^{n-k-q-1}y^{j-q}\right) I_{i_1,i_2} x_1^2\, y dx_1 dy = (n-k-q)\iint_{\tilde{S}_0} \left(x_1^{n-k-q-1}y^{j-q}\right) I_{i_1,i_2} x_1^2\, y dx_1 dy + (n-k-q)\iint_{S_0+S_i+S_1} \left(x_1^{n-k-q-1}y^{j-q}\right) I_{i_1,i_2} x_1^2\, y dx_1 dy$$

$$= (n-k-q)\int_0^1 \int_{\frac{b}{x_1}}^{b} \left(x_1^{n-k-q-1}y^{j-q}\right) I_{i_1,i_2} x_1^2\, y dx_1 dy + (n-k-q)\int_{LB}^{UB}\int_0^1 \left(x_1^{n-k-q-1}y^{j-q}\right) I_{i_1,i_2} x_1^2\, y dx_1 dy$$

$$= \frac{-(n-k-q)(-b)^{j-q+2}}{(i_1+1)\left[(n-k+i_1)-(q-3)\right]\left[(n-k+i_1)-(j-1)\right]}\tilde{J}_p\left(-\frac{1}{B}\right) + \frac{n-k-q}{(i_1+1)(n-k-q+i_1+3)}\left\{\sum_{f=0}^{i_2}(-1)^f C_f^{i_2} l^{i_2-f}\right.$$

$$\left.\times\left[\sum_{t_5=0}^{j-q+1}(-1)^{t_5} C_{t_5}^{j-q+1} l^{j-q+1-t_5}\left(\int_{\frac{1}{B}}^{\frac{1}{B}}(l-y)^{i_1+t_5+1} I_g dy + \int_{\frac{1}{B}}^{1}(l-y)^{i_1+t_5+1} I_g dy\right)\right] + \left(\int_b^{\frac{1}{B}} y^{j-q+1}\tilde{J}_p dy + \int_{\frac{1}{B}}^{\frac{1}{B}} y^{j-q+1}\tilde{J}_p dy\right)\right\}$$

(C-38)

$$\iint_S \left(x_1^{n-k-q}y^{j-q}\right) I_{i_1,i_2} x_1^2\, y dx_1 dy = \iint_{\tilde{S}_0} \left(x_1^{n-k-q}y^{j-q}\right) I_{i_1,i_2} x_1^2\, y dx_1 dy + \iint_{S_0+S_i+S_1} \left(x_1^{n-k-q}y^{j-q}\right) I_{i_1,i_2} x_1^2\, y dx_1 dy$$

$$= \int_0^1 \int_{\frac{b}{x_1}}^{b} \left(x_1^{n-k-q}y^{j-q}\right) I_{i_1,i_2} x_1^2\, y dx_1 dy + \int_{LB}^{UB}\int_0^1 \left(x_1^{n-k-q}y^{j-q}\right) I_{i_1,i_2} x_1^2\, y dx_1 dy$$

$$= \frac{-(-b)^{j-q+2}}{(i_1+1)\left[(n-k+i_1)-(q-4)\right]\left[(n-k+i_1)-(j-2)\right]}\tilde{J}_p\left(-\frac{1}{B}\right) + \frac{1}{(i_1+1)(n-k-q+i_1+4)}\left\{\sum_{f=0}^{i_2}(-1)^f C_f^{i_2} l^{i_2-f}\right.$$

$$\left.\times\left[\sum_{t_5=0}^{j-q+1}(-1)^{t_5} C_{t_5}^{j-q+1} l^{j-q+1-t_5}\left(\int_{\frac{1}{B}}^{\frac{1}{B}}(l-y)^{i_1+t_5+1} I_g dy + \int_{\frac{1}{B}}^{1}(l-y)^{i_1+t_5+1} I_g dy\right)\right] + \left(\int_b^{\frac{1}{B}} y^{j-q+1}\tilde{J}_p dy + \int_{\frac{1}{B}}^{\frac{1}{B}} y^{j-q+1}\tilde{J}_p dy\right)\right\}$$

(C-39)

$$\int_S \left(x_1^{n-k-q} y^{j-q}\right)\frac{\partial I_{i_1,i_2}}{\partial x_1} x_1^2 y dx_1 dy = \int_{\tilde{S}_0} \left(x_1^{n-k-q} y^{j-q}\right)\frac{\partial I_{i_1,i_2}}{\partial x_1} x_1^2 y dx_1 dy + \int_{S_0+S_i+S_1} \left(x_1^{n-k-q} y^{j-q}\right)\frac{\partial I_{i_1,i_2}}{\partial x_1} x_1^2 y dx_1 dy$$

$$= \int_0^1 \int_{\frac{b}{x_1}}^b \left(x_1^{n-k-q} y^{j-q}\right)\frac{\partial I_{i_1,i_2}}{\partial x_1} x_1^2 y dx_1 dy + \int_{LB}^{UB} \int_0^1 \left(x_1^{n-k-q} y^{j-q}\right)\frac{\partial I_{i_1,i_2}}{\partial x_1} x_1^2 y dx_1 dy$$

$$= \frac{-(-b)^{j-q+2}}{[(n-k+i_1)-(q-3)][(n-k+i_1)-(j-1)]}\tilde{J}_p\left(-\frac{1}{B}\right) + \frac{1}{n-k-q+i_1+3}\left\{\sum_{f=0}^{i_2}(-1)^f C_f^{i_2} l^{i_2-f+1}\right.$$

$$\times\left[\sum_{t_7=0}^{j-q+1}(-1)^{t_7} C_{t_7}^{j-q+1} l^{j-q+1-t_7}\left(\int_{\frac{1}{B}}^{\frac{1}{B}}(l-y)^{i_1+t_7} I_g dy + \int_{\frac{1}{B}}^{\frac{1}{B}}(l-y)^{i_1+t_7} I_g dy\right)\right] + \left(\int_b^{\frac{1}{B}} y^{j-q+1}\tilde{J}_p dy + \int_{\frac{1}{B}}^{\frac{1}{B}} y^{j-q+1}\tilde{J}_p dy\right)\Bigg\}$$

$$-\frac{1}{(n-k-q+i_1+3)(i_1+1)}\left\{\sum_{f=0}^{i_2}(-1)^f C_f^{i_2} l^{i_2-f}\left[\sum_{t_9=0}^{j-q+2}(-1)^{t_9} C_{t_9}^{j-q+2} l^{j-q+2-t_9}\left(\int_{\frac{1}{B}}^{\frac{1}{B}}(l-y)^{i_1+1+t_9} dI_g\right)\right] + \left(\int_{\frac{1}{B}}^{\frac{1}{B}} y^{j-q+2} d\tilde{J}_p\right)\right\}. \quad \text{(C-40)}$$

Similarly, detailed equations for solving integrals in Eq.(C-32) ~ (C-40) are solved by the recurrence formulae and given in the following sections.

## C-5: Recurrence formulae for the integral $I_a$

Consider the recurrence integral defined as

$$I_a = \int \frac{y^a}{\sqrt{1-B^2y^2}} dy, \text{ for } a \geq 0. \quad \text{(C-41)}$$

First, define an auxiliary integral $A_1$ as

$$A_1 = \int y^a \sqrt{1-B^2y^2}\, dy = \int \frac{y^a}{\sqrt{1-B^2y^2}} dy - B^2 \int \frac{y^{a+2}}{\sqrt{1-B^2y^2}} dy. \quad \text{(C-42)}$$

In turn, by integrating by parts for $A_1$, one concludes that

$$A_1 = \int y^a \sqrt{1-B^2y^2}\,dy = \frac{y^{a+1}}{a+1}\sqrt{1-B^2y^2} + \frac{B^2}{a+1}\int \frac{y^{a+2}}{\sqrt{1-B^2y^2}}dy. \tag{C-43}$$

Substituting Eq.(C-43) into the definition of the auxiliary integral $A_1$, we obtain

$$I_a = -\frac{y^{a-1}\sqrt{1-B^2y^2}}{aB^2} + \frac{(a-1)}{aB^2} I_{a-2}, \text{ for } a \geq 1. \tag{C-44}$$

The value of integral at a = 0 is given by,

$$I_a = \int \frac{1}{\sqrt{1-B^2y^2}}dy = \frac{1}{B}\sin^{-1}(By). \tag{C-45}$$

The recurrence integral $I_a$ is evaluated from $y = -\frac{1}{B}$ to $y = \frac{1}{B}$.

For $a = 0$,

$$I_a = \int_{-\frac{1}{B}}^{\frac{1}{B}} \frac{1}{\sqrt{1-B^2y^2}}dy = \frac{\pi}{B}. \tag{C-46}$$

For $a \geq 1$,

$$I_a = \int_{-\frac{1}{B}}^{\frac{1}{B}} \frac{y^a}{\sqrt{1-B^2y^2}}dy = \frac{a-1}{aB^2} I_{a-2}. \tag{C-47}$$

## C-6: Recurrence formulae for the integral $I_b$

Consider the recurrence integral defined as

$$I_b = \int y^b \sqrt{1-B^2y^2}\,dy, \text{ for } b \geq 0. \tag{C-48}$$

Similarly, the recurrence formulae for integral $I_b$ is derived as

$$I_b = -\frac{y^{b-1}\left(1-B^2y^2\right)^{3/2}}{(b+2)B^2} + \frac{b-1}{(b+2)B^2} I_{b-2}, \text{ for } b \geq 1. \tag{C-49}$$

The value of integral at $b = 0$ is given by

$$I_b = \int \sqrt{1-B^2y^2}\,dy = \frac{1}{2}y\sqrt{1-B^2y^2} + \frac{1}{2B}\sin^{-1}(By), \text{ for } b = 0. \tag{C-50}$$

In turn, the recurrence integral $I_b$ is evaluated from $y = -\frac{1}{B}$ to $y = \frac{1}{B}$.

For $b = 0$,

$$I_b = \int_{-b}^{b} \sqrt{1 - B^2 y^2}\, dy = \frac{\pi}{2B}. \tag{C-51}$$

For $b \geq 1$

$$I_b = \frac{b-1}{(b+2)B^2} I_{b-2}. \tag{C-52}$$

## C-7: Recurrence formulae for integral $\int (l-y)^m I_g dy$

Consider the recurrence integral defined as

$$I_g^* = \int (l-y)^m I_g dy. \tag{C-53}$$

For $g = 1$,

$$I_g^* = \frac{2}{\sqrt{B^2 l^2 - 1}} \int (l-y)^m \cos^{-1} \sqrt{\frac{(1-By)(1+Bl)}{2B(l-y)}}\, dy = \frac{2}{\sqrt{B^2 l^2 - 1}} \left( \sum_{q=0}^{m} (-1)^q C_q^m l^{m-q} \int y^q \cos^{-1} \sqrt{\frac{(1-By)(1+Bl)}{2B(l-y)}}\, dy \right)$$

$$= \frac{2}{\sqrt{B^2 l^2 - 1}} \left[ \sum_{q=0}^{m} (-1)^q C_q^m l^{m-q} \left( \frac{y^{q+1} - l^{q+1}}{q+1} \cos^{-1} \sqrt{\frac{(1+Bl)(1-By)}{2B(l-y)}} + \frac{\sqrt{B^2 l^2 - 1}}{2(q+1)} \sum_{a=0}^{q} l^{q-a} I_a \right) \right]. \tag{C-54}$$

For $g \geq 2$,

$$I_g^* = \frac{1}{(g-1)(1-B^2 l^2)} \left[ \int (l-y)^{[m-(g-1)]} \sqrt{1 - B^2 y^2}\, dy + B^2 l (3-2g) I_{g-1}^* + B^2 (g-2) I_{g-2}^* \right]$$

$$= \frac{1}{(g-1)(1-B^2 l^2)} \left[ \left( \sum_{a=0}^{[m-(g-1)]} (-1)^a C_a^{[m-(g-1)]} l^{[m-(g-1)]-a} \left( I_a - B^2 I_{a+2} \right) \right) + B^2 l (3-2g) I_{g-1}^* + B^2 (g-2) I_{g-2}^* \right], \tag{C-55}$$

where from section C.5, $I_a = \int \frac{y^a}{\sqrt{1 - B^2 y^2}}\, dy$.

The recurrence integral $I_g^*$ is evaluated from $y=\frac{1}{B}$ to $y=l$, where $I_g$ is constant, and is given by,

For $g=1$,

$$I_g^* = \int_{\frac{1}{B}}^{l}(l-y)^m I_g dy = \frac{1}{m+1}\left(l-\frac{1}{B}\right)^{m+1}\frac{\pi}{\sqrt{B^2l^2-1}}. \tag{C-56}$$

For $g \geq 2$,

$$I_g^* = \int_{\frac{1}{B}}^{l}(l-y)^m I_g dy = \frac{1}{m+1}\left(l-\frac{1}{B}\right)^{m+1}\frac{1}{(1-B^2l^2)}\left[B^2l\frac{3-2g}{g-1}I_{g-1}+B^2\frac{g-2}{g-1}I_{g-2}\right], \tag{C-57}$$

where for g = 1, $I_g = \frac{\pi}{\sqrt{B^2l^2-1}}$.

The recurrence integral $I_g^*$ is evaluated from $y=-\frac{1}{B}$ to $y=\frac{1}{B}$, where $I_g$ is function of $y$, and is given by,

For $g=1$,

$$I_g^* = \int_{\frac{1}{B}}^{\frac{1}{B}}(l-y)^m I_g dy = \frac{2}{\sqrt{B^2l^2-1}}\left[\sum_{q=0}^{m}(-1)^q C_q^m l^{m-q}\left(\frac{\left(B^{-1}\right)^{q+1}-l^{q+1}}{q+1}\frac{\pi}{2}+\frac{\sqrt{B^2l^2-1}}{2(q+1)}\sum_{a=0}^{q}l^{q-a}I_a\right)\right]. \tag{C-58}$$

For $g \geq 2$,

$$I_g^* = \int_{\frac{1}{B}}^{\frac{1}{B}}(l-y)^m I_g dy = \frac{1}{(g-1)(1-B^2l^2)}\left[\left(\sum_{a=0}^{[m-(g-1)]}(-1)^a C_a^{[m-(g-1)]}l^{[m-(g-1)]-a}\left(I_a-B^2I_{a+2}\right)\right)+B^2l(3-2g)I_{g-1}^*+B^2(g-2)I_{g-2}^*\right] \tag{C-59}$$

## C-8: Recurrence formulae for integral $\int_{\frac{1}{B}}^{\frac{1}{B}}(l-y)^m dI_g$

By integrating by parts, we obtain,

$$\int_{\frac{1}{B}}^{\frac{1}{B}}(l-y)^m dI_g = (l-y)^m I_g(y)\Big|_{\frac{1}{B}}^{\frac{1}{B}} + m\int_{\frac{1}{B}}^{\frac{1}{B}}(l-y)^{m-1}I_g dy$$

$$= \left(l-\frac{1}{B}\right)^m I_g\left(\frac{1}{B}\right) + m\int_{\frac{1}{B}}^{\frac{1}{B}}(l-y)^{m-1}I_g dy. \tag{C-60}$$

Thus, for $g = 1$,

$$\int_{\frac{1}{B}}^{\frac{1}{B}} (l-y)^m dI_g = \left(l-\frac{1}{B}\right)^m \frac{\pi}{\sqrt{B^2l^2-1}} + \frac{2m}{\sqrt{B^2l^2-1}}\left[\sum_{q=0}^{m-1}(-1)^q C_q^{m-1} l^{m-1-q}\left(\frac{\left(B^{-1}\right)^{q+1}-l^{q+1}}{q+1}\frac{\pi}{2} + \frac{\sqrt{B^2l^2-1}}{2(q+1)}\sum_{a=0}^{q} l^{q-a} I_a\right)\right] \tag{C-61}$$

For $g \geq 2$,

$$\int_{\frac{1}{B}}^{\frac{1}{B}} (l-y)^m dI_g = \left(l-\frac{1}{B}\right)^m \frac{1}{\left(1-B^2l^2\right)}\left[B^2 l \frac{3-2g}{g-1} I_{g-1} + B^2 \frac{g-2}{g-1} I_{g-2}\right]$$

$$+\frac{m}{(g-1)\left(1-B^2l^2\right)}\left[\left(\sum_{a=0}^{[m-1-(g-1)]}(-1)^a C_a^{[m-1-(g-1)]} l^{[m-1-(g-1)]-a}\left(I_a - B^2 I_{a+2}\right)\right) + B^2 l(3-2g) I_{g-1}^* + B^2(g-2) I_{g-2}^*\right], \tag{C-62}$$

where $I_g$ and $I_g^*$ are given as follows for g = 1.

$$I_g = \frac{\pi}{\sqrt{B^2l^2-1}}. \tag{C-63}$$

$$I_g^* = \int_{\frac{1}{B}}^{\frac{1}{B}} (l-y)^{m-1} I_g dy = \frac{2}{\sqrt{B^2l^2-1}}\left[\sum_{q=0}^{m-1}(-1)^q C_q^{m-1} l^{m-1-q}\left(\frac{\left(B^{-1}\right)^{q+1}-l^{q+1}}{q+1}\frac{\pi}{2} + \frac{\sqrt{B^2l^2-1}}{2(q+1)}\sum_{a=0}^{q} l^{q-a} I_a\right)\right]. \tag{C-64}$$

## C-9: Recurrence formulae for integral $\int (l+y)^n J_g dy$

Consider the recurrence integral defined by

$$J_g^* = \int (l+y)^n J_g dy. \tag{C-65}$$

For $g = 1$,

$$J_g^* = \frac{2}{\sqrt{B^2l^2-1}}\int (l+y)^n \cos^{-1}\sqrt{\frac{(1+By)(1+Bl)}{2B(l+y)}}dy = \frac{2}{\sqrt{B^2l^2-1}}\left(\sum_{q=0}^{n} C_q^n l^{n-q}\int y^q \cos^{-1}\sqrt{\frac{(1+By)(1+Bl)}{2B(l+y)}}dy\right)$$

$$= \frac{2}{\sqrt{B^2l^2-1}}\left[\sum_{q=0}^{n} C_q^n l^{n-q}\left(\frac{y^{q+1}+(-1)^q l^{q+1}}{q+1}\cos^{-1}\sqrt{\frac{(1+Bl)(1+By)}{2B(l+y)}} + \frac{\sqrt{B^2l^2-1}}{2(q+1)}\sum_{a=0}^{q}(-l)^a I_{q-a}\right)\right]. \tag{C-66}$$

For $g \geq 2$,

$$J_g^* = \frac{1}{(g-1)(1-B^2l^2)}\left[\int (l+y)^{[n-(g-1)]}\sqrt{1-B^2y^2}\,dy + B^2l(3-2g)J_{g-1}^* + B^2(g-2)J_{g-2}^*\right]$$

$$= \frac{1}{(g-1)(1-B^2l^2)}\left[\left(\sum_{a=0}^{[n-(g-1)]} C_a^{[n-(g-1)]} l^{[n-(g-1)]-a}\left(I_a - B^2 I_{a+2}\right)\right) + B^2l(3-2g)J_{g-1}^* + B^2(g-2)J_{g-2}^*\right], \tag{C-67}$$

where from section C.5, $I_{q-a} = \int \frac{y^{q-a}}{\sqrt{1-B^2y^2}}dy$ and $I_a = \int \frac{y^a}{\sqrt{1-B^2y^2}}dy$.

The recurrence integral $J_g^*$ is evaluated from $y = -l$ to $y = -\frac{1}{B}$, where $J_g$ is constant, and is given

For $g = 1$,

$$J_g^* = \int_{-l}^{-\frac{1}{B}} (l+y)^n J_g\,dy = \frac{1}{n+1}\left(l - \frac{1}{B}\right)^{n+1} \frac{\pi}{\sqrt{B^2l^2-1}}. \tag{C-68}$$

For $g \geq 2$,

$$J_g^* = \int_{-l}^{-\frac{1}{B}} (l+y)^n J_g\,dy = \frac{1}{n+1}\left(l - \frac{1}{B}\right)^{n+1} \frac{1}{(1-B^2l^2)}\left[B^2l\frac{3-2g}{g-1}J_{g-1} + B^2\frac{g-2}{g-1}J_{g-2}\right], \tag{C-69}$$

where for g = 1, $J_g = \frac{\pi}{\sqrt{B^2l^2-1}}$.

The recurrence integral $J_g^*$ is evaluated from $y = -\frac{1}{B}$ to $y = \frac{1}{B}$, where $J_g$ is function of $y$, and is given by,

For $g = 1$,

$$J_g^* = \int_{-\frac{1}{B}}^{\frac{1}{B}} (l+y)^n J_g\,dy = \frac{2}{\sqrt{B^2l^2-1}}\left[\sum_{q=0}^{n} C_q^n l^{n-q}\left(\frac{\left(-B^{-1}\right)^{q+1} - (-l)^{q+1}}{q+1}\frac{\pi}{2} + \frac{\sqrt{B^2l^2-1}}{2(q+1)}\sum_{a=0}^{q}(-l)^a I_{q-a}\right)\right]. \tag{C-70}$$

For $g \geq 2$,

$$J_g^* = \int_{-\frac{1}{B}}^{\frac{1}{B}} (l+y)^n J_g\,dy = \frac{1}{(g-1)(1-B^2l^2)}\left[\left(\sum_{a=0}^{[n-(g-1)]} C_a^{[n-(g-1)]} l^{[n-(g-1)]-a}\left(I_a - B^2 I_{a+2}\right)\right) + B^2l(3-2g)J_{g-1}^* + B^2(g-2)J_{g-2}^*\right] \tag{C-71}$$

## C-10: Recurrence formulae for integral $\int_{\frac{1}{B}}^{\frac{1}{B}}(l+y)^n dJ_g$

By integrating by parts, we have

$$\int_{\frac{1}{B}}^{\frac{1}{B}}(l+y)^n dJ_g = (l+y)^n J_g(y)\Big|_{\frac{1}{B}}^{\frac{1}{B}} - n\int_{\frac{1}{B}}^{\frac{1}{B}}(l+y)^{n-1} J_g dy = -\left(l-\frac{1}{B}\right)^n J_g(\frac{1}{B}) - n\int_{\frac{1}{B}}^{\frac{1}{B}}(l+y)^{n-1} J_g dy \tag{C-72}$$

Thus, for $g = 1$,

$$\int_{\frac{1}{B}}^{\frac{1}{B}}(l+y)^n dJ_g = -\left(l-\frac{1}{B}\right)^n \frac{\pi}{\sqrt{B^2l^2-1}} - \frac{2n}{\sqrt{B^2l^2-1}}\left[\sum_{q=0}^{n-1} C_q^{n-1} l^{n-1-q}\left(\frac{\left(-B^{-1}\right)^{q+1}-(-l)^{q+1}}{q+1}\frac{\pi}{2} + \frac{\sqrt{B^2l^2-1}}{2(q+1)}\sum_{a=0}^{q}(-l)^a I_{q-a}\right)\right] \tag{C-73}$$

For $g \geq 2$,

$$\int_{\frac{1}{B}}^{\frac{1}{B}}(l+y)^n dJ_g = -\left(l-\frac{1}{B}\right)^n \frac{1}{\left(1-B^2l^2\right)}\left[B^2 l\frac{3-2g}{g-1}J_{g-1} + B^2\frac{g-2}{g-1}J_{g-2}\right]$$

$$-\frac{n}{(g-1)\left(1-B^2l^2\right)}\left[\left(\sum_{a=0}^{[n-1-(g-1)]} C_a^{[n-1-(g-1)]} l^{[n-1-(g-1)]-a}\left(I_a - B^2 I_{a+2}\right)\right) + B^2 l(3-2g)J_{g-1}^* + B^2(g-2)J_{g-2}^*\right], \tag{C-74}$$

where $J_g$ and $J_g^*$ are given as follows for g = 1.

$$J_g = \frac{\pi}{\sqrt{B^2l^2-1}}. \tag{C-75}$$

$$J_g^* = \int_{\frac{1}{B}}^{\frac{1}{B}}(l+y)^{n-1} J_g dy = \frac{2}{\sqrt{B^2l^2-1}}\left[\sum_{q=0}^{n-1} C_q^{n-1} l^{n-1-q}\left(\frac{\left(-B^{-1}\right)^{q+1}-(-l)^{q+1}}{q+1}\frac{\pi}{2} + \frac{\sqrt{B^2l^2-1}}{2(q+1)}\sum_{a=0}^{q}(-l)^a I_{q-a}\right)\right]. \tag{C-76}$$

## C-11: Recurrence formulae for integral $\int y^n \tilde{J}_p dy$

Consider the recurrence integral defined by

$$\tilde{J}_p^* = \int y^n \tilde{J}_p dy . \tag{C-77}$$

For $p = 0$,

$$\tilde{J}_p^* = \int y^n \tilde{J}_p dy = \frac{1}{B}\int y^n \left[\frac{\pi}{2} - \sin^{-1}(By)\right] dy = \frac{\pi}{2B}\frac{y^{n+1}}{n+1} - \frac{1}{B}\int y^n \sin^{-1}(By) dy$$

$$= \frac{y^{n+1}}{B(n+1)}\left(\frac{\pi}{2} - \sin^{-1}(By)\right) + \frac{1}{n+1}\int \frac{y^{n+1}}{\sqrt{1-B^2y^2}} dy$$

$$= \frac{y^{n+1}}{B(n+1)}\left(\frac{\pi}{2} - \sin^{-1}(By)\right) + \frac{1}{n+1} I_{a(a=n+1)} . \tag{C-78}$$

For $p = 1$,

$$\tilde{J}_p^* = \int y^n \tilde{J}_p dy = \frac{2}{B^2}\int y^n \sqrt{1-B^2y^2}\, dy = \frac{2}{B^2} I_{b(b=n)} . \tag{C-79}$$

For $p \geq 2$,

$$\tilde{J}_p^* = \int y^n \tilde{J}_p dy = \frac{1}{pB^2} I_{b(b=n+p-1)} + \frac{p-1}{pB^2}\tilde{J}_{p-2}^* , \tag{C-80}$$

where from section C-5 and C-6, $I_{a(a=n+1)} = \int \frac{y^{n+1}}{\sqrt{1-B^2y^2}} dy$ and $I_{b(b=n)} = \int y^n \sqrt{1-B^2y^2}\, dy$.

The recurrence integral is then evaluated from $y = -b$ to $y = -\frac{1}{B}$, where $\tilde{J}_p$ is constant in such integration domain, and is given by,

For $p = 0$,

$$\tilde{J}_p^* = \int_{-b}^{-\frac{1}{B}} y^n \tilde{J}_p dy = \frac{1}{n+1}\left[\left(-\frac{1}{B}\right)^{n+1} - (-b)^{n+1}\right]\frac{\pi}{B} \tag{C-81}$$

For $p = 1$,

$$\tilde{J}_p^* = \int_{-b}^{-\frac{1}{B}} y^n \tilde{J}_p dy = 0 . \tag{C-82}$$

For $p \geq 2$,

$$\tilde{J}_p^* = \int_b^{\frac{1}{B}} y^n \tilde{J}_p dy = \frac{1}{n+1}\left[\left(-\frac{1}{B}\right)^{n+1} - (-b)^{n+1}\right]\frac{p-1}{pB^2}\tilde{J}_{p-2}. \tag{C-83}$$

where, for $p = 0$, $\tilde{J}_p = \frac{\pi}{B}$; for $p = 1$, $\tilde{J}_p = 0$.

The recurrence integral is then evaluated from $y = -\frac{1}{B}$ to $y = \frac{1}{B}$, where $\tilde{J}_p$ is yet function of $y$, and is given by,

For $p = 0$,

$$\tilde{J}_p^* = \int_{\frac{1}{B}}^{\frac{1}{B}} y^n \tilde{J}_p dy = -\frac{\left(-B^{-1}\right)^{n+1}}{B(n+1)}\pi + \frac{1}{n+1} I_{a(a=n+1)}. \tag{C-84}$$

For $p = 1$,

$$\tilde{J}_p^* = \int_{\frac{1}{B}}^{\frac{1}{B}} y^n \tilde{J}_p dy = \frac{2}{B^2}\int_{\frac{1}{B}}^{\frac{1}{B}} y^n \sqrt{1-B^2y^2}\, dy = \frac{2}{B^2} I_{b(b=n)}. \tag{C-85}$$

For $p \geq 2$,

$$\tilde{J}_p^* = \int_{\frac{1}{B}}^{\frac{1}{B}} y^n \tilde{J}_p dy = \frac{1}{pB^2} I_{b(b=n+p-1)} + \frac{p-1}{pB^2}\tilde{J}_{p-2}^*. \tag{C-86}$$

## C-12: Recurrence formulae for integral $\int_{\frac{1}{B}}^{\frac{1}{B}} y^n d\tilde{J}_p$

By integrating by parts, we have

$$\int_{\frac{1}{B}}^{\frac{1}{B}} y^n d\tilde{J}_p = y^n \tilde{J}_p(y)\Big|_{\frac{1}{B}}^{\frac{1}{B}} - n\int_{\frac{1}{B}}^{\frac{1}{B}} y^{n-1}\tilde{J}_p dy$$

$$= -\left(-B^{-1}\right)^n \tilde{J}_p\left(-\frac{1}{B}\right) - n\int_{\frac{1}{B}}^{\frac{1}{B}} y^{n-1}\tilde{J}_p dy. \tag{C-87}$$

Thus, for p = 0,

$$\int_{\frac{1}{B}}^{\frac{1}{B}} y^n d\tilde{J}_p = -\left(-B^{-1}\right)^n \frac{\pi}{B} - n\left(-\frac{\pi\left(-B^{-1}\right)^n}{B(n)} + \frac{1}{n} I_{a(a=n)}\right). \tag{C-88}$$

For p = 1,

$$\int_{\frac{1}{B}}^{\frac{1}{B}} y^n d\tilde{J}_p = -\frac{2n}{B^2} I_{b(b=n-1)}. \tag{C-89}$$

For $p \geq 2$,

$$\int_{\frac{1}{B}}^{\frac{1}{B}} y^n d\tilde{J}_p = -\left(-B^{-1}\right)^n \frac{p-1}{pB^2} \tilde{J}_{p-2}\left(-\frac{1}{B}\right) - n\left(\frac{1}{pB^2} I_{b(b=n+p-2)} + \frac{p-1}{pB^2} \tilde{J}^*_{p-2}\right). \tag{C-90}$$

## C-13: Integrals related to $I_g^*$ and $J_g^*$, for $g = 1$.

Consider the following two integrals of inverse triangular functions given by,

$$\int y^q \cos^{-1}\sqrt{\frac{(1+Bl)(1-By)}{2B(l-y)}}\,dy = \frac{y^{q+1}}{q+1}\cos^{-1}\sqrt{\frac{(1+Bl)(1-By)}{2B(l-y)}} - \frac{\sqrt{B^2l^2-1}}{2(q+1)}\int \frac{y^{q+1}}{(l-y)\sqrt{1-B^2y^2}}\,dy, \tag{C-91}$$

$$\int y^q \cos^{-1}\sqrt{\frac{(1+Bl)(1+By)}{2B(l+y)}}\,dy = \frac{y^{q+1}}{q+1}\cos^{-1}\sqrt{\frac{(1+Bl)(1+By)}{2B(l+y)}} + \frac{\sqrt{B^2l^2-1}}{2(q+1)}\int \frac{y^{q+1}}{(l+y)\sqrt{1-B^2y^2}}\,dy. \tag{C-92}$$

Note that $\frac{y^{q+1}}{(l-y)}$ and $\frac{y^{q+1}}{(l+y)}$ can be recast by,

$$\frac{y^{q+1}}{(l-y)} = -\frac{-y^{q+1}+l^{q+1}}{(l-y)} + \frac{l^{q+1}}{(l-y)} = -\sum_{j=0}^{q} l^{q-j} y^j + \frac{l^{q+1}}{(l-y)}, \tag{C-93}$$

$$\frac{y^{q+1}}{(l+y)} = \frac{y^{q+1}+(-1)^q l^{q+1}}{(l+y)} - \frac{(-1)^q l^{q+1}}{(l+y)} = \sum_{j=0}^{q} (-l)^j y^{q-j}\left(-\frac{(-1)^q l^{q+1}}{(l+y)}\right). \tag{C-94}$$

We apply general factorization equation for expanding $\left(y^{q+1}+(-1)^q l^{q+1}\right)$ and $\left(l^{q+1}-y^{q+1}\right)$.

$$y^{q+1}+(-1)^q l^{q+1} = (l+y)\sum_{j=0}^{q} l^{q-j}(-y)^j, \tag{C-95}$$

$$l^{q+1} - y^{q+1} = (l-y)\sum_{j=0}^{q} l^{q-j} y^{j} \,. \tag{C-96}$$

By arranging the terms, one concludes,

$$\int y^{q} \cos^{-1} \sqrt{\frac{(1+Bl)(1-By)}{2B(l-y)}}\, dy$$

$$= \frac{y^{q+1} - l^{q+1}}{q+1} \cos^{-1} \sqrt{\frac{(1+Bl)(1-By)}{2B(l-y)}} + \frac{\sqrt{B^2 l^2 - 1}}{2(q+1)} \sum_{j=0}^{q} l^{q-j} \int \frac{y^{j}}{\sqrt{1-B^2 y^2}}\, dy \,. \tag{C-97}$$

$$\int y^{q} \cos^{-1} \sqrt{\frac{(1+Bl)(1+By)}{2B(l+y)}}\, dy$$

$$= \frac{y^{q+1} + (-1)^{q} l^{q+1}}{q+1} \cos^{-1} \sqrt{\frac{(1+Bl)(1+By)}{2B(l+y)}} + \frac{\sqrt{B^2 l^2 - 1}}{2(q+1)} \sum_{j=0}^{q} (-l)^{j} \int \frac{y^{q-j}}{\sqrt{1-B^2 y^2}}\, dy \,. \tag{C-98}$$

# Appendix D: General integral and integration limits for calculation of aerodynamics coefficients for delta and trapezoidal wings

## D-1: Case of thin delta wing

$I_{i_1,i_2}$ can be written in the form as

$$I_{i_1,i_2} = \iint_{\sigma} \frac{X^{i_1} Y^{i_2}}{\Re} dXdY = \frac{[x_1(l-y)]^{i_1+1}}{i_1+1} \int_{\frac{1}{B}}^{f(y)} \frac{Y^{i_2}}{(l-Y)^{i_1+1}\Re} dY + \frac{[x_1(l+y)]^{i_1+1}}{i_1+1} \int_{f(y)}^{\frac{1}{B}} \frac{Y^{i_2}}{(l+Y)^{i_1+1}\Re} dY. \quad \text{(D-1)}$$

In turn, two integrals in Eq.(D-1) can be carried out analytically by the Newton binomial formula as

$$\int_{\frac{1}{B}}^{f(y)} \frac{Y^{i_2}}{(l-Y)^{i_1+1}\Re} dY = \sum_{f=0}^{i_2} (-1)^f C_f^{i_2} l^{i_2-f} \int_{\frac{1}{B}}^{f(y)} \frac{1}{(l-Y)^{i_1-f+1}\Re} dY, \quad \text{(D-2)}$$

$$\int_{f(y)}^{\frac{1}{B}} \frac{Y^{i_2}}{(l+Y)^{i_1+1}\Re} dY = \sum_{f=0}^{i_2} (-1)^{i_2-f} C_f^{i_2} l^{i_2-f} \int_{f(y)}^{\frac{1}{B}} \frac{1}{(l+Y)^{i_1-f+1}\Re} dY. \quad \text{(D-3)}$$

Then, we denote two integrals in Eq.(D-2) and (D-3) by $I_g$ and $J_g$, respectively, where $g = i_1 - f + 1$.

$$I_g = \int_{\frac{1}{B}}^{f(y)} \frac{1}{(l-Y)^g \Re} dY, \quad \text{(D-4)}$$

$$J_g = \int_{f(y)}^{\frac{1}{B}} \frac{1}{(l+Y)^g \Re} dY. \quad \text{(D-5)}$$

Analytical solutions can be drawn out successively by means of recurrence formulae technique for $I_g$ and $J_g$ straightforward. We conclude that

$$I_g = \frac{1}{(1-B^2 l^2)} \left[ \frac{\sqrt{1-B^2[f(y)]^2}}{(g-1)[l-f(y)]^{g-1}} + B^2 l \frac{3-2g}{g-1} I_{g-1} + B^2 \frac{g-2}{g-1} I_{g-2} \right], \text{ for } g \geq 2. \quad \text{(D-6)}$$

$$I_g = \frac{1}{B} \left[ \sin^{-1}(Bf(y)) + \frac{\pi}{2} \right], \text{ for } g = 0. \quad \text{(D-7)}$$

$$I_g = \frac{2}{\sqrt{B^2 l^2 - 1}} \cos^{-1} \sqrt{\frac{(1-Bf(y))(1+Bl)}{2B(l-f(y))}}, \text{ for } g = 1. \quad \text{(D-8)}$$

where, $I_g = \int_{\frac{1}{B}}^{f(y)} \frac{1}{(l-Y)^g \Re} dY$; $I_{g-1} = \int_{\frac{1}{B}}^{f(y)} \frac{1}{(l-Y)^{g-1} \Re} dY$; $I_{g-2} = \int_{\frac{1}{B}}^{f(y)} \frac{1}{(l-Y)^{g-2} \Re} dY$

And

$$J_g = \frac{1}{(1-B^2l^2)}\left[\frac{\sqrt{1-B^2[f(y)]^2}}{(g-1)[l+f(y)]^{g-1}} + B^2 l\frac{3-2g}{g-1}I_{g-1} + B^2\frac{g-2}{g-1}I_{g-2}\right], \text{ for } g \geq 2. \quad \text{(D-9)}$$

$$J_g = \frac{1}{B}\left[\frac{\pi}{2} - \sin^{-1}(Bf(y))\right], \text{ for } g = 0. \quad \text{(D-10)}$$

$$J_g = \frac{2}{\sqrt{B^2l^2-1}}\cos^{-1}\sqrt{\frac{(1+Bf(y))(1+Bl)}{2B(l+f(y))}}, \text{ for } g = 1. \quad \text{(D-11)}$$

where, $J_g = \int_{f(y)}^{\frac{1}{B}} \frac{1}{(l+Y)^g \Re} dY$; $J_{g+1} = \int_{f(y)}^{\frac{1}{B}} \frac{1}{(l+Y)^{g+1} \Re} dY$; $J_{g+2} = \int_{f(y)}^{\frac{1}{B}} \frac{1}{(l+Y)^{g+2} \Re} dY$

Accordingly, the general integral, $I_{i_1,i_2}$, and its derivative with limits are given separately by considering the location of point $P(x_1, x_2)$.

**For position outside the Mach cone to the right,** $\frac{1}{B} \leq y \leq l$ and $f(y) = \frac{1}{B}$.

$$I_{i_1,i_2} = \frac{[x_1(l-y)]^{i_1+1}}{i_1+1}\int_{\frac{1}{B}}^{\frac{1}{B}} \frac{Y^{i_2}}{(l-Y)^{i_1+1}\Re} dY. \quad \text{(D-12)}$$

$$\frac{\partial}{\partial x_1} I_{i_1,i_2} = l[x_1(l-y)]^{i_1}\int_{\frac{1}{B}}^{\frac{1}{B}} \frac{Y^{i_2}}{(l-Y)^{i_1+1}\Re} dY. \quad \text{(D-13)}$$

**For position inside the Mach cone,** $-\frac{1}{B} \leq y \leq \frac{1}{B}$ and $f(y) = y$.

$$I_{i_1,i_2} = \frac{[x_1(l-y)]^{i_1+1}}{i_1+1}\int_{\frac{1}{B}}^{y} \frac{Y^{i_2}}{(l-Y)^{i_1+1}\Re} dY + \frac{[x_1(l+y)]^{i_1+1}}{i_1+1}\int_{y}^{\frac{1}{B}} \frac{Y^{i_2}}{(l+Y)^{i_1+1}\Re} dY. \quad \text{(D-14)}$$

$$\frac{\partial}{\partial x_1} I_{i_1,i_2} = l[x_1(l-y)]^{i_1}\int_{\frac{1}{B}}^{y} \frac{Y^{i_2}}{(l-Y)^{i_1+1}\Re} dY + \frac{[x_1(l-y)]^{i_1+1}}{i_1+1}\frac{\partial}{\partial x_1}\left(\int_{\frac{1}{B}}^{y} \frac{Y^{i_2}}{(l-Y)^{i_1+1}\Re} dY\right) +$$

$$l[x_1(l+y)]^{i_1}\int_{y}^{\frac{1}{B}} \frac{Y^{i_2}}{(l+Y)^{i_1+1}\Re} dY + \frac{[x_1(l+y)]^{i_1+1}}{i_1+1}\frac{\partial}{\partial x_1}\left(\int_{y}^{\frac{1}{B}} \frac{Y^{i_2}}{(l+Y)^{i_1+1}\Re} dY\right) \quad \text{(D-15)}$$

In addition, the derivative of integral $\int_{\frac{1}{B}}^{y}\frac{Y^{i_2}}{(l-Y)^{i_1+1}\Re}dY$ and $\int_{y}^{\frac{1}{B}}\frac{Y^{i_2}}{(l+Y)^{i_1+1}\Re}dY$ with respect to $x_1$ can be derived further as follows.

$$\frac{\partial}{\partial x_1}\left(\int_{\frac{1}{B}}^{y}\frac{Y^{i_2}}{(l-Y)^{i_1+1}\Re}dY\right)=\sum_{f=0}^{i_2}(-1)^f C_f^{i_2} l^{i_2-f}\frac{\partial I_g}{\partial x_1}=-\frac{x_2}{x_1^2}\sum_{f=0}^{i_2}(-1)^f C_f^{i_2} l^{i_2-f}\frac{\partial I_g}{\partial y} \tag{D-16}$$

$$\frac{\partial}{\partial x_1}\left(\int_{y}^{\frac{1}{B}}\frac{Y^{i_2}}{(l+Y)^{i_1+1}\Re}dY\right)=\sum_{f=0}^{i_2}(-1)^{i_2-f} C_f^{i_2} l^{i_2-f}\frac{\partial J_g}{\partial x_1}=-\frac{x_2}{x_1^2}\sum_{f=0}^{i_2}(-1)^{i_2-f} C_f^{i_2} l^{i_2-f}\frac{\partial J_g}{\partial y} \tag{D-17}$$

And the derivative of $I_g$ and $J_g$ with respect to y are then given by the recurrence formulae as,

For $g \geq 2$,

$$\frac{\partial I_g}{\partial y}=\frac{1}{1-B^2l^2}\left[\frac{(g-1)\left|1-B^2y^2\right|-B^2y(l-y)}{(g-1)(l-y)^g\sqrt{1-B^2y^2}}+B^2l\frac{3-2g}{g-1}\frac{\partial I_{g-1}}{\partial y}+B^2\frac{g-2}{g-1}\frac{\partial I_{g-2}}{\partial y}\right]. \tag{D-18}$$

$$\frac{\partial J_g}{\partial y}=\frac{1}{1-B^2l^2}\left[\frac{(g-1)\left|1-B^2y^2\right|-B^2y(l+y)}{(g-1)(l+y)^g\sqrt{1-B^2y^2}}+B^2l\frac{3-2g}{g-1}\frac{\partial J_{g-1}}{\partial y}+B^2\frac{g-2}{g-1}\frac{\partial J_{g-2}}{\partial y}\right]. \tag{D-19}$$

For $g = 1$,

$$\frac{\partial I_g}{\partial y}=\frac{1}{(l-y)\sqrt{1-B^2y^2}}. \tag{D-20}$$

$$\frac{\partial J_g}{\partial y}=\frac{-1}{(l+y)\sqrt{1-B^2y^2}}. \tag{D-21}$$

**For position outside the Mach cone to the left,** $-l \leq y \leq -\frac{1}{B}$ and $f(y)=-\frac{1}{B}$.

$$I_{i_1,i_2}=\frac{[x_1(l+y)]^{i_1+1}}{i_1+1}\int_{\frac{1}{B}}^{\frac{1}{B}}\frac{Y^{i_2}}{(l+Y)^{i_1+1}\Re}dY. \tag{D-22}$$

$$\frac{\partial}{\partial x_1}I_{i_1,i_2}=l[x_1(l+y)]^{i_1}\int_{\frac{1}{B}}^{\frac{1}{B}}\frac{Y^{i_2}}{(l+Y)^{i_1+1}\Re}dY. \tag{D-23}$$

## D-2: Case of thin trapezoidal wing

$I_{i_1,i_2}$ can be written in the form as

$$I_{i_1,i_2} = \iint_S \frac{X^{i_1} Y^{i_2}}{\Re} dXdY = \frac{[x_1(l-y)]^{i_1+1}}{i_1+1} \int_{\frac{1}{B}}^{f(y)} \frac{Y^{i_2}}{(l-Y)^{i_1+1}\Re} dY + \frac{x_1^{i_1+1}}{i_1+1} \int_{f(y)}^{\frac{1}{B}} \frac{Y^{i_2}}{\Re} dY. \quad \text{(D-24)}$$

The analytical solutions to the first integral in Eq.(D-24) have been established in Eq.(D-6) ~ (D-8), and the second integral can also be solved analytical by the recurrence formulae. We conclude that

$$\tilde{J}_p = \int_{f(y)}^{\frac{1}{B}} \frac{Y^p}{\Re} dY = \frac{p-1}{B^2 p}\left( \frac{\sqrt{1-B^2(f(y))^2}}{p-1}(f(y))^{p-1} + \tilde{J}_{p-2} \right), \text{ for } p \geq 2. \quad \text{(D-25)}$$

$$\tilde{J}_p = \int_{f(y)}^{\frac{1}{B}} \frac{1}{\Re} dY = \frac{1}{B}\left( \frac{\pi}{2} - \sin^{-1}(Bf(y)) \right), \text{ for } p = 0. \quad \text{(D-26)}$$

$$\tilde{J}_p = \int_{f(y)}^{\frac{1}{B}} \frac{\bar{Y}}{\underline{R}} d\bar{Y} = \frac{1}{B^2}\sqrt{1-B^2(f(y))^2}, \text{ for } p = 1, \quad \text{(D-27)}$$

where $\tilde{J}_p = \int_{f(y)}^{\frac{1}{B}} \frac{Y^p}{\Re} dY$ and $\tilde{J}_{p-2} = \int_{f(y)}^{\frac{1}{B}} \frac{Y^{p-2}}{\Re} dY$.

As a consequence, the general integral $I_{i_1,i_2}$ and its derivative in respect to $x_1$ with limits are determined as follows based on the location of point $P(x_1, x_2)$.

**For position in area** $S_1$, $\frac{1}{B} \leq y \leq l_1$ and $f(y) = \frac{1}{B}$.

$$I_{i_1,i_2} = \frac{[x_1(l-y)]^{i_1+1}}{i_1+1} \int_{\frac{1}{B}}^{\frac{1}{B}} \frac{Y^{i_2}}{(l-Y)^{i_1+1}\Re} dY. \quad \text{(D-28)}$$

$$\frac{\partial}{\partial x_1} I_{i_1,i_2} = l[x_1(l-y)]^{i_1} \int_{\frac{1}{B}}^{\frac{1}{B}} \frac{Y^{i_2}}{(l-Y)^{i_1+1}\Re} dY. \quad \text{(D-29)}$$

**For position in area** $S_i$, $-\frac{1}{B} \le y \le \frac{1}{B}$ and $f(y) = y$

$$I_{i_1,i_2} = \frac{[x_1(l-y)]^{i_1+1}}{i_1+1} \int_{\frac{1}{B}}^{f(y)} \frac{Y^{i_2}}{(l-Y)^{i_1+1}\Re} dY + \frac{x_1^{i_1+1}}{i_1+1} \int_{f(y)}^{\frac{1}{B}} \frac{Y^{i_2}}{\Re} dY. \quad \text{(D-30)}$$

$$\frac{\partial}{\partial x_1} I_{i_1,i_2} = l[x_1(l-y)]^{i_1} \int_{\frac{1}{B}}^{y} \frac{Y^{i_2}}{(l-Y)^{i_1+1}\Re} dY + \frac{[x_1(l-y)]^{i_1+1}}{i_1+1} \frac{\partial}{\partial x_1} \left( \int_{\frac{1}{B}}^{y} \frac{Y^{i_2}}{(l-Y)^{i_1+1}\Re} dY \right) +$$

$$x_1^{i_1} \int_{y}^{\frac{1}{B}} \frac{Y^{i_2}}{\Re} dY + \frac{x_1^{i_1+1}}{i_1+1} \frac{\partial}{\partial x_1} \left( \int_{y}^{\frac{1}{B}} \frac{Y^{i_2}}{\Re} dY \right). \quad \text{(D-31)}$$

where the derivative of integral $\int_{\frac{1}{B}}^{y} \frac{Y^{i_2}}{(l-Y)^{i_1+1}\Re} dY$ and $\int_{y}^{\frac{1}{B}} \frac{Y^{i_2}}{\Re} dY$ with respect to $x_1$ in Eq.(D-31) can be given by,

$$\frac{\partial}{\partial x_1} \left( \int_{\frac{1}{B}}^{y} \frac{Y^{i_2}}{(l-Y)^{i_1+1}\Re} dY \right) = \sum_{f=0}^{i_2} (-1)^f C_f^{i_2} l^{i_2-f} \frac{\partial I_g}{\partial x_1} = -\frac{x_2}{x_1^2} \sum_{f=0}^{i_2} (-1)^f C_f^{i_2} l^{i_2-f} \frac{\partial I_g}{\partial y}. \quad \text{(D-32)}$$

$$\frac{\partial}{\partial x_1} \left( \int_{y}^{\frac{1}{B}} \frac{Y^{i_2}}{\Re} dY \right) = \frac{\partial \tilde{J}_p}{\partial x_1} = -\frac{y}{x_1} \frac{p-1}{B^2 p} \frac{\partial}{\partial y} \left( \frac{\sqrt{1-B^2y^2}}{p-1} y^{p-1} + \tilde{J}_{p-2} \right)$$

$$= -\frac{y}{x_1} \frac{p-1}{B^2 p} \left( \frac{-B^2}{p-1} \frac{y^p}{\sqrt{1-B^2y^2}} + \sqrt{1-B^2y^2} \times y^{p-2} + \frac{\partial \tilde{J}_{p-2}}{\partial y} \right), \text{ for } p \ge 2 \quad \text{(D-33)}$$

The derivative of $I_g$ and $\tilde{J}_g$ with respect to y in the above two equations is given by the recurrence formulae as,

For $g \ge 2$

$$\frac{\partial I_g}{\partial y} = \frac{1}{1-B^2l^2} \left[ \frac{(g-1)|1-B^2y^2| - B^2y(l-y)}{(g-1)(l-y)^g \sqrt{1-B^2y^2}} + B^2 l \frac{3-2g}{g-1} \frac{\partial I_{g-1}}{\partial y} + B^2 \frac{g-2}{g-1} \frac{\partial I_{g-2}}{\partial y} \right]. \quad \text{(D-34)}$$

For $g = 1$,

$$\frac{\partial I_g}{\partial y} = \frac{1}{(l-y)\sqrt{1-B^2y^2}}. \quad \text{(D-35)}$$

For $p = 0$,

$$\frac{\partial \tilde{J}_p}{\partial x_1} = \frac{\partial}{\partial x_1}\left( \int_y^{\frac{1}{B}} \frac{1}{\Re} dY \right) = \frac{y}{x_1 \sqrt{1 - B^2 y^2}}. \tag{D-36}$$

For $p = 1$,

$$\frac{\partial \tilde{J}_p}{\partial x_1} = \frac{\partial}{\partial x_1}\left( \int_y^{\frac{1}{B}} \frac{Y}{\Re} dY \right) = \frac{y^2}{x_1 \sqrt{1 - B^2 y^2}}. \tag{D-37}$$

**For position in area $\tilde{S}_0$ and $S_0$, $-l_2 \le y \le -\frac{1}{B}$ and $f(y) = -\frac{1}{B}$.**

$$I_{i_1, i_2} = \frac{x_1^{\,i_1+1}}{i_1 + 1} \int_{-\frac{1}{B}}^{\frac{1}{B}} \frac{Y^{i_2}}{\Re} dY. \tag{D-38}$$

$$\frac{\partial}{\partial x_1} I_{i_1, i_2} = x_1^{\,i_1} \int_{-\frac{1}{B}}^{\frac{1}{B}} \frac{Y^{i_2}}{\Re} dY. \tag{D-39}$$

# Bibliography


1. Abbott, H., and Von Doenhoff, A.E., *Theory of wing sections*, Dover, New York, 1959.
2. Carafoli E., Mateescu D., and Nastase A., *Wing Theory in Supersonic Flow*, Pergamon Press, 1969.
3. Carafoli E., *Supersonic Aerodynamics*, Pergamom Press, Oxford, New York, 1962.
4. Chipman, R.R., "An improved Mach-Box approach for the calculations of supersonic oscillatory pressure distributions", *Proceedings AIAA/ASME/SAE, 17th Structures, Structural Dynamics, and Materials Conference*, pp. 615-625, 1976.
5. Courant R. and Friedrichs K.O., "Supersonic flow and shock waves", *Interscience Publishers Inc.*, New York, 1948.
6. Fénain M., "Trainée d'ailes delta symetriques à incidence nulle en regime supersonique", *La recherché Aeronautique*, No. 16, 1950.
7. Fénain M., *La théorie des écoulements à potential homogène et ses applications au calcul des ailes en regime supersonique*, Pergamom Press, London, 1967.
8. Geissler W., "Investigation of unsteady airloads on wings with oscillating control for active control purposes", *Neuilly sur Seine*, France, AGARD, 1981.
9. Germain P. and Fénain M., "Determination of Optimum Delta Wings with sonic leading edges", *O.N.E.R.A. Publ.* No.86, 1962.
10. Germain P. and Vallée D., "Effect de dièsur une aile delta en regime supersonique", *La recherché Aeronautique*, No. 52, pp. 3-20, 1962.

11. Germain P., "La théorie des mouvement coniques et ses application a l'Aerodinamique supersonique", *O.N.E.R.A. Publ.* No.34, 1949.

12. Germain P., "La théorie des mouvement homogène et son application au calcul de certain ailes delta en regime supersonique", *La recherché Aeronautique*, No. 7, pp. 3-16, 1949.

13. Hirsch C., *Numerical Computation of Internal and External Flows, Vol. 1: Fundamentals of Numerical Discretization*, John Wiley & Sons, New York, 2000.

14. Hirsch C., *Numerical Computation of Internal and External Flows, Vol. 2: Computational Methods for Inviscid and Viscous Flows*, John Wiley & Sons, New York, 2000.

15. Jameson A., "Numerical calculation of the transonic flow past a swept wing", *ERDA Mathematics and Computing Laboratory Press*, Courant Institute of Mathematical Sciences, New York University, 1977.

16. Jameson A., Schmidt W., and Turkel E., "Numerical simulation of the Euler equations by finite volume methods using Runge-Kutta time stepping schemes", *AIAA Paper 81-1259*, AIAA 5th Computational Fluid Dynamics Conference, 1981.

17. Jameson A., "Transonic aerofoil calculations using the Euler equations", in P.L. Roe (ed.), *Numerical Methods in Aeronautical Fluid Dynamics*, New York: Academic Press, 1982.

18. Jameson A., and Baker T.J., "Solutions of the Euler equations for complex configurations", *AIAA Paper 83-1929*, AIAA 6th Computational Fluid Dynamics Conference.

19. Jameson A., and Baker T.J., "Multigrid solutions of the Euler equations for aircraft configurations", *AIAA Paper 84-0093*, AIAA 22nd Aerospace Sciences Meeting.

20. Jameson A., *Frontiers of computational fluid dynamics*, Wiley, Chichester, New York, 1994.

21. John D. Anderson, Jr., *Computational Fluid Dynamics*, 1st Edition, McGraw-Hill, New York, 1995.

22. John D. Anderson, Jr., *Fundamentals of Aerodynamics*, 2nd Edition, McGraw-Hill, New York, 1997.

23. John D. Anderson, Jr., *Modern Compressible Flow with Historical Perspective*, 2nd Edition, McGraw-Hill, New York, 1990.

24. Krasilschiova E.A., "The wing of finite span in compressible stream", Gostehizdat, Moscow, 1952.

25. Krasilschiova E.A., "Unsteady motion of a wing of infinite aspect ratio", Gostehizdat, Moscow, 1954.

26. Krasilschiova E.A., "Unsteady motion of finite wing span in a compressible motion", Gostehizdat, Moscow, 1964.

27. Lennart Råde, Bertil Westergren, *Mathematics Handbook for Science and Engineering*, Birkhäuser, Sweden, 1995.

28. MacCormack R.W., "The effect of viscosity in hypervelocity impact cratering", *AIAA Paper 69-354*, 1969.

29. MacCormack R.W., "Numerical solutions of the interaction of a shock wave with a laminar boundary layer", *Proc. Second International Conference on Numerical Methods in Fluid Dynamics*, pp. 151-163, *Lecture Notes in Physics*, Vol. 8, Berlin: Springer Verlag, 1971.

30. MacCormack R.W., and Paullay A.J., "Computational efficiency achieved by time splitting for finite difference operators", *AIAA Paper 72-154*, San Diego, 1972.

31. MacCormack R.W., and Baldwin B.S., "A numerical method for solving the Navier-Stokes equations with application to shock-boundary layer interaction" *AIAA Paper 75-1*, 1975.

32. MacCormack R.W., "Current status of numerical solutions of the Navier-Stokes equations", *AIAA Paper 88-0513*, 1988.

33. Mateescu D. and Lauzon M., "An explicit Euler method for internal flow computation", *Computers and Experiments in Fluid Flow, Editors G.M. Carlomagno and C.A. Brebbia, Computational Mechanics Publication*, Springer-Verlag, Berlin, pp. 41-50, 1989.

34. Mateescu D. and Newman B.G., "Analysis of flexible-membrane and jet-flapped aerofoil using velocity singularities", *AIAA Journal*, Vol. 28, No. 11, pp. 789-795, 1991.

35. Mateescu D., "A hybrid panel method for airfoil aerodynamics", *Boundary Elements XII, Vol. 2, Applications in Fluid Mechanics and Field Problems*, Springer-Verlag, Berlin, pp. 3-14, 1990.

36. Mateescu D., "A solution of the conically cambered delta wings in supersonic flow", *Revue de Mécanique Appliquée*, No. 2, pp. 189-216, 1975.

37. Mateescu D., "Computational solutions of unsteady viscous flows with oscillating boundaries", *Computational Methods and Experimental Measurements VIII, Editors P. Anagnostopoulos, G.M. Carlomagno and C.A. Brebbia*, Computational Mechanics Publications, Southampton & Boston, pp. 331-340, 1997.

38. Mateescu D., "Cruciform wings and tails fitted with conical bodies in supersonic flow II – high order conical flow", *Revue de Mécanique Appliquée*, No. 1, pp. 53-76, 1969.

39. Mateescu D., "Cruciform wings and tails fitted with conical bodies in supersonic flow I – conical flow", *Revue de Mécanique Appliquée*, No. 2, pp. 189-216, 1975.

40. Mateescu D., "Low frequency oscillations of the tail-body system in supersonic flow", *Revue de Mécanique Appliquée*, No. 6, pp. 1225-1244, 1969.

41. Mateescu D., "Oscillatory motions of the polygonal wings in supersonic flow", *Revue de Mécanique Appliquée*, No. 1, pp. 105-129, 1970.

42. Mateescu D., "Two hybrid spectral methods for the analysis of unsteady viscous flows with oscillating boundaries", *Computational Mechanics '95, Theory and Application, Editors S.N. Atluri, G. Yagawa, T. Cruse*, Springer, Berlin, pp. 792-798, 1995.

43. Mateescu D., and Chocron L., "Solutions for jet-flapped airfoils and aerodynamic nozzle design based on a Lagrangian computational method", *Proceedings of the 15th International Conference on Numerical Methods in Fluid Dynamics*, Monterey, California, pp. 254-255, 1996.

44. Mateescu D., and Nasrallah P., "Computational solutions based on a Lagrangian formulation for aerodynamic problems of unspecified geometry", *Computational Methods and Experimental Measurements VII, Editors G.M. Carlomagno and C.A. Brebbia*, Computational Mechanics Publications, Southampton & Boston, pp. 317-325, 1995.

45. Mateescu D., and Stanescu D., "A biased flux method for solving the Euler equations in subsonic, transonic, and supersonic flows", *Computational Methods and Experimental Measurements VII, Editors G.M. Carlomagno and C.A. Brebbia*, Computational Mechanics Publications, Southampton & Boston, pp. 327-335, 1995.

46. Mateescu, D., "Wing and Conical Body of Arbitrary Cross Section in Supersonic Flow", *J. AIRCRAFT*, Vol. 24, No.4, pp. 239-247, 1999.

47. Mateescu, D., *Lecture Notes of Computational Aerodynamics*, McGill University, 2001.

48. Mateescu, D., *Lecture Notes of High Speed Aerodynamics*, McGill University, 2000.

49. Mateescu, D., *Lecture Notes of Subsonic Aerodynamics*, McGill University, 1999.

50. Mateescu, D., *Lecture Notes of Unsteady Aerodynamics*, McGill University, 2001.

51. Mateescu, D., *Private Communications*, McGill University, 2002.

52. Miles, J.W., *The Potential Theory of Unsteady Supersonic Flow*, Cambridge University Press, 1959.

53. Milne-Thomson, L.M., *Theoretical Aerodynamics*, 4th Edition, Dover, New York, 1966.

54. Pines S. and Dugundgi J., "Application of aerodynamics flutter derivatives to flexible wings with supersonic and subsonic edges", *Republic Aviation Corporation*, Rep. E-SAF-2, 1954.